UNIVERSIDAD COMPLUTENSE DE MADRID
FACULTAD DE CIENCIAS QUÍMICAS

TESIS DOCTORAL

Melatonin-and resveratrol-based multitarget-directed agents for Alzheimer's disease and photoswitchable muscular nicotinic receptor ligands

Agentes multidiana derivados de melatonina y resveratrol para la enfermedad de Alzheimer y ligandos fotomodulables del receptor nicotínico muscular

MEMORIA PARA OPTAR AL GRADO DE DOCTOR

PRESENTADA POR

Clara Herrera Arozamena

Directora

María Isabel Rodríguez Franco

Madrid

UNIVERSIDAD COMPLUTENSE MADRID

CSIC
Consejo Superior de Investigaciones Científicas

Melatonin- and resveratrol-based multitarget-directed agents for Alzheimer's disease and photoswitchable muscular nicotinic receptor ligands

Agentes multidiana derivados de melatonina y resveratrol para la enfermedad de Alzheimer y ligandos fotomodulables del receptor nicotínico muscular

Clara Herrera Arozamena

PhD candidate

Dra. María Isabel Rodríguez Franco

Supervisor

Facultad de Ciencias Químicas
Instituto de Química Médica
Consejo Superior de Investigaciones Científicas
MADRID 2019

UNIVERSIDAD COMPLUTENSE MADRID

DECLARACIÓN DE AUTORÍA Y ORIGINALIDAD DE LA TESIS PRESENTADA PARA OBTENER EL TÍTULO DE DOCTOR

D./Dña. Clara Herrera Arozamena,
estudiante en el Programa de Doctorado Doctorado en Química Orgánica RD99/2011,
de la Facultad de Ciencias Químicas de la Universidad Complutense de Madrid, como autor/a de la tesis presentada para la obtención del título de Doctor y titulada:

Agentes multidiana derivados de melatonina y resveratrol para la enfermedad de Alzheimer y ligandos fotomodulables del receptor nicotínico muscular

y dirigida por: María Isabel Rodríguez Franco

DECLARO QUE:

La tesis es una obra original que no infringe los derechos de propiedad intelectual ni los derechos de propiedad industrial u otros, de acuerdo con el ordenamiento jurídico vigente, en particular, la Ley de Propiedad Intelectual (R.D. legislativo 1/1996, de 12 de abril, por el que se aprueba el texto refundido de la Ley de Propiedad Intelectual, modificado por la Ley 2/2019, de 1 de marzo, regularizando, aclarando y armonizando las disposiciones legales vigentes sobre la materia), en particular, las disposiciones referidas al derecho de cita.

Del mismo modo, asumo frente a la Universidad cualquier responsabilidad que pudiera derivarse de la autoría o falta de originalidad del contenido de la tesis presentada de conformidad con el ordenamiento jurídico vigente.

En Madrid, a 27 de junio de 2019

Fdo.: 

Esta DECLARACIÓN DE AUTORÍA Y ORIGINALIDAD debe ser insertada en la primera página de la tesis presentada para la obtención del título de Doctor.

Esta Tesis Doctoral se ha realizado en el Instituto de Química Médica del CSIC, en el laboratorio de la Dra. María Isabel Rodríguez Franco a quien agradezco la oportunidad que me brindó y la confianza depositada en mi trabajo durante estos años. Además, parte de esta tesis se ha realizado en la University of the Pacific (California) en el laboratorio del Dr. Carlos A. Villalba Galea, a quien agradezco haberme aceptado en su grupo y adentrarme en el complejo campo de la electrofisiología. Asimismo, me gustaría destacar todos los buenos recuerdos de las dos estancias.

De igual manera, agradezco a toda la financiación, sin la que no habría sido posible este trabajo: el Ministerio de Educación Cultura y Deporte por los proyectos SAF2012-31035 y SAF2015-64948, gracias a los que pude tener dos contratos con los que comencé mi tesis. A este mismo organismo por la beca Formación del Personal Universitario (FPU) y la FPU de estancias, gracias a esta última esta tesis va a tener mención internacional. Además, a la Agencia Estatal de Investigación por el proyecto RTI2018-093955 (AEI) y a la Comunidad de Madrid por B2017/BMD-3827. A todos, nuestro reconocimiento.

Además, me gustaría agradecer a todo el Instituto de Química Médica, en especial a la directora Dra. Ana Castro Morera y la anterior, Dra. María Jesús Pérez Pérez, al gerente Pedro Pastur y al gestor José María Nicolás por su trabajo y haber estado siempre tan atentos. De igual modo a todo el personal de HPLC, Guadalupe Romero y Felipe Pérez, y de RMN, a Maite Benito Gómez por toda su ayuda en el registro de los espectros del segundo capítulo.

Asimismo, me gustaría dar las gracias a la Dra. María Luz López Rodríguez de la Universidad Complutense de Madrid, por su papel como tutora.

Quiero agradecer también a la Sociedad Española de Química Terapéutica (SEQT), por haberme permitido presentar mi trabajo en diversos congresos gracias a sus becas y haber reconocido mi trabajo en el "XIX Premio para Investigadores Nóveles", asimismo agradecer a la compañía farmacéutica Lilly por escoger mi trabajo. A la Sociedad Internacional de Neuroquímica que me concedió la beca para presentar mi trabajo en su Meeting en París y a la Sociedad Internacional de Biofísica por la beca para defender el

trabajo del segundo capítulo en su Meeting en Baltimore (Maryland), donde pude adquirir una visión más multidisciplinar.

También quiero expresar mi agradecimiento a todos los colaboradores que menciono a continuación.

Al Dr. Federico Gago y Alberto Mills de la Universidad de Alcalá por estar dispuestos a introducirse en el apasionado mundo de la melatonina, haciendo estudios computacionales en los tres receptores. Gracias, en especial a Federico por los buenos días que he pasado allí, por estar siempre dispuesto a ayudar, por preocuparse y por tener siempre buenas palabras.

A las Dras. Begoña Gómez Miguel y Ana María Martínez Díaz de la Universidad Complutense de Madrid por toda su paciencia, cariño y permitirme tener mi primer contacto con la biología realizando ensayos de neuroprotección en células SHSY5Y.

A los Dres. Rafael León y Manuela G. López del Instituto Teófilo Hernando donde se han realizado los estudios de Nrf2 y neuroprotección. En especial a la Dra. Patrycja Miclaska por ayudarme esos dos meses en los que estuve aprendiendo y al Dr. Felipe Franco por los estudios computacionales en Nrf2.

A la Dra. Dolores Viña de la Universidad Santiago de Compostela por realizar parte de los ensayos en monoaminoxidasas y ciclooxigenasas.

A los Dres. José A Morales-García y Ana Pérez Castillo del Instituto de Investigaciones Biomédicas “Alberto Sols” por realizar los estudios de neurogénesis.

Agradecer también a la bióloga del grupo, la Dra. Concepción Pérez quien ha realizado los ensayos de MAOs, ORAC y LOX-5, además de otros no incluidos en esta memoria.

Quiero dar las gracias a los profesores del Dpto. de Química Orgánica I de la Universidad Complutense de Madrid, los Dres. Rafael Gómez Aspe, Cristina Aragoncillo y Ángeles Canales, con los que he impartido prácticas de laboratorio y han hecho esa experiencia muy gratificante.

Gracias a todos los que han estado dispuestos siempre a ayudar. A María Elena Zoghbi por su trabajo, sus correcciones y todo el tiempo compartido. A la Dra. Lissa Carrillo, por ser siempre atenta y generosa. A Karlira por todos los momentos californianos compartidos juntas, tanto dramas como risas. A todos los compañeros con los que he compartido vitrina y los que ya me ha tocado ordenador. Especialmente a Cristina Tortosa por todo su trabajo, su alegría y locura particular, que hacía el laboratorio un ambiente más agradable. A Olaia Martí, Patricia López, Yalda Barlas y Jorge Manuel Rubio a los que he tenido la oportunidad de supervisar sus trabajos. En particular, con cariño a Olaia por todas nuestras profundas conversaciones.

Por otra parte, me gustaría agradecer a mis queridos compañeros de la Academia OF, los Dres. Mar Blanco, Juan Carlos y Jorge Jabonero por haberme ayudado con el millón de dudas que me han ido surgiendo a lo largo de estos años y todas sus aportaciones, además de los buenos ratos juntos.

A todos los amigos y compañeros con los que he compartido grandes momentos, en los primeros años, Guadalupe, Asier, Oskía, Belén, Pili, Paco Fueyo; a los que los han ido llegando más tarde, Gabi, Carol, Cristina, Santi, Lucía; Tania, Carlos y a los que siempre han estado, Paco Sánchez, Cumella, Patrick, Laura, Felipe. En especial a Jose Cumella por tener la paciencia del recuento de protón y carbono de la parte experimental.

Gracias a mi familia, porque sin mis padres, sin su apoyo incondicional y todos sus esfuerzos, llegar hasta aquí habría sido imposible. Gracias por estar siempre a mi lado sin importar la distancia, siempre tan dispuestos a ayudarme a alcanzar cualquier meta y hacerme feliz. A mi hermano Miguel por estar atento y preocupado.

Finalmente, agradecer inmensamente al Dr. Martín Estrada, “el MEV”, por haber sido mi pilar desde que puse los pies en el laboratorio 310. Gracias por tus recristalizaciones, por tus infinitas correcciones, por tus ánimos cuando me veía en un pozo sin salida, por tu infinita calma, por tu generosidad, por todos los grandes momentos compartidos... Simplemente gracias por estar a mi lado, compañero.

Gracias a todos los que habéis estado ahí durante estos casi cinco años.

TABLE OF CONTENTS

ABBREVIATIONS AND ACRONYMS

Throughout this thesis, abbreviations and acronyms recommended by the American Chemical Society in the Organic Chemistry and Medicinal Chemistry areas have been employed (revised in the *Journal of Organic Chemistry* and *Journal of Medicinal Chemistry* on April 2019; http://pubs.acs.org/paragonplus/submission/joceah/joceah_abbreviations.pdf and http://pubs.acs.org/paragonplus/submission/jmcmar/jmcmar_abbreviations.pdf). Furthermore, those indicated below have also been used.

AAPH	2,2'-Azobis-(amidinopropane) dihydrochloride
ACN	Acetonitrile
ARE	Antioxidant response element
BisQ	3,3'-Bis[α-(trimethylammonium)methyl]azobenzene dibromide
BOP	(Benzotriazol-1-yloxy)tris(dimethylamino)phosphonium hexafluorophosphate
CDI	1,1′-Carbonyldiimidazole
Cul3	Cullin-dependent E3 ubiquitin ligase
DAPI	4′,6-Diamidine-2′-phenylindole dihydrochloride
DCFDA	Dichlorofluorescin diacetate
DMEM	Dulbecco's Modified Eagle's Medium
EDG	Electron donate group
EDC	*N*-(3-Dimethylaminopropyl)-*N*′-ethylcarbodiimide
FBS	Fetal bovine serum
FL	Fluorescein
GSK-3β	Glycogen Synthase-3β
g.t.	Gradient time
HBSS	Hanks' balanced salt solution
HEPES	4-(2-Hydroxyethyl)-1-piperazineethanesulfonic acid
HO1	Hemoxygenase-1

HOBt	1-Hydroxybenzotriazole
HTRF	Homogeneous Time Resolved Fluorescence
KEAP1	Kelch like ECH associated protein 1
LED	Light emitting diode
LOX-5	Lipoxygenase-5
MAO	Monoamino oxidase
MAP-2	Microtubule-associated protein 2
MT	Melatonin
MTDL	Multi-target-directed ligand
MTR	Melatonin receptors
MTT	3-[4,5-Dimethylthiazol-2-yl]-2,5-diphenyltetrazolium bromide / Thiazolyl Blue Tetrazolium Bromide
mw	Microwave
nAChR	Nicotinic acetylcholine receptors
ND	Neurodegenerative disease
NDGA	Nordihydroguaiaretic acid
NFTs	Neurofibrillary tangles
NMBA	Neuromuscular blocking agent
NQO1	NAD(P)H quinone oxidoreductase 1
Nrf2	Nuclear transcriptor factor (erythroid-derived 2)–like 2
NRH	*N*-ribosyldihydronicotinamide
NS	Neurospheres
NSC	Neuronal stem cells
OA	Okadaic acid
ORAC	Oxygen radical absorbance capacity
OS	Oxidative stress
Oxone®	$[(KHSO_5)_2 \cdot KHSO_4 \cdot K_2SO_4]$
PBL	Porcine brain lipid
Pd-C	Palladium over charcoal
P_e	Permeability
PI	Propidium iodide

PTL	Photochromic-tethered ligands
QBr	3-(α-Bromomethyl)-3'-[α -(trimethylammonium)methyl]azobenzene bromide
QR2/NQO2	Quinone reductase 2
RNS	Reactive Nitrogen Species
SD	Standard deviation
SEM	Standard error of the mean
SGZ	Subgranular zones
TEA	Triethylamine
TEVC	Two-electrode voltage-clamp
tg	Transgenic
TuJ1	Human β-III-tubulin

ABSTRACT

ABSTRACT

Chapter I. Melatonin- and resveratrol-based multitarget-directed agents for Alzheimer's disease

Introduction

Alzheimer´s disease (AD) is a complex multifactorial illness with no effective treatment, characterized by irreversible global cognitive impairment. As only symptomatic treatments are available with drugs acting at one single target, exploration of molecules active in different pathological targets is required. In this chapter, our objective was to develop new families of multitarget directed ligands (MTDLs) focused on some pathological pathways underlying AD, namely, oxidative stress and neuroinflammation. Thus, we design melatonin- and resveratrol-based MTDLs looking for activity in melatonin receptors ($MT_{1-3}Rs$), monoaminoxidases (MAO-A/B), lipoxygenase-5 (LOX-5), and nuclear factor erythroid 2-related factor 2 (Nrf2). Considering the neuroprotective and neurogenic properties found in melatonin and resveratrol, we reasonably expected these activities in our MTDLs.

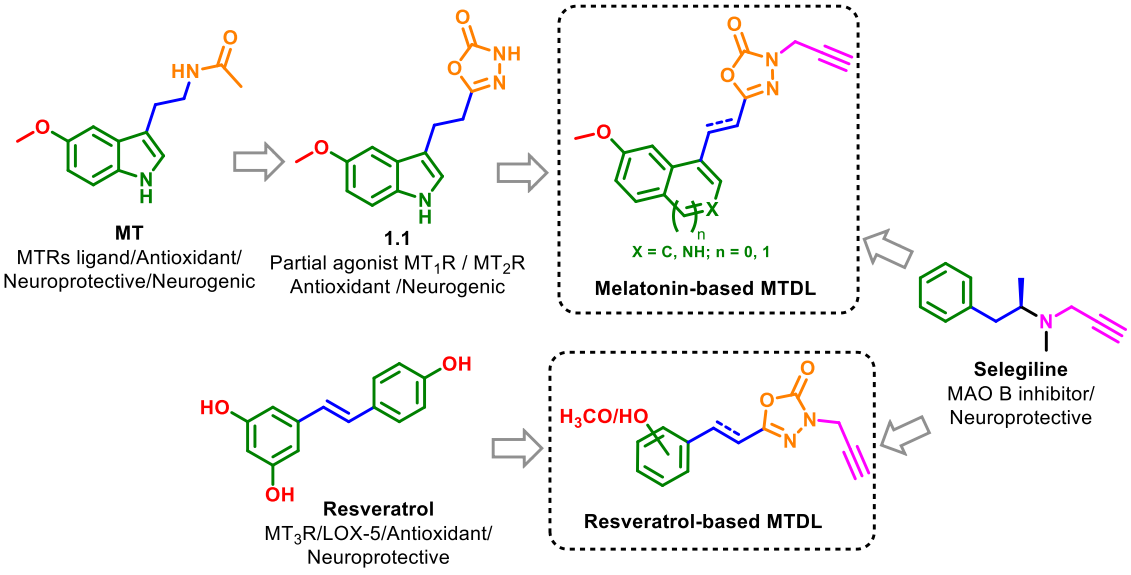

Figure 1. MTDL strategy design for the novel melatonin- and resveratrol-based families

Results and discussion

The main synthetic strategy started by a *Knoevenagel-Doebner* reaction from aromatic aldehydes to afford the corresponding α,β-unsaturated acids, which yielded the saturated acid by hydrogenation. Both acids were transformed into hydrazides or amides. Then, hydrazides were cycled to yield oxadiazolone derivatives, which in some cases were alkylated to give the desired melatonin- and resveratrol-based compounds (Scheme 1).

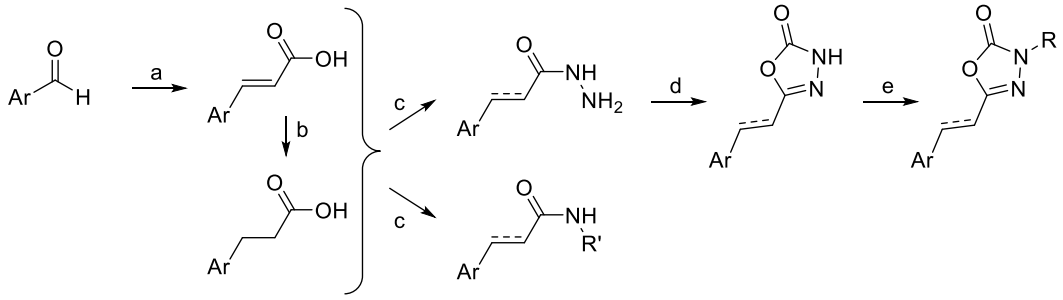

Scheme 1. Reagents and conditions. (a) Malonic acid, piperidine, pyridine, 70 ºC; (b) H_2/Pd-C (5%), EtOH, rt; (c) EDC·HCl, HOBt, DMAP, ACN; $N_2H_4 \cdot H_2O$/NH_2R', rt.; (d) CDI, DMF, mw, 130 ºC, 25 min; (e) K_2CO_3, RX/R-OTs, acetone, mw, 120 ºC, 10 min.

The new MTDLs were tested in the above-mentioned targets, ranking their affinity or inhibition constants between the nanomolar and micromolar order. Some compounds were good radical scavengers and could penetrate into the central nervous system (CNS), according to the *in vitro* PAMPA-BBB assay. A structure-activity relationship (SAR) has been stablished in each target, which has guided the optimization of new MTDLs. Furthermore, some of them displayed neurogenic properties in phenotypic experiments. Moreover, selected MTDLs were evaluated in *in vitro* AD-models of increasing complexity.

Conclusions

From SAR studies, we conclude that the nature of the aromatic ring is the more influential feature in the radical scavenging properties, being the indole the most favourable. The unsaturated linker was the most important structural characteristic in the potency and selectivity towards MT_3R and Nrf2. The *N*-propargyloxadiazolone ring was the most favoured polar moiety in the potency and selectivity toward MAO-B and Nrf2. The best low-micromolar *h*LOX-5 inhibitors had a catechol in their structure. The most potent and selective *h*MAO-B inhibitors were resveratrol-derivatives with a propargyl radical in the oxadiazolone, being also excellent Nrf2 inducers, and effective neurogenic and neuroprotective agents in *in vitro* models of AD. Derivatives with the better MTD-profile were predicted to be CNS-permeable, acting in their cerebral targets.

5-(4-Methoxystyryl)-3-(prop-2-yn-1-yl)-1,3,4-oxadiazol-2(3*H*)-one (**1.107**) emerges as an interesting AD-MTDL. In the low-micromolar range, **1.107** is a potent Nrf2 inducer, a *h*MAO-B inhibitor and a MT_3R ligand. And in phenotypic assays, it displays neuroprotective and neurogenic properties. Consequently, **1.107** can be considered a promising prototype in the searching for innovative treatments for AD.

Chapter II. Photoswitchable muscular nicotinic receptor ligands

Introduction

Neuromuscular blockers acting at the neuromuscular junction generally present severe side-effects, some of them attributable to a poor selectivity between muscular and neuronal nicotinic acetylcholine receptors (nAChRs). Here, we developed a new family of photoswitchable neuromuscular ligands, named azocuroniums, with manageable or null CNS side-effects. They are based on an azobenzene structure bearing *N*-methyl-*N*-carbocyclic quaternary ammonium groups in *meta*- or *para*-positions. Azocuroniums could be photoswitched between the (*E*)-(*Z*)-isomers by irradiation at blue or UV light, allowing the fine spatial and temporal control of their activity.

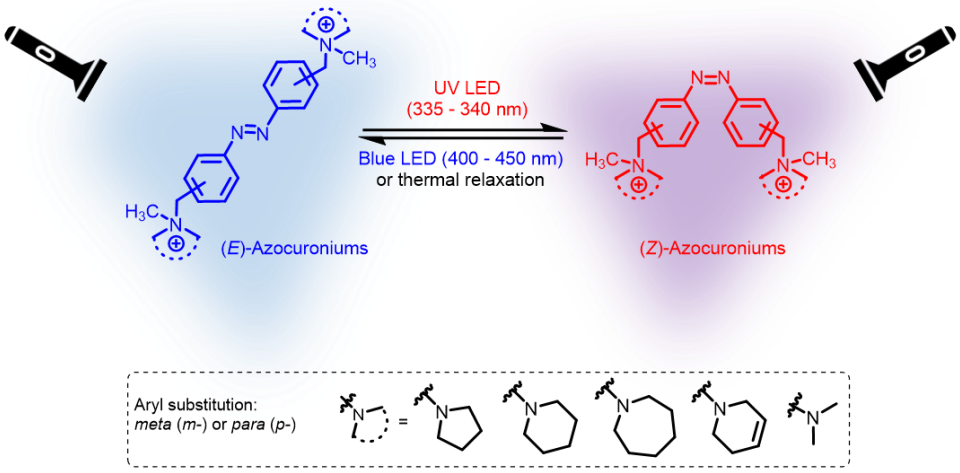

Figure 2. (*E*)-(*Z*)-Azocuroniums and their photoisomerization.

Results and discussion

The synthetic route for the symmetric azocuroniums consisted of a reductive coupling between the corresponding nitrobenzenes, obtained previously from *meta*- or *para*-nitrobenzyl bromide and the corresponding *NH*-cycle. Then, the amino groups were quaternized to generate the azocuronium. In the asymmetric *m*-**2.14b**, azocoupling took place by a Mills reaction between aniline *m*-**2.4b** and nitrosobenzene (Scheme 2).

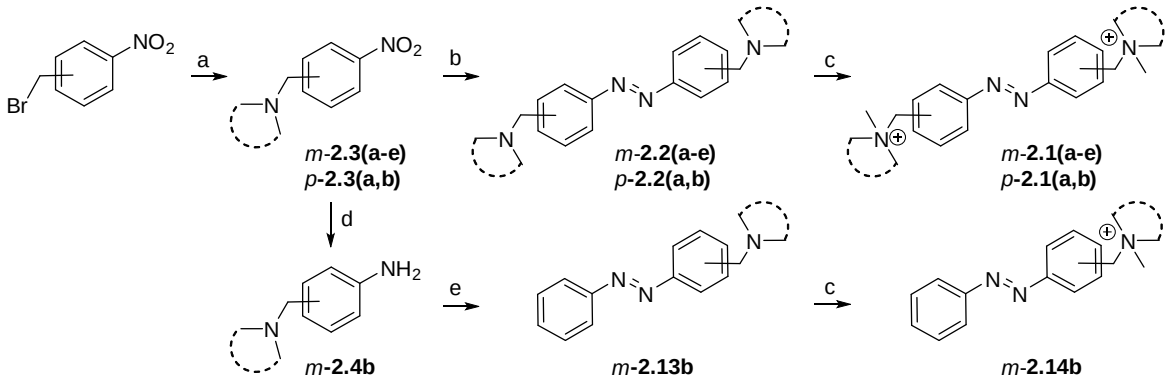

Scheme 2. Reagents and conditions. (a) K_2CO_3, amine, acetone, mw, 120 ºC, 10 min; (b) $LiAlH_4$, Et_2O, -78 ºC to rt; (c) CH_3I, DMF, mw, 120 ºC, 12 min; (d) H_2/Pd-C (5%), EtOH, overnight; (e) nitrosobenzene, AcOH, toluene, 60 ºC, overnight.

In radioligand binding assays at nAChRs, *meta*-azocuroniums were more potent and selective towards muscular receptors than their *para*-counterparts. Derivatives with smaller cationic heads (*meta*-pyrrolidine *m*-**2.1a** and *meta*-piperidine *m*-**2.1b**) emerged as the most potent and selective ligands in muscle-type nAChRs (K_is = 42 and 35 nM, respectively). In contrast, azocuroniums with increased volume or rigidity in the *N*-carbocycle (*m*-azepane *m*-**2.1c** and *m*-1,2,3,6-tetrahydropyridine *m*-**2.1d**) showed reduced binding constants in muscular-type nAChR (K_is = 220 and 100 nM, respectively) with diminished selectivity indexes.

Using the two-electrode voltage-clamp technique, we evaluated the functional activity of *meta*-azocuroniums *m*-**2.1(a-d)** and *m*-**2.5b** in muscular nAChR expressed in *Xenopus laevis* oocytes. By irradiation with blue or UV LED, in all cases the (*E*)-isomer was found

to be more potent than the (*Z*)-form. The volume and hydrophobic character of the ammonium groups seemed to determine the functional character. All *meta*-azocuroniums behaved as antagonists of muscular nAChR, with the exception of the smallest pyrrolidine derivative *m*-**2.1a**.

Conclusions

In this chapter, potent photoswitchable neuromuscular ligands named azocuroniums, has been developed. They can be photoswitched between the (*E*)- and (*Z*)-isomers by blue or UV LED. *Meta*-azocuroniums were more potent and selective toward muscular nAChRs compared to neuronal subtypes, showed good solubility in physiologic media, negligible cell toxicity, and would not reach the CNS.

Electrophysiological studies in muscle-type nAChRs showed that (*E*)-azocuroniums were more potent and two ammonium groups are required for high activity. All *meta*-azocuroniums were antagonists, except the pyrrolidine derivative that was an agonist. These *meta*-azocuroniums, which can be modulated *ad libitum* by light, could be employed as photoswitchable tools to better understand the pharmacology of muscle-type nAChRs.

RESUMEN

RESUMEN

Capítulo I. Agentes multidiana derivados de melatonina y resveratrol para la enfermedad de Alzheimer

Introducción

La enfermedad de Alzheimer (EA) es un desorden multifactorial sin cura efectiva, caracterizada por un deterioro cognitivo global. Los tratamientos disponibles son sólo sintomáticos con fármacos que actúan sobre una sola diana, siendo necesarias moléculas activas por diferentes vías. En este capítulo, nuestro objetivo es desarrollar nuevas familias de ligandos multidiana (MTDL) enfocados hacia vías patológicas de la EA, concretamente, el estrés oxidativo y neuroinflamación. Así, desarrollamos MTDLs basados en melatonina y resveratrol buscando actividad en receptores de melatonina ($MT_{1\text{-}3}Rs$), monoamino oxidasas (MAO-A/B), lipoxigenasa-5 (LOX-5) y el factor nuclear (erythroid-derived 2)-like 2 (Nrf2). Considerando las propiedades neuroprotectoras y neurogénicas de la melatonina y el resveratrol, esperamos razonablemente estas actividades en nuestros MTDLs.

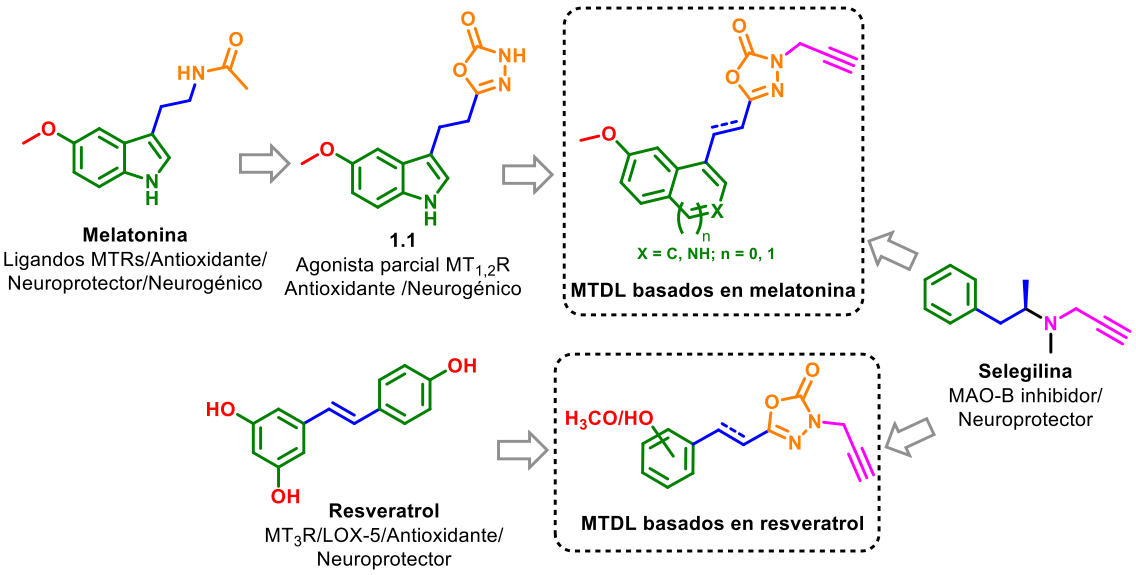

Figura 1. Estrategia de diseño MTDL para las familias basadas en melatonina y resveratrol

Resultados y Discusión

La estrategia sintética seguida en este capítulo comenzó por una reacción de *Knoevenagel-Doebner* desde aldehídos aromáticos para obtener ácidos α,β-insaturados, los cuales dieron lugar a los ácidos saturados por hidrogenación. Ambos ácidos fueron transformados en hidrazidas o amidas. A continuación, se ciclaron las hidrazidas, obteniendo los derivados de oxadiazolona, los cuales en algunos casos se alquilaron para dar los derivados deseados de melatonina y resveratrol (Esquema 1).

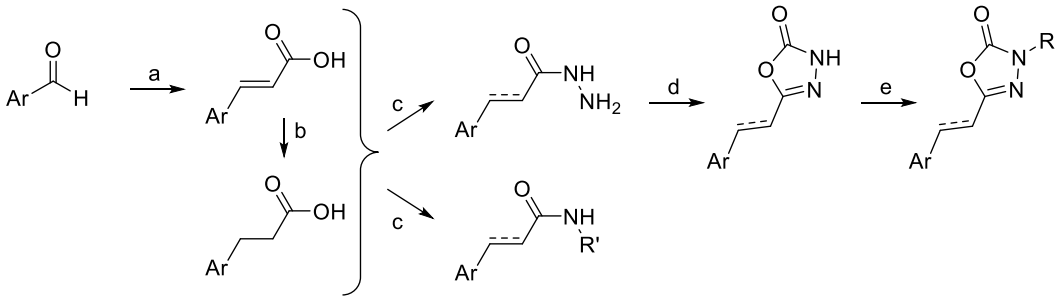

Esquema 1. Reactivos y condiciones. (a) Ácido malónico, piperidina, piridina, 70 ºC; (b) H_2/Pd-C (5%), EtOH, ta; (c) EDC·HCl, HOBt, DMAP, ACN; $N_2H_4 \cdot H_2O/NH_2R'$, ta; (d) CDI, DMF, mw, 130 ºC, 25 min; (e) K_2CO_3, RX /R-OTs, acetona, mw, 120 ºC, 10 min.

Los nuevos MTDLs fueron evaluados en las dianas mencionadas anteriormente, estando sus constantes de afinidad o inhibición comprendidos entre los rangos nanomolar y micromolar. Algunos compuestos presentaron buenas capacidades antioxidantes y penetraron en el sistema nervioso central (SNC) (ensayo *in vitro* PAMPA-BBB). Se ha establecido una relación estructura-actividad (SAR), la cual ha permitido la optimización de nuevos MTDLs. Además, algunos mostraron propiedades neurogénicas empleado células madre murinas. Los MTDLs seleccionados fueron evaluados en modelos *in vitro* de EA de creciente complejidad.

Conclusiones

A partir de los estudios SAR, concluimos que la naturaleza del anillo aromático es la propiedad más influyente en la capacidad antioxidante, siendo el indol el más favorable. La cadena insaturada fue la característica estructural más importante en potencia y selectividad hacia MT_3R y Nrf2. El anillo *N*-propargiloxadiazolona fue el más favorecido en la potencia y selectividad hacia *h*MAO-B y Nrf2. El mejor inhibidor de LOX-5 en micromolar bajo tenía un catecol en su estructura. Los inhibidores más potentes y selectivos de *h*MAO-B fueron los derivados de resveratrol con un radical propargilo en la oxadiazolona, siendo también excelentes inductores de Nrf2 y agentes neurogénicos y neuroprotectores en modelos *in vitro* de la EA. Los derivados con mejor perfil multidiana alcanzarían el SNC, actuando en las dianas cerebrales.

5-(4-Metoxiestiril)-3-(prop-2-in-1-il)-1,3,4-oxadiazol-2(3*H*)-ona (**1.107**) resulta un interesante MTDL para la EA. En el rango micromolar bajo, **1.107** es un potente inductor de Nrf2, inhibidor de *h*MAO-B y ligando de MT_3R. En ensayos fenotípicos, muestra propiedades neuroprotectoras y neurogénicas. Por lo tanto, **1.107** puede ser considerado un prometedor prototipo en la búsqueda de tratamientos innovadores para la EA.

Capítulo II. Ligandos fotomodulables del receptor nicotínico muscular

Introducción

Los bloqueantes neuromusculares que actúan en la sinapsis neuromuscular presentan por lo general efectos secundarios graves, algunos de ellos atribuibles a una escasa selectividad entre los receptores nicotínicos (nAChRs) de tipo muscular y neuronal. En este capítulo, hemos desarrollado una nueva familia de ligandos musculares fotoconmutables, llamados azocuronios, con efectos secundarios manejables o nulos en el SNC. Están basados en la estructura de azobenceno sustituido en *meta*- o *para*- por grupos amonio cuaternarios *N*-metil-*N*-carbocíclico. Los azocuronios serían modulables entre los isómeros (*E*)-(*Z*) por irradiación con luz azul o UV, controlando su actividad espacial y temporalmente.

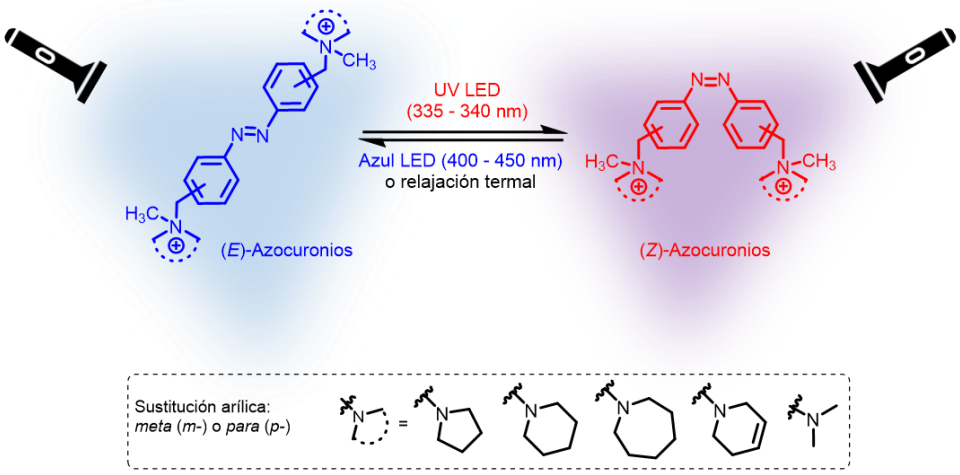

Figura 2. (*E*)-(*Z*)-Azocuronios y su fotoisomerización.

Resultados y Discusión

La ruta sintética optimizada para los azocuronios simétricos consistió en un acoplamiento reductor entre los correspondientes nitrobencenos, obtenidos previamente desde bromuro de *meta*/*para*-nitrobenzilo y el correspondiente *NH*-ciclo. Después, los grupos amino fueron cuaternizados para dar los azocuronios. En el asimétrico *m*-**2.14b**, el azoacoplamiento tuvo lugar por una reacción de Mills entre la anilina *m*-**2.4b** y el nitrosobenceno (Esquema 2).

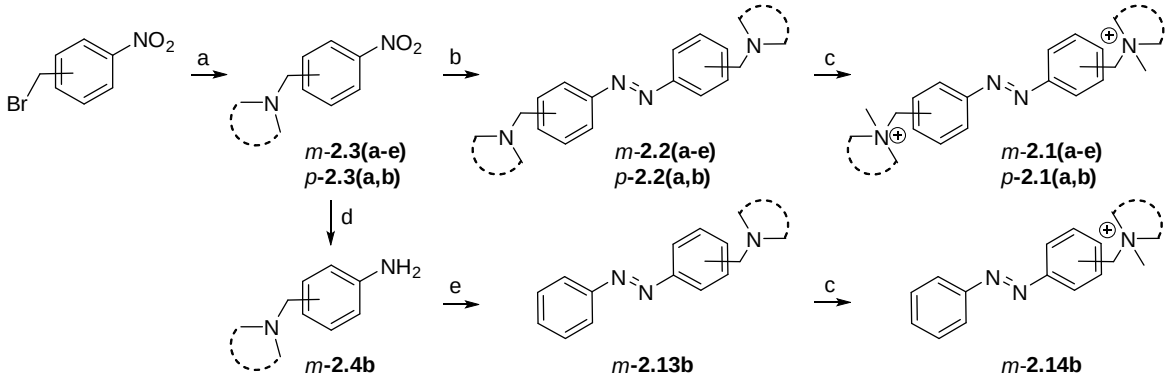

Esquema 2. Reactivos y condiciones. (a) K_2CO_3, correspondiente amina, acetona, mw, 120 ºC, 10 min; (b) $LiAlH_4$, Et_2O, -78 ºC a ta; (c) CH_3I, DMF, mw, 120 ºC, 12 min; (d) H_2/Pd-C (5%), EtOH, overnight; (e) nitrosobenceno, AcOH, tolueno, 60 ºC.

En nAChRs los *meta*-azocuronios fueron más potentes y selectivos hacia los receptores musculares que sus homólogos *para*-. Aquellos con grupos catiónicos más pequeños (*meta*-pirrolidina *m*-**2.1a** y *meta*-piperidina *m*-**2.1b**) resultaron los más potentes y selectivos en musculares (K_is = 42 y 35 nM, respectivamente). Por el contrario, los azocuronios con mayor volumen o rigidez en el *N*-carbociclo (*m*-azepan *m*-**2.1c** y *m*-1,2,3,6-tetrahidropiridina *m*-**2.1d**) mostraron constantes de unión en receptores musculares (K_is = 220 y 100 nM, respectivamente) con menores índices de selectividad.

Empleando la técnica *voltage-clamp* de dos electrodos, evaluamos el carácter funcional de los *meta*-azocuronios *m*-**2.1(a-d)** y *m*-**2.14b** en nAChR muscular expresados en ovocitos de *Xenopus laevis*. Por irradiación con LED azul o UV, en todos los casos el isómero (*E*) fue

más potente que el (*Z*). El volumen y el carácter hidrofóbico de los grupos amonio parece determinar el carácter funcional. Todos los *meta*-azocuronios resultaron antagonistas de nAChR muscular, excepto el derivado de pirrolidina más pequeño *m*-**2.1a**.

Conclusiones

Se ha desarrollado una nueva serie de potentes ligandos neuromusculares fotoconmutables, azocuronios. Pueden isomerizarse reversiblemente [(*E*)-(*Z*)]- con luz azul o UV. Los m*eta*-azocuronios fueron más potentes y selectivos hacia los nAChRs musculares comparado con los neuronales. Mostraron buena solubilidad, despreciable toxicidad neuronal y no alcanzan el SNC.

Los estudios de electrofisiología en nAChRs muscular mostraron que los (*E*)-azocuronios fueron más potentes y que dos grupos amonio son necesarios para una alta actividad. Todos los *meta*-azocuronios fueron antagonistas, excepto el derivado de pirrolidina que fue agonista. Estos *meta*-azocuronios, los cuales pueden ser fotomodulados *ad libitum*, se podrían emplear como herramienta para entender mejor la farmacología del nAChR muscular.

CHAPTER I

Melatonin- and resveratrol-based multitarget-directed agents for Alzheimer's disease

INTRODUCTION

INTRODUCTION

Alzheimer's disease (AD) is the most common age-associated neurodegenerative disorder (ND), currently becoming an alarming social, familiar, and economic burden in world-wide countries.[1] The origin of this disease is not completely understood, although different factors that trigger cognitive symptoms and memory loss have been postulated, such as abnormal hyper-phosphorylation of tau, oxidative stress (OS), neuro-inflammation, mitochondrial dysfunction, etc. The main AD hallmarks are the extracellular deposits of the neurotoxic amyloid-β peptide (Aβ), the intracellular accumulation of the hyperphosphorylated microtubule-associated tau protein and a massive neuronal loss.[2]

Abnormal cleavage of the amyloid precursor protein (APP) by β-secretase and γ-secretase causes Aβ. This peptide is prone to aggregation, first in insoluble Aβ fibrils and then in bulkier aggregates named senile plaques. Hyperphosphorylated microtubule-associated tau protein is the main component of neurofibrillary tangles (NFTs). Moreover, the neuronal loss diminishes the levels of the neurotransmitter acetylcholine (ACh), in charge of neuronal transmission. There are strong evidences that correlate protein aggregates anomalies and neuronal loss with OS and neuroinflammation.[3]

Oxidative Stress

OS is produced by the over accumulation of unpaired electrons of reactive oxygen species (ROS) and reactive nitrogen species (RNS), which leads to an increased risk of suffering neurodegeneration. In fact, post-mortem studies of AD brains have linked the increased levels of peroxided biomolecules with the progression of the disorder.[4] Furthermore, imbalance of the antioxidant defense system produces OS, causing abnormal protein aggregates.[5] Although the brain has its own antioxidant defense system, it is limited and lost with aging. Thereby, control of transcription factors involved in the regulation of oxidative genes and inhibition of the main enzymes that cause overproduction of ROS and RNS, such as monoamine oxidases (MAOs) or quinone reductase 2 (QR2), would be a valuable strategy to treat AD.[6]

Nuclear transcriptor factor (erythroid-derived 2)–like 2

The key elements that regulate the expression of cytoprotective antioxidant and anti-inflammatory enzymes are the DNA promotor region antioxidant response element (ARE) and the nuclear transcriptor factor (erythroid-derived 2)–like 2 (Nrf2).[7] Under no pathological conditions, Nrf2 is mainly located in the cytosol, bound to Kelch like ECH associated protein 1 (Keap1), which allows Cul3 (Cullin-dependent E3 ubiquitin ligase) ubiquitination of the Neh2 domain of Keap1-bound Nrf2, followed proteasomal degradation. In these conditions, Nrf2 levels remain low because of the negatively regulation by ubiquitination and degradation.[8] However, under OS conditions, Keap1 changes its conformation, breaking its binding to Nrf2. Thus, the latter is accumulated and translocated to the cell nucleus, where it forms a transcription factor complex that binds to ARE and induces gene expression of antioxidant enzymes, such as NAD(P)H quinone oxidoreductase 1 (NQO1) or hemoxygenase-1 (HO1) (Figure 1.1).[9,10] There are two pharmacological ways to activate Nrf2, involving either an electrophilic or a non-electrophilic mechanism. In the electrophilic mechanism, a covalent binding between electrophilic activator molecules and the cysteines of Keap1 produces either a subsequent Cul3 dissociation or a hinge and latch effect which finally releases Nrf2. These electrophilic activator molecules bind unspecifically to different nucleophiles in the cell and consequently they trend to produce undesired effects.[11,12] A huge amount of electrophilic Nrf2 inducers have been described, some representative examples are sulforaphane, dimethyl fumarate (approved for multiple sclerosis in 2013)[13] or bardoxolone methyl (currently under phase 3 clinical trials for the treatment of advanced chronic kidney disease in patients with type 2 diabetes mellitus)[14] (Figure 1.1).

In contrast, in the non-electrophilic mechanism, the Keap1-Nrf2 protein-protein interaction is disrupted by a peptide or a small-molecule by a non-covalent binding. Since this is a more specific mechanism, it is the preferred option in current research and several compounds have been designed looking for disrupting this interaction.[15-19]

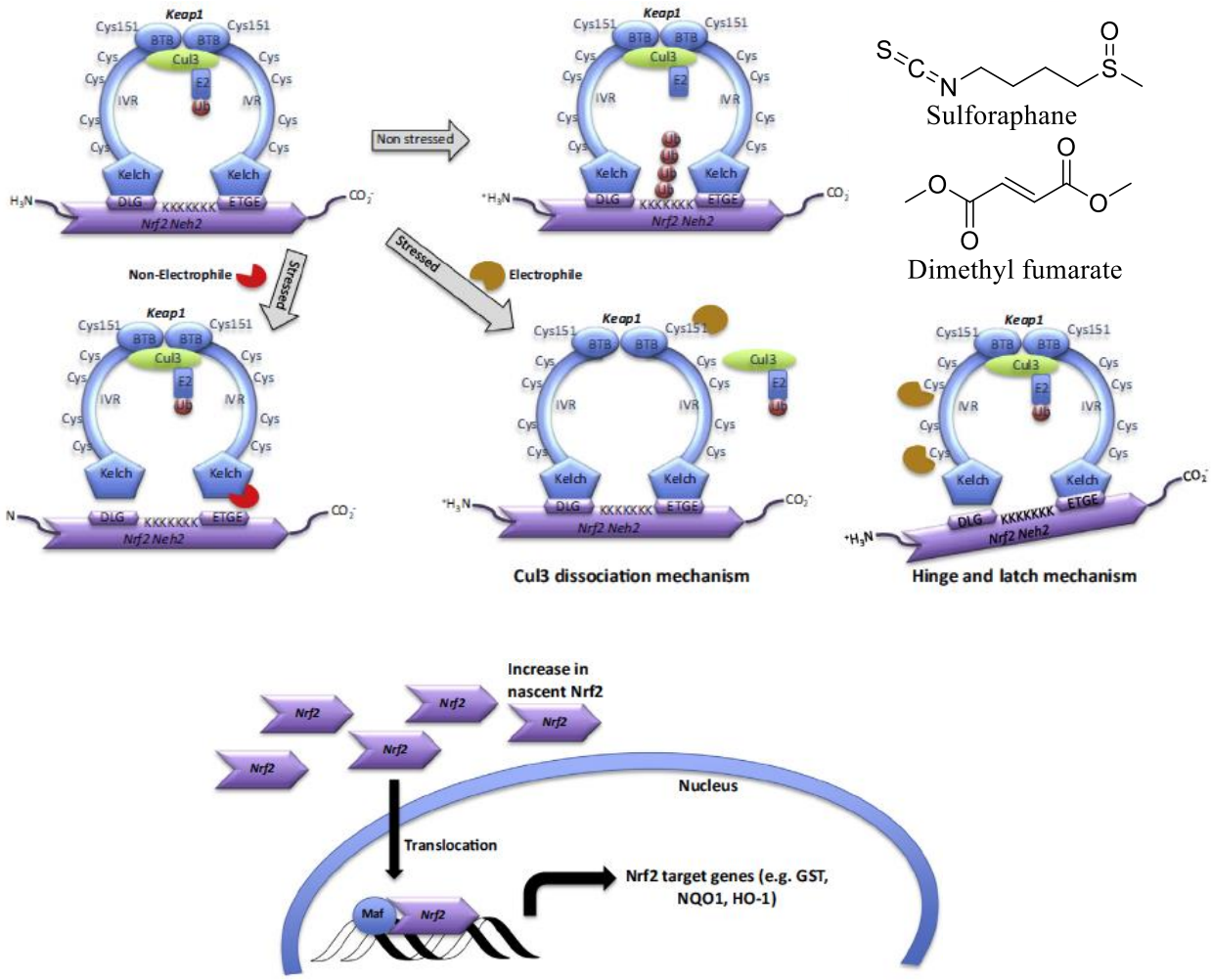

Figure 1.1. Schematic representation of Nrf2 activation by substrate adaptor protein Keap1. Under non-stressed conditions, Nrf2 is bound to Keap1. Nrf2 activation through either a non-electrophilic or by an electrophilic mechanism. In both cases, Nrf2 is translocated to the nucleus, where it binds with small Maf proteins and leads to transcription of Nrf2 target genes. Chemical structures of electrophilic Nrf2 inducers. Reproduced from [16]

In addition to its antioxidant role, Nrf2 acts as endogenous defense by inducing autophagy, and regulates neurogenic processes. In fact, Nrf2 over-expression promotes proliferation and differentiation to neuronal cells in primary cultures of rat stem cells.[20,21] Thus, inducers of Nrf2-ARE are promising therapeutic agents against OS, and accordingly for treatment of AD.[22,23]

Monoamino oxidases

MAO (E.C. 1.4.3.4) is an outer mitochondrial membrane-bound flavoprotein, which catalyzes the oxidative deamination of monoamines, such as neurotransmitters [serotonin (5-HT), dopamine (DA), norepinephrine (NE)] or other biogenic amines (tyramine or phenethylamine).[24] In mammals there are two isoforms differently distributed in the organism (brain, gastrointestinal tract, platelets…), distinguished by their structures[25] and consequently, by the affinity toward the different subtracts. MAO-A mainly metabolizes 5-HT, NE and DA, and therefore, it is involved in depressive and anxiety disorders. In fact, the mechanism of action of some antidepressant drugs such as clorgyline and moclobedine (Figure 1.2) is mainly based on the inhibition of MAO-A. In contrast, MAO-B that is responsible of 75% of the brain activity, catalyzes essentially the deamination of DA (5-HT and NE slowly), reason why its inhibitors, such as rasagiline and selegiline (Figure 1.2), act as anti-parkinsonian drugs.[26,27]

The oxidative reaction catalyzed by both isoenzymes generates hydrogen peroxide (H_2O_2) and the corresponding imine, which is hydrolyzed to the respective carbonyl group and either ammonia (in primary amines) (Figure 1.2) or a substituted amine (in secondary amines).[28] An excess of H_2O_2 produces ROS contributing to neurodegeneration. Moreover, overexpression of MAO-B intensifies the expression of γ-secretase, producing the formation of Aβ from APP.[29] In this sense, MAO inhibition could provide neuroprotection against AD, regulating the neurotransmitters levels, reducing the amyloid plaques formation and OS.[30,31]

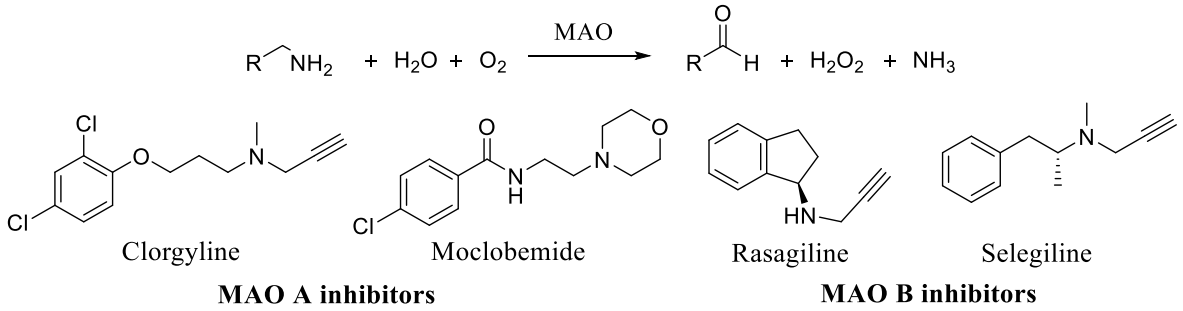

Figure 1.2. (Upper) Oxidative reaction of amines in the presence of H_2O and O_2 leads to the corresponding aldehyde, H_2O_2 and NH_3. (Lower) chemical structures of some MAOs inhibitors.

Melatonin receptors

Melatonin receptors (MTRs)[32] in mammals consist of the well-known MT_1R and MT_2R, G-protein coupled receptors (GPCRs),[33] and the third MTR (MT_3R), which has been identified as the flavin adenine dinucleotide (FAD)-dependent enzyme QR2 (EC 1.10.99.2).[34] Melatonin (MT, Figure 1.3) displays sub-nanomolar affinities toward MT_1R and MT_2R (around 10^{-10} M), whereas its affinity for MT_3R is about 100-fold lower, with an IC_{50} of 84 nM.[35-38] These receptors are involved in several physiological and pharmacological actions, like circadian and seasonal rhythms' regulation, immune and antioxidant systems modulation, and promotion of endogenous brain neurogenesis.[39] In addition of MT itself, there are three agonists in the market targeting MT_1R/MT_2R, namely, agomelatine (Valdoxan® for major depression),[40] ramelteon (Rozerem® for sleeping disorders)[41] and tasimelteon (Hetlioz® for non-24-h sleep-wake disorder) (Figure 1.3).[42,43]

MT_3R/QR2 uses *N*-ribosyldihydronicotinamide (NRH) or different NRH derivatives as electron donors to catalyze the two-electron reduction of quinones into unstable hydroquinones,[44] which are either excreted through conjugations or returned in the presence of oxygen to quinones while producing ROS.[45] It has been found that levels of QR2 are increased in the hippocampus of AD patients.[46] Thus, the inhibition of this enzyme would reduce OS,[47] being a promising target for this dementia.[48]

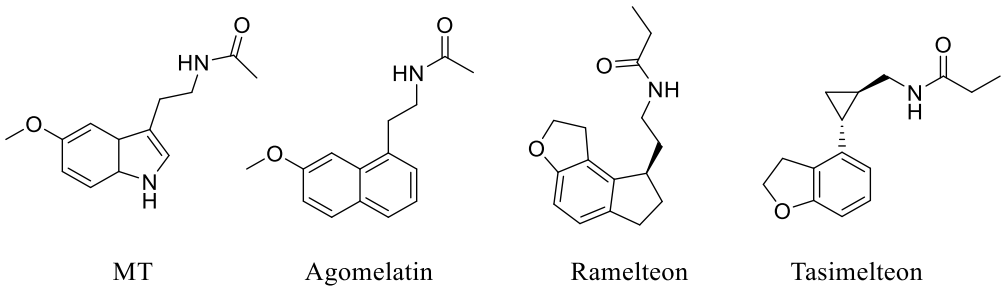

Figure 1.3. Chemical structures of MT and other marketed MT agonists

Neuroinflammation

In addition of OS, another possible pathway leading to the progression of neurodegeneration is the increase of neuroinflammation in some regions of the brain.[49] Inflammatory processes begin with the activation of microglia and astrocytes that bond to amyloid plaques, in an attempt to eliminate them. After this unsuccessful action, proinflammatory cytokines and neurotoxins are released, leading to neuronal damage and death.[50]

Lipoxygenase-5 (LOX-5)

LOX-5 (EC 1.13.11.34) is an iron-containing enzyme that catalyzes the oxidation of the arachidonic acid (AA) to 5-HPETE (5-hydroxy-peroxy-eicosatetraenoic acid) and subsequently to 5-HETE (5-hydroxy-eicosatetraenoic acid), which can be then metabolized into different pro-inflammatory leukotriene eicosanoids, acting as mediators of the inflammatory response.[51] LOX-5 is present in the CNS particularly in the hippocampus, where its levels appear to increase during aging and in AD.[52-54] Interestingly, it has been seen that blockade of the lipoxygenase-5 (LOX-5) in transgenic mice diminishes microgliosis and astrocytosis and consequently, reduces pro-inflammatory cytokines levels, as well as decreases both Aβ and tau pathology.[55] Indeed, in a model of AD-like amyloidosis, the LOX-5 gene disruption reduced the Aβ plaques and γ secretase activity.[56] Moreover, in the AD-triple transgenic mouse model with high density of plaques and tangles (3xTg), overexpression of LOX-5 led to a clear exacerbation of memory deficits and increased burdens of both *tau* and amyloid deposits.[57] Furthermore, 3xTg mice treated with the LOX-5 inhibitor zileuton (Figure 1.4) presented an improvement in memory, cognition, synaptic integrity and a reduction in amyloid and tau pathologies.[58] These findings suggest a functional role of LOX-5 in the AD-pathogenesis, pointing out the interest of LOX-5 inhibitors as valuable therapeutic agents, as they could reduce neuro-inflammation and the main AD-hallmarks, amyloid plaques and NFTs.[59, 55]

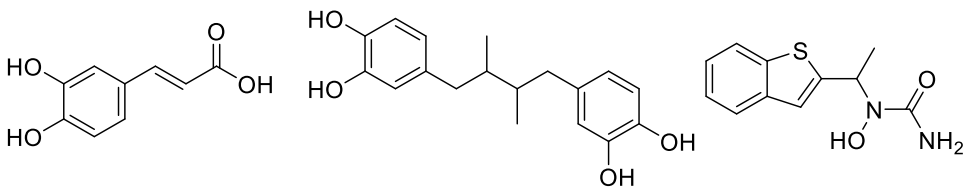

Caffeic acid NDGA Zileuton

Figure 1.4. Chemical structures of some LOX-5 inhibitors, caffeic acid, nordihydroguaiaretic acid (NDGA) and zileuton

Neurogenesis

Apart from Aβ and tau pathologies, AD is also characterized by a massive neuronal loss. The neuronal regeneration was thought to be restricted to embryonic development until 1962, when Altman showed neurogenic processes in the adult brain of rats.[60] However, the therapeutic potential of neurogenesis gained strength in the late 1990s when Eriksson *et al.* demonstrated neurogenesis in the brain of adult humans, pointing out that the hippocampus is able to develop and integrate new neuronal cells during adult life.[61] Adult neurogenesis is restricted to two brain niches, the subventricular zone (SVZ) lining the lateral ventricles and the subgranular zone (SGZ) in the dentate gyrus (DG) of hippocampus.[62] This process is sequential: activation of quiescent neural stem-cells (NSCs) and proliferation, migration to different areas of the CNS, differentiation and maturation to specific cell types, and integration in the brain circuitry (Figure 1.5). Neurogenesis modulates learning and memory integration processes and is sensitive to physiological, pathological and pharmacological stimuli. For instance, ageing, neurodegenerative, and some mental diseases are associated with an exponential decrease in hippocampal neurogenesis. Therefore, the controlled pharmacological stimulation of adult neurogenesis might counteract the age-related loss of memory and cognitive deterioration in pathological processes.[63,64] In this sense, a neurogenic inducer would induce the differentiation of NSCs into mature neurons capable to replace those lost by neurodegeneration, allowing the brain to recover its own self-renewal capacity. In this regenerative approach, a hopeful compound is the steroid allopregnanolone that has demonstrated to promote neurogenic processes and

reverse cognitive deficits in a mouse AD-model and that recently has completed phase-I studies.[65,66]

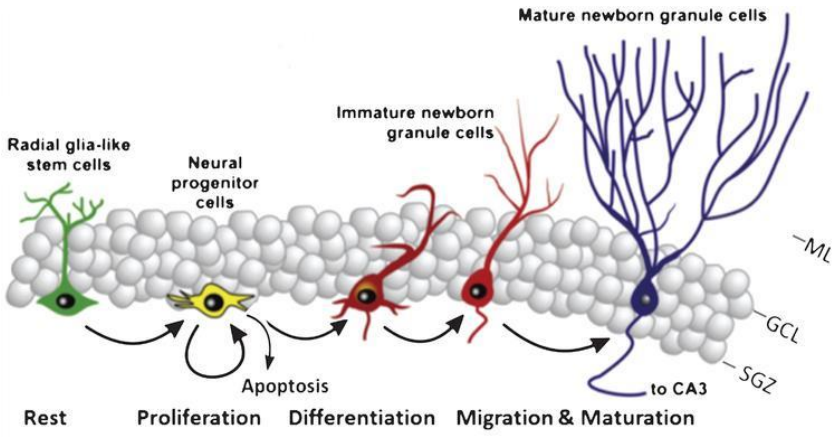

Figure 1.5. Schematic diagram illustrating the different phases of neurogenesis in the dentate gyrus (taken from Ref.[67])

In last years, numerous molecular targets and signalling cascades involved in neurogenesis have been identified and, as a consequence, different types of drugs have been evaluated in neuronal regeneration. For example, neurogenic properties have been found in MTRs' ligands, Nrf2 activators, antioxidants and anti-inflammatory agents.[68]

MT plasma levels decline along with age in a similar manner as the endogenous neurogenic rate does. Whether the two phenomena are related or not, remains unclear, albeit MT positively modulates hippocampal neurogenesis by increasing both precursor cell proliferation and survival in the hippocampi of aged mice.[69] Given that MT displays outstanding neurogenic activity, many research groups (including ours) have devoted many efforts aiming to identify new MT ligands and to study their molecular pathways.[70-73] Recently, we studied the effects *in vivo* of the MT analogue IQM316, developed in our group. We found that this compound is capable of inducing hippocampal neurogenesis in mice at a healthy and sustainable rate, preserving previous memories.[74,75]

In addition to its pivotal role in the endogenous defense, Nrf2 is an important player in the regulation of neurogenesis. Overexpression of Nrf2 and its downstream genes increased neuronal cell proliferation and differentiation in the human neuroblastoma cell line SH-SY5Y and in rat NSC-derived neurospheres.[20,21] The above data support the use of activators of the Nrf2-ARE signalling pathway as neurogenic agents for the treatment of ND. An example is the natural polyphenol resveratrol, which enhances hippocampal neurogenesis and the expression of many antioxidant defensive enzymes such as HO1, catalase, glutathione peroxidase, and superoxide dismutase.[76,77] Such resveratrol benefits could be achieved by regulating various protective signalling pathways, including Nrf2.[78]

Multi-Target-Directed Ligand strategy

In spite of the great advances in the knowledge of AD, nowadays there is no effective therapy to treat this multifactorial disorder. Only palliative drugs are available in the market, three inhibitors of acetylcholinesterase (AChE, donepezil, rivastigmine, and galantamine) and one antagonist of the *N*-methyl-D-aspartate receptor (memantine).[79] These drugs are mainly active in a single target and can hardly modify the progression of the disease.[79] This failure led to two new approaches to fight the multifactorial character of AD: multiple-medication therapy that is, the administration of a "cocktail of drugs", acting by diverse action mechanisms; and multiple-compound medication, that consists of joining different molecules administrated in the same pill. However, the possible interaction among the drugs administrated, has led to the development to multi-target-directed ligands paradigm (MTDLs). This approach is based on the design of molecules capable interact with several pharmacological targets involved in a given disease, minimizing adverse effect and improving pharmacokinetic and ADMET profile.[80-82] In the field of AD, the MTDLs must hit targets located upstream in the neurotoxic cascades to achieve maximum efficiency in stopping or delaying neurodegeneration.[83,84]

Nowadays, the MTDL approach is giving good results and in the last decade an increasing number of new MTD-drugs have been developed for the treatment of several complex diseases. In the field of NDs,[85] safinamide was approved in Europe in February 2015 and in

the United States in March 2017 for the treatment of Parkinson's disease (PD), due to its MTD-profile that combines dopaminergic (MAO-B and dopamine reuptake inhibition) and non-dopaminergic properties (blockade of voltage-dependent Na^+ and Ca^{2+} channels).[86]

OBJECTIVES AND WORK PLAN

In this chapter, the general objective was the design, synthesis and biological evaluation of new families of MTDLs with potential application in the treatment of AD. Our goal was the development of new molecules that were active in key targets related to OS and neuroinflammation, namely $MT_{1\text{-}3}$Rs, MAOs, LOX-5, and Nrf2. Furthermore, according to bibliographic precedents, neuroprotective and neurogenic properties were also expected.

For designing new prototypes, our inspiration came from natural or synthetic bioactive compounds with advantageous pharmacological profiles, namely MT, resveratrol and selegiline. As explained, the neurohormone MT is involved in a plethora of physiological processes, displaying anti-inflammatory, antioxidant, neurogenic and neuroprotective properties against toxic events related to neurodegenerative diseases.[87] Resveratrol is a potent Nrf2 inducer[77] and cinnamic derivatives, such as the well-known antioxidants ferulic and caffeic acids, are potent dual inhibitors of MT_3R (QR2) and LOX-5.[88-90] Selegiline is a selective MAO-B inhibitor with neuroprotective properties,[91] which is used to reduce symptoms in early-stages of PD.

Thus, the design of new MTD-families was based on the combination of fragments derived from the above-mentioned bioactive compounds, using classical medicinal chemistry strategies, such as bioisosterism and scaffold hopping.

In a previous work, we described the bioisosteric replacement of the acetamide group of melatonin by a series of reversed amides and azoles.[72] Among these azole derivatives, 5-(2-(5-methoxy-1*H*-indol-3-yl)ethyl)-1,3,4-oxadiazol-2(3*H*)-one (**1.1**) was the most potent partial agonist in the human MTRs, displaying the highest affinity for both *h*MT_1R and *h*MT_2R (K_i = 35, 4 nM, respectively). Moreover, this compound also showed potent neurogenic properties *in vitro*, better than MT itself, but it was predicted that **1.1** could not enter to the CNS according to the *in vitro* PAMPA-BBB assay.

Therefore, our first objective was to develop a new melatonin-based family that could improve pharmacokinetics of **1.1** and also incorporate additional activities in targets related to OS and neuroinflammation. For this purpose, we modified each part of the starting

molecule by: (i) adding different substituents in the *NH*-oxadiazolone, in special the propargyl group present in selegiline; (ii) the incorporation of a double bond in the linker; and (iii) the replacement of the indole by a dihydronaphthalene or naphthalene ring. The replacement of the above-mentioned aromatic scaffolds by benzene could produce the resveratrol-based MTDLs, in which we planned to incorporate structural fragments similar to those of the previous melatonin-based family. Like resveratrol, we also scheduled the introduction of hydroxyl groups into the benzene that could improve antioxidant properties (Figure 1.6).

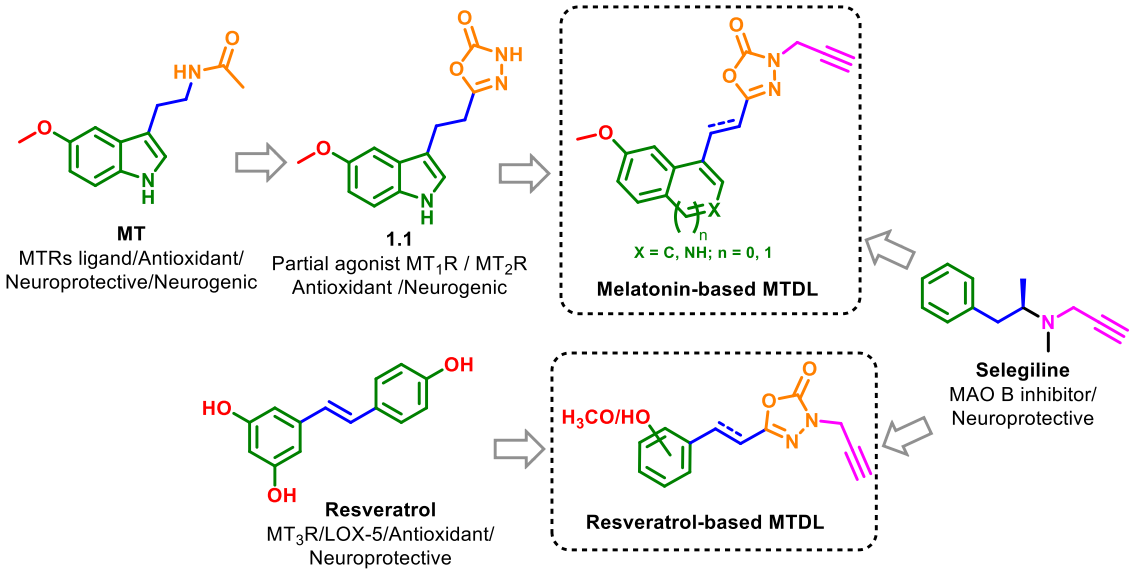

Figure 1.6. MTDL strategy design for the novel neurogenic and neuroprotective agents

The work plan was outlined as follows: (1) synthesis of proposed melatonin- and resveratrol-based families; (2) evaluation of new molecules in $MT_{1\text{-}3}R$, MAOs, LOX-5, and Nrf2; (3) measurement of their oxygen radical absorbance capacity and their probable permeability in the CNS; (4) study of the structure-activity relationship (SAR) in each biological target; (5) assessment of neurogenic properties in primary cultures of rat NSC; (6) neuroprotection studies in *in vitro* models of AD of increasing complexity.

RESULTS AND DISCUSSION

RESULTS AND DISCUSSION

Chemistry Results

Synthesis of 1,3,4-oxadiazole-2-one derivatives

Previously, we reported the synthesis of 5-(2-(5-methoxy-1*H*-indol-3-yl)ethyl)-1,3,4-oxadiazol-2(3*H*)-one (**1.1**) according to steps a-c depicted in Scheme 1.1.[72] The treatment of commercially available 5-methoxyindole with ethyl acrylate, catalyzed by anhydrous zirconium (IV) chloride ($ZrCl_4$)[92] at room temperature (rt), gave ethyl 3-(5-methoxy-1*H*-indol-3-yl)propanoate (**1.2**) in 71% yield. This intermediate was then transformed into the corresponding hydrazide **1.3** by a microwave (mw)-promoted hydrazinolysis in quantitative yield. Finally, the mw-heating of this hydrazide with 1,1'-carbonyldiimidazole (CDI) at 130 ºC for 25 min afforded the desired 1,3,4-oxadiazol-2-one **1.1** in 86% yield.

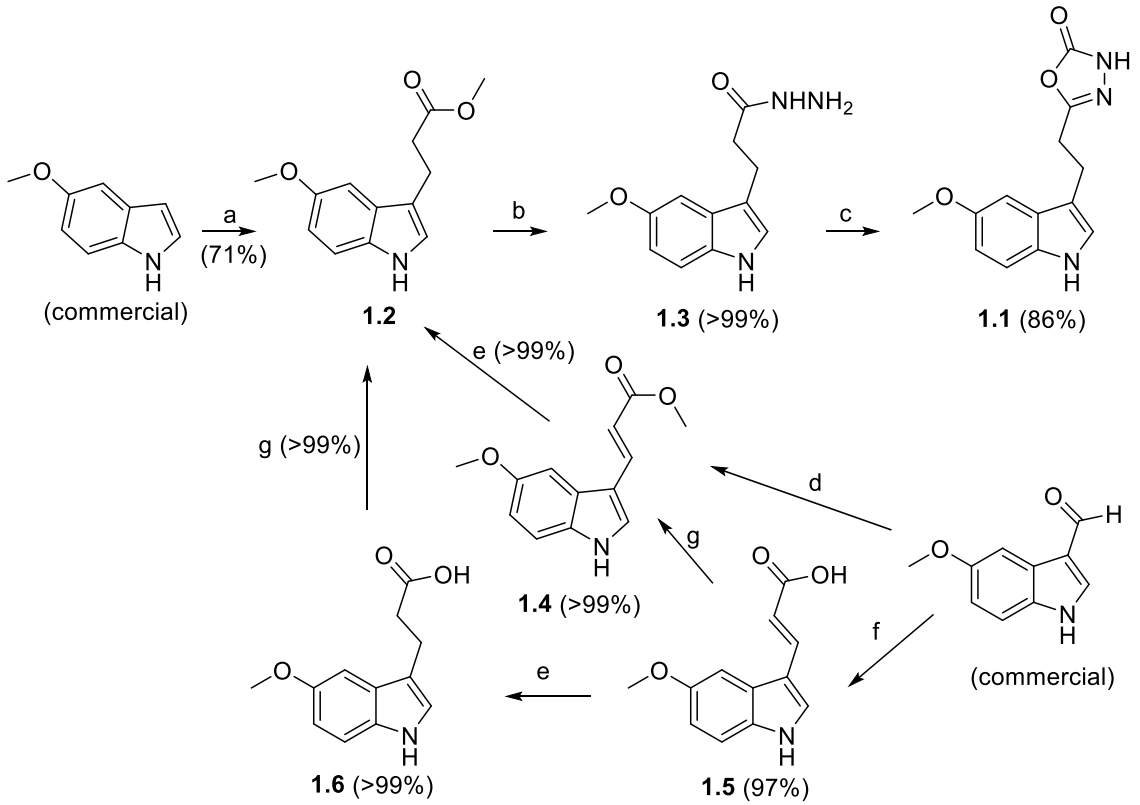

Scheme 1.1. Reagents and conditions. (a) Ethyl acrylate, $ZrCl_4$, DCM, rt; (b) $N_2H_4 \cdot H_2O$, mw, 150 °C, 45 min; (c) CDI, DMF, mw, 130 ºC, 25 min; (d) Methyl (triphenylphosphoranylidene)acetate, toluene, reflux, overnight; (e) H_2/Pd-C (5%), EtOH,

rt, overnight; (f) malonic acid, piperidine, pyridine, 70 ºC, overnight; (g) CH_3I, K_2CO_3, acetone, rt, overnight.

Following route a-c, **1.1** can be obtained in good overall yield (61%). However, in this work we explored two alternative ways for the synthesis of the intermediate ester **1.2**, to avoid the use of the toxic ethyl acrylate in the step a. In both routes, we used the commercially available 5-methoxy-1*H*-indole-3-carbaldehyde as starting material (Scheme 1.1).

A first approach consisted on a *Wittig* reaction, in which the 5-methoxy-1*H*-indole-3-carbaldehyde was reacted with methyl (triphenylphosphoranylidene)acetate in refluxing toluene overnight, yielding methyl 3-(5-methoxy-1*H*-indol-3-yl)acrylate **1.4** in quantitative yield. In the ^{1}H-NMR spectrum of this compound we observed that the alkene protons showed a coupling constant of 16.0 Hz, pointing out that the major species of this α,β-unsaturated ester was the (*E*)-isomer. Then, the double bond of derivative **1.4** was reduced using catalytic hydrogenation at rt overnight, yielding the saturated ester **1.2** in quantitative yield (Scheme 1.1, steps d and e).

Alternatively, ester **1.2** was obtained from 5-methoxy-1*H*-indole-3-carbaldehyde that was treated with malonic acid in basic media to generate the α,β-unsaturated acid **1.5**, by a *Knoevenagel-Doebner* reaction. Then, **1.5** was subjected to an esterification by treatment with potassium carbonate (K_2CO_3) and methyl iodide (CH_3I), giving **1.4** in quantitative yield. Subsequently, reduction of **1.4** with hydrogen and palladium over charcoal at 5% [Pd-C (5%)] provided **1.2** in quantitative yield (Scheme 1.1, steps f-g-e). Otherwise, **1.5** was hydrogenated to yield the saturated acid **1.6** and finally esterified to the ester **1.2** (Scheme 1.1, steps e-g).

Despite these new synthetic alternatives to synthetize the ester **1.2** consisted of 2 or 3 synthetic steps and the use of the toxic CH_3I, the global yield was improved in whatever of these pathways.

Saturated ester **1.2** was then transformed into the hydrazide **1.3** (quantitative yield) by treatment with hydrazine hydrate ($N_2H_4 \cdot H_2O$) under mw irradiation at 150 ºC during 45 min. Such hydrazide derivative was cyclized in an mw oven at 130 ºC for 25 min in the presence of CDI to obtain **1.1** in high yield (86%) (Scheme 1.1).

Structural modifications in the oxadiazolone ring of derivative 1.1

Alkylation of the *NH*-group in the oxadiazolone ring of **1.1** was carried out by an mw-assisted bimolecular nucleophilic substitution (S_N2) (120 ºC, 10 min), using the corresponding alkyl halide or alkyl tosylate, to afford derivatives **1.7–1.20**. Initially, dimethylformamide (DMF) was used as solvent, obtaining moderated yields (60-70%). However, the replacement of DMF by acetone improved considerably the yields (80–90%) because of its easier elimination from the crude of reaction (Scheme 1.2, step a).

Not available alkyl halides were replaced by alkyl tosylates (**1.21** and **1.22**), which were synthesized from the corresponding commercial alcohol and tosyl chloride (TsCl) under basic conditions in high yields (Scheme 1.2, step b).

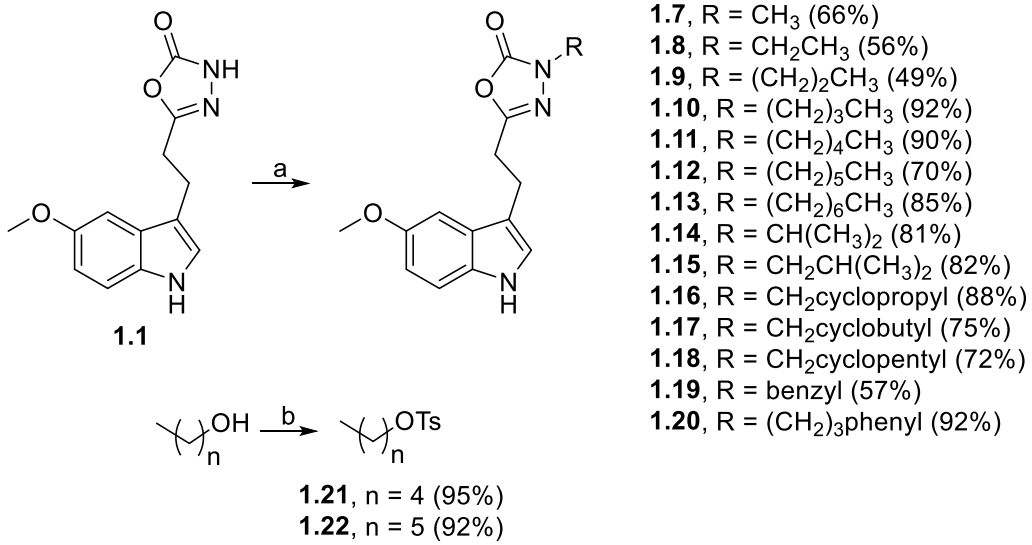

Scheme 1.2. Reagents and conditions. (a) K_2CO_3, acetone, RX or R-OTs, mw, 120 ºC, 10 min; (b) TsCl, DMAP, TEA, DCM, rt, overnight.

On the other hand, the carbonyl group of the oxadiazolone ring of **1.1** was replaced by methyl or ethyl amine. Treatment of **1.1** with (benzotriazol-1-yloxy)tris(dimethylamino)phosphonium hexafluorophosphate (BOP), triethylamine (TEA) and either methyl- or ethylamine in DMF, yielded the corresponding oxadiazol-2-amine **1.23** and **1.24**, respectively. In general, the reaction conversions were satisfactory, although we had some difficulties in the isolation and purification of the products that eventually led to low yields (18 and 6%) (Scheme 1.3). Due to such synthetic difficulties and to the fact that resulting compounds didn't improve biological activities as explained below, we decided to continue with the design and synthesis of other different derivatives.

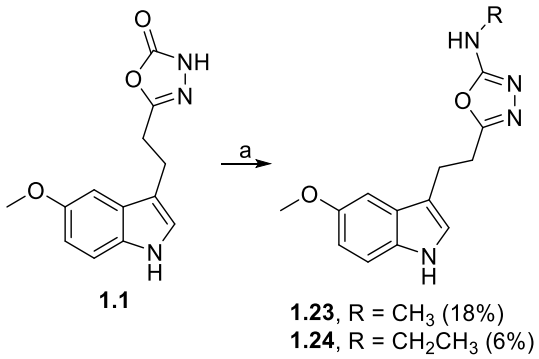

Scheme 1.3. Reagents and conditions. (a) RNH_2, BOP, TEA, DMF, rt, overnight

Linker Modification

Introduction of the conjugated double bond required a different approach in the synthetic strategy, because the treatment of the α,β-unsaturated ester **1.4** with $N_2H_4 \cdot H_2O$ in EtOH (same conditions as Scheme 1.1, step b) afforded a complex mixture of compounds. In such mixture we identified by HPLC-MS the pyrazolidinone **1.25** as the result of a sequential hydrazinolysis and an undesired Michael-type cyclization, as previously described by Zhang *et al.*[93] (Scheme 1.4, step a). For this reason, we decided to activate first the unsaturated acid with hydroxybenzotriazole (HOBt) and *N*-(3-dimethylaminopropyl)-*N*′-ethylcarbodiimide hydrochloride (EDC·HCl) as coupling agents, and a catalytic amount of 4-dimethylaminopyridine (DMAP) (rt, 1 - 3 h). Then, the addition of $N_2H_4 \cdot H_2O$ yielded the

hydrazide **1.26** in quantitative yield. It is worth-mentioning that the order of addition of the reagents is crucial for obtaining the desired intermediate **1.26** in high yield.

Once the hydrazide is formed, cyclization occurred under the same conditions of procedure c in Scheme 1.1 to afford compound **1.27** in good yield (85%) (Scheme 1.4)

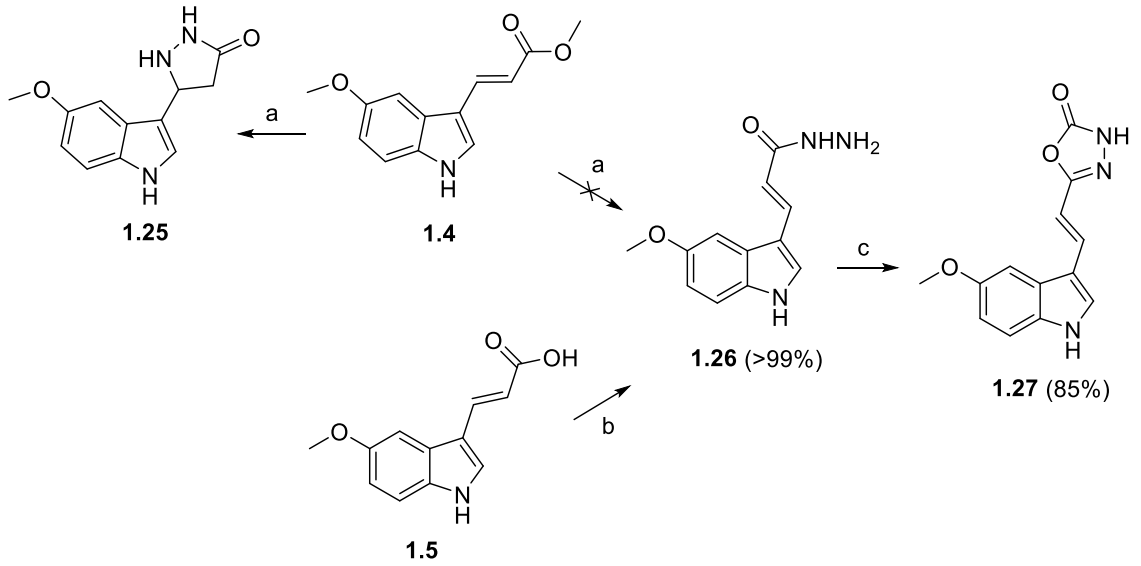

Scheme 1.4. Reagents and conditions. (a) $N_2H_4 \cdot H_2O$, mw, 150 °C, 45 min; (b) i. EDC·HCl, HOBt, DMAP, ACN; ii. $N_2H_4 \cdot H_2O$, rt.; (c) CDI, DMF, mw, 130 ºC, 25 min.

Introduction a methyl group in *alpha*-position with respect to the ester, was carried out from the commercially available 5-methoxy-1*H*-indole-3-carbaldehyde and (carbethoxyethylidene)triphenylphosphorane by a *Wittig* reaction, giving the corresponding α,β-unsaturated ester **1.28** in high yields (95%). Then, **1.28** was reduced by catalytic hydrogenation to the saturated ester **1.29**, followed by its transformation into the corresponding hydrazide and further cyclization to yield compound **1.30** in 48% yield (Scheme 1.5).

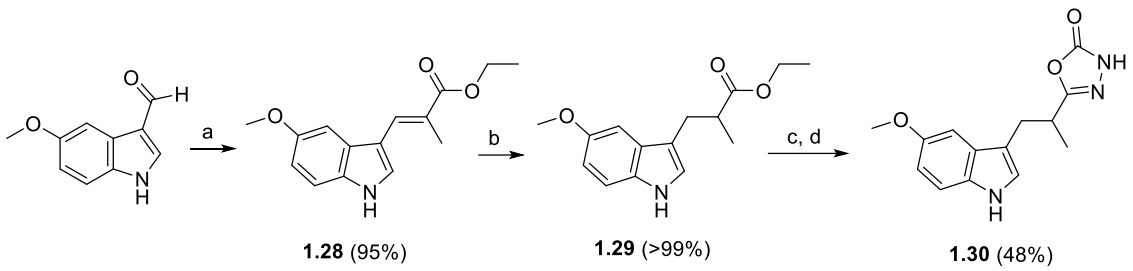

Scheme 1.5. Reagents and conditions. (a) (Carbethoxyethylidene)triphenylphosphorane, DCM, reflux, overnight; (b) H_2/Pd-C (5%), EtOH, rt, overnight; (c) $N_2H_4 \cdot H_2O$, mw, 150 °C, 45 min; (d) CDI, DMF, mw, 130 ºC, 25 min.

The synthesis of derivatives with the methyl group in the *beta*-position was attempted from the commercial 5-methoxyindole using different routes, all of them with unsuccessful results. Firstly, starting indole was transformed into 1-(5-methoxy-1*H*-indol-3-yl)ethan-1-one (**1.31**) (Scheme 1.6, step a) by the treatment with acetyl chloride in the presence of the Lewis acid $AlCl_3$. In order to avoid indole polymerization, nitromethane (CH_3NO_2), was added as cosolvent, moreover, increasing the solubility of the solid indole-Lewis acid complex in the reaction media, minimizing the reaction time and improving yields due to its strong solvent effect.[94]

However, the indole methyl ketone **1.31** did not react either through the *Knoevenagel-Doebner* or the *Wittig* reaction toward the desired intermediates (Scheme 1.6, steps b or c, respectively), even using higher temperatures and reaction times. These failures clearly contrast with the synthesis of compound with the methyl group in the *alpha*-position (**1.30**), which was successfully obtained by a *Wittig* reaction. These differences could be expected due to the decrease in the electrophilic character of keto group compared to aldehyde.

Taking into account the tendency of N*H*-indoles to polymerize in the presence of a Lewis acid,[95] we studied the overnight reaction of 5-methoxyindole with $ZrCl_4$ at rt, which gave the biindole derivative **1.32** in 53% yield (Scheme 1.6).

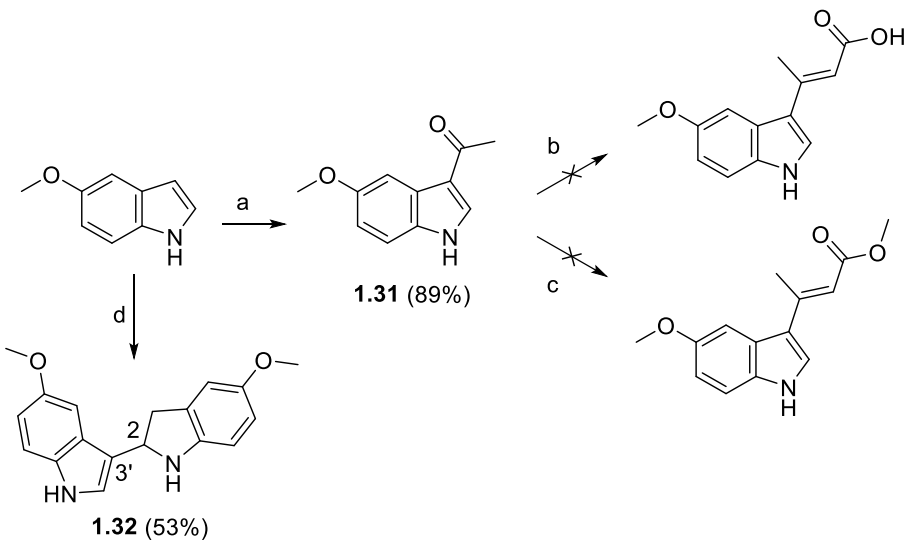

Scheme 1.6. Reagents and conditions. (a) Acetyl chloride, $AlCl_3$, CH_3NO_2, DCM; (b) Malonic acid, piperidine, pyridine, reflux, 2 days; (c) Methyl (triphenylphosphoranylidene)acetate, toluene, reflux, 5 days; (d) ethyl acrylate, $ZrCl_4$, DCM, N_2, rt.

From ^{1}H and ^{13}C NMR spectra of **1.32** we deduced a dimeric structure in which an indole and an indoline were directly linked. However, the binding positions between both rings were not completely clear, even after analysing the HSQC and HMBC two-dimensional experiments. For this reason, we crystallized **1.32** that was subjected to an X-ray analysis, which demonstrated that it was the racemic mixture of 5,5'-dimethoxy-2,3-dihydro-1*H*,1'*H*-2,3'-biindole (Figure 1.7).

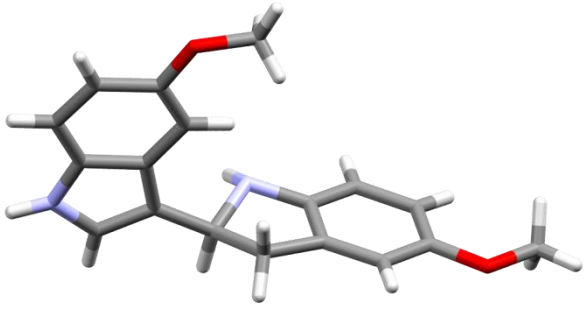

Figure 1.7. Structure of **1.32** by X-ray analysis

This dimerization behaviour of *NH*-indole is not surprising, because it has previously been described with other Lewis acids (e.g. $BiCl_3$, $SnCl_4$, $InCl_3$)[95,96] or by direct treatment with acidic medium (TsOH or HCl).[97-99]

CORE MODIFICATION

Naphthalene and dihydronaphthalene derivatives

Indole scaffold replacement by either a dihydronaphthalene or naphthalene ring was carried out from 7-methoxy-1-tetralone by two different synthetic routes.

Firstly, commercial 7-methoxy-1-tetralone was treated with a solution of methyl magnesium iodide (CH_3MgI) in ether at rt for 3 h to afford the corresponding alcohol (non-isolated intermediate), which was treated with HCl to yield the dihydronaphthalene **1.33** in quantitative yield.[100] Aromatization of **1.33** with 2,3-dichloro-5,6-dicyano-1,4-benzo-quinone (DDQ) led to 1-methyl-7-methoxy-1-methylnaphthalene **1.34** in high yield (95%).[101] Oxidation of the methyl group at position 1 of compound **1.34** to aldehyde was attempted using bromine (Br_2) and DMSO (Scheme 1.7, step c), testing different number of equivalents and times of reaction. However, in all cases we isolated a mixture of the desired 1-naphthaldehyde **1.35** and the corresponding 8-bromo-1-naphthaldehyde **1.36**, as much with 20% yield each.[102]

Given such poor yields, a new strategy was attempted from dihydronaphthalene **1.33**, by introduction of the aldehyde in allyl position with selenium dioxide (SeO_2) to obtain aldehyde **1.37**.[103] However, due to the easy aromatization of dihydronaphthalene, a low yield was obtained under these oxidative conditions, giving a mixture of dihydronaphthalene **1.37** and naphthalene **1.35** in 25% and 20% yields, respectively (Scheme 1.7, step d).

Then, we planned to transform the dihydronaphthalene derivative **1.37** into the unsaturated acid **1.38** by the treatment with malonic acid in *Knoevenagel-Doebner* conditions, obtaining unexpected ^1H- and ^{13}C-NMR data for the isolated product. A deeper NMR

analysis (COSY, HSQC, and HMBC) demonstrated that this structure corresponded to lactone **1.39**, formed under basic conditions (piperidine and pyridine treatment, Scheme 1.7, step e) by an intramolecular cyclization. Carboxylate group attacked the intracyclic double bond forming the enol intermediate, which developed to lactone **1.39**, as shown in Scheme 1.7. Nevertheless, given that in solution this cyclization is an equilibrium, acid activation was possible after treatment with coupling reagents (EDC·HCl, HOBt). Further treatment with $N_2H_4 \cdot H_2O$ and CDI, led to the desired dihydronaphthalene-based oxadiazolone **1.40**, although in low yield (15%), probably due to the easy aromatization that gave also the corresponding naphthalene (non-isolated).

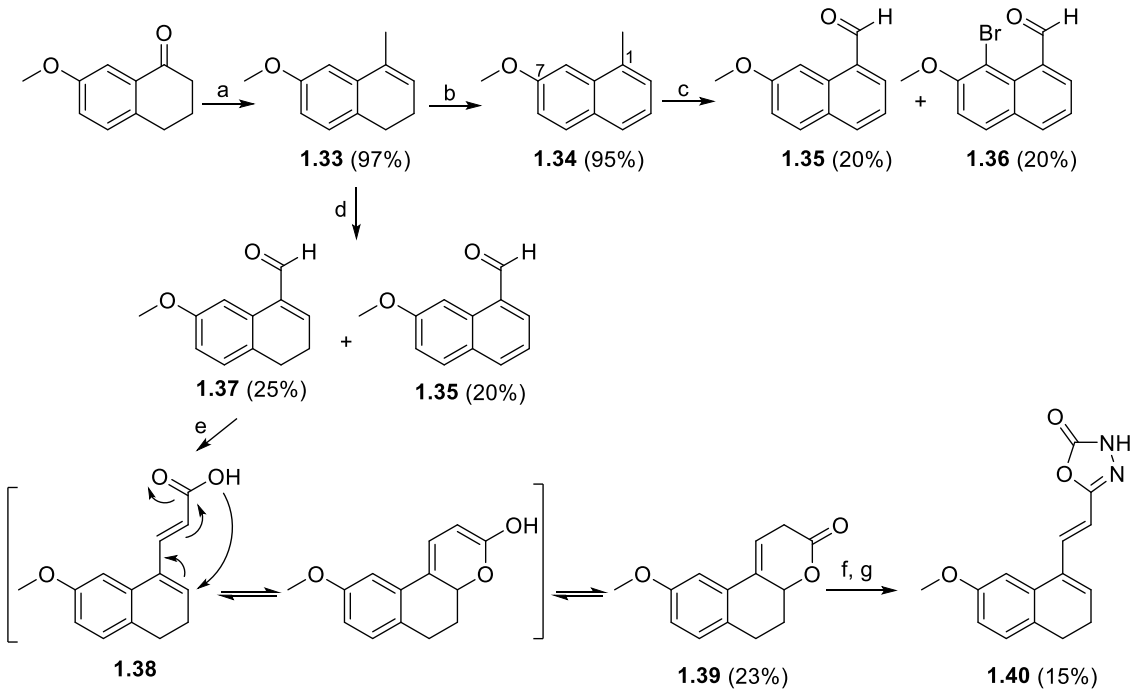

Scheme 1.7. Reagents and conditions. (a) i. CH_3MgI, Et_2O, 3 h, rt, ii. HCl 2 M; (b) DDQ, DCM, rt, 10 min; (c) Br_2, DMSO, dioxane; (d) SeO_2, EtOH:H_2O 10:1; (e) Malonic acid, piperidine, pyridine, 70 ºC, overnight; (f) i. EDC·HCl, HOBt, DMAP, ACN, ii. $N_2H_4 \cdot H_2O$, rt; (g) CDI, DMF, mw, 130 ºC, 25 min.

Aiming to improve the yield of the oxadiazolone derivative with a dihydronaphthalene core **1.40**, another alternative synthetic route was explored. 7-Methoxy-1-tetralone was reacted with trifluoromethanesulfonic anhydride (Tf_2O) and 2-chloropyridine as base to yield the vinyl triflate **1.41** in good yield (78%)[104] (Scheme 1.8, step a).

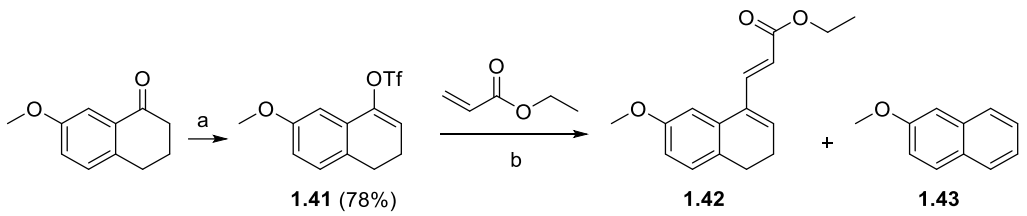

Scheme 1.8. Reagents and conditions. (a) Tf_2O, 2-chloropyridine, DCM, 2 h, rt; (b) $Pd(PPh_3)_2Cl_2$, ethyl acrylate, TEA, mw, 105 ºC, 15 min.

The introduction of an α,β-unsaturated ester was carried out by olefination of vinyl triflates under palladium-catalyzed conditions (Heck reaction, Scheme 1.8, step b), using ethyl acrylate and TEA (3.5 equiv) as base. Since first attempts to obtain **1.42** in good yields failed, different conditions (catalyst, ligand, temperature, time…) were evaluated and major subproducts were isolated and characterized, as explained in table 1.1. In the presence of triphenylphosphine (PPh_3), 2-methoxynaphthalene (**1.43**) was formed as main product, whereas only 10% of the desired ester **1.42** was observed by HPLC-MS (Table 1.1, entries 1-5). When reactions were performed without PPh_3 better conversions of **1.42** were obtained, although in all cases starting material **1.41** was also detected. Optimized conditions for the synthesis of **1.42**, resulted from the use of bis(triphenylphosphine)palladium (II) dichloride ($Pd(PPh_3)_2Cl_2$), as catalyst and mw irradiation at 105 ºC for 15 min, obtaining the desired ester derivative in 87% isolated yield (Table 1.1, entry 10).

Table 1.1. Experimental conditions probed in the synthesis of **1.42**.

Entry	Catalyst (equiv)	Ligand (equiv)	Acrylate equiv	Conditions T (ºC), t (min)	Conversions (%)
1	[a]$Pd(OAc)_2$ (5 mol%)	PPh_3 (3 equiv)	2.2	mw 140 ºC, 30 min	**1.42**: 10% **1.43**: >80%
2	[a]$Pd(OAc)_2$ (5 mol %)	PPh_3 (0.5 equiv)	2.2	1) mw 140 ºC, 15 min 2) mw 140 ºC, 30 min	**1.42**: 10% **1.43**: >80%
3	[a]$Pd(OAc)_2$ (5 mol %)	PPh_3 (0.5 equiv)	2.2	mw 120 ºC, 30 min	**1.42**: 10% **1.43**: >80%
4	[a]$Pd(OAc)_2$ (5 mol %)	PPh_3 (3 equiv)	2.2	mw 120 ºC, 15 min	**1.42**: 10% **1.43**: >80%
5	$Pd(PPh_3)_2Cl_2$ (2.2 mol %)	PPh_3 (10 mol %)	2.2	mw 140 ºC, 30 min	**1.42**: 10% **1.43**: >80%
6	[b]$Pd(PPh_3)_2Cl_2$ (5 mol %)	none	2.2	1) 80 ºC, overnight 2) mw 130 ºC, 39 min	**1.42**: 38% **1.41**: 31%
7	$Pd(PPh_3)_2Cl_2$ (2.2 mol %)	none	2.2	mw 140 ºC, 30 min	**1.42**:15%
8	$Pd(PPh_3)_2Cl_2$ (2.2 mol %)	none	3.0	mw 130 ºC, 15 min	**1.42**:10%
9	$Pd(PPh_3)_2Cl_2$ (2.2 mol %)	none	2.2	mw 100 ºC, 10 min	**1.42**: 32% **1.41**: 68%
10	$Pd(PPh_3)_2Cl_2$ (2.2 mol %)	none	2.2	mw 105 ºC, 15 min	**1.42**: 89% **1.41**: 11%

[a]Conditions adapted from Ref.[105] [b]Conditions adapted from Ref. [106]

Then, ester **1.42** was hydrolyzed under basic condition with lithium hydroxide (LiOH) followed by acid treatment with HCl to obtain the corresponding acid. This acid was not isolated but transformed to the corresponding hydrazide, followed by cyclization with CDI to afford the final dihydronaphthalene-based oxadiazolone **1.40** in low yields (21%) due to its easy aromatization. In fact, the aromatic analogue was detected by HPLC (Scheme 1.9).

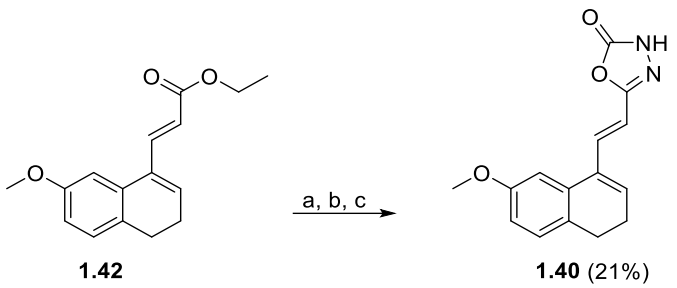

1.42 **1.40** (21%)

Scheme 1.9. Reagents and conditions. (a) i. LiOH, THF:H_2O 1:1, rt, overnight; ii. 1 M HCl; (b) i. EDC·HCl, HOBt, DMAP, ACN, ii. $N_2H_4 \cdot H_2O$, rt; (c) CDI, DMF, mw, 130 ºC, 25 min.

Given that the best yields were obtained using the second synthetic route (triflate formation, followed by Heck coupling), this strategy was applied for synthesis of naphthalene derivatives **1.51** and **1.52** (Scheme 1.10).

The conditions previously used in the synthesis of the vinyl triflate **1.41** (Scheme 1.8) were extended to the dimethoxylated derivative **1.44** (Scheme 1.10, step a). However, this derivative was obtained with low yields due to the formation of several by-products, probably due to the lesser electrophilic character of the carbonyl group. According to bibliographic precedents, this yield could be improve using bulkier bases, such as 2,6-lutidine[107] or 2,6-di-tert-butylpyridine.[108] Aromatization of triflates **1.41** and **1.44** with DDQ at rt, led to naphthalenes **1.45** and **1.46**, respectively (Scheme 1.10, conditions b). Then, the ethyl acrylic moiety was introduced by a Heck reaction,[109] treating the corresponding triflate with ethyl acrylate in the presence of palladium (II) acetate ($Pd(OAc)_2$) as catalyst, 1,10-phenanthroline as ligand and TEA as base, to yield the corresponding esters **1.47** and **1.48** in high yields (90 and 81%, respectively).

As mentioned before (Scheme 1.9, step a), methoxy and dimethoxy esters were hydrolyzed under basic conditions, obtaining acids **1.49** and **1.50**, in quantitative yields. Acids were transformed into the corresponding hydrazides, followed by cyclization to afford final compounds **1.51** and **1.52** in good yields. (91 and 85%, respectively).

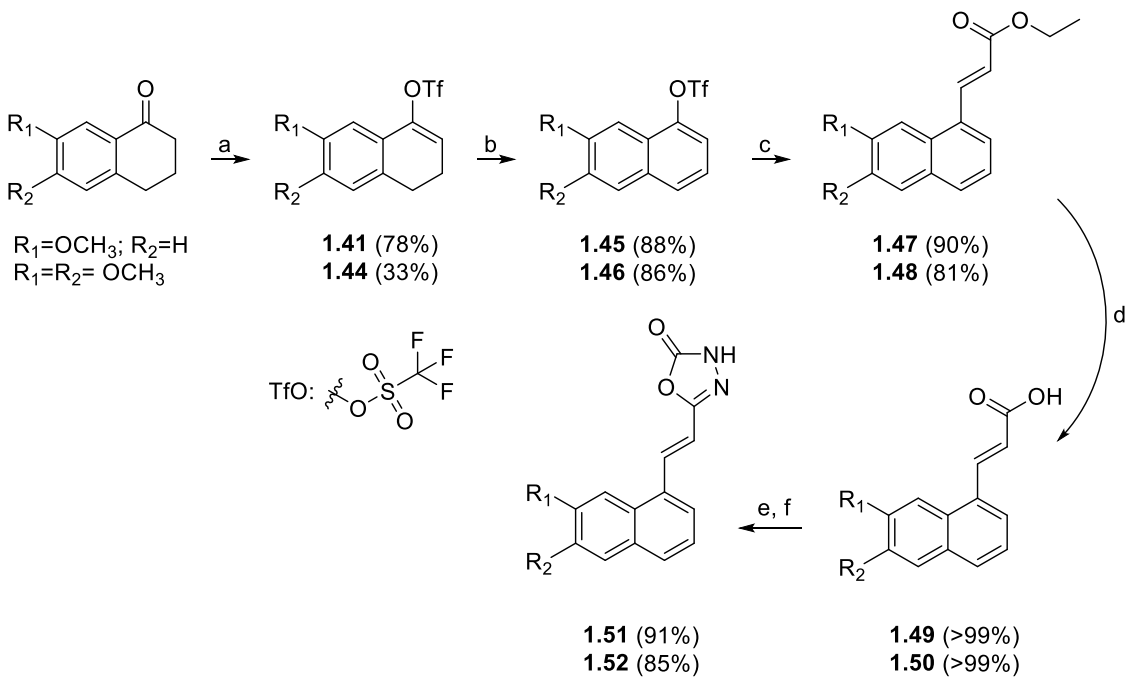

Scheme 1.10. Reagents and conditions. (a) Tf_2O, 2-chloropyridine, DCM, rt, 2 h; (b) DDQ, DCM, rt, 10 min; (c) ethyl acrylate, $Pd(OAc)_2$, 1,10-phenanthroline, DMF, mw, 150 ºC, 1 h; (d) i. LiOH, THF:H_2O 1:1, rt, overnight; ii. 1 M HCl; (e) i. EDC·HCl, HOBt, DMAP, ACN; ii. $N_2H_4 \cdot H_2O$, rt; (f) CDI, DMF, mw, 130 ºC, 25 min.

Resveratrol-like derivatives

Next, we performed the replacement of the aromatic scaffold by a phenyl ring, with the aim of obtaining resveratrol-like derivatives. The synthesis was carried out from cinnamic acids, bearing functional groups (methoxy, hydroxyl, nitrile, nitro and amino) in different positions of the cycle. Many of these starting acids were commercially available, whereas non-commercial acids (**1.53** and **1.54**) were synthetized from the corresponding aldehyde by a *Knoevenagel-Doebner* reaction in high yields (Scheme 1.11, step a). Then, acids were transformed into the corresponding α,β-unsaturated hydrazides (**1.55**–**1.65**) in quantitative yields, which were used without further purification. Subsequent cyclocondensation of these hydrazides in presence of CDI under mw irradiation gave the corresponding 1,3,4-

oxadiazole-2-one heterocycle (**1.66**–**1.76**) in good yields (54–94%, yields of both steps) (Scheme 1.11).

Otherwise, conversion of cinnamic acids to the corresponding saturated 3-phenylpropanoic acids took place by hydrogenation in quantitative yields, using H_2 with Pd-C 5% (Scheme 1.11, step d). Then, same conditions for the hydrazide formation and the final cyclization as in the saturated analogues were used to give final saturated **1.86** – **1.90** in good yields (Scheme 1.11, steps b, c).

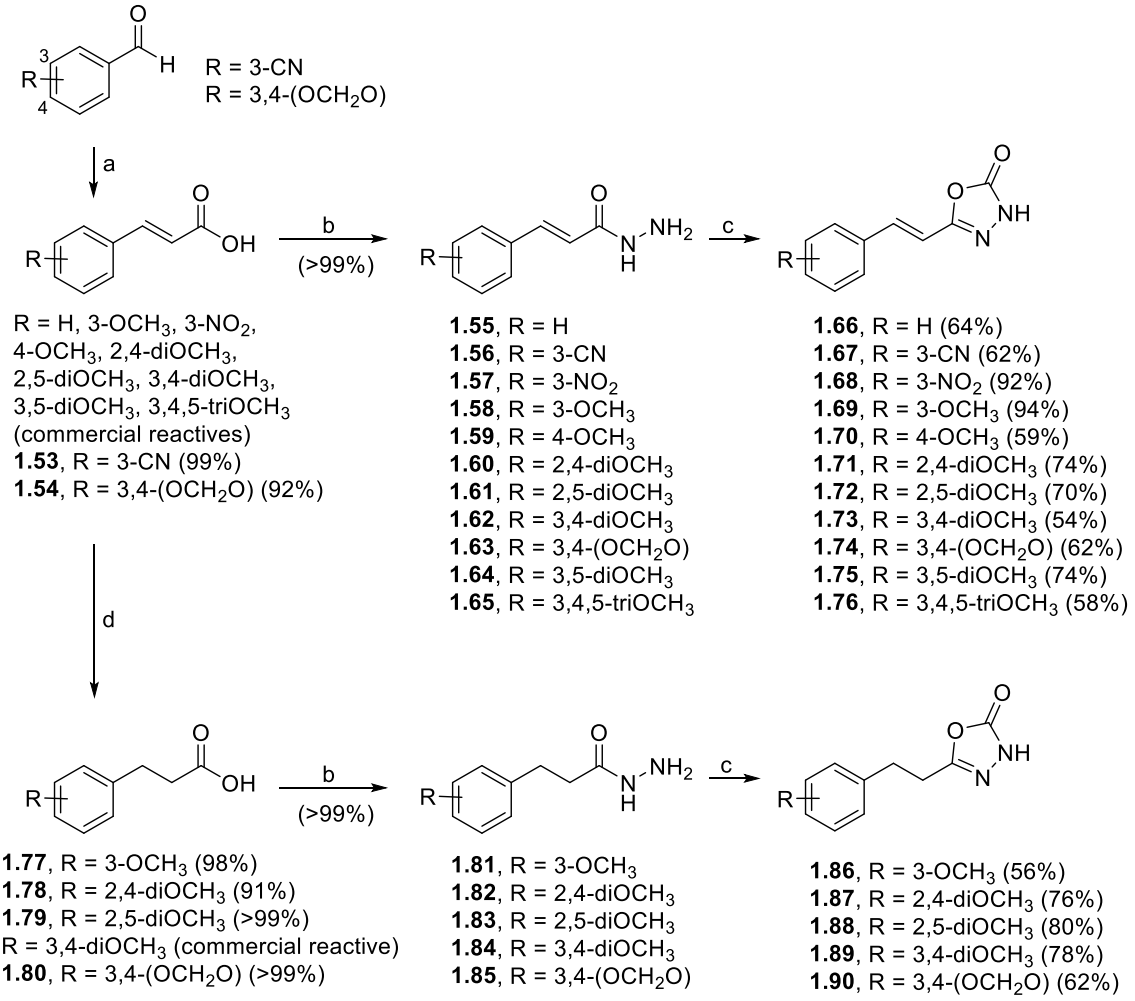

Scheme 1.11. Reagents and conditions. (a) Malonic acid, piperidine, pyridine, 70 ºC, overnight; (b) i. EDC·HCl, HOBt, DMAP, ACN, rt; ii. $N_2H_4 \cdot H_2O$, rt; (c) CDI, DMF, mw, 130 ºC, 25 min; (d) H_2/Pd-C (5%).

Hydroxylated derivatives **1.91**–**1.97** were obtained via deprotection of the corresponding methoxylated compounds, by treatment with boron tribromide (BBr_3) in DCM at rt overnight. For achieving good yields in these transformations (63-96%) it was necessary to use one BBr_3 equivalent for each ether group to be cleavage plus an additional equivalent for each heteroatom present in the molecule, due to the well-known complexation ability of the boron atom.[110,111] But using the same reaction conditions, the deprotection of compounds containing a methoxy group at position 2 (namely **1.71** and **1.72**) did not lead to good results, although different conditions were tested. Desired products were identified in the crude of reaction by HPLC-MS but were not isolated from the chromatography column, probably due to the facile oxidation to the corresponding quinones. The only 2,5-dihydroxyl compound that could be isolated was **1.96**, although in poor yields (16%) (Scheme 1.12).

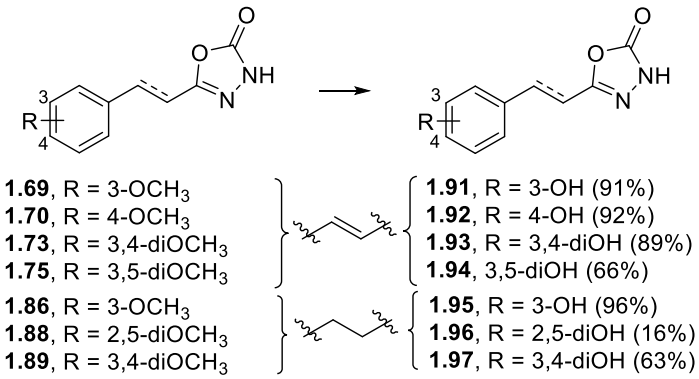

Scheme 1.12. Reagents and conditions. BBr_3, DCM, rt, overnight.

Compound **1.98**, containing one amino group at *meta* position was synthesized in high yield (87%) by the reduction of the nitro derivative **1.68**, using iron-ammonium chloride in neutral medium (Scheme 1.13).[112]

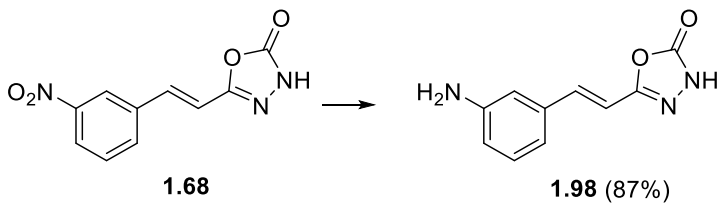

Scheme 1.13. Reagents and conditions. Fe/NH_4Cl, EtOH, reflux 1 h.

Substitution of the methoxy by allyloxy group at position *meta*- was carried out by a *Williamson* alkylation of the 3-hydroxy derivative with allyl bromide under mw irradiation and acetone as solvent. Under these conditions, three compounds were obtained: the desired product of the *O*-allylation (**1.99**, 49% yield); the product of an aldolic condensation between the aldehyde and acetone (**1.100**, 4% yield); and the product of both reactions (**1.101**, 6% yield). Aldolic condensation could be the result of a higher pressure and traces of water present in the mw vial. Then, aldehyde **1.99** led to the acid **1.102** by a *Knoevenagel* reaction, which by treatment with hydrazine hydrate followed by cyclization in the presence of CDI gave the final compound **1.104** (Scheme 1.14).

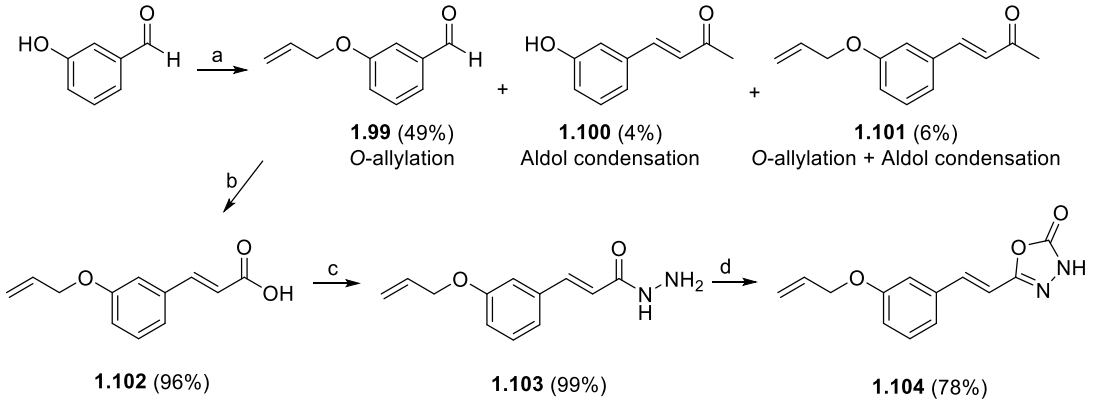

Scheme 1.14. Reagents and conditions. (a) Allyl bromide, K_2CO_3, acetone, mw, 140 ºC, 20 min; (b) malonic acid, piperidine, pyridine, 70 ºC, overnight; (c) i. EDC·HCl, HOBt, DMAP, ACN, rt, 3 h, ii. $N_2H_4 \cdot H_2O$; (d) CDI, DMF, mw, 130 ºC, 25 min.

Introduction of the propargyl group in cinnamic derivatives **1.66**, **1.69**, **1.70**, **1.91** and indole derivative **1.27** was developed by alkylation of the NH group of the oxadiazole under the same conditions as Scheme 1.2 (K_2CO_3, acetone, mw, 120 ºC, 10 min or rt overnight) to afford the final compounds **1.105–1.109**, in moderate to good yields. Alkylation of hydroxylated derivative **1.91**, led to compound **1.108** in 44% of yield. This reaction was carried out at rt in order to avoid possible secondary reactions through the hydroxyl group (Scheme 1.15).

It is worthy to note the low yield achieved (17%) for the indole derivative **1.109**. In this case the (*E*)-isomer was not as favored as in phenyl derivatives, complicating the isolation from its (*Z*)-isomer, which was identified by HPLC-MS. In fact, the purification was attempted by flash chromatography in conventional (hexane:EtOAc) and reverse phase (H_2O:ACN) with limited success. Only semipreparative HPLC allowed the isolation of the (*E*)-isomer of **1.109** with high purity (Scheme 1.15).

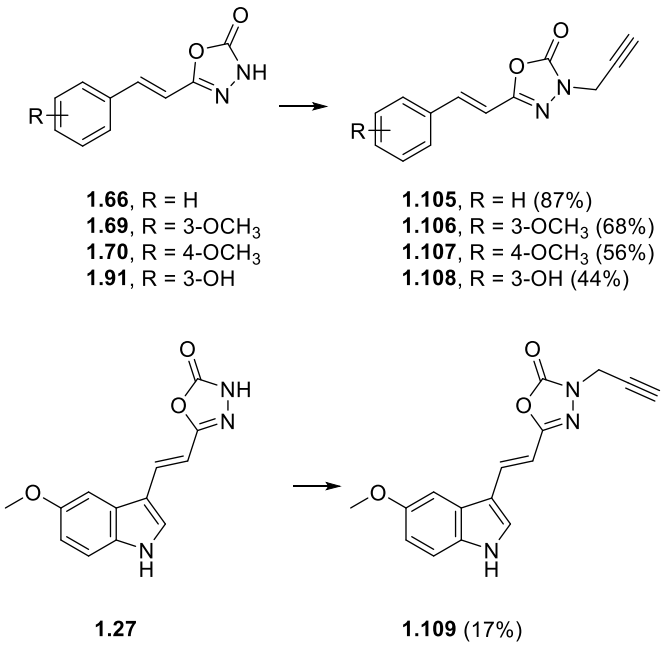

Scheme 1.15. Reagents and conditions. K_2CO_3, acetone, mw, 120 ºC, 10 min or rt overnight.

Replacement of oxadiazolone by amide or amine

Amides

Bioisosteric replacement of the oxadiazolone ring by an amide group was carried out from either acid **1.53** (Scheme 1.11), or commercially available 3- or 4-methoxycinammic acids by condensation with propargyl or allyl amine under the same conditions as Scheme 1.4, step b (Scheme 1.16, step a).

5-Methoxyindole derivatives (**1.117** and **1.118**) were synthesized from acid **1.5** (Scheme 1.1) using same above-mentioned procedure, although lower yields were obtained. (Scheme 1.16, conditions a).

N-Methylation of amide **1.111**, using sodium hydride (NaH) and CH_3I gave tertiary amide **1.113** in good yield. At rt and using MeOD as solvent, the 1H-NMR spectrum showed a mixture of rotamers in a proportion of 1:0.7. Signal rotamers were solved by a temperature gradient, employing DMSO-d_6 as solvent.

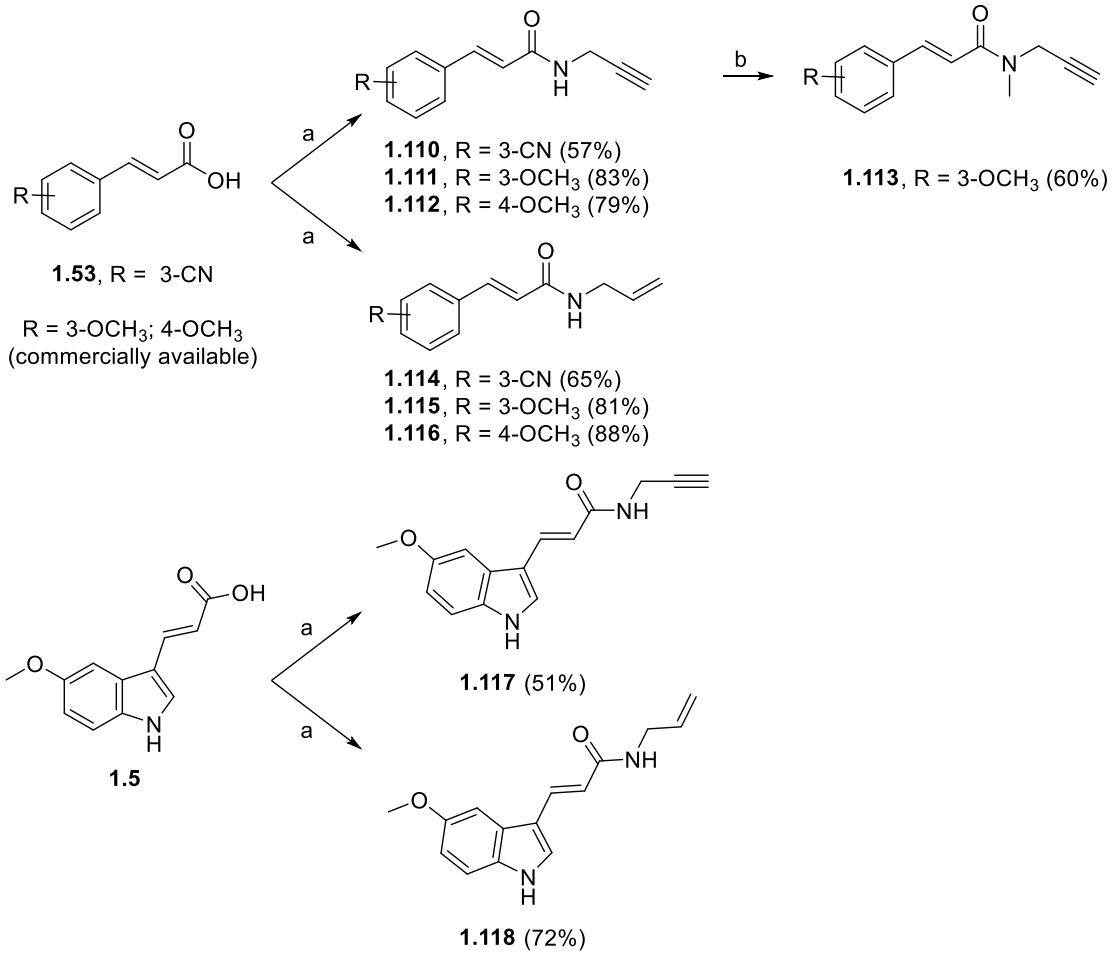

Scheme 1.16. Reagents and conditions. (a) i. EDC·HCl, HOBt, DMAP, ACN, rt; ii. Corresponding amine; (b) i. NaH, THF, -20 ºC to rt; ii. CH_3I, rt, overnight.

Deprotection of methoxylated allylamides **1.115** and **1.116** by treatment with BBr_3 at rt overnight gave the desired hydroxyl compounds **1.119** and **1.120** in good yields (Scheme 1.17).

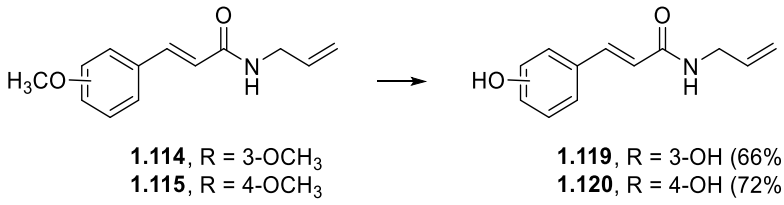

Scheme 1.17. Reagents and conditions. BBr_3, DCM, rt, overnight.

However, demethylation of the alkyne analogues did not afford the desired product in good yield and, only a 20% of conversion was detected by HPLC-MS. This could be due to the fact that bromoboration of terminal alkynes leads to (*Z*)-(2-bromo-1-alkenyl)dibromoboranes via Markovnikov *cis*-addition of bromo-boron to terminal triple bond stereo- and regioselectively by kinetic control, as previously described (Scheme 1.18).[113-115]

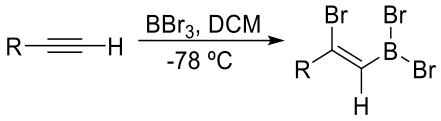

Scheme 1.18. Bromoboration of terminal alkynes.

Given that demethylation of alkyne derivatives was not possible by treatment with BBr_3, condensation with propargylamine was carried out directly with the commercially available acids with free hydroxyl groups. Although the conversion was not as good as in methoxylated derivatives and more subproducts were formed, the desired phenols **1.121 – 1.124** were isolated in good yields (Scheme 1.19).

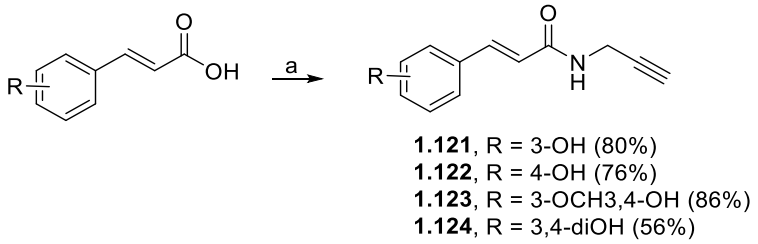

Scheme 1.19. Reagents and conditions. (a) i. EDC·HCl, HOBt, DMAP, ACN, rt; ii. Propargylamine, rt.

Amine

Reduction of amides to obtain the corresponding amines was attempted under different experimental procedures, with limited successful results. Lithium aluminum hydride ($LiAlH_4$) was used either as 2 M solution in THF or as solid, at reflux up to 2 days.[116,117] In both cases, desired amines could not be detected by HPLC-MS.

Alternatively, a reductive amination was carried out. The treatment of the commercially available ferulic aldehyde with 5 equiv of propargylamine gave the intermediate imine, which was not isolated but reduced with sodium borohydride ($NaBH_4$) to give the amine **1.125** in good yields (62%) (Scheme 1.20).[118]

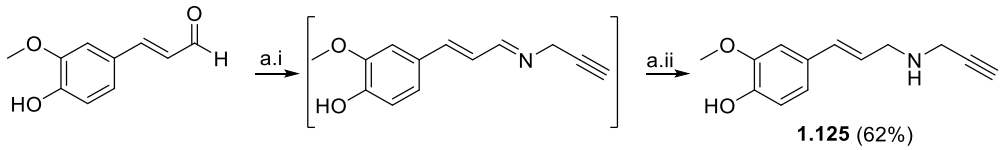

Scheme 1.20. Reagents and conditions. (a) i. Propargylamine, THF, rt, overnight; ii. $NaBH_4$, MeOH.

Biological Results

As previously explained, the 5-(2-(5-methoxy-1*H*-indol-3-yl)ethyl)-1,3,4-oxadiazol-2(3*H*)-one **1.1** was found to be a potent partial agonist in human MT_1R and MT_2R, displaying nanomolar affinity values for both receptors (K_i = 35 and 4 nM, respectively) with a slight selectivity for MT_2R. This compound was also a good radical scavenger (ORAC = 2.7 trolox equiv) and displayed potent neurogenic properties *in vitro*, better than melatonin itself.[72] However, it could not penetrate into the CNS, according to the *in vitro* parallel artificial membrane permeation assay for the blood-brain barrier (PAMPA-BBB).[119]

Thus, we began the biological evaluation of the new compounds by measuring their affinity for melatonin receptors and their antioxidant properties.

Evaluation in melatonin receptors

Evaluation of the affinities of new compounds in MTRs was carried out at Eurofins-CEREP SA (France) using radioligand binding assays. Experiments in human MT_1R and MT_2R were performed in Chinese hamster ovary cells (CHO), where these receptors were stably transfected. Assays in MT_3R (or QR2) were carried out in membrane homogenates of hamster brains. In all cases, displacement of the radioligand 2-[^{125}I]iodomelatonin was measured in the absence or presence of the tested compound and nonspecific binding was determined in the presence of MT, following described protocols.[120-122]

Firstly, radioligand displacements were measured at a fixed concentration of compound (10 μM or 100 nM) in each receptor subtype. Then, binding constants (K_i) were calculated only for compounds with a radioligand displacement above 80%. MT was tested for comparative purposes and results are gathered in Table 1.2 for indole and naphthalene derivatives and in Table 1.3 for the phenyl series.

Table 1.2. Binding constants at MTRs K_i (nM), or percentage of radioligand displacement at the specified concentration (in brackets), and antioxidant properties (ORAC assay) of indole and naphthalene derivatives

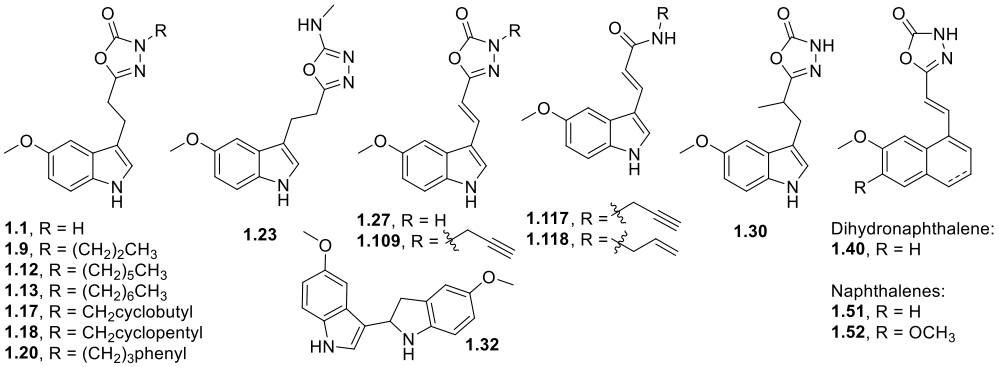

Compd.	K_i (nM)[a]			ORAC (Trolox equiv)[b]
	hMT_1R	hMT_2R	MT_3R	
1.1	35 ± 1	4.0 ± 0.5	$>10^2$ (5%)	2.7 ± 0.3
1.9	$>10^4$	$>10^4$	~10^4 (68%)	3.0 ± 0.2
1.12	$>10^4$	530 ± 40	n.d.	2.1 ± 0.2
1.13	$>10^4$	300 ± 30	n.d.	2.2 ± 0.1
1.17	550 ± 40	230 ± 20	n.d.	2.8 ± 0.2
1.18	$>10^4$	390 ± 30	n.d.	2.7 ± 0.2
1.20	690 ± 60	320 ± 20	n.d.	1.8 ± 0.2
1.23	550 ± 40	110 ± 20	330 ± 30	2.3 ± 0.1
1.27	$>10^2$ (8%)	$>10^2$ (17%)	6.6 ± 0.4	2.4 ± 0.1
1.109	$>10^2$ (0%)	$>10^2$ (0%)	3.2 ± 0.2	1.8 ± 0.1
1.117	$>10^2$ (13%)	~10^2 (58%)	9.3 ± 0.5	1.3 ± 0.1
1.118	$>10^2$ (34%)	~10^2 (78%)	110 ± 10	1.8 ± 0.1
1.30	$>10^2$ (37%)	12 ± 0.9	220 ± 20	2.3 ± 0.1
1.32	~10^4 (58%)	620 ± 40	7.5 ± 0.5	2.3 ± 0.1
1.40	~10^4 (46%)	260 ± 20	250 ± 20	0.4 ± 0.04
1.51	260 ± 20	5.1 ± 0.4	270 ± 20	< 0.1
1.52	~10^4 (63%)	69 ± 6	35 ± 2	< 0.1
MT	0.27 ± 0.03	0.13 ± 0.02	84 ± 1	2.3 ± 0.1

[a]Results are the mean ± SEM (n = 3). [b]Results are the mean ± SD (n = 3).
n.d., not determined.

The indole–*NH*-oxadiazolone **1.1** presented high binding values in MT_1R and MT_2R (K_i = 35 and 4 nM, respectively).[72] In contrast, **1.1** did not show affinity toward MT_3R, as at 100 nM it only displaced a 5% of the radioligand (Table 1.2).

The introduction of radicals in the NH- group of the oxadiazolone ring to give derivatives **1.7** – **1.20** caused a great decrease in the affinity for all melatonin receptors, reaching in some cases the total loss of activity. Only compounds with longer chains namely, **1.12** [R = $(CH_2)_5CH_3$], **1.13** [R = $(CH_2)_6CH_3$], **1.17** (R = CH_2cyclobutyl), **1.18** (R = CH_2cyclopentyl), and **1.20** [R = $(CH_2)_3$phenyl] showed a slight selectivity to MT_2R *vs.* MT_1R, with binding constants around 10^{-7} M in MT_2R. This decrease in the activity could be due to a possible hydrogen bond between the NH of the oxadiazolone ring of **1.1** and the receptor, which is lost when it is substituted. The evaluation of derivative **1.9** in MT_3R gave only a 68% displacement at 10 µM, so its K_i was not calculated and the rest of the indole-oxadiazolones were not evaluated in MT_3R.

The replacement of the oxadiazolone ring by a 1,3,4-oxadiazol-2-amine to give **1.23** provided binding constants in the hundred-nanomolar range for the three melatonin receptors, K_i = 550, 110, 330 nM, MT_1, MT_2 and MT_3R, respectively. Thus, this change maintained the binding constants for MT_1R and MT_2R and improved results in MT_3R, compared to some *N*-substituted oxadiazolone derivatives (e.g., **1.17** and **1.20**).

The addition of a methyl group in the aliphatic linker of **1.1** to give the *alpha*-methyl derivative **1.30**, resulted in a complete loss of affinity toward MT_1R, a similar binding constant for MT_2R (K_i = 12 nM) and a better union to MT_3R (K_i = 230 nM), in comparison with **1.1**.

In the indole series, the introduction of a double bond in the linker provided interesting effects in the behaviour of these unsaturated oxadiazolones (**1.27** and **1.109**) and amides (**1.117** and **1.118**). These four derivatives lost their affinity toward MT_1R and MT_2R (K_is > 10^2 nM), while improved drastically their binding in MT_3R. Unsaturated indole-oxadiazolone derivatives, whatever the substitution in the oxadiazolone ring (**1.27** R = hydrogen or **1.109** R = propargyl group), and the propargyl amide derivative **1.117** showed K_is between 3.2 and 9.3 nM in MT_3R, better than MT itself (K_i = 84 nM).

By comparing with **1.1**, the affinity of biindole **1.32** was lost for MT_1R (58% at 10 µM), was reduced to the 10^{-7} M for MT_2R and was clearly improved for MT_3R reaching the low-namolar rage (K_i = 7.5 nM).

According to previous results described in the bibliography,[123] we also found that the NH-indole fragment was not indispensable for activity in melatonin receptors. In fact, the 7-methoxy-3,4-dihydronaphthalene **1.40** showed affinities toward MT_2R and MT_3R in the 10^{-7} M range (K_i = 410 and 260 nM, respectively), although resulted inactive in MT_1R. Ring aromatization to give the naphthalene counterpart greatly modified the profile towards MTRs, as **1.51** recovered a moderated affinity for MT_1R (K_i = 260 nM), maintained a similar affinity for MT_3R (K_i = 270 nM), and interestingly, displayed a potent binding to MT_2R in the low-nanomolar range (K_i = 5.1 nM). The introduction of a second methoxy group in position 6 of the naphthalene ring was partially detrimental for affinity, since **1.52** was inactive in MT_1R, not as active as **1.51** in MT_2R (K_i = 69 nM), although **1.52** was one order of magnitude more active in MT_3R (K_i = 35 nM).

5-(2-(7-Methoxynaphthalen-1-yl)vinyl)-1,3,4-oxadiazol-2(3*H*)-one (**1.51**), which displayed the most potent affinity for hMT_2R, was also functionally characterized by measuring its effects on cAMP modulation, in Eurofins-CEREP SA according to a described HTRF-detection protocol.[121,124] Compound **1.51** was found to be a potent full agonist in MT_2R with a half maximal effective concentration in the low-nanomolar range (EC_{50} = 1.1 nM) and a maximum activity of 85% with respect to melatonin.

In the phenyl series, we prioritized methoxy-substituted compounds to be tested in melatonin receptors, due to their more structural similarity with the endogenous ligand MT. Given that a first selection of these derivatives, namely **1.86**, **1.89**, and **1.111** at 10 µM gave radioligand displacement in MT_1R below 80%, the rest of the series was not evaluated in this receptor subtype (Table 1.3).

In general, phenyl–oxadiazolone derivatives with an unsaturated linker were selective toward MT_3R compared to MT_2R, strengthening the idea that the presence of a double bond in the linker favours MT_3R activity.

Table 1.3. Binding constants at melatonin receptors K_i (nM), or percentage of radioligand displacement at 10 μM (in brackets), and antioxidant properties (ORAC assay) of phenyl derivatives

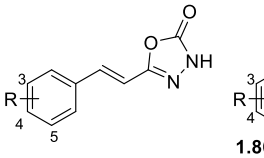

1.69, R = 3-OCH_3
1.70, R = 4-OCH_3
1.75, R = 3,5-diOCH_3
1.91, R = 3-OH
1.92, R = 4-OH
1.98, R = 3-NH_2
1.104, R = 3-$OCH_2CH{=}CH_2$

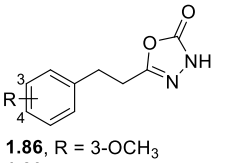

1.86, R = 3-OCH_3
1.89, R = 3,4-diOCH_3
1.95, R = 3-OH

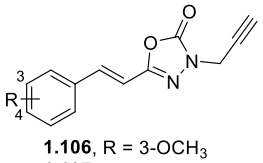

1.106, R = 3-OCH_3
1.107, R = 4-OCH_3
1.108, R = 3-OH

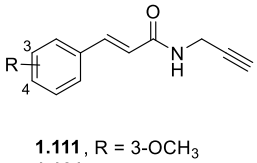

1.111, R = 3-OCH_3
1.121, R = 3-OH
1.124, R = 3,4-diOH

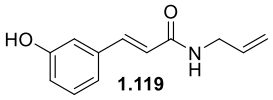

1.119

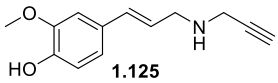

1.125

Compd.	K_i (μM)[a]			ORAC (Trolox equiv)[b]
	hMT_1R	*h*MT_2R	MT_3R	
1.69	n.d.	>10 (15%)	>10 (76%)	< 0.1
1.70	n.d.	n.d.	>10 (68%)	< 0.1
1.75	n.d.	>10 (2%)	<10 (106%)	< 0.1
1.91	n.d.	~10 (58%)	n.d.	3.8 ± 0.1
1.92	n.d.	n.d.	n.d.	3.2 ± 0.1
1.98	n.d.	n.d.	n.d.	0.9 ± 0.03
1.104	n.d.	>10 (12%)	~10 (66%)	< 0.1
1.86	~10 (53%)	1.1 ± 0.1	>10 (36%)	0.4 ± 0.07
1.89	>10 (32%)	~10 (49%)	n.d.	< 0.1
1.95	n.d.	n.d.	n.d.	2.2 ± 0.3
1.106	n.d.	>10 (25%)	~10 (78%)	0.3 ± 0.06
1.107	n.d.	n.d.	<10 (91%)	< 0.1
1.108	n.d.	n.d.	<10 (90%)	2.7 ± 0.2
1.111	~10 (65%)	1.4 ± 0.1	~10 (76%)	< 0.1
1.121	n.d.	n.d.	n.d.	3.0 ± 0.3
1.124	n.d.	n.d.	n.d.	1.9 ± 0.1
1.119	n.d.	n.d.	n.d.	2.3 ± 0.2
1.125	n.d.	>10 (32%)	0.19 ± 0.01	2.1 ± 0.1
MT	0.27 ± 0.03	0.13 ± 0.02	84 ± 1	2.3 ± 0.1

[a]Results are the mean ± SEM (n = 3). [b]Results are the mean ± SD (n = 3).
n.d., not determined.

Furthermore, introduction of a propargyl fragment in the oxadiazolone NH (**1.106**-**1.108**) no produced drastic differences in comparison to their unsubstituted analogues in MTRs. All of them resulted selective toward MT_3R with radioligand displacement values around 80 – 90% at 10 µM.

The 3-methoxyphenyl–oxadiazolone **1.86** bearing a dimethylene linker showed the opposite selectivity, with binding constants of 1.7 µM in MT_2R and around 10 µM in MT_1R, whereas it displayed a modest 36% displacement at 10 µM in MT_3R.

In the case of amides, the 3-methoxyphenyl derivative **1.111** considerably enhanced its affinity toward MT_2R (K_i = 1.4 µM) respect to the oxadiazolone analogues without the propargyl group **1.69** (15% displacement at 10 µM) or with this fragment **1.106** (25% displacement at 10 µM). However, in MT_3R these three compounds showed similar radioligand displacement (around 76%).

Otherwise, amine derivative **1.125** demonstrated to be a potent and selective ligand of MT_3R with a binding constant in the sub-micromolar range (K_i = 190 nM) (Table 1.3).

Conformational analysis of indole and naphthalene derivatives (1.27 and 1.51)

As explained, the indole–*NH*-oxadiazolone derivative **1.27** showed a marked selectivity towards MT_3R (K_i = 6.6 nM), in comparison with MT_1R and MT_2R (K_i = 100 nM). In contrast, substitution of the indole heterocycle for a naphthalene ring gave **1.51**, which was a potent and selective agonist in MT_2R (EC_{50} = 1.1 nM), compared to MT_1R and MT_3R (K_i = 260 and 270 nM, respectively).

With the aim of explaining this different behaviour in *NH*-oxadiazolone derivatives that only differed in the nature of the other heterocycle, we performed a conformational analysis of **1.27** and **1.51** using the *ab initio* Hartree-Fock method.

The conformational analysis of torsional angle among carbons 1-4 determined that the energy barriers for both compounds are different (Figure 1.8). The indole–*NH*-oxadiazolone **1.27** showed high energy barriers (around 5 kcal mol^{-1}) and the most stable

conformation at 180º torsion angle, denoting a completely flat arrangement between the two heterocycles. In contrast, the more stable conformation of the naphthalene derivative **1.51** showed a dihedral angle of about 40°, which prevented the steric hindrance of the hydrogen of naphthalene with the hydrogen chain in carbon 3 (Figure 1.8). Although theoretical calculations are required with the 3D-structures of the receptors, these results seem to indicate that the flat conformation of **1.27** favoured the interaction with MT_3R, while the torsional disposition of **1.51** is preferred for its agonist activity in MT_2R.

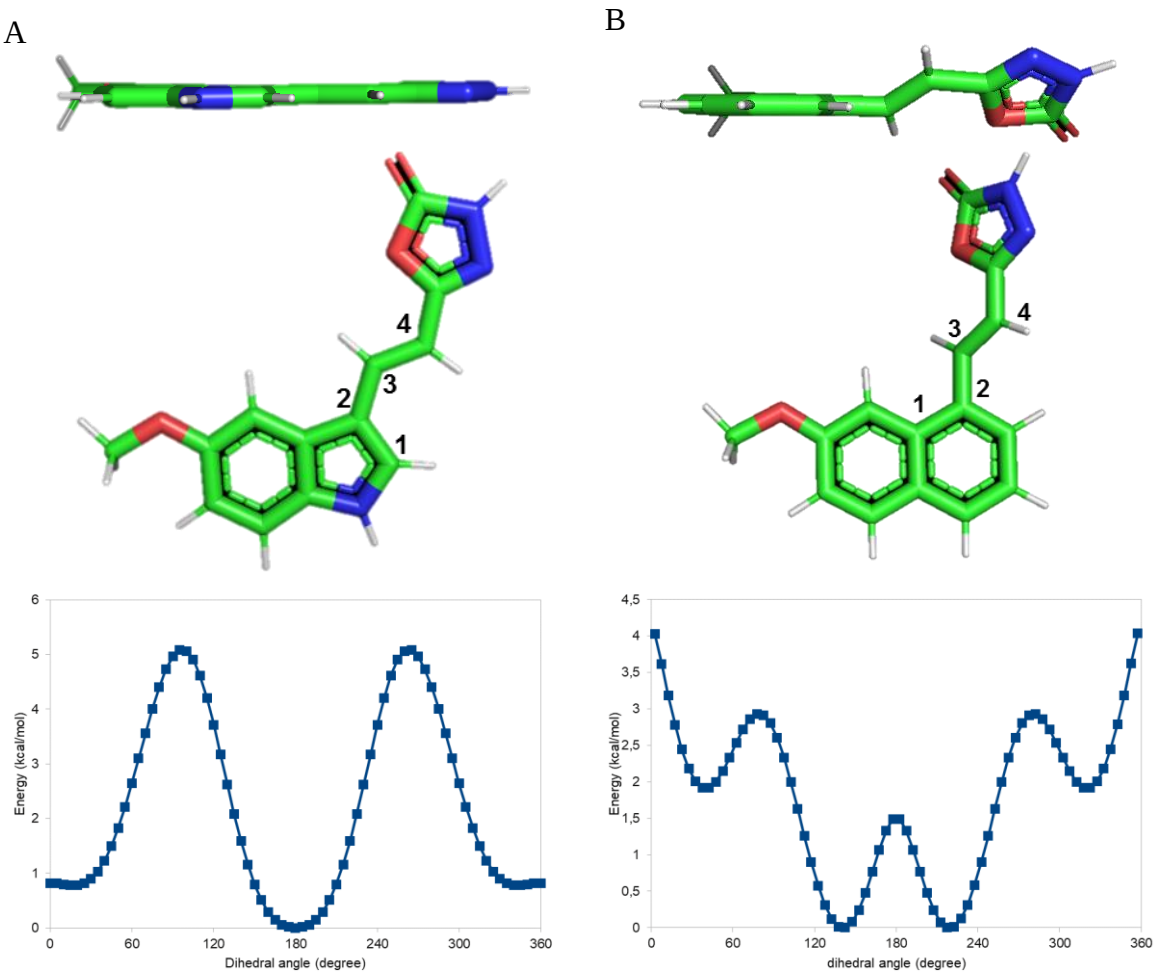

Figure 1.8. Conformational analysis of indole–*NH*-oxadiazolone **1.27** (**A**) and naphthalene–*NH*-oxadiazolone **1.51** derivatives (**B**). Minimum energy structures for **1.27** and **1.51**. Energy scans of dihedral angle between indole or naphthalene scaffold and oxadiazolone (bellow).

Evaluation of the oxygen radical absorbance capacity (ORAC)

The oxygen radical absorbance capacity (ORAC) of new compounds was determined as a measure of their antioxidant properties, following described protocols.[125-128] Trolox [(±)-6-hydroxy-2,5,7,8-tetramethylchromane-2-carboxylic acid], the aromatic part of vitamin E responsible for its scavenging properties, was used as internal standard with the arbitrary value of ORAC = 1.0. Results are expressed as trolox equivalents (trolox mmol / tested compd mmol) in a comparative scale that indicates if a compound is a better (ORAC > 1.0) or a worse oxygen radical scavenger (ORAC < 1.0) than vitamin E. MT was also evaluated for comparative purposes, giving an ORAC value 2.3-fold higher than trolox. This activity fully agrees with the ORAC value previously described by Sofic *et al.* (2.0 trolox equiv),[129] pointing out the reliability of our experiments.

ORAC values are gathered in Table 1.2 for indole and naphthalene derivatives and in Table 1.3 for the phenyl series.

As shown in Table 1.2, all indole derivatives **1.3**-**1.20**, **1.23**, **1.27**, **1.30**, **1.32 1.109**, **1.117** and **1.118** presented ORAC values between 1.3 and 3.0 trolox equiv with independence of the nature of the substituent attached to the position 3 of indole heterocycle. Consequently, they could be considered as excellent antioxidant agents. It was unexpected that the unsaturated derivative **1.27** did not show a significant difference in the ORAC value (2.4 trolox equiv) compared to its saturated analogue **1.3** (2.7 trolox equiv), in spite of the increase of the conjugation between the indole and oxadiazolone rings would suggest an increase in antioxidant properties.

Replacement of indole by a dihydronaphthalene or naphthalene core was detrimental to the antioxidant activity in the ORAC assay. Dihydronaphthalene **1.40** displayed a reduced ORAC value (0.4 trolox equiv) and naphthalenes **1.51** and **1.52** were inactive at the maximum concentration tested (10 μM).

In summary, it can be inferred that in this first series the radical absorbance capacity was mainly due to the presence of the indole ring, rather than other structural motifs.

Regarding the phenyl-based family, only derivatives with hydroxyl groups exhibited remarkable antioxidant capacity (ORAC = 1.7 – 3.8 trolox equiv), whereas the 3-aminophenyl oxadiazolone **1.98** showed a similar ORAC value as trolox (0.9 trolox equiv) and methoxylated derivatives were not antioxidant at the maximum concentration tested (10 μM) (Table 1.3).

In the hydroxyphenyl-oxadiazolones, the best ORAC values were obtained with derivatives bearing a double bond in the linker, such as **1.91** (R = 3-OH) and **1.92** (R = 4-OH) that displayed ORAC values of 3.8 and 3.2 trolox equiv, respectively. The replacement of the double bond for a saturated linker provoked a decrease in the ORAC value, **1.95** (R = 3-OH) being an example (ORAC = 2.2 trolox equiv).

The 3-hydroxyphenyl-propargyl amide **1.121** showed a better ORAC value (3.0 trolox equiv) than its allyl counterpart **1.119** (ORAC = 2.3 trolox equiv). It should be noted that introduction of a second hydroxyl group in **1.121** to give the catechol derivative **1.124** reduced the antioxidant capacity (ORAC = 1.9 trolox equiv). Reduction of amide group to give the 3-methoxy-4-hydroxyphenyl-propargyl amine **1.125** lowered slightly the antioxidant capacity (ORAC = 2.1 trolox equiv) (Table 1.3).

Inhibition of human MAO and LOX-5

All compounds were evaluated as inhibitors of human MAO-A, MAO-B and LOX-5 and the results of the most representative compounds are gathered in Table 1.4 (indole and naphthalene derivatives) and in Table 1.5 (phenyl derivatives). For clarifying, data of inactive compounds in the three enzymes are omitted.

The *h*MAO-A/B inhibition was determined by the production of oxygen peroxide from a common substrate for both isoenzymes (*p*-tyramine) and quantified by the Amplex Red MAO assay kit.[130] (*R*)-Deprenyl, iproniazid and moclobemide were also tested for comparative purposes.

The inhibition of *h*LOX-5 was performed following the fluorescence-based method described by Pufahl *et al.*,[131] using the two well-known inhibitors zileuton and NDGA as internal references.

Table 1.4. Inhibition (IC_{50}, μM)[a] of human monoamine oxidases (*h*MAO-A and *h*MAO-B) and human lipoxygenase-5 (*h*LOX-5) of indole and naphthalene derivatives.[b]

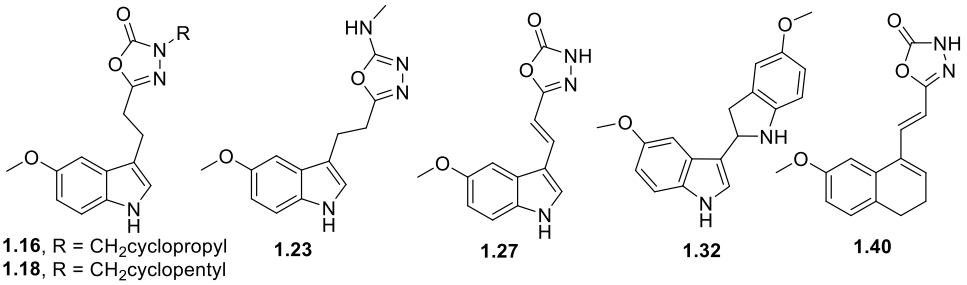

Compd.	*h*MAO-A	*h*MAO-B	*h*LOX-5
1.16	> 50	> 50	74.2 ± 2.2
1.18	> 50	> 50	22.5 ± 1.8
1.23	> 50	37.0 ± 0.7	60.6 ± 2.6
1.27	53.0 ± 3.5	68.3 ± 4.6	> 100
1.32	2.54 ± 0.56	3.69 ± 0.33	5.3 ± 0.3
1.40	40.6 ± 1.1	35.7 ± 3.3	12.5 ± 0.3
(*R*)-Deprenyl	68.7 ± 4.2	0.017 ± 0.002	n.d.
Iproniazid	6.7 ± 0.8	7.5 ± 0.4	n.d.
Moclobemide	161.4 ± 19.4	> 100	n.d.
(*R*,*S*)-Zileuton	n.d.	n.d.	0.15 ± 0.03
NDGA	n.d.	n.d.	0.097 ± 0.019

[a]Results are the mean ± SEM of three independent experiments.
[b]Data of inactive compounds are not shown

In general, saturated indole–oxadiazolone derivatives did not show appreciable inhibition of *h*MAOs or *h*LOX-5 (IC_{50} > 50), with the exception of **1.16** and **1.18** that displayed a modest inhibition of *h*LOX-5 (IC_{50} = 74.2 and 22.5 µM, respectively). The 5-methoxyindole-oxadiazolamine **1.23** inhibited both *h*MAO-B and *h*LOX-5 (IC_{50} = 37.0 and 60.6 µM, respectively). Introduction of a double bond in the linker changed this profile, as the 5-methoxyindole-oxadiazole **1.27** displayed moderate inhibition of MAO-A and MAO-B (IC_{50} = 53.0 and 68.3 µM, respectively) although it was inactive in LOX-5 (IC_{50} > 100 µM). This positive effect of the double bond in the linker was not valid for the naphthalene-oxadiazole and the indole-amide series, because **1.51**, **1.52**, **1.117** and **1.118** were inactive in the three enzymes (data not shown). Surprisingly, the introduction of a propargyl radical in the oxadiazolone ring of the MAO-A/B inhibitor **1.27** to give **1.109** caused a total lack of activity in these enzymes (data not shown). Unlike, the dihydronaphthalene-oxadiazolone **1.40** inhibited *h*MAO-A, *h*MAO-B and *h*LOX-5 with IC_{50} values of 40.6, 35.7 and 12.5 µM, respectively (Table 1.4).

The biindole **1.32** deserves a special mention, because it was the best inhibitor in the three enzymes with IC_{50} values in the low-micromolar range: 2.54, 3.69, and 5.3 µM in *h*MAO-A, *h*MAO-B and *h*LOX-5, respectively.

In the resveratrol-based series, the nature, number and position of the substituents exerted a notorious influence over the inhibition of *h*MAOs and *h*LOX-5. Generally, methoxybenzene–*NH*-oxadiazolones did not display a significant inhibition of *h*MAOs and *h*LOX-5, with the exception of the 3,4-dioxolanphenyl derivative **1.74** with a moderate inhibition of MAO-B (IC_{50} = 27.6 µM). Unlike, the 3-nitrophenyl–*NH*-oxadiazolone **1.68** was a potent and selective MAO-B inhibitor with IC_{50} in the low-micromolar range (IC_{50} = 1.1 µM) (Table 1.5).

Table 1.5. Inhibition (IC_{50}, μM)[a] of human monoamine oxidases (*h*MAO-A and *h*MAO-B) and human lipoxygenase-5 (*h*LOX-5) of phenyl derivatives.[b]

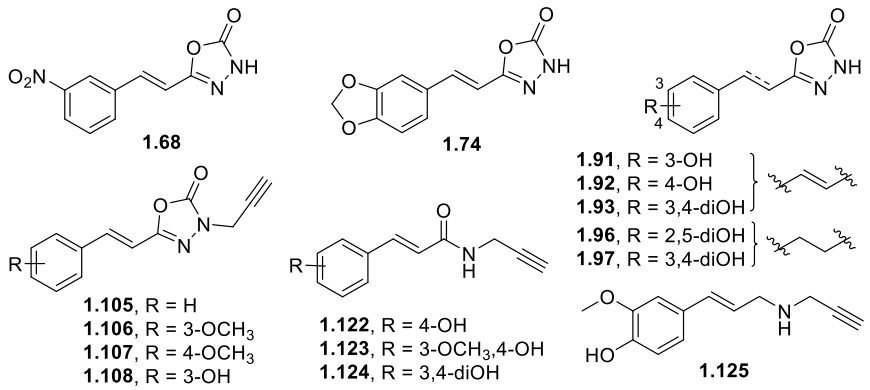

Compd.	*h*MAO-A	*h*MAO-B	*h*LOX-5
1.68	> 50	1.1 ± 0.1	> 100
1.74	> 50	27.6 ± 0.9	> 100
1.91	> 50	> 50	187 ± 13
1.92	51.5 ± 3.4	45.7 ± 3.0	> 100
1.93	3.41 ± 0.23	5.84 ± 0.39	1.25 ± 0.12
1.96	n.d.	n.d.	42.8 ± 2.7
1.97	> 50	> 50	10.2 ± 0.6
1.105	> 50	9.87 ± 0.9	> 100
1.106	> 50	0.64 ± 0.06	> 100
1.107	> 50	8.05 ± 0.8	n.d.
1.108	> 50	3.53 ± 0.15	> 100
1.122	> 50	31.1 ± 1.6	28.9 ± 1.5
1.123	> 50	> 50	31.2 ± 2.0
1.124	47.0 ± 1.0	> 50	8.72 ± 0.5
1.125	30.3 ± 2.5	> 50	66.8 ± 3.3
(*R*)-Deprenyl	68.7 ± 4.2	0.017 ± 0.002	n.d.
Iproniazid	6.7 ± 0.8	7.5 ± 0.4	n.d.
Moclobemide	161.4 ± 19.4	> 100	n.d.
(*R,S*)-Zileuton	n.d.	n.d.	0.15 ± 0.03
NDGA	n.d.	n.d.	0.097 ± 0.019

[a]Results are the mean ± SEM of three independent experiments. [b]Data of inactive compounds are not shown

As expected, introduction of hydroxyl groups in positions 3- and 4- of benzene generally improved IC_{50}s in the three enzymes and the presence of a double bond in the linker connecting both cycles resulted important as well. Whereas the unsaturated 3-hydroxybenzene–*NH*-oxadiazolone **1.91** was almost inactive in all enzymes, its 4-hydroxyl counterpart **1.92** displayed a moderate inhibition in both *h*MAO-A and *h*MAO-B (IC_{50} = 51.1 and 45.7 µM, respectively). Remarkably, introduction of two hydroxyl groups in positions 3 and 4 of the benzene gave the catechol **1.93**, which was among the most potent inhibitors in *h*MAOs and *h*LOX-5 discovered in this work, with IC_{50}s in the low-micromolar range, namely 3.41, 5.84 and 1.25 µM, respectively. The saturated analogue of **1.93** (**1.97**) was not active in MAOs and its LOX-5 inhibition (IC_{50} = 10.2 µM) was one of magnitude worse than **1.93**, confirming the importance of the presence of a double bond in the linker for a successful activity in these enzymes.

In the methoxy- or hydroxyl-phenyl–oxadiazolone derivatives, the incorporation of a propargylic radical in the oxadiazolone ring remarkably improved *h*MAO-B inhibition, while completely lost the activity in *h*MAO-A and *h*LOX-5. Thus, derivatives **1.105**, **1.107** and **1.108** were potent and selective inhibitors of *h*MAO-B, with IC_{50} values in the low-micromolar range (IC_{50} = 9.87, 8.05, and 3.53 µM, respectively), reaching the submicromolar magnitude in the case of **1.106** (IC_{50} = 0.64 µM). Thus, 5-(3-methoxystyryl)-3-(prop-2-yn-1-yl)-1,3,4-oxadiazol-2(3*H*)-one (**1.106**) was emerged as the most potent and selective *h*MAO-B inhibitor here described.

In the phenyl–propargylamide series, only hydroxyl-substituted derivatives resulted active in *h*LOX-5. In general, they displayed IC_{50}s in the two-digit micromolar range, namely **1.122**, **1.123**, and **1.125** (IC_{50} = 28.9, 31.2 and 66.8 µM, respectively), highlighting the catechol **1.124** as the most active (IC_{50} = 8.7 µM). Moreover, **1.122** displayed also an interesting inhibition of *h*MAO-B (IC_{50} = 31.1 µM), whereas amide **1.124** and amino **1.125** were moderated inhibitors of MAO-A (IC_{50} = 47.0 and 30.3 µM, respectively).

Nrf2 induction

The ability to induce Nrf2 transcription factor was evaluated using a Nrf2-dependent luciferase reporter assay in the AREc32 cell line.[132,133] Cells were cultured for 24 h and then treated with increasing concentrations of the corresponding compound (0.3, 3, 10 and 30 μM). A selection of new compounds, covering different structural features was tested as Nrf2 inducers and results are gathered in Table 1.6. For simplicity, inactive compounds are omitted. Sulforaphane was used as reference and data are expressed as the concentration needed to duplicate the specific activity of the luciferase reporter (CD).

Table 1.6. Nrf2 induction capability of selected compounds (CD, μM)[a,b]

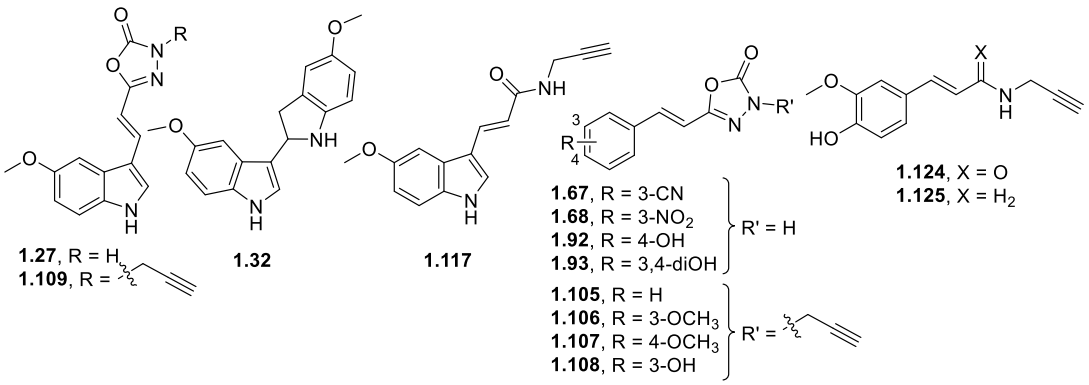

Compd.	Nrf2 induction (CD, μM)	Compd.	Nrf2 induction (CD, μM)
1.27	15.1 ± 0.9	**1.105**	16.9 ± 0.4
1.32	0.56 ± 0.05	**1.106**	7.44 ± 0.34
1.109	1.76 ± 0.20	**1.107**	9.83 ± 0.20
1.117	27.4 ± 1.5	**1.108**	8.05 ± 0.41
1.67	13.7 ± 1.1	**1.124**	19.2 ± 1.4
1.68	8.42 ± 0.9	**1.125**	22.3 ± 2.1
1.92	22.7 ± 1.3	Sulforaphane	0.54 ± 0.07
1.93	21.3 ± 1.6		

[a]Results are the mean ± SEM (n > 3). [b]Data of inactive compounds are not shown

In general, saturated indole-oxadiazolone derivatives (e.g., **1.9**) did not show activity at the maximum concentration tested (30 μM). Unlike, the unsaturated indole-oxadiazolone **1.27** and its *N*-propargylic counterpart **1.109** were able to increase luciferase activity, with CD values of 15.1 and 1.8 μM, respectively. The elimination of the oxadiazolone ring in **1.109** to give the propargylic amide **1.117** provoked a decrease in one order of magnitude in the Nrf2 activation (CD = 27.4 μM) (Table 1.6). When propargyl radical was replaced by an allyl fragment (**1.118**) the activity *vs.* Nrf2 was lost. Dihydronaphthalene and naphthalene analogues resulted inactive (data not shown).

In the phenyl series, unsaturated compounds showed also higher induction values than the saturated analogues. Among the phenyl–*NH*-oxadiazolone compounds with a double bond in the linker, the most active were the 3-cyanophenyl **1.67** (CD = 13.7 μM), 3-nitrophenyl **1.68** (CD = 8.42 μM), 4-hydroxylphenyl **1.92** (CD = 22.6 μM), and 3,4-dihydroxyphenyl **1.93** derivatives (CD = 21.3 μM).

Introduction of a propargyl radical in the NH of the oxadiazolone heterocycle produced again an increase in the activity, obtaining values in low micromolar range for the phenyl **1.105** (CD = 16.9 μM), 3-methoxyphenyl **1.106** (CD = 7.44 μM), 4-methoxyphenyl **1.107** (CD = 9.83 μM), and 3-hydroxyphenyl **1.108** (CD = 8.05 μM) derivatives.

Among the phenyl–propargyl amides, catechol **1.124** was the only active compound (CD = 19.2 μM). Amine **1.125** displayed moderated activity (CD = 22.3 μM), although it was enhanced with respect to its amide analogue **1.123** (CD > 60 μM).

The biindole **1.32** emerges as the most potent Nrf2 inducer of the compounds here tested, with a CD value of 0.56 μM, in the same range as sulforaphane.[134] It is worth-mentioning that **1.32** does not have any electrophilic character, reason why its mode of action may involve a disruption of the Nrf2 – Keap1 interaction, instead of an electrophilic mechanism. Thus, it could be expected that **1.32** was less promiscuous than electrophilic inducers, as explained in the introduction.

In vitro blood−brain barrier permeation assay (PAMPA-BBB)

In order to know the capability of new compounds to cross the blood-brain barrier (BBB) and reach their CNS-targets, we evaluated them in the *in vitro* parallel artificial membrane permeability assay for the BBB (PAMPA-BBB) described by Di *et al.*,[135] and modified by our group for testing molecules with limited water-solubility.[126,127,136-138] The passive CNS-permeation of new compounds through a lipid extract of porcine brain was measured at room temperature. In each experiment, 11 commercial drugs of known brain permeability were also tested and their permeability values normalised to the reported PAMPA-BBB data (See Experimental Section). As previously established in the literature,[135] compounds with $P_e > 4.0 \cdot 10^{-6}$ cm·s^{-1} would be able to cross the BBB (cns+), whereas those displaying $P_e < 2.0 \cdot 10^{-6}$ cm·s^{-1} would not reach the CNS (cns-). Between these values, the predicted CNS permeability was uncertain (cns +/-).

In the melatonin-based family, the indole–*NH*-oxadiazolone **1.1** and its *alpha*-methyl analogue **1.30** (both bearing a saturated linker) were predicted as not CNS-permeable ($P_e < 2 \cdot 10^{-6}$ cm·s^{-1}). In contrast, all indole–*N*-substituted oxadiazolone derivatives (**1.7**-**1.20**), showed permeability values exceeding 4.0 10^{-6} cm·s^{-1} and thus, they were predicted to be CNS-permeable. The indole–oxadiazolamine **1.23** displayed negative CNS permeation, whereas the indole–oxadiazolone **1.27** that is the unsaturated analogue of **1.1**, displayed a permeability value in the ambiguous range ($P_e = 3.2 \cdot 10^{-6}$ cm·s^{-1}). The introduction of a propargylic radical in the NH of the oxadiazolone ring of **1.27** gave **1.109** that as expected, was found to be CNS-permeable. Unsaturated amides **1.117** and **1.118** showed negative CNS-permeability.

Interestingly, biindole **1.32** presented a P_e value of 12.9 10^{-6} cm·s^{-1}, revealing that clearly it can cross the BBB by passive diffusion and reach the CNS.

The exchange of the indole heterocycle by a dihydronaphthalene (**1.40**) or a naphthalene (**1.51** and **1.52**) generated compounds with good CNS-permeability values (P_e = 9.0, 9.8 and 4.5 10^{-6} cm·s^{-1}, respectively), even retaining the NH-unsubstituted oxadiazolone ring.

From these experiments, we can conclude that in general the new indole and naphthalene derivatives with a single NH-unsubstituted motif were expected to be CNS-penetrating, whereas compounds with two NH groups experienced more difficulties to reach the CNS.

In the case of the phenyl–*NH*-oxadiazolone family, compounds bearing a methoxy group (**1.69**, **1.70**, and **1.86**) were found to be CNS-permeable (P_e = 4.6, 6.5 and 7.3 10^{-6} cm s^{-1}, respectively), whereas the introduction of an additional methoxy fragment gave compounds that in general displayed an uncertain CNS-permeation (cns+/-). When there was a cyano-, nitro-, hydroxyl- or amino-phenyl fragment, the resulting phenyl–*NH*-oxadiazolones (**1.67**, **1.68**, **1.91**, **1.92**, **1.98**…), cannot cross the blood-brain barrier (P_e < 2.0 10^{-6} cm s^{-1}). However, all derivatives bearing a propargyl group in the *NH*-oxadiazolone are predicted to enter into the CNS by passive permeation, even bearing a hydroxyl group such as the case of **1.108** (P_e = 4.7 10^{-6} cm s^{-1}).

Regarding amides derivatives, only those with methoxy groups were able to go through the blood-brain barrier. Unfortunately, either the 3-methoxy-4-hydroxylphenyl or the catechol propargyl amide (**1.124** and **1.123**) with remarkable activity in *h*LOX-5, does not permeate into the CNS by passive diffusion (P_e < 2.0 10^{-6} cm s^{-1}). The same disappointing results were found in the indole amides **1.117** and **1.118**, which were very potent ligands of *h*MT_3R.

The amine **1.125** showed a better P_e value (8.7 10^{-6} cm s^{-1}) than its amide analogue **1.123** (P_e < 2.0 10^{-6} cm s^{-1}), confirming that the presence of a carbonyl group decreased CNS-permeability.

Neurogenic studies

A selection of new compounds, covering different structural features, was screened in primary cultures of NSCs to study their neurogenic properties. Adult mice NSCs were isolated from SGZ of the dentate gyrus of the hippocampus, and grown as free-floating neurospheres (NS).[139,140] Tested compounds (at 10 μM) were added to NS culture for 7 days and then, NS were fixed to a substrate and allowed to differentiate in the presence of each compound for a 3-days additional period.

The neurogenic potential of each compound was determined using fluorescence confocal microscopy, by direct observation of the expression of two immunostained markers namely, human β-III-tubulin (TuJ-1 clone; green) and microtubule-associated protein 2 (MAP-2), and cell nuclei were identified by staining with 4',6-diamidino-2-phenylindole (DAPI). TuJ-1 is expressed in NSCs in early stages of their differentiation, whereas the expression of MAP-2 indicates a consolidated neuronal stage.[141] Control (basal) experiments (vehicle-treated cultures) only showed a few positive cells for TuJ-1 or MAP-2, whereas in cultures treated with neurogenic compounds the number of both TuJ-1 and MAP-2 marked cells was clearly increased.

In the melatonin-based family several compounds promoted the expression of TuJ-1 and MAP-2, indicating positive neurogenic activities (Figure 1.9). Comparing derivatives with a dimethylene liker, the indole –*N*-propyloxadiazolone **1.9** displayed good neurogenic properties, whereas its indole–oxadiazolamine counterpart **1.23** was inactive, pointing out the importance of the presence of an oxadiazolone ring for a successful neurogenesis.

Among indole compounds bearing a double bond in the linker, the indole–*N*-propargyloxadiazolone **1.109** was one of the most active compounds, as it greatly increased the expression of both TuJ-1 and MAP-2. Conversely, its analogue indole–*NH*-oxadiazolone **1.27** was inactive, suggesting that the *N*-propargyloxadiazolone ring is beneficial for activity.

The biindole **1.32** turned out to be the most potent compound of the melatonin-based series at stimulating neurogenesis *in vitro*. It induced both early neurogenesis (TuJ-1) and cell maturation (MAP-2), showing also the typical neuronal morphology.

Both naphthalene–*NH*-oxadiazolone derivatives **1.51** and **1.52** showed positive effects in the expression of TuJ-1 and MAP-2. In contrast, the dihydronaphthalene analogue **1.40** was inactive suggesting that naphthalene is more useful for neurogenesis.

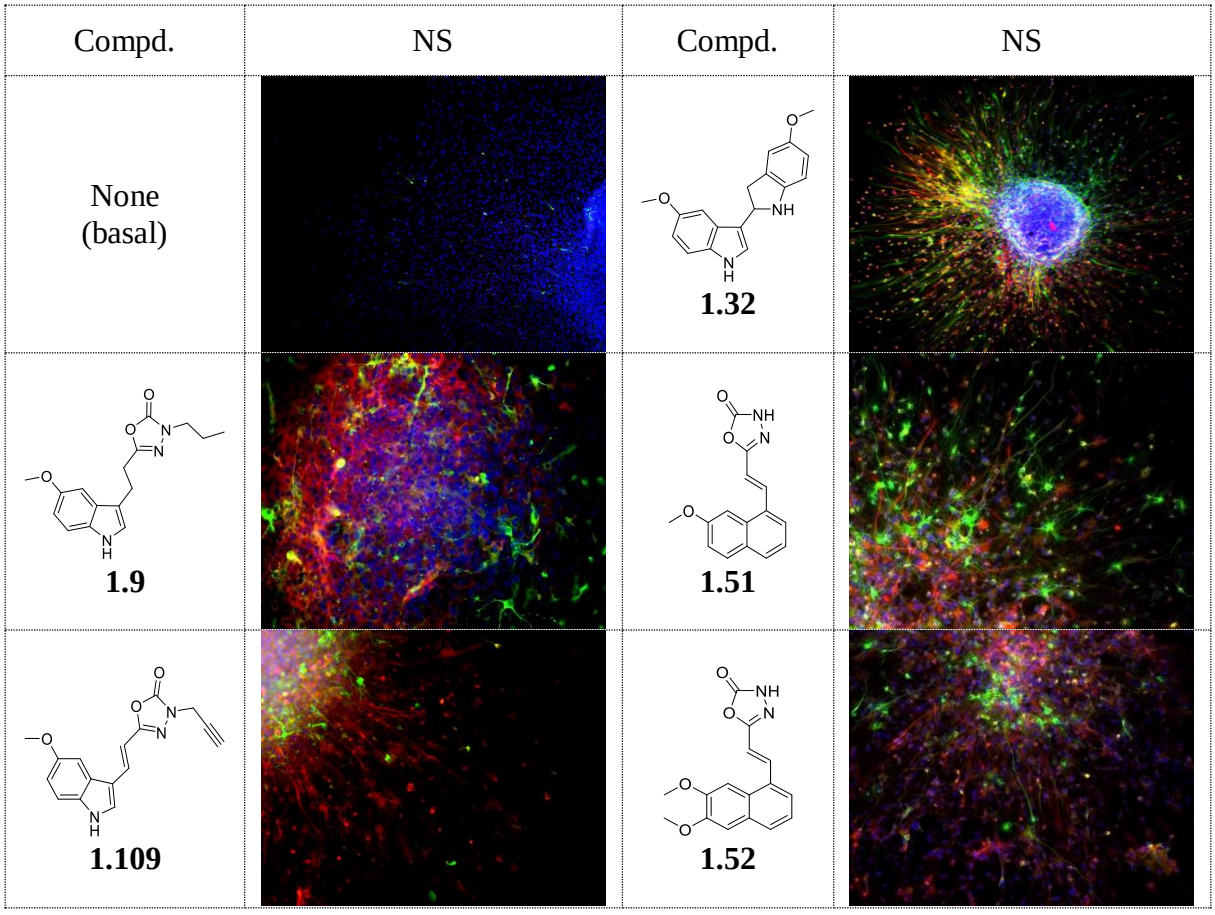

Figure 1.9. Expression of TuJ-1 (green) and MAP-2 (red) in cultured SGZ-derived NS in the presence of different melatonin-based compounds at 10 µM. DAPI (blue) was used as a nuclear marker (images of inactive compounds are not shown).

In the phenyl–oxadiazolone series bearing a dimethylene linker, we found that the 3-methoxyphenyl–*NH*-oxadiazolone **1.86** showed good neurogenic properties, in contrast with the lack of activity of their 3-hydroxyl- and 3,5-dihydroxyl counterparts **1.95** and **1.97**, respectively (Figure 1.10).

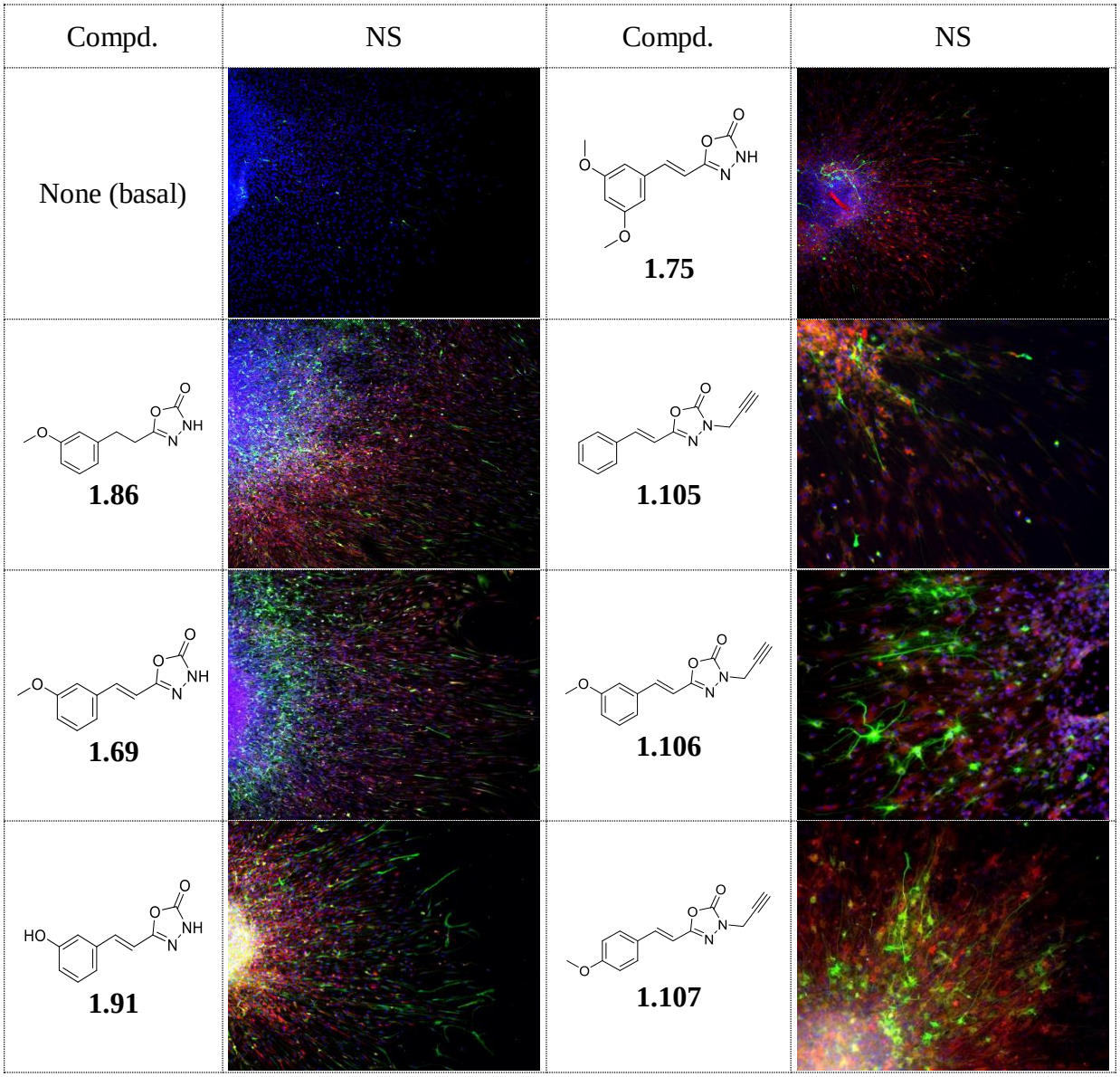

Figure 1.10. Expression of TuJ-1 (green) and MAP-2 (red) in cultured SGZ-derived NS in the presence of different resveratrol-based compounds at 10 µM. DAPI (blue) was used as a nuclear marker (images of inactive compounds are not shown).

Comparing phenyl–oxadiazolone family with a double bond in the linker, we observed that compounds with a *meta*-substituent in the benzene ring either a methoxy (**1.69**, **1.75** and **1.106**) or a hydroxyl group (**1.91**) promoted more remarkably the maturation than the early neurogenesis. However, the transformation of the 3,5-dimethoxy groups of **1.75** in 3,5-dihydroxyl group gave a total lack of activity in **1.94**.

Incorporation of a propargyl group in the oxadiazolone ring notably increased the expression of both TuJ-1 and MAP-2, compared with their *NH*-oxadiazolone analogues. Specifically, 3- and 4-methoxyphenyl –*N*-propargyloxadiazolone derivatives (**1.106** and **1.107**, respectively) were the most neurogenic agents of this family. In contrast, **1.105** with no substitution in the benzene and the 3-hydroxylphenyl analogue **1.108** showed poor capacity to differentiate NSCs (Figure 1.10).

Neuroprotection studies in models related to Alzheimer's disease

Toxicity and neuroprotection properties in the human neuroblastoma SH-SY5Y line

In order to determine the toxicity of the most representative compounds at 100 µM (one hundred times higher concentrations than neuroprotective assays) a study of cell viability was carried out by MTT assay in the neuroblastoma cell line SH-SY5Y. The data normalized respect to the basal condition (100% viability) showed that none of these compounds are toxic at that concentration (Figure 1.11A).

Then, the neuroprotective properties were evaluated using different *in vitro* AD models of increasing complexity. Firstly, we used okadaic acid (OA) as toxic insult in SY5Y cells. This toxin inhibits the phosphatase action, inducing hyperphosphorylation of tau and cell death, which are outstanding AD hallmarkrs.[142]

Tested compounds (1 µM) were cultured in SH-SY5Y cells for 24 h, followed by co-treatment with OA (10 nM) and the corresponding compound for an additional 24 h. Cell survival was assessed by MTT assay, normalizing data respect to basal condition. MT (10

µM) was used as a positive control.[143] Whereas, OA produced a cell viability of 63%, five compounds were able to remarkably protect the cellular line, increasing the survival respect to the toxic (Figure 1.11B). Such neuroprotective compounds were the 3-nitrophenyl–*NH*-oxadiazolone **1.68** (cell viability = 73%), the 4-hydroxyphenyl–*NH*-oxadiazolone **1.92** (cell viability = 75%), the 3,4-dihydroxyphenyl–*NH*-oxadiazolone **1.93** (cell viability = 71%), the 4-methoxyphenyl–*N*-propargyloxadiazolone **1.107** (cell viability = 73%) and 3,4-dihydroxyphenyl–propargylamide **1.124** (cell viability = 78%).

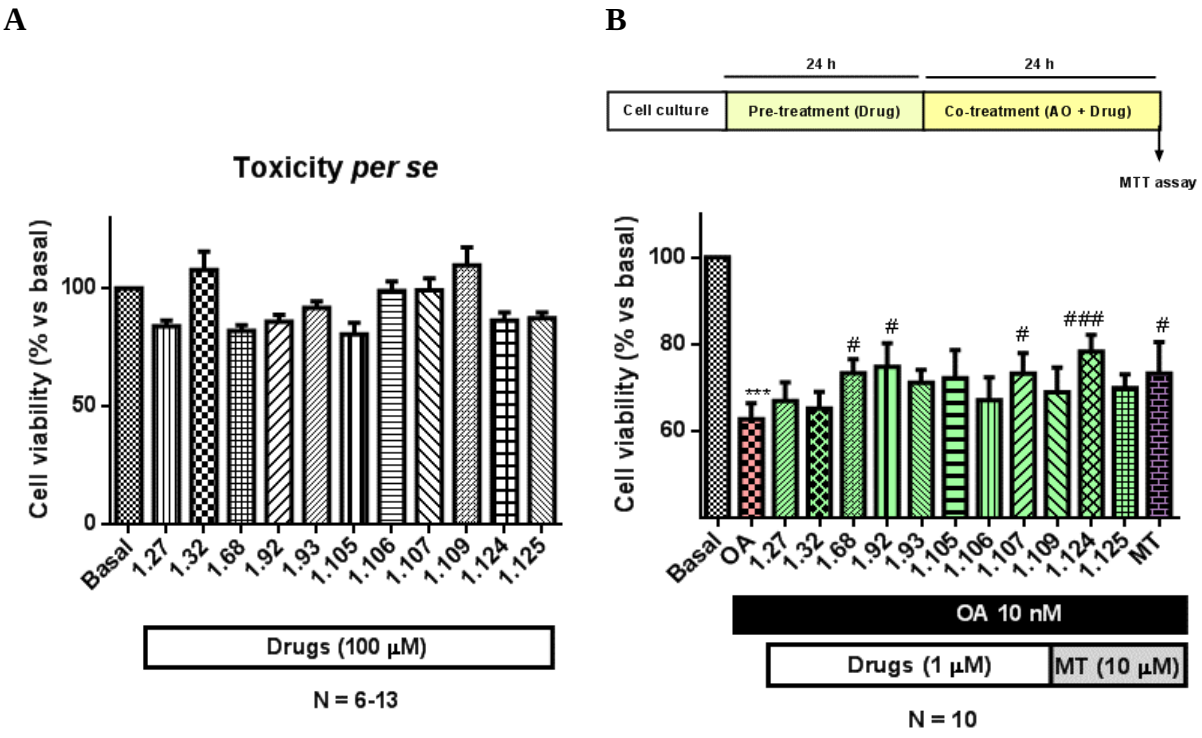

Figure 1.11. None compound resulted toxic and **1.93, 1.68, 1.92, 1.107, 1.124** neuroprotective agents against OA in the SY5Y cell line. Data normalized respect to the basal condition and represented as cell viability percentage. (**A**) Toxicity *per se* at 100 µM (N = 6-13). (**B**) Protocol scheme and cell viability determined by MTT assay. **1.93**, **1.68**, **1.92**, **1.107**, **1.124** protected against OA at 1 µM (N = 10). Statistical differences are represented as * p-value < 0.05 respect to the basal and # p-value <0.05 with respect to OA. Results are the mean of triplicates ± SD.

Compounds **1.68** and **1.93** had a worse neuroprotective profile, thus they were not further studied. We selected **1.92**, **1.107**, and **1.124** (Figure 1.12) for continuing with their biological evaluation.

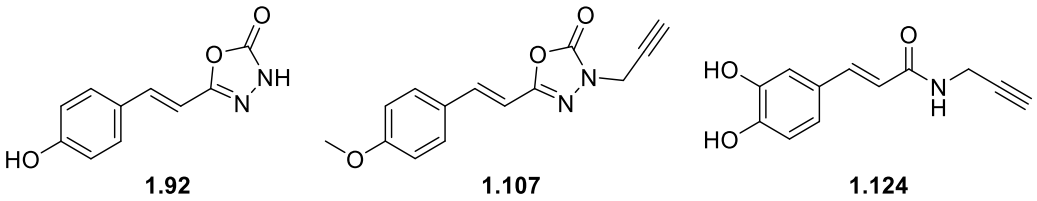

Figure 1.12. Structures of selected compounds for further phenotypic experiments

Studies in rat cortical neurons exposed to okadaic acid

Compounds **1.92**, **1.107**, and **1.124** were then evaluated in primary neuron cultures from rat embryos cortex obtained from 18-day pregnant rats and exposed to OA. Primarily, the preparation of the cells took place extracting the brain cortices, suspending in Dulbecco's Modified Eagle's Medium (DMEM)/F12, seeding in well plates and culturing for 2 h. Then, the medium was replaced by neurobasal medium (NB) and cultured for 7-10 days (Figure 1.13A). Once neurons were prepared, the assay was carried out following the above explained protocol, in the presence of OA. MT (10 µM) was used as positive control. Cell viability was determined by MTT assay and the data was normalized respect to the basal (100% viability).

While OA (10 nM) decreased the cell viability to 50%, **1.107** and **1.124** (both at 1 µM) considerably reversed the cell viability to 70% and 89%, respectively. In contrast, **1.92** (1 µM) was not able to protect significantly against OA at that concentration (Figure 1.13B) nevertheless; the around 11% increasing of cell surviving is biologically significant.

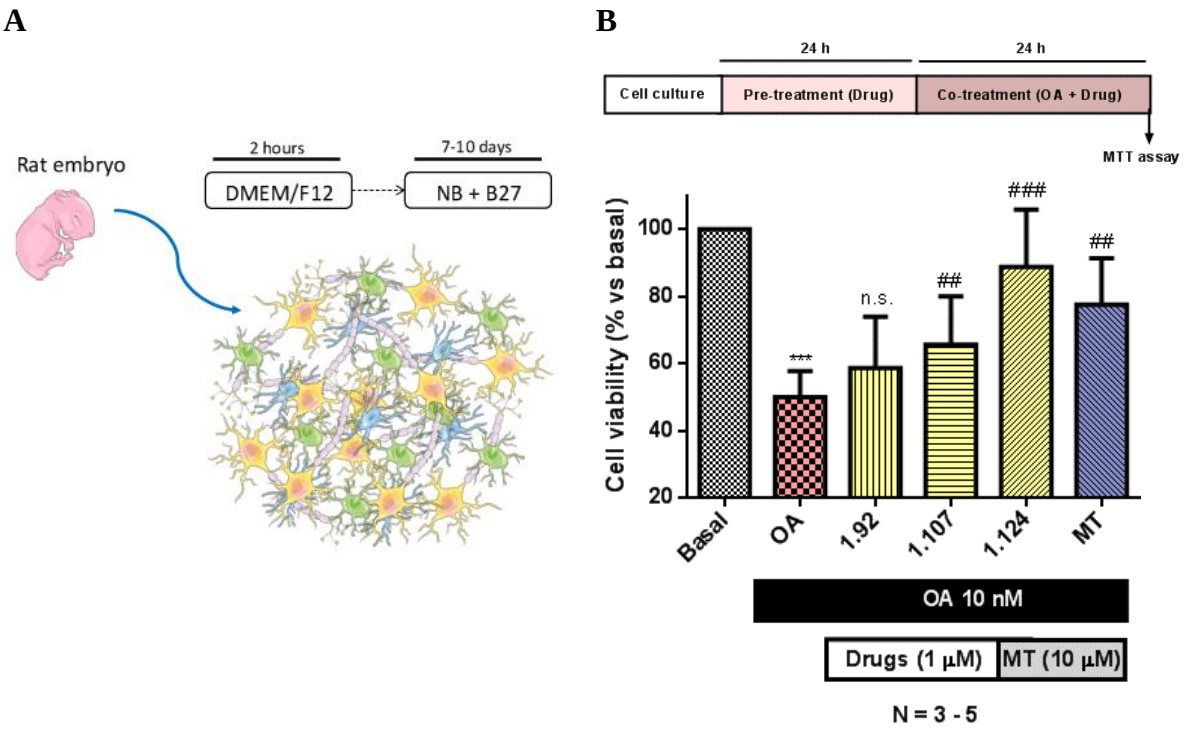

Figure 1.13. (**A**) Scheme of preparation of rat cortical neurons. (**B)** Protocol scheme. Compounds **1.107** and **1.124** (1 µM) increased remarkably cell viability in neurons exposed to OA (10 nM) in primary cortical neurons cultures. **1.92** did not increase significantly the cell viability. Data is represented as cell viability percentage normalized to the basal condition. Statistical differences are represented as * p-value <0.05 respect to the basal and # p-value <0.05 respect to OA. n.s.: not significant. Results are the mean of triplicates ± SD (N = 3-5).

Studies in mice hippocampal slices exposed to okadaic acid

The three selected compounds **1.92**, **1.107**, and **1.124** were assessed in mice hippocampal slices, a more complex *in vitro* AD model to study the tau pathology in the hippocampus during this disorder. These slices were extracted and stabilized for 45 min and exposed to OA (1 µM) for 6 h, testing the three compounds at 1 µM. Cell viability was measured in CA1 region of hippocampus by both MTT and propidium iodide (PI) fluorescence, a red marker of cell death, normalizing in both cases respect to basal condition (100% viability) (Figure 1.14).

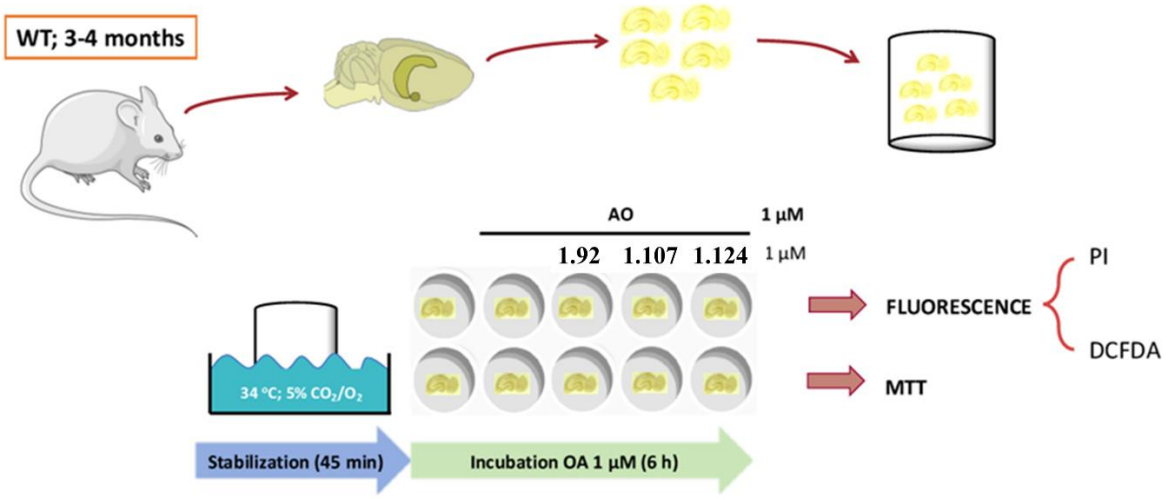

Figure 1.14. Scheme of the procedure for neuroprotection assay in hippocampal slices. Firstly, preparation of the slice from 3 – 4 months old mice, then toxicity induction and incubation with **1.107**, **1.92** and **1.124** compounds and measure by either MTT or fluorescence probes (PI or DCFDA).

In the MTT assay, OA (1 µM) induced a decreasing of cell viability to 60%, while **1.92** and **1.124** reversed this cell death to 81% and 73% of cell viability, respectively. Conversely, **1.107** was not able to restore significantly the cell survival at 1 µM. MT (10 µM) was again employed as a positive reference (Figure 1.15).

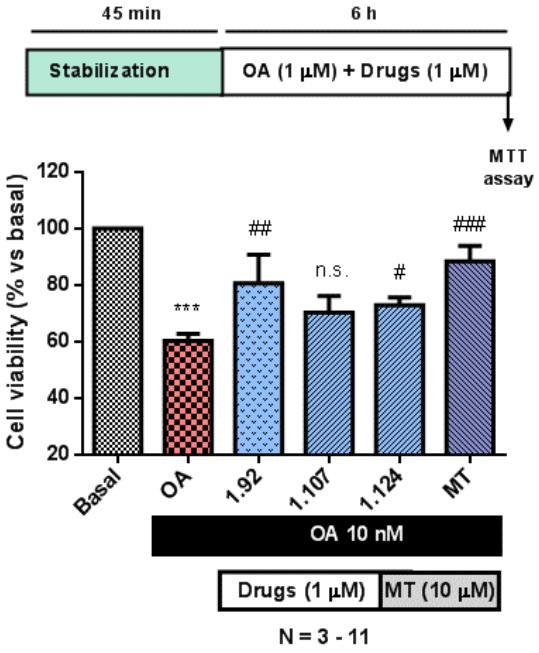

Figure 1.15. Compounds **1.92** and **1.124** protected against OA in mice hippocampal slices. However, **1.107** was not able to reverse notoriously the cell viability because of the OA-induced toxicity. Protocol scheme. Data represented as cell viability percentage normalized respect to basal condition. Statistical differences are represented as * p-value <0.05 respect to the basal and # p-value <0.05 respect to OA. n.s.: not significant. Results are the mean of triplicates ± SD (N = 3-11).

In contrast, the detection by the fluorescent marker PI (1 µg/µL), which was added after 5 h incubation, led to different results. In this case, PI data was normalized respect to Hoechst (1 µg/µL), a nuclear marker. While OA (1 µg) produced a 1.5-fold increasing in PI fluorescence (150%) in the CA1 region, in the presence of either **1.92, 1.107** or **1.124**, the fluorescence decreased to 96%, 69% and 74%, respectively (Figure 1.16).

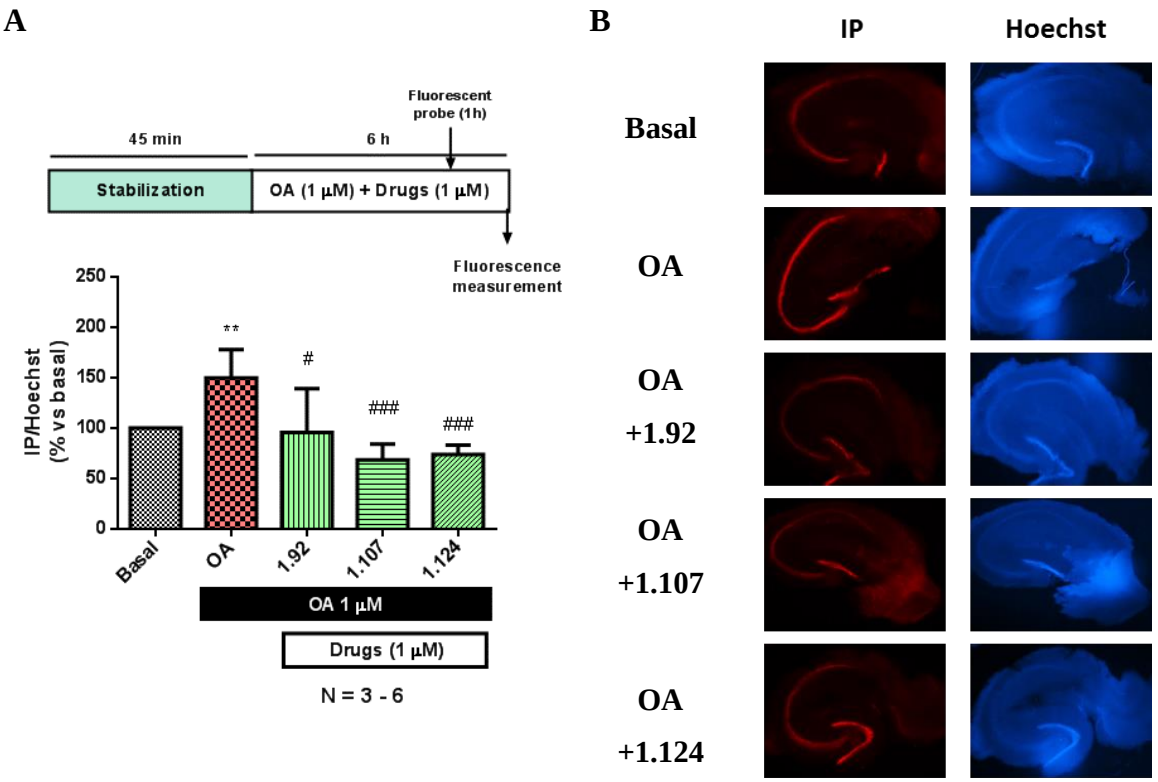

Figure 1.16. Compounds **1.92, 1.107** and**1.124** give back the cell viability of OA-treated hippocampal slices. (**A**) Scheme of protocol employed. Fluorescence analysis (PI/Hoechst ratio). Statistical differences are represented as * p-value <0.05 respect to the basal; # p-value <0.05 respect to OA. Results are the mean ± SD in triplicates (N = 3 - 6). (**B**) Illustrative hippocampi slice sections (10X objective). While OA increases PI fluorescence in CA1 respect to control, **1.92**, **1.107** and **1.124** remarkably decrease PI fluorescence in the same area (left). Nuclei staining with Hoechst are represented for each slice (right).

The incongruence in the **1.107** case (inactive by MTT and potent by PI fluorescence) may be due to the fact that MTT is a less accurate method than PI fluorescence, because MTT does not depend on the state of the mitochondrial dehydrogenase. Or it may due to a not enough sample size for this compound in MTT assay.

Evaluation of antioxidant capacity of compounds in mice hippocampal slices

As previously explained, OS contributes to the AD progression. Although the antioxidant capacity was determined by the ORAC assay, a more precise measure of ROS generated by OA treatment in the hippocampi slices was carried out. In this case the fluorescent probe used was 2′,7′-dichlorofluorescein diacetate (DCFDA, 10 µg/µL), which dyes ROS in CA1 region of the hippocampus (Figure 1.17). Thus, normalizing DCFDA data against Hoechst was possible determining that OA increased 1.75-fold of DCFDA fluorescence (175%), indicating an increasing of ROS production. Nevertheless, the fluorescence decreased in the presence of **1.92, 1.107** and **1.124** at 1 µM (84, 63 and 73%, respectively), showing a clear capacity to reduce ROS production (Figure 1.17).

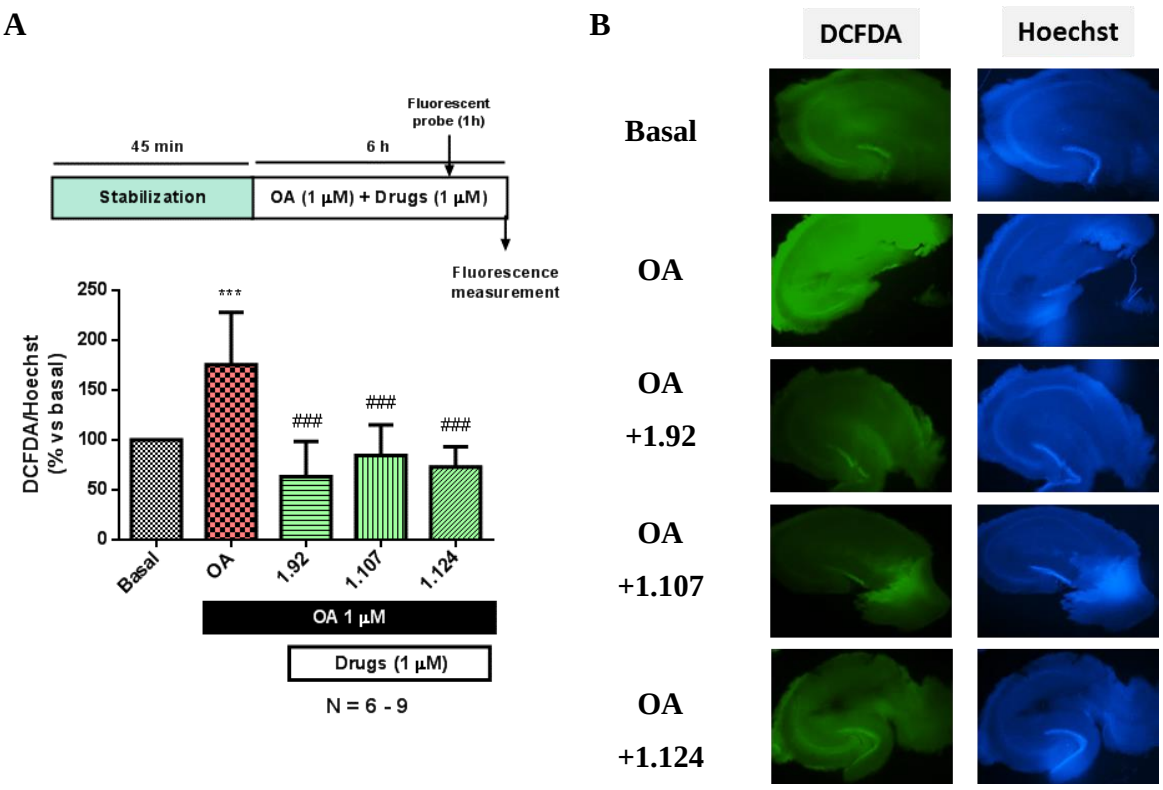

Figure 1.17. Compounds **1.92**, **1.107** and **1.124** reduce ROS in OA-treated hippocampal slices. (**A**) Protocol representation. Fluorescence analysis (DCFDA/Hoechst ratio) Statistical differences are represented as * p-value <0.05 respect to the basal; # p-value <0.05 respect to OA. Results are the mean ± SD in triplicates (N = 3-5). (**B**) OA increased

ROS compared with basal condition in CA1. Nuclei staining with Hoechst are represented for each slice.

From these results we can conclude that the three selected compounds could be interesting candidates for continuing for their biological evaluation. However, **1.124** was previously described in the bibliography and **1.92** displayed worse multitarget profile than **1.107**. Thus, we highlighted the 4-methoxyphenyl–*N*-propargyloxadiazolone **1.107** as a promising candidate for advanced pharmacological evaluation.

CONCLUSIONS

CONCLUSIONS

We have developed new melatonin- and resveratrol-based families as MTDLs with potential application in the treatment of AD. Design was inspired in several natural or synthetic bioactive compounds with advantageous pharmacologic profile namely, MT, resveratrol and selegiline, from which classical medicinal chemistry strategies have been applied, for instance bioisosterism and scaffold hopping. New molecules combined structural features of these ligands, which can be summarized as an aromatic ring (indole, dihydronaphthalene, naphthalene or benzene) linked to a polar moiety (five-membered heterocycle, amide or amine group) through a saturated or unsaturated chain of two carbons. We also synthetized a biindole derivative, as the result of the dimerization of 5-methoxyindole.

The new melatonin- and resveratrol-based MTDLs were active in several key targets involved in OS and neuroinflammation, such as $MT_{1\text{-}3}$Rs, MAOs, LOX-5 and Nrf2. Several compounds were good radical scavengers and could penetrate the CNS, according to the *in vitro* PAMPA-BBB assay. In phenotypic experiments, some of these MTDLs displayed interesting neuroprotective and neurogenic properties.

From the SAR studies performed in each target, we can conclude that the nature of the aromatic ring is the more influential feature in the radical scavenging properties, being the indole scaffold the most favourable. The double bond in the linker resulted to be the most important structural characteristic in the potency and selectivity towards MT_3R and Nrf2. The *N*-propargyloxadiazolone ring was the most favoured polar moiety in the potency and selectivity toward MAO-B and Nrf2.

Moreover, the best low-micromolar *h*LOX-5 inhibitors had a catechol in their structure. The most potent and selective *h*MAO-B inhibitors were resveratrol-cinnamic derivatives with a propargyl group in the oxadiazolone ring. Such analogues were also excellent Nrf2 inductors, and effective neurogenic and neuroprotective agents in *in vitro* models of AD. Derivatives with the better multitarget profile were predicted to be CNS-permeable, thus they could act in their cerebral targets.

In the melatonin-based family, 5,5'-dimethoxy-2,3-dihydro-1*H*,1'*H*-2,3'-biindole (**1.32**) is a potent neurogenic agent, displaying also outstanding activities in key targets related to AD. It shows nanomolar affinity for MT_3R, is a 2.3-fold more potent radical scavenger than vitamin E, and inhibits *h*MAO-A/B and *h*LOX-5 in the low-micromolar range. Moreover, **1.32** is the most potent Nrf2 inducer of the compounds here developed, with a CD value in the sub-micromolar range close to the marketed sulforaphane. Interestingly, **1.32** is not an electrophilic compound, so it could be expected that its mode of action could involve a disruption of the Nrf2 – Keap1 interaction. Thus, **1.32** is an interesting MTDL in the search of innovative treatments for AD.

It is worth-mentioning that the 4-methoxyphenyl– *N*-propargyloxadiazolone **1.107** showed an interesting biological profile in *in vitro* experiments related to AD. Its structure consists of a styrene scaffold (based on resveratrol), an oxadiazolone fragment (bioisosteric replacement of the melatonin acetamide moiety) and a propargyl radical (from selegiline). In the low-micromolar range, **1.107** is a potent Nrf2 inducer, a *h*MAO-B selective inhibitor and a MT_3R ligand. Furthermore, in phenotypic assays, it displays neuroprotective properties against OA and promotes the differentiation and maturation of NSC. Consequently, 5-(4-methoxystyryl)-3-(prop-2-yn-1-yl)-1,3,4-oxadiazol-2(3*H*)-one (**1.107**) emerges as a promising candidate for continuing its pharmacological study.

EXPERIMENTAL SECTION

EXPERIMENTAL SECTION

Synthesis

Along this thesis, reagents and solvents were purchased as high-grade products from common commercial suppliers, mostly Sigma-Aldrich, and were used without further purification. Reactions were controlled by analytical thin-layer chromatography (TLC), ran on Merck silica gel 60 F254 plates, with detention by UV-light (λ = 254 or 365 nm) and/or stained with 10% wt. phosphomolybdic acid solution in EtOH, ninhydrin solution or vanillin solution; or by High-Performance Liquid Chromatography – Mass Spectrometry (HPLC-MS), performed on a Waters analytical (Alliance Watters 2695) equipped with a SunFire C_{18} (3.5 μm, 4.6 mm x 50 mm) column, a UV-visible photodiode array detector (λ = 190 - 700 nm) coupled to quadrupole mass spectrometer (Micromass ZQ), spectra were acquired in an Electrospray Ionization (ESI) interface working in the positive or negative-ion mode. Reactions under mw irradiation were performed in a Biotage Initiator 2.5 reactor. Unless otherwise stated, products were purified by automatized flash chromatography using an IsoleraOne (Biotage) equipment, with different cartridges of silica gel Biotage ZIP KP-Sil 50 μm. Alternatively, preparative TLC on Merck silica gel 60 F254 plates or by semipreparative HPLC on Waters Autopurification system with UV-visible photodiode array detector (λ = 190 - 700 nm) coupled to a quadrupole mass spectrometer (3100 Mass Detector) were used. HPLC analyses were used to confirm the purity of all compounds (≥ 95%) and were performed on Waters 2690 equipment, at a flow rate of 1.0 mL/min, with a UV-visible photodiode array detector (λ = 190 - 700 nm), using SunFire C_{18} (3.5 μm, 4.6 mm x 50 mm) column. The gradient mobile phase consisted of H_2O:ACN with 0.1% formic acid as solvent modifiers, and the gradients time (g.t.) are indicated for each compound. Melting points (mp) (uncorrected) were determined in a MP70 apparatus (Mettler Toledo). Nuclear magnetic resonance (^{1}H NMR and ^{13}C NMR) spectra were obtained in MeOD, acetone-d_6, D_2O, DMSO-d_6 or $CDCl_3$ solutions using the following NMR spectrometers: Varian INOVA-300 (^{1}H, 300 MHz; ^{13}C, 75 MHz), Varian INOVA-400, Varian Mercury-400 (^{1}H, 400 MHz; ^{13}C, 100 MHz) or Varian Unity-500 (^{1}H, 500 MHz; ^{13}C, 125 MHz). Chemical shifts (δ) are reported in parts per million (ppm) relatives to internal tetramethylsilane scale, coupling constants (J) values in hertz (Hz). The

following abbreviations are used to describe peak patterns when appropriate: s (singlet), d (doublet), t (triplet), q (quartet), m (multiplet), app (apparent), and b (broad). 2D NMR experiments -homonuclear correlation spectroscopy (H, H-COSY), heteronuclear multiple quantum correlation (HMQC) and heteronuclear multiple bond correlation (HMBC) of the compounds were acquired to assign protons and carbons of new structures. The High Resolution Mass Spectra (HR-MS) analysis was carried out by using an Agilent 1200 Series LC system (equipped with a binary pump, an autosampler, and a column oven) coupled to a 6520 quadrupole-time of flight (QTOF) mass spectrometer. ACN:H_2O (75:25, v:v) was used as mobile phase at 0.2 mL/min. The ionization source was an ESI interface working in the positive-ion mode. The electrospray voltage was set at 4.5 kV, the fragmentor voltage at 150 V and the drying gas temperature at 300 °C. Nitrogen (99.5% purity) was used as nebulizer (207 kPa) and drying gas (6 L/min).

General procedures

I. Wittig reaction[144]

The mixture of the corresponding aldehyde (1.0 equiv) and (Carbethoxyethylidene) triphenylphosphorane (1.3 equiv) was dissolved in DCM or toluene. The reaction solution was refluxed overnight. The solvent was evaporated under reduced pressure. The residue was purified by column flash chromatography in the appropriated gradient.

II. Synthesis of α,β-unsaturated acids by Knoevenagel-Doebner reaction[145]

To a solution of the commercial aldehyde (1 equiv) in pyridine (7 mL/mmol), malonic acid (2 equiv) and piperidine (13 µL/mmol) were added. The mixture of reaction was stirred at 70 ºC overnight under N_2 atmosphere. The solvent was evaporated under reduced pressure. EtOAc was added and the organic layer washed with H_2O (x3), 10% citric acid solution, dried over Mg_2SO_4, filtered, and evaporated under reduced pressure. In the case of initial amount was over at 500 mg, acid was precipitated from pyridine with H_2O, filtered and washed several times with H_2O. The crude was dried to obtain the corresponding α,β-unsaturated acid.

III. Hydrogenation of alkenes to alkanes or nitrobenzenes to anilines

To a solution of the either commercial α,β-unsaturated acid or nitrobenzene in EtOH (10 mL/mmol), catalytic amount of Pd-C 5% was added under N_2 atmosphere. After that, N_2 was displaced by H_2 and the flask was sealed up with a septum. A balloon with H_2 was connected with a needle to stir at 30 ºC overnight. The mixture was filtrated, and the solvent was removed under reduced pressure. In most of cases, it was not necessary further purification.

IV. Synthesis of amides and hydrazides from acids[146]

To a suspension of the corresponding acid (1 equiv) and activated 4 Å molecular sieves in anhydrous ACN (15 mL/mmol) at rt under N_2 atmosphere, HOBt (1.2 equiv), EDC·HCl (1.2 equiv) and DMAP (0.12 equiv) were added orderly. The reaction was stirred until complete activation of the acid (30 min - 3 h) at rt. Either an excess of $N_2H_4 \cdot H_2O$ or the corresponding amine (1.2 equiv) was added. Once finished the reaction (upon the end of addition in most of cases), H_2O was added. The mixture was extracted with DCM (x3) and washed with saturated $NaHCO_3$ (aq). The organic layers were joined, and the solvent was evaporated under reduced pressure to obtain the corresponding *N*-acylhydrazines. In the case of amides, organic layer was dried over Mg_2SO_4, filtered, and evaporated under reduced pressure. Final compounds were purified with the appropriated gradient.

V. Synthesis of the corresponding 1,3,4-oxadiazol-2(3H)-one

To a solution of the corresponding hydrazide (1 equiv) in anhydrous DMF (10 mL/mmol), CDI (1.2 equiv) was added under N_2 atmosphere. The reaction was heated at 120 ºC for 25 min under mw irradiation. The solvent was removed, EtOAc was added, extracted (x3), washed with brine, dried over Mg_2SO_4, filtered, and evaporated under reduced pressure. The compound was purified in the adequate gradient to obtain the corresponding 1,3,4-oxadiazol-2(3*H*)-one.

VI. S_N2 in either N-alkylation of 1,3,4-oxadiazol-2(3H)-one or in benzyl bromide

A solution of either 1,3,4-oxadiazol-2(3*H*)-one derivatives or benzyl bromide and K_2CO_3 (1.2 equiv) in acetone (7 mL/mmol) (previously dry with K_2CO_3) was stirred at rt for 10 min. Corresponding halide or tosyl alkyl (1.2 equiv) was added. The mixture was heating under mw irradiation at 120 ºC for 10 min. In hydroxyl derivatives, the mixture of reaction was left at rt overnight instead of using mw. The solvent was evaporated under reduced pressure. EtOAc was added and the organic layer washed with H_2O (x3) and brine, dried over Mg_2SO_4, filtered, and evaporated under reduced pressure. The crude was purified by chromatography using the appropriate eluent to afford the corresponding alkyl derivative.

VII. Demethoxylation to obtain phenols

To a solution of the corresponding methoxylated compound in the minimum amount of anhydrous DCM, a 1 M BBr_3 solution in DCM was added dropwise under N_2 atmosphere (1 equiv of BBr_3 per each heteroatom present in the molecule). The mixture was left at rt overnight. Reaction was quenched with MeOH (dropwise until end of effervescence) and the solvent evaporated under reduced pressure to remove the remaining BBr_3, this process was repeated several times until no fumes were observed when adding MeOH. In most of cases, purification was not necessary to obtain the corresponding phenol.

VIII. Aromatization of 1,2-dihydronaphathalenes[101]

To a solution of the corresponding dihydronaphthalene (1 equiv) in DCM (5 mL/mmol), a solution of DDQ (1.2 equiv) in DCM (5 mL/mmol) was added. The reaction was stirred for necessary time (from 10 min to overnight) and washed with a saturated solution of $NaHCO_3$, brine, dried over $MgSO_4$, filtrated and the solvent was removed under reduced pressure. The crude was purified by chromatography using the appropriate eluent to afford the corresponding naphthalene.

IX. Heck reaction from triflate naphthalene

Adaptation from [109]. To a solution of the corresponding triflate (1 equiv), 1,10-phenanthroline (5.5% mol), ($Pd(OAc)_2$, 5% mol) in anhydrous DMF (5 mL/mmol), TEA

(1.2 equiv) and ethyl acrylate (5 equiv) were added successively. The reaction was heated under mw irradiation at 150 ºC for 1 h. The solvent was evaporated. The product was purified by flash column in the corresponding gradient to yield the corresponding α,β-unsaturated ester.

X. Hydrolysis of α,β-unsaturated esters[109]

To a solution of the corresponding α,β-unsaturated ester in THF:H_2O 1:1 (7.5 mL/mmol), LiOH (1.3 equiv) was added and the reaction was stirred at rt overnight. The solution was adjusted to pH = 1 by addition of 1 M HCl. The product was precipitated, washed with H_2O until neutral pH, centrifuging to avoid losing product, and lyophilized to remove water traces to obtain the corresponding acid.

Synthesis of indole derivatives

5-(2-(5-Methoxy-1*H*-indol-3-yl)ethyl)-1,3,4-oxadiazol-2(3*H*)-one (1.1)

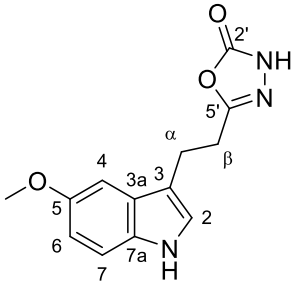

Derivative **1.1** was synthesized from hydrazide **1.2** (146 mg, 0.62 mmol), according to the procedure V as a white solid (138 mg, 86%). Spectra corresponding with described in [72].

Ethyl 3-(5-methoxy-1*H*-indol-3-yl)propanoate (1.2)

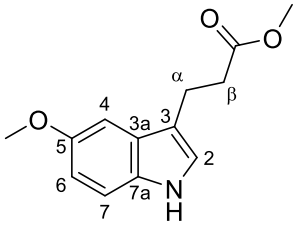

To solution of commercial 5-methoxy-1*H*-indole (5.0 g, 34 mmol) in anhydrous DCM (40 mL) ethyl acrylate (21.7 mL, 0.2 mol) was added. Finally, anhydrous $ZrCl_4$ (1.0 g, 4.29 mmol) is added to the solution. The mixture was kept stirring at rt for 18 h, after which the

catalyst was filtered off and the solvent and excess of ethyl acrylate were removed under vacuum and collected in a cold trap. The resulting crude was purified by flash chromatography in DCM to afford **1.1** (6.1 g, 71%) as a white pearly solid. Spectra corresponding with described in Ref.[72].

3-(5-Methoxy-1*H*-indol-3-yl)propanehydrazide (1.3)

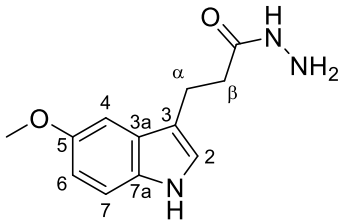

A mixture of **1.2** (3.0 g, 12.1 mmol), and excess of $N_2H_4 \cdot H_2O$ (5 mL) in EtOH (6 mL) was heated to 155 °C for 45 min under mw irradiation. After removing the solvent, the crude was suspended in H_2O (70 mL) and extracted with EtOAc (x6). The organic layer was dried over $MgSO_4$, filtrated and solvent removed to give **1.3** (2.8 g, >99%), without further purification, as a white solid. Spectra corresponding with described in Ref.[72].

Methyl (2*E*)-3-(5-methoxy-1*H*-indol-3-yl)prop-2-enoate (1.4)

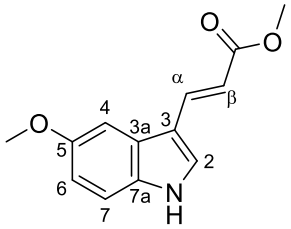

A solution of acid **1.5** (800 mg, 3.68 mmol) and K_2CO_3 (1.2 equiv) in the minimum amount of THF (not completely soluble in acetone) was stirred at rt 10 min. Then, CH_3I (1.2 equiv) was added. The reaction was left at rt overnight. Solvent was evaporated under reduced pressure and the crude was extracted with DCM (x3), dried over $MgSO_4$ and filtrated. The product was precipitated with hexane to give ester **1.5** without further purification in quantitative yield (850 mg, 3.7 mmol) as a brown-yellow solid. Mp: 177 - 180 ºC (lit. 177 - 179 ºC)[147]. ^{1}H NMR (300 MHz, DMSO-d_6) δ 7.91 (s, 1H, H_2), 7.87 (d, J = 16.2 Hz, 1H, H_α), 7.36 (d, J = 8.7 Hz, 1H, H_7), 7.27 (d, J = 2.4 Hz, 1H, H_4), 6.84 (dd, J = 8.7, 2.5 Hz, 1H, H_6), 6.32 (d, J = 16.0 Hz, 1H, H_β), 3.82 (s, 3H, C_5OCH_3), 3.70 (s, 3H, CO_2CH_3). ^{13}C NMR (75 MHz, DMSO-d_6) δ 167.9 (CO), 154.8 (C_5), 139.2 (C_α), 132.2 (C_{7a}), 132.0 (C_2),

125.6 (C_{3a}), 113.1 (C_7), 112.4 (C_6), 111.5 (C_β), 110.0 (C_3), 101.7 (C_4), 55.5 ($C_5O\underline{C}H_3$), 51.0 ($CO_2\underline{C}H_3$). HPLC-MS (15:95- g.t.5 min) ^tR 4.22 min, *m/z* = 232.37 $[M+H]^+$, calcd. for $[C_{13}H_{11}N_3O_3+H]^+$ 232.25.

(2*E*)-3-(5-Methoxy-1*H*-indol-3-yl)prop-2-enoic acid (1.5)

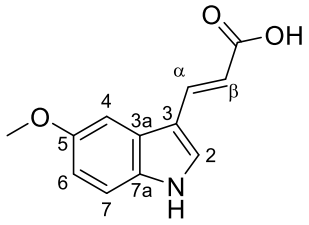

Following the general procedure II by a *Knoevenagel-Doebner* reaction from commercial 5-methoxy-1*H*-indole-3-carbaldehyde (500 mg, 2.8 mmol), the acid **1.5** was afforded as a white solid in 97% yield (600 mg, 2.8 mmol). Mp: 208 - 211 ºC. ^{1}H NMR (300 MHz, DMSO-d_6) δ 11.85 (bs, 1H, OH), 11.60 (s, 1H, NH), 7.86 (d, *J* = 3.0 Hz, 1H, H_2), 7.80 (d, *J* = 16.0 Hz, 1H, H_α), 7.35 (d, *J* = 8.8 Hz, 1H, H_7), 7.26 (d, *J* = 2.5 Hz, 1H, H_4), 6.84 (dd, *J* = 8.7, 2.4 Hz, 1H, H_6), 6.25 (d, *J* = 16.0 Hz, 1H, H_β), 3.82 (s, 3H, CH_3). ^{13}C NMR (75 MHz, DMSO-d_6) δ 168.6 (CO), 154.7 (C_5), 138.5 (C_α), 132.2 (C_{7a}), 131.3 (C_2), 125.7 (C_{3a}), 113.0 (C_7), 112.3 (C_6), 111.5 (C_β), 111.5 (C_3), 101.6 (C_4), 55.4 (CH_3). HPLC-MS (15:95- g.t.5 min) ^tR 3.40 min, *m/z* = 218.26 $[M+H]^+$, calcd. for $[C_{12}H_{11}NO_3+H]^+$ 218.22.

3-(5-Methoxy-1*H*-indol-3-yl)propanoic acid (1.6)

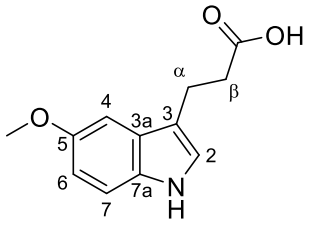

Following the general procedure III of hydrogenation, the saturated acid **1.6** was obtained from the unsaturated acid **1.5** (200 mg, 0.92 mmol), without further purification in quantitative yield (200 mg, 0.91 mmol). Mp: 126 - 129 ºC (lit. 133 - 135 ºC)[148]. ^{1}H NMR (300 MHz, $CDCl_3$) δ 7.86 (bs, 1H), 7.25 (d, *J* = 8.8 Hz, 1H, H_7), 7.04 (d, *J* = 2.5 Hz, 1H, H_4), 7.00 (d, *J* = 2.4 Hz, 1H, H_2), 6.87 (dt, *J* = 9.0, 2.3 Hz, 1H, H_6), 3.87 (s, 3H, CH_3), 3.08 (t, *J* = 7.5 Hz, 2H, H_α), 2.77 (t, *J* = 7.5 Hz, 2H, H_β). ^{13}C NMR (75 MHz, $CDCl_3$) δ 179.1 (CO), 154.2 (C_5), 131.5 (C_{7a}), 127.6 (C_{3a}), 122.4 (C_2), 114.5 (C_3), 112.5 (C_6), 112.0 (C_7),

100.6 (C_4), 56.1 (CH_3), 34.6 (C_β), 20.5 (C_α). HPLC-MS (15:95- g.t.5 min) ^tR 3.47 min, *m/z* = 220.28 $[M+H]^+$, calcd. for $[C_{12}H_{13}NO_3+H]^+$ 220.24.

***N*-oxadiazolone substituted derivatives**

All compounds of this series were synthetized following the general procedure VI from 5-(2-(5-methoxy-1*H*-indol-3-yl)ethyl)-1,3,4-oxadiazol-2(3*H*)-one (**1.1**) and obtained as white solids.

5-[2-(5-Methoxy-1*H*-indol-3-yl)ethyl]-3-methyl-1,3,4-oxadiazol-2(3*H*)-one (1.7)

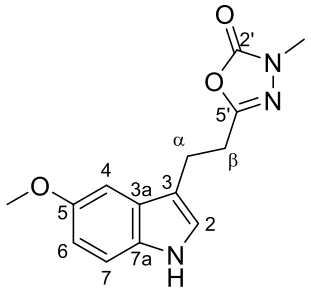

Final compound **1.7** was obtained from **1.1** (150 mg, 0.58 mmol) and CH_3I in 66% yield (106 mg, 0.39 mmol). Chromatography: DCM to DCM:MeOH 95:5. Mp: 83 - 86 ºC. ^1H NMR (500 MHz, $CDCl_3$) δ 7.97 (s, 1H, NH), 7.25 (d, *J* = 8.6 Hz, 1H, H_7), 7.00 (d, *J* = 2.5 Hz, 1H, H_2), 6.99 (d, *J* = 2.4 Hz, 1H, H_4), 6.87 (dd, *J* = 8.7, 2.4 Hz, 1H, H_6), 3.87 (s, 3H, OCH_3), 3.35 (s, 3H, NCH_3), 3.12 (t, *J* = 7.7 Hz, 2H, H_α), 2.92 (t, *J* = 7.7 Hz, 2H, H_β). ^{13}C NMR (126 MHz, $CDCl_3$) δ 155.9 ($C_{5'}$), 154.4 ($C_{2'}$), 154.2 (C_5), 131.5 (C_{7a}), 127.4 (C_{3a}), 122.5 (C_2), 113.6 (C_3), 112.6 (C_6), 112.2 (C_7), 100.3 (C_4), 56.1 (OCH_3), 32.5 (NCH_3), 27.4 (C_β), 21.5 (C_α). HPLC-MS (15:95- g.t.5 min) ^tR 3.97 min, *m/z* = 274.20 $[M+H]^+$, calcd. for $[C_{14}H_{15}N_3O_3+H]^+$ 274.29. HRMS $[ESI^+]$ *m/z* = 273.11145 $[M]^+$, calcd. for $[C_{14}H_{15}N_3O_3]^+$ 273.11134.

3-Ethyl-5-[2-(5-methoxy-1*H*-indol-3-yl)ethyl]-1,3,4-oxadiazol-2(3*H*)-one (1.8)

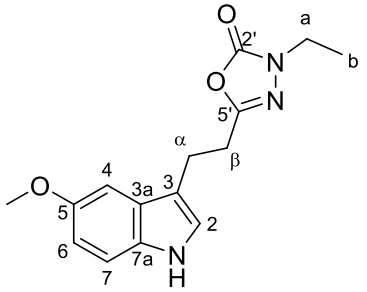

Final derivative **1.8** was obtained from oxadiazolone **1.1** (60 mg, 0.23 mmol) and iodoethane in 56% yield (37 mg, 0.13 mmol). Chromatography: DCM to DCM:MeOH 95:5. Mp: 69 - 72 ºC. ^{1}H NMR (500 MHz, $CDCl_3$) δ 7.90 (s, 1H, NH), 7.26 (d, *J* = 8.8 Hz, 1H, H_7), 7.01 (d, *J* = 2.5 Hz, 1H, H_2), 6.99 (d, *J* = 2.3 Hz, 1H, H_4), 6.87 (dd, *J* = 8.8, 2.4 Hz, 1H, H_6), 3.87 (s, 3H, OCH_3), 3.71 (q, *J* = 7.2 Hz, 2H, H_a), 3.15 – 3.11 (m, 2H, H_α), 2.95 – 2.90 (m, 2H, H_β), 1.28 (t, *J* = 7.2 Hz, 3H, H_b). ^{13}C NMR (126 MHz, $CDCl_3$) δ 155.9 ($C_{5'}$), 154.3 (C_5), 154.0 ($C_{2'}$), 131.5 (C_{7a}), 127.5 (C_{3a}), 122.5 (C_2), 113.8 (C_3), 112.7 (C_6), 112.1 (C_7), 100.3 (C_4), 56.1 (OCH_3), 40.8 (C_a), 27.6 (C_β), 21.6 (C_α), 13.5 (C_b). HPLC-MS (15:95-g.t.5 min) ^{t}R 4.21 min, *m/z* = 288.15 $[M+H]^+$, calcd. for $[C_{15}H_{17}N_3O_3+H]^+$ 288.32. HRMS [ESI$^+$] *m/z* = 287.1275$[M]^+$, calcd. for $[C_{15}H_{17}N_3O_3]^+$ 287.12699.

5-[2-(5-Methoxy-1*H*-indol-3-yl)ethyl]-3-propyl-1,3,4-oxadiazol-2(3*H*)-one (1.9)

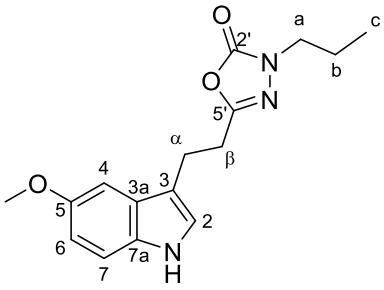

Final compound **1.9** was obtained from **1.1** (60 mg, 0.23 mmol) and 1-iodopropane in 49% yield (34 mg, 0.11 mmol). Chromatography: DCM to DCM:MeOH 95:5. Mp: 95 – 98 ºC. ^{1}H NMR (500 MHz, DMSO-d_6) δ 10.67 (s, 1H, NH), 7.21 (dd, *J* = 8.7, 0.5 Hz, 1H, H_7), 7.11 (d, *J* = 2.5 Hz, 1H, H_2), 6.97 (d, *J* = 2.4 Hz, 1H, H_4), 6.70 (dd, *J* = 8.8, 2.4 Hz, 1H, H_6), 3.75 (s, 3H, OCH_3), 3.53 (t, *J* = 6.8 Hz, 2H, H_a), 3.00 (t, *J* = 7.4 Hz, 2H, H_α), 2.90 (t, *J* = 7.5 Hz, 2H, H_β), 1.57 (h, *J* = 7.2 Hz, 2H, H_b), 0.78 (t, *J* = 7.4 Hz, 3H, H_c). ^{13}C NMR (126 MHz, DMSO-d_6) δ 155.6 ($C_{5'}$), 153.5 ($C_{2'}$), 153.0 (C_5), 131.3 (C_{7a}), 127.1 (C_{3a}), 123.3 (C_2),

112.1 (C_7), 111.9 (C_3), 111.2 (C_6), 99.7 (C_4), 55.3 (OCH_3), 46.4 (C_a), 26.9 (C_β), 21.0 (C_b), 20.8 (C_α), 10.6 (C_c). HPLC-MS (15:95- g.t.5 min) ^tR 4.48 min, *m/z* = 302.28 $[M+H]^+$, calcd. for $[C_{16}H_{19}N_3O_3+H]^+$ 302.35. HRMS $[ESI^+]$ *m/z* = 301.14327 $[M]^+$, calcd. for $[C_{16}H_{19}N_3O_3]^+$ 301.14264.

3-butyl-5-[2-(5-methoxy-1*H*-indol-3-yl)ethyl]-1,3,4-oxadiazol-2(3*H*)-one (1.10)

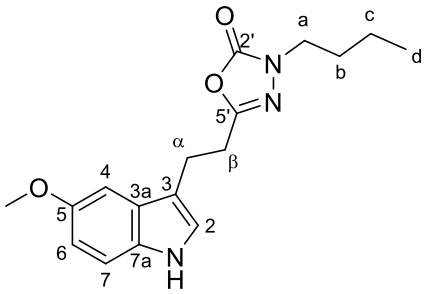

Final compound **1.10** was obtained from **1.1** (80 mg, 0.31 mmol) and 1-chlorobutane in 92% yield (90 mg, 0.28 mmol). Chromatography: DCM. Mp: 64 - 65 ºC. ^{1}H NMR (500 MHz, DMSO-d_6) δ 10.67 (s, 1H, NH), 7.21 (d, *J* = 8.7 Hz, 1H, H_7), 7.10 (d, *J* = 2.4 Hz, 1H, H_2), 6.96 (d, *J* = 2.5 Hz, 1H, H_4), 6.70 (dd, *J* = 8.7, 2.4 Hz, 1H, H_6), 3.75 (s, 3H, OCH_3), 3.55 (t, *J* = 6.9 Hz, 2H, H_a), 3.00 (t, *J* = 7.4 Hz, 2H, H_α), 2.91 (t, *J* = 7.5 Hz, 2H, H_β), 1.52 (p, *J* = 7.0 Hz, 2H, H_b), 1.17 (h, *J* = 7.4 Hz, 2H, H_c), 0.83 (t, *J* = 7.4 Hz, 3H, H_d). ^{13}C NMR (126 MHz, DMSO-d_6) δ 155.6 ($C_{5'}$), 153.4 ($C_{2'}$), 153.0 (C_5), 131.3 (C_{7a}), 127.1 (C_{3a}), 123.3 (C_2), 112.1 (C_7), 111.9 (C_3), 111.2 (C_6), 99.7 (C_4), 55.3 (OCH_3), 44.4 (C_a), 29.5 (C_b), 26.9 (C_β), 20.8 (C_α), 18.8 (C_c), 13.3 (C_d). HPLC-MS (15:95- g.t.5 min) ^tR 4.79 min, *m/z* = 316.11 $[M+H]^+$, calcd. for $[C_{17}H_{21}N_3O_3+H]^+$ 316.37. HRMS $[ESI^+]$ *m/z* = 315.15838 $[M]^+$, calcd. for $[C_{17}H_{21}N_3O_3]^+$ 315.15829.

5-[2-(5-Methoxy-1*H*-indol-3-yl)ethyl]-3-pentyl-1,3,4-oxadiazol-2(3*H*)-one (1.11)

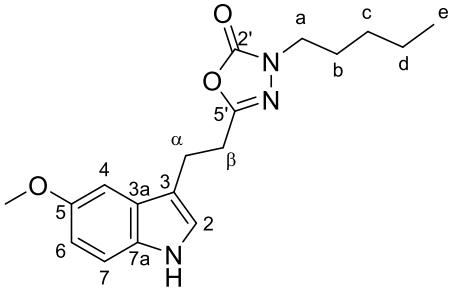

Final compound **1.11** was obtained from **1.1** (80 mg, 0.31 mmol) and tosylate **1.21** in 90% yield (92 mg, 0.28 mmol). Chromatography: DCM. Mp: 48 - 51 ºC. ^{1}H NMR (500 MHz,

$CDCl_3$) δ 7.90 (s, 1H, NH), 7.25 (d, *J* = 8.5 Hz, 1H, H_7), 7.01 (d, *J* = 2.5 Hz, 1H, H_2), 6.99 (d, *J* = 2.4 Hz, 1H, H_4), 6.87 (dd, *J* = 8.8, 2.5 Hz, 1H, H_6), 3.87 (s, 3H, OCH_3), 3.63 (t, *J* = 7.2 Hz, 2H, H_a), 3.13 (t, *J* = 7.4 Hz, 2H, H_α), 2.92 (t, *J* = 7.5 Hz, 2H, H_β), 1.67 (p, *J* = 7.3 Hz, 2H, H_b), 1.36 – 1.30 (m, 2H, H_d), 1.30 – 1.21 (m, 2H, H_c), 0.89 (t, *J* = 7.2 Hz, 3H, H_e). ^{13}C NMR (126 MHz, $CDCl_3$) δ 155.8 ($C_{5'}$), 154.3 (C_5), 154.3 ($C_{2'}$), 131.5 (C_{7a}), 127.5 (C_{3a}), 122.5 (C_2), 113.7 (C_3), 112.7 (C_6), 112.1 (C_7), 100.3 (C_4), 56.1 (OCH_3), 45.8 (C_a), 28.6 (C_c), 27.9 (C_b), 27.6 (C_β), 22.3 (C_d), 21.6 (C_α), 14.1 (C_e). HPLC-MS (30:95- g.t.5 min) ^{t}R 4.60 min, (50:95- g.t.5 min) ^{t}R 3.17 min, *m/z* = 330.13 $[M+H]^+$, calcd. for $[C_{18}H_{23}N_3O_3+H]^+$ 330.40. HRMS $[ESI^+]$ *m/z* = 329.17515 $[M]^+$, calcd. for $[C_{18}H_{23}N_3O_3]^+$ 329.17394.

3-Hexyl-5-[2-(5-methoxy-1*H*-indol-3-yl)ethyl]-1,3,4-oxadiazol-2(3*H*)-one (1.12)

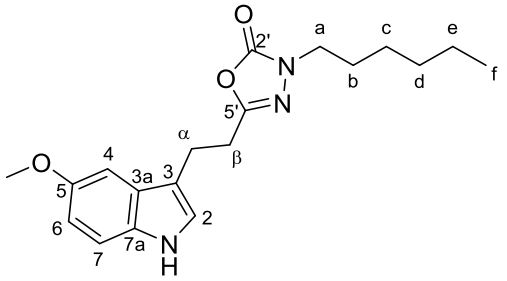

Final compound **1.12** was obtained from **1.1** (80 mg, 0.31 mmol) and tosylate **1.22** in 70% yield (74 mg, 0.22 mmol), as a colorless oil. Chromatography: hexane to DCM. ^{1}H NMR (500 MHz, MeOD) δ 7.20 (d, *J* = 8.7 Hz, 1H, H_7), 7.03 (bs, 1H, H_2), 6.95 (d, *J* = 2.4 Hz, 1H, H_4), 6.74 (dd, *J* = 8.8, 2.4 Hz, 1H, H_6), 3.82 (s, 3H, OCH_3), 3.57 (t, *J* = 6.9 Hz, 2H, H_a), 3.11 (t, *J* = 7.2 Hz, 2H, H_α), 2.92 (t, *J* = 7.2 Hz, 2H, H_β), 1.56 (p, *J* = 7.0 Hz, 2H, H_b), 1.30 – 1.21 (m, 4H, H_d, H_e), 1.20 – 1.10 (m, 2H, H_c), 0.88 (t, *J* = 6.9 Hz, 3H, H_f). ^{13}C NMR (126 MHz, MeOD) δ 157.6 ($C_{5'}$), 156.0 ($C_{2'}$), 155.1 (C_5), 133.3 (C_{7a}), 128.7 (C_{3a}), 124.1 (C_2), 113.6 (C_3), 113.0 (C_7), 112.8 (C_6), 100.7 (C_4), 56.2 (OCH_3), 46.4 (C_a), 32.3 (C_d), 28.9 (C_b), 28.7 (C_β), 26.9 (C_c), 23.5 (C_e), 22.4 (C_α), 14.3 (C_f). HPLC-MS (50:95- g.t.5 min) ^{t}R 3.77 min, *m/z* = 344.38 $[M+H]^+$, calcd. for $[C_{19}H_{25}N_3O_3+H]^+$ 344.43. HRMS $[ESI^+]$ *m/z* = 343.18957 $[M]^+$, calcd. for $[C_{19}H_{25}N_3O_3]^+$ 343.18959.

3-Heptyl-5-[2-(5-methoxy-1*H*-indol-3-yl)ethyl]-1,3,4-oxadiazol-2(3*H*)-one (1.13)

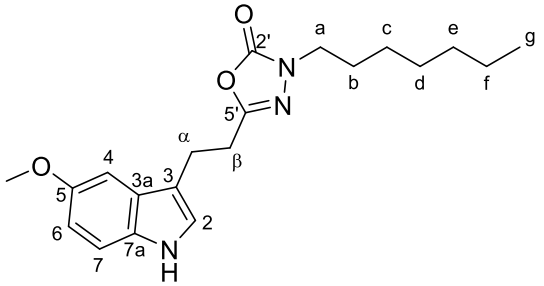

Final compound **1.13** was obtained from **1.1** (80 mg, 0.31 mmol) and 1-iodoheptane in 85% yield (94 mg, 0.26 mmol), as a yellow oil. Chromatography: hexane to DCM. ^{1}H NMR (300 MHz, $CDCl_3$) δ 7.95 (s, 1H, NH), 7.25 (d, *J* = 8.9 Hz, 1H, H_7), 7.02 – 6.95 (m, 2H, H_2, H_4), 6.86 (dd, *J* = 8.8, 2.4 Hz, 1H, H_6), 3.87 (s, 3H, OCH_3), 3.63 (t, *J* = 7.2 Hz, 2H, H_a), 3.13 (dd, *J* = 8.6, 6.3 Hz, 2H, H_α), 2.92 (dd, *J* = 8.6, 6.4 Hz, 2H, H_β), 1.67 (p, *J* = 7.3 Hz, 2H, H_b), 1.34 – 1.19 (m, 8H, H_c, H_d, H_e, H_f), 0.88 (t, *J* = 6.7 Hz, 3H, H_g). ^{13}C NMR (75 MHz, $CDCl_3$) δ 155.9 ($C_{5'}$), 154.3 (C_5), 154.3 ($C_{2'}$), 131.5 (C_{7a}), 127.5 (C_{3a}), 122.5 (C_2), 113.7 (C_3), 112.6 (C_6), 112.1 (C_7), 100.3 (C_4), 56.1 (OCH_3), 45.8 (C_a), 31.8 (C_e), 28.9 (C_d), 28.2 (C_b), 27.6 (C_β), 26.4 (C_c), 22.7 (C_f), 21.6 (C_α), 14.2 (C_g). HPLC-MS (70:95- g.t.5 min) ^{t}R 1.56 min, *m/z* = 358.25 $[M+H]^+$, calcd. for $[C_{20}H_{27}N_3O_3+H]^+$ 358.45. HRMS [ESI$^+$] *m/z* = 357.2056 $[M]^+$, calcd. for $[C_{20}H_{27}N_3O_3]^+$ 357.20524.

5-[2-(5-Methoxy-1*H*-indol-3-yl)ethyl]-3-(propan-2-yl)-1,3,4-oxadiazol-2(3*H*)-one (1.14)

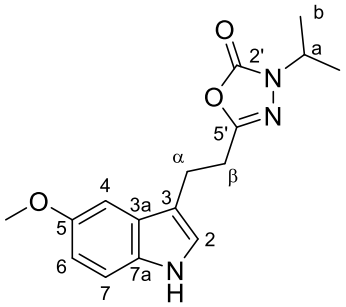

Final compound **1.14** was obtained from **1.1** (80 mg, 0.31 mmol) and 2-bromopropane in 81% yield (76 mg, 0.25 mmol). Chromatography: DCM. Mp: 130 - 133 ºC. ^{1}H NMR (500 MHz, $CDCl_3$) δ 7.88 (bs, 1H, NH), 7.25 (d, *J* = 7.8 Hz, 1H, H_7), 7.01 (d, *J* = 2.4 Hz, 1H, H_2), 6.99 (d, *J* = 2.4 Hz, 1H, H_4), 6.86 (dd, *J* = 8.8, 2.4 Hz, 1H, H_6), 4.25 – 4.21 (m, 1H, H_a), 3.87 (s, 3H, OCH_3), 3.13 (dd, *J* = 7.6 Hz, 2H, H_α), 2.92 (dd, *J* = 7.7 Hz, 2H, H_β), 1.30 (d, *J* = 6.7 Hz, 6H, H_b). ^{13}C NMR (126 MHz, $CDCl_3$) δ 155.8 ($C_{5'}$), 154.3 (C_5), 153.6 ($C_{2'}$),

131.5 (C_{7a}), 127.6 (C_{3a}), 122.5 (C_2), 113.9 (C_3), 112.7 (C_6), 112.1 (C_7), 100.3 (C_4), 56.1 (OCH_3), 47.9 (C_a), 27.7 (C_β), 21.6 (C_α), 20.8 (C_b). HPLC-MS (15:95- g.t.5 min) ^tR 4.49 min, *m/z* = 302.35 $[M+H]^+$, calcd. for $[C_{16}H_{19}N_3O_3+H]^+$ 302.35. HRMS $[ESI^+]$ *m/z* = 301.14244 $[M]^+$, calcd. for $[C_{16}H_{19}N_3O_3]^+$ 301.14264.

5-[2-(5-Methoxy-1*H*-indol-3-yl)ethyl]-3-(2-methylpropyl)-1,3,4-oxadiazol-2(3*H*)-one (1.15)

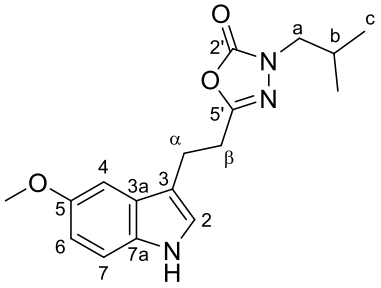

Final compound **1.15** was obtained from **1.1** (80 mg, 0.31 mmol) and 1-chloro-2-methylpropane in 82% yield (80 mg, 0.25 mmol). Chromatography: DCM. Mp: 54 - 56 ºC. ^1H NMR (500 MHz, DMSO-*d*$_6$) δ 10.67 (s, 1H, NH), 7.21 (d, *J* = 8.7 Hz, 1H, H_7), 7.10 (d, *J* = 2.4 Hz, 1H, H_2), 6.97 (d, *J* = 2.4 Hz, 1H, H_4), 6.70 (dd, *J* = 8.7, 2.4 Hz, 1H, H_6), 3.75 (s, 3H, OCH_3), 3.37 (d, *J* = 7.1 Hz, 2H, H_a), 3.00 (t, *J* = 7.3 Hz, 2H, H_α), 2.91 (t, *J* = 7.2 Hz, 2H, H_β), 1.90 – 1.87 (m, 1H, H_b), 0.79 (d, *J* = 6.7 Hz, 6H, H_c). ^{13}C NMR (126 MHz, DMSO-*d*$_6$) δ 155.6 ($C_{5'}$), 153.7 ($C_{2'}$), 153.0 (C_5), 131.3 (C_{7a}), 127.1 (C_{3a}), 123.3 (C_2), 112.1 (C_7), 111.9 (C_3), 111.2 (C_6), 99.7 (C_4), 55.3 (OCH_3), 51.8 (C_a), 27.4 (C_b), 26.9 (C_β), 20.8 (C_α), 19.4 (C_c). HPLC-MS (15:95- g.t.5 min) ^tR 4.77 min, *m/z* = 316.34 $[M+H]^+$, calcd. for $[C_{17}H_{21}N_3O_3+H]^+$ 316.37. HRMS $[ESI^+]$ *m/z* = 315.15958 $[M]^+$, calcd. for $[C_{17}H_{21}N_3O_3]^+$ 315.15829.

3-(Cyclopropylmethyl)-5-[2-(5-methoxy-1*H*-indol-3-yl)ethyl]-1,3,4-oxadiazol-2(3*H*)-one (1.16)

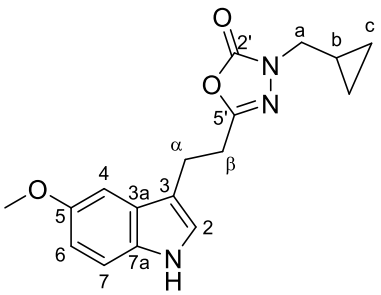

Final compound **1.16** was obtained from **1.1** (80 mg, 0.31 mmol) and (bromomethyl)cyclopropane in 88% yield (85 mg, 0.27 mmol). Chromatography: DCM. Mp: 94 - 97 ºC. ^{1}H NMR (500 MHz, $CDCl_3$) δ 7.89 (s, 1H, NH), 7.26 (d, *J* = 8.8 Hz, 1H, H_7), 7.02 (d, *J* = 2.4 Hz, 1H, H_2), 7.00 (d, *J* = 2.7 Hz, 1H, H_4), 6.87 (dd, *J* = 8.8, 2.4 Hz, 1H, H_6), 3.87 (s, 3H, CH_3), 3.52 (d, *J* = 7.2 Hz, 2H, H_a), 3.13 (q, *J* = 7.0 Hz, 2H, H_α), 2.96 – 2.90 (m, 2H, H_β), 1.19 – 1.09 (m, 1H, H_b), 0.57 – 0.51 (m, 2H, H_c), 0.34 (dt, *J* = 6.2, 4.8 Hz, 2H, H_c). ^{13}C NMR (126 MHz, $CDCl_3$) δ 155.9 ($C_{2'}$), 155.8 ($C_{5'}$), 154.3 (C_5), 131.5 (C_{7a}), 127.5 (C_{3a}), 122.5 (C_2), 113.8 (C_3), 112.7 (C_6), 112.1 (C_7), 100.3 (C_4), 56.1 (CH_3), 50.5 (C_a), 27.5 (C_β), 21.6 (C_α), 10.0 (C_b), 3.6 (C_c). HPLC-MS (15:95- g.t.5 min) ^{t}R 4.57 min, *m/z* = 314.03 $[M+H]^+$, calcd. for $[C_{17}H_{19}N_3O_3+H]^+$ 314.36. HRMS $[ESI^+]$ *m/z* = 313.14324 $[M]^+$, calcd. for $[C_{17}H_{19}N_3O_3]^+$ 313.14264.

3-(Cyclobutylmethyl)-5-[2-(5-methoxy-1*H*-indol-3-yl)ethyl]-1,3,4-oxadiazol-2(3*H*)-one (1.17)

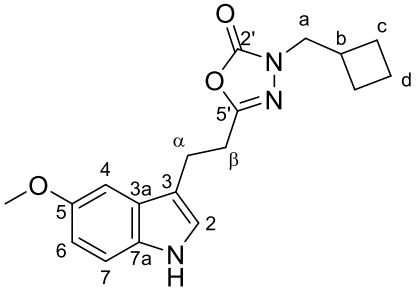

Final compound **1.17** was obtained from **1.1** (80 mg, 0.31 mmol) and (bromomethyl)cyclobutane in 75% yield (76 mg, 0.23 mmol). Chromatography: hexane to DCM. Mp: 74 - 76 ºC. ^{1}H NMR (500 MHz, $CDCl_3$) δ 7.88 (bs, 1H, NH), 7.25 (d, *J* = 8.0 Hz, 1H, H_7), 7.00 (d, *J* = 2.4 Hz, 1H, H_2), 6.99 (d, *J* = 2.5 Hz, 1H, H_4), 6.87 (dd, *J* = 8.8, 2.4 Hz, 1H, H_6), 3.87 (s, 3H, CH_3), 3.66 (d, *J* = 7.3 Hz, 2H, H_a), 3.12 (dd, *J* = 8.6, 6.7 Hz, 2H, H_α), 2.91 (dd, *J* = 8.4, 6.9 Hz, 2H, H_β), 2.68 (p, *J* = 7.7 Hz, 1H, H_b), 2.06 – 1.96 (m, 2H, H_c), 1.93 – 1.83 (m, 2H, d), 1.81 – 1.69 (m, 2H, H_c). ^{13}C NMR (126 MHz, $CDCl_3$) δ 155.7 ($C_{5'}$), 154.5 ($C_{2'}$), 154.3 (C_5), 131.5 (C_{7a}), 127.5 (C_{3a}), 122.5 (C_2), 100.3 (C_4), 56.1 (CH_3), 50.6 (C_a), 34.3 (C_b), 27.6 (C_β), 25.7 (C_c), 21.5 (C_α), 18.3 (C_d). HPLC-MS (50:95- g.t.5 min) ^{t}R 2.35 min, *m/z* = 328.37 $[M+H]^+$, calcd. for $[C_{18}H_{21}N_3O_3+H]^+$ 328.38. HRMS $[ESI^+]$ *m/z* = 327.15892 $[M]^+$, calcd. for $[C_{18}H_{21}N_3O_3]^+$ 327.15829.

3-(Cyclopentylmethyl)-5-[2-(5-methoxy-1*H*-indol-3-yl)ethyl]-1,3,4-oxadiazol-2(3*H*)-one (1.18)

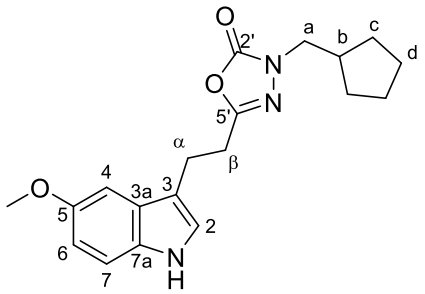

Final compound **1.18** was obtained from **1.1** (80 mg, 0.31 mmol) and (bromomethyl)cyclopentane in 72% yield (76 mg, 0.22 mmol). Chromatography: hexane to DCM. Mp: 81 - 84 ºC. ^{1}H NMR (500 MHz, $CDCl_3$) δ 7.88 (bs, 1H, NH), 7.25 (d, *J* = 8.8 Hz, 1H, H_7), 7.01 (d, *J* = 2.5 Hz, 1H, H_2), 6.99 (d, *J* = 2.4 Hz, 1H, H_4), 6.86 (dd, *J* = 8.8, 2.4 Hz, 1H, H_6), 3.87 (s, 3H, CH_3), 3.56 (d, *J* = 7.4 Hz, 2H, H_a), 3.13 (t, *J* = 7.6 Hz, 2H, H_α), 2.92 (t, *J* = 7.6 Hz, 2H, H_β), 2.29 (p, *J* = 7.6 Hz, 1H, H_b), 1.70 – 1.59 (m, 4H, H_d, H_c), 1.58 – 1.50 (m, 2H, H_d), 1.27 – 1.16 (m, 2H, H_c). ^{13}C NMR (126 MHz, $CDCl_3$) δ 155.7 ($C_{5'}$), 154.5 ($C_{2'}$), 154.3 (C_5), 131.5 (C_{7a}), 127.5 (C_{3a}), 122.5 (C_2), 113.7 (C_3), 112.7 (C_6), 112.1 (C_7), 100.3 (C_4), 56.1 (CH_3), 50.5 (C_a), 39.0 (C_b), 30.1 (C_c), 27.6 (C_β), 25.2 (C_d), 21.6 (C_α). HPLC-MS (50:95- g.t.5 min) ^{t}R 3.14 min, *m/z* = 342.20 $[M+H]^+$, calcd. for $[C_{19}H_{23}N_3O_3+H]^+$ 342.41. HRMS [ESI$^+$] *m/z* = 341.17482 $[M]^+$, calcd. for $[C_{19}H_{23}N_3O_3]^+$ 341.17394.

3-Benzyl-5-[2-(5-methoxy-1*H*-indol-3-yl)ethyl]-1,3,4-oxadiazol-2(3*H*)-one (1.19)

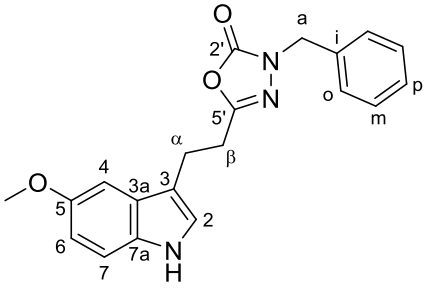

Final compound **1.19** was obtained from **1.1** (80 mg, 0.31 mmol) and benzyl bromide in 57% yield (62 mg, 0.18 mmol). Chromatography: DCM. Mp: 118 - 121 ºC. ^{1}H NMR (500 MHz, $CDCl_3$) δ 7.85 (s, 1H, NH), 7.38 – 7.33 (m, 2H, H_o), 7.32 – 7.30 (m, 1H, H_p), 7.30 – 7.21 (m, 3H, H_m, H_7), 6.98 (d, *J* = 2.4 Hz, 1H, H_4), 6.94 (s, 1H, H_2), 6.87 (dd, *J* = 8.7, 2.4

Hz, 1H, H_6), 4.81 (s, 2H, H_a), 3.86 (s, 3H, CH_3), 3.11 (t, *J* = 7.6 Hz, 2H, H_α), 2.90 (t, *J* = 7.6 Hz, 2H, H_β). ^{13}C NMR (126 MHz, $CDCl_3$) δ 156.1 ($C_{5'}$), 154.3 (C_5), 154.2 ($C_{2'}$), 135.1 (C_i), 131.4 (C_{7a}), 129.0 (C_o), 128.4 (C_p), 128.3 (C_m), 127.4 (C_{3a}), 122.5 (C_2), 113.6 (C_3), 112.7 (C_6), 112.1 (C_7), 100.2 (C_4), 56.0 (CH_3), 49.5 (C_a), 27.6 (C_β), 21.5 (C_α). HPLC-MS (30:95- g.t.5 min) ^{t}R 4.23 min, *m/z* = 350.26 $[M+H]^+$, calcd. for $[C_{20}H_{19}N_3O_3+H]^+$ 350.14. HRMS $[ESI^+]$ *m/z* = 349.14257$[M]^+$, calcd. for $[C_{20}H_{19}N_3O_3]^+$ 349.14264.

5-[2-(5-Methoxy-1*H*-indol-3-yl)ethyl]-3-(3-phenylpropyl)-1,3,4-oxadiazol-2(3*H*)-one (1.20)

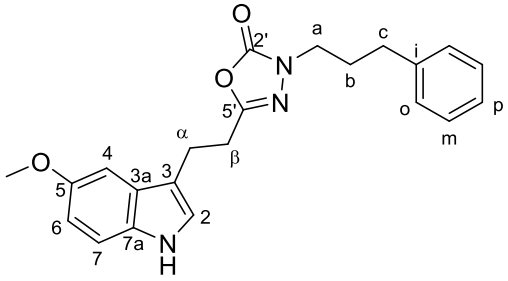

Final compound **1.20** was obtained from **1.1** (80 mg, 0.31 mmol) and (3-bromopropyl)benzene in 92% yield (108 mg, 0.28 mmol), as a brown oil. Chromatography: hexane to hexane:DCM 8:2. ^{1}H NMR (500 MHz, $CDCl_3$) δ 7.85 (s, 1H, NH), 7.32 – 7.09 (m, 6H, H_7, H_o, H_m, H_p), 6.98 (bs, 2H, H_2, H_4), 6.85 (dd, *J* = 8.8, 2.5 Hz, 1H, H_6), 3.86 (s, 3H, CH_3), 3.68 (t, *J* = 7.0 Hz, 2H, H_a), 3.12 (dd, *J* = 8.6, 6.4 Hz, 2H, H_α), 2.91 (dd, *J* = 8.3, 6.4 Hz, 2H, H_β), 2.58 (t, *J* = 7.6 Hz, 2H, H_c), 2.00 (p, *J* = 7.2 Hz, 2H, H_b). ^{13}C NMR (125 MHz, $CDCl_3$) δ 155.9 ($C_{5'}$), 154.3 (C_5), 154.2 ($C_{2'}$), 140.9 (C_i), 131.5 (C_{7a}), 128.6 (C_{Ar}), 128.5 (C_{Ar}), 126.3 (C_p), 122.5 (C_2), 113.7 (C_3), 112.7 (C_6), 112.1 (C_7), 100.3 (C_4), 56.1 (CH_3), 45.2 (C_a), 32.7 (C_c), 29.7 (C_b), 27.6 (C_β), 21.5 (C_α). HPLC-MS (50:95- g.t.5 min) ^{t}R 3.42 min, *m/z* = 378.31$[M+H]^+$, calcd. for $[C_{22}H_{23}N_3O_3+H]^+$ 378.44. HRMS $[ESI^+]$ *m/z* = 377.1737$[M]^+$, calcd. for $[C_{22}H_{23}N_3O_3]^+$ 377.17394.

Synthesis of tosylates: pentyl 4-methylbenzene-1-sulfonate (**1.21**) and hexyl 4-methylbenzene-1-sulfonate (**1.22**) (adapted from Ref.[149,150])

To a solution of the corresponding alcohol (1 equiv) in dry DCM (9.5 mL/mmol) at -20 ºC and under N_2 atmosphere, TsCl (1.5 equiv) and anhydrous pyridine (0.5 mL/mmol) were added. The reaction mixture was allowed to warm to rt overnight. Then, concentrated HCl was carefully added and the resulting solution was extracted with EtOAc (x3). The combined organic extracts were sequentially washed with H_2O and brine, dried over $MgSO_4$, filtered, and evaporated under reduced pressure to give the corresponding tosylate, without further purification. The spectroscopic data correspond with those previously reported.

Oxadiazolamine derivatives

5-[2-(5-Methoxy-1*H*-indol-3-yl)ethyl]-*N*-methyl-1,3,4-oxadiazol-2-amine (1.23)

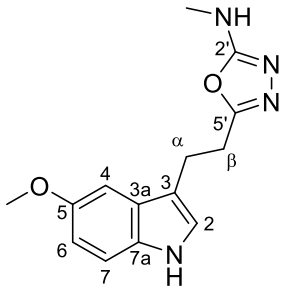

(Adapted from Ref.[151]) To a solution of **1.1** (150 mg, 0.58 mmol) in 5.8 mL (10 mL/mmol) of anhydrous DMF, TEA (162 µL, 1.16 mmol, 2 equiv), BOP (282 mg, 0.64 mmol, 1.1 equiv) and methyl amine (580 µL of a 2M solution in THF) were slowly added. The mixture was stirred at rt for 2 h. The solvent was removed under reduced pressure. The crude was extracted with EtOAc (x3) and washed with H_2O (x2) and brine. The organic layers were joined, dried over $MgSO_4$ and the solvent was evaporated. The crude was purified by flash chromatography (DCM to DCM:MeOH 9:1) and washed with hexane to afford the final compound **1.23** in 18% yield (29 mg, 0.11 mmol). Mp: 145 - 148 ºC. ^{1}H NMR (500 MHz, DMSO-d_6) δ 10.65 (bs, 1H, NH_{indole}), 7.24 (t, J = 4.9 Hz, 1H, N<u>H</u>CH_3), 7.21 (d, J = 8.9 Hz, 1H, H_7), 7.08 (d, J = 2.5 Hz, 1H, H_2), 6.93 (d, J = 2.5 Hz, 1H, H_4), 6.70 (dd, J = 8.7, 2.4 Hz, 1H, H_6), 3.75 (s, 3H, OCH_3), 2.99 (m, 4H, H_α, H_β), 2.75 (d, J = 4.9 Hz, 3H, NHC<u>H</u>$_3$). ^{13}C NMR (126 MHz, DMSO-d_6) δ 164.0 ($C_{2'}$), 159.5 ($C_{5'}$), 153.0 (C_5), 131.3

(C_{7a}), 127.1 (C_{3a}), 123.2 (C_2), 112.4 (C_3), 112.0 (C_7), 111.2 (C_6), 99.8 (C_4), 55.3 (OCH_3), 29.0 ($NHCH_3$), 25.8 (C_β), 22.0 (C_α). HPLC-MS (15:95- g.t.5 min) ^tR 3.17 min, *m/z* = 273.34 $[M+H]^+$, calcd. for $[C_{14}H_{16}N_4O_2+H]^+$ 273.31. HRMS $[ESI^+]$ *m/z* = 272.12816 $[M]^+$, calcd. for $[C_{14}H_{16}N_4O_2]^+$ 272.12733.

_N_-Ethyl-5-[2-(5-methoxy-1_H_-indol-3-yl)ethyl]-1,3,4-oxadiazol-2-amine (1.24)

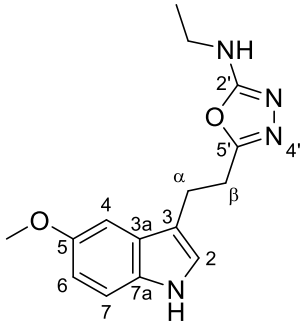

Ethyl derivate **1.24** (85 mg, 0.33 mmol) was synthesized from **1.1** following the same procedure as **1.23**. In this case, a flash chromatography (DCM to DCM:MeOH 9:1) and semi preparative HPLC (20:80 g.t. 60 min, isocratic gradient) were necessary to purified it, obtaining **1.23** in 6% yield (6 mg, 0.02 mmol). ^1H NMR (500 MHz, DMSO-d_6) δ 10.65 (bs, 1H, NH_{indole}), 7.32 (t, *J* = 5.6 Hz, 1H, N<u>H</u>CH_2), 7.21 (dd, *J* = 8.7, 0.5 Hz, 1H, H_7), 7.09 (d, *J* = 2.3 Hz, 1H, H_2), 6.94 (d, *J* = 2.4 Hz, 1H, H_4), 6.70 (dd, *J* = 8.7, 2.4 Hz, 1H, H_6), 3.75 (s, 3H, OCH_3), 3.15 (qd, *J* = 7.2, 5.6 Hz, 2H, C<u>H</u>$_2CH_3$), 3.04 – 2.95 (m, 4H, 4H, H_α, H_β), 1.11 (t, *J* = 7.2 Hz, 3H, CH_2C<u>H</u>$_3$). ^{13}C NMR (126 MHz, DMSO-d_6) δ 163.3 ($C_{2'}$), 159.3 ($C_{5'}$), 153.0 (C_5), 131.3 (C_{7a}), 127.2 (C_{3a}), 123.2 (C_2), 112.4 (C_3), 112.0 (C_7), 111.2 (C_6), 99.8 (C_4), 55.3 (OCH_3), 37.3 (<u>C</u>H_2CH_3), 25.8 (C_β), 22.0 (C_α), 14.5 (CH_2<u>C</u>H_3). HPLC-MS (15:95- g.t.5 min) ^tR 3.53 min, *m/z* = 287.11 $[M+H]^+$, calcd. for $[C_{19}H_{25}N_3O_3+H]^+$ 287.34. HRMS $[ESI^+]$ *m/z* = 286.14359 $[M]^+$, calcd. for $[C_{15}H_{18}N_4O_2]^+$ 286.14298.

Linker modification

5-[(*E*)-2-(5-Methoxy-1*H*-indol-3-yl)ethenyl]-1,3,4-oxadiazol-2(3*H*)-one (1.27)

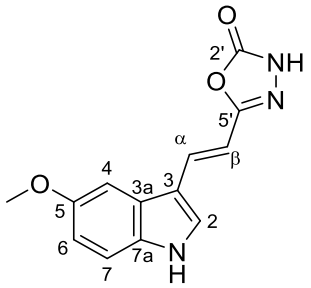

Acid **1.5** (500 mg, 2.30 mmol) was transformed into the corresponding hydrazide following experimental procedure IV without isolation, identified by HPLC-MS (15:95- g.t.5), ^{t}R 1.99 min, *m/z* = 232.39 $[M+H]^+$, calcd. for $[C_{12}H_{13}N_3O_2+H]^+$ 232.26, which was reacted with CDI following procedure V to obtain the oxadiazolone **1.27** in 85% yield (502 mg, 1.95 mmol). Chromatography: hexane to hexane:EtOAc 1:1. Mp: 206 - 209 ºC. ^{1}H NMR (500 MHz, DMSO-*d*$_6$) δ 11.53 (bs, 1H, NH_{indole}), 7.85 (d, *J* = 2.8 Hz, 1H, H_2), 7.49 (d, *J* = 16.4 Hz, 1H, H_α), 7.34 (d, *J* = 2.7 Hz, 1H, H_4), 7.34 (d, *J* = 8.5 Hz, 1H, H_7), 6.82 (dd, *J* = 8.8, 2.3 Hz, 1H, H_6), 6.59 (d, *J* = 16.4 Hz, 1H, H_β), 3.82 (s, 3H, CH_3). ^{13}C NMR (126 MHz, DMSO-*d*$_6$) δ 155.4 ($C_{5'}$), 154.6 (C_5), 154.4 ($C_{2'}$), 132.0 (C_{7a}), 131.1 (C_α), 129.7 (C_2), 125.5 (C_{3a}), 112.9 (C_7), 112.3 (C_6), 111.9 (C_3), 103.9 (C_β), 101.5 (C_4) 55.5 (CH_3). HPLC-MS (15:95- g.t.10 min) ^{t}R 4.95 min, *m/z* = 258.32 $[M+H]^+$, calcd. for $[C_{13}H_{11}N_3O_3+H]^+$ 258.25. HRMS [ESI$^+$] *m/z* = 257.08107 $[M]^+$, calcd. for $[C_{13}H_{11}N_3O_3]^+$ 257.08004.

Ethyl (2*E*)-3-(5-methoxy-1*H*-indol-3-yl)-2-methylprop-2-enoate (1.28)

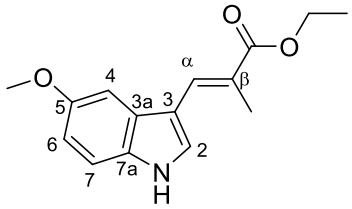

Following the general procedure I of *Wittig* reaction, the ester **1.28** was obtained from the commercial 5-methoxy-1*H*-indole-3-carbaldehyde (1000 mg, 5.7 mmol), in 95% yield (1400 mg, 5.40 mmol). Chromatography: hexane to hexane: EtOAc 1:1. Mp: 116 - 117 ºC. ^{1}H NMR (500 MHz, DMSO-*d*$_6$) δ 11.65 (s, 1H, NH), 7.92 (s, 1H, H_α), 7.71 (s, 1H, H_2), 7.36 (d, *J* = 8.7 Hz, 1H, H_7), 7.17 (d, *J* = 2.4 Hz, 1H, H_4), 6.84 (dd, *J* = 8.7, 2.4 Hz, 1H,

H_6), 4.20 (q, *J* = 7.1 Hz, 2H, CH_2), 3.81 (s, 3H, OCH_3), 2.11 (s, 3H, $C_\beta CH_3$), 1.29 (t, *J* = 7.1 Hz, 3H, $CH_2C\underline{H}_3$). ^{13}C NMR (126 MHz, DMSO-d_6) δ 168.2 (CO), 154.3 (C_5), 130.7 (C_{7a}), 130.3 (C_α), 128.1 (C_2), 127.9 (C_{3a}), 120.3 (C_β), 112.8 (C_7), 112.5 (C_6), 111.1 (C_3), 99.7 (C_4), 60.0 (CH_2), 55.4 (OCH_3), 14.9 ($C_\beta\underline{C}H_3$), 14.4 ($CH_2\underline{C}H_3$). HPLC-MS (15:95- g.t.5 min) ^{t}R 4.79 min, *m/z* = 266.33 $[M+H]^+$, calcd. for $[C_{15}H_{17}NO_3+H]^+$ 260.12.

Ethyl 3-(5-methoxy-1*H*-indol-3-yl)-2-methylpropanoate (1.29)

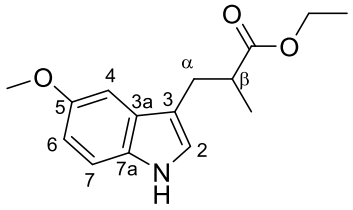

Following the general procedure III of hydrogenation, the saturated ester **1.29** was obtained from the ester **1.28** (500 mg, 1.93 mmol), without further purification in quantitative yield. ^{1}H NMR (400 MHz, $CDCl_3$) δ 7.88 (bs, 1H, NH), 7.23 (d, *J* = 8.7 Hz, 1H, H_7), 7.03 (d, *J* = 2.4 Hz, 1H, H_2), 6.98 (d, *J* = 2.3 Hz, 1H, H_4), 6.85 (dd, *J* = 8.8, 2.4 Hz, 1H, H_6), 4.10 (q, *J* = 7.2 Hz, 3H, $C\underline{H}_2CH_3$), 3.87 (s, 3H, OCH_3), 3.20 – 3.08 (m, 1H, H_α), 2.88 – 2.74 (m, 2H, H_α, H_β), 1.21 (dd, *J* = 6.7, 2.3 Hz, 3H, $CH_\beta C\underline{H}_3$), 1.19 (t, *J* = 7.1 Hz, 3H, $CH_2C\underline{H}_3$). ^{13}C NMR (101 MHz, $CDCl_3$) δ 176.8 (CO), 154.1 (C_5), 131.5 (C_{7a}), 128.1 (C_{3a}), 123.2 (C_2), 113.7 (C_3), 112.2 (C_7), 111.9 (C_6), 101.0 (C_4), 60.4 ($\underline{C}H_2CH_3$), 56.1 (OCH_3), 40.6 (C_β), 29.4 (C_α), 17.3 ($CH_\beta\underline{C}H_3$), 14.3 ($CH_2\underline{C}H_3$). HPLC-MS (15:95- g.t.5 min) ^{t}R 4.77 min, *m/z* = 262.27 $[M+H]^+$, calcd. for $[C_{15}H_{19}NO_3+H]^+$ 262.32.

5-[1-(5-Methoxy-1*H*-indol-3-yl)propan-2-yl]-1,3,4-oxadiazol-2(3*H*)-one (1.30)

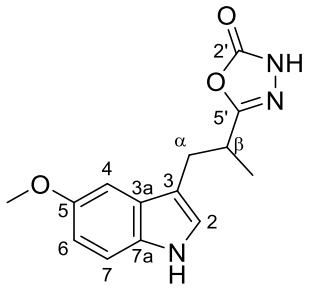

Ester **1.29** (360 mg, 1.38 mmol) was transformed into the corresponding hydrazide following the procedure IV to synthetize the corresponding hydrazide without isolation, identified by HPLC-MS (15:95- g.t.5), ^{t}R 2.97 min, *m/z* = 248.17 $[M+H]^+$, calcd. for

$[C_{13}H_{17}N_3O_2+H]^+$ 248.30, which was reacted with CDI following procedure V to obtain the oxadiazolone **1.30** in 48% yield (180 mg, 0.66 mmol). Chromatography: hexane to hexane:EtOAc 1:1. Mp: 90 - 93 ºC. ^{1}H NMR (400 MHz, $CDCl_3$) δ 8.40 (bs, 1H, NHCO), 7.91 (bs, 1H, NH_{indole}), 7.25 (d, *J* = 9.0 Hz, 1H, H_7), 6.98 (d, *J* = 2.4 Hz, 1H, H_2), 6.97 (d, *J* = 2.4 Hz, 1H, H_4), 6.86 (dd, *J* = 8.8, 2.4 Hz, 1H, H_6), 3.87 (s, 3H, OCH_3), 3.19 (dd, *J* = 13.7, 6.7 Hz, 1H, ½H_α), 3.11 (h, *J* = 6.8 Hz, 1H, H_β), 2.94 (dd, *J* = 13.8, 7.0 Hz, 1H, ½H_α), 1.32 (d, *J* = 6.8 Hz, 3H, $CH_\beta C\underline{H}_3$). ^{13}C NMR (101 MHz, $CDCl_3$) δ 161.4 ($C_{5'}$), 155.0 ($C_{2'}$), 154.3 (C_5), 131.4 (C_{7a}), 127.8 (C_{3a}), 123.4 (C_2), 112.6 (C_6), 112.3 (C_3), 112.1 (C_7), 100.4 (C_4), 56.1 (OCH_3), 33.7 (C_β), 29.4 (C_α), 16.9 ($CH_\beta\underline{C}H_3$). HPLC-MS (40:95- g.t.10 min) ^{t}R 1.24 min, *m/z* = 274.22 $[M+H]^+$, calcd. for $[C_{14}H_{15}N_3O_3+H]^+$ 274.29. HRMS [ESI$^+$] *m/z* = 273.11073 $[M]^+$, calcd. for $[C_{14}H_{15}N_3O_3]^+$ 273.11134.

1-(5-Methoxy-1*H*-indol-3-yl)ethan-1-one (1.31)

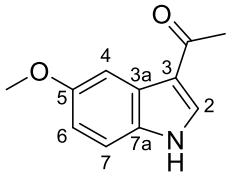

Commercial 5-methoxyindole (350 mg, 2.38 mmol) and $AlCl_3$ (3801 mg, 2.86 mmol, 1.2 equiv) were solved in 4 mL of DCM at 0 ºC. After remaining the mixture 5 min at this temperature, it was stirred at rt for 30 min. Acetyl chloride was added in small portions (187 µL, 2.62 mmol, 1.1 equiv) and CH_3NO_2 (3.57 mL, 15 mL/mmol). The reaction was stirred for 2 h. Ice was added, crude was filtered and extracted with EtOAc, dried over $MgSO_4$, filtered and solvent was removed under reduced pressure. Product was purified by flash chromatography using hexane to hexane:EtOAc 1:1 as gradient, to afford **1.31** in 89% yield (400 mg, 2.12 mmol). Mp: 181 - 183 ºC decomposes (lit. 170 ºC decomposes)[152].^{1}H NMR (500 MHz, $CDCl_3$) δ 8.55 (bs, 1H, NH), 7.90 (d, *J* = 2.5 Hz, 1H, H_4), 7.82 (d, *J* = 3.1 Hz, 1H, H_2), 7.29 (dd, *J* = 8.9, 0.6 Hz, 1H, H_7), 6.93 (dd, *J* = 8.9, 2.6 Hz, 1H, H_6), 3.90 (s, 3H, OCH_3), 2.53 (s, 3H, $COCH_3$). ^{13}C NMR (126 MHz, $CDCl_3$) δ 193.7 (CO), 156.6 (C_5), 131.7 (C_2), 131.2 (C_{3a}), 126.4 (C_{7a}), 118.6 (C_3), 114.5 (C_6), 112.2 (C_7), 103.7 (C_4), 55.9 (OCH_3), 27.6 ($CO\underline{C}H_3$). HPLC-MS (15:95- g.t.5 min) ^{t}R 3.20 min, *m/z* = 190.44 $[M+H]^+$, calcd. for $[C_{11}H_{11}NO_2+H]^+$ 190.21.

5,5'-Dimethoxy-2,3-dihydro-1*H*,1'*H*-2,3'-biindole (1.32)

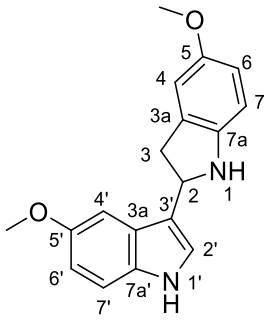

A solution of 5-methoxyindole (30 mg, 0.20 mmol) and $ZrCl_4$ (48 mg, 0.20 mmol) in anhydrous DCM (50 mL) was stirred at rt overnight under N_2. DCM (50 mL) was added to the reaction and extracted with $NaHCO_3$ solution (aq) (x3) and brine (x3). The organic layer was dried over $MgSO_4$, filtrated and the solvent was evaporated under vacuum. The mixture was purified by flash chromatography in hexane to hexane:EtOAc 7:3 gradient. The product was crystallized in EtOH, obtaining **1.32** as colorless crystals (16 mg, 0.05 mmol, 53%). Mp: 168 – 170 ºC (lit. 169 – 170 ºC).[95] ^{1}H NMR (500 MHz, Acetone-d_6) δ 9.87 (s, 1H, $H_{1'}$), 7.27 (dt, J = 8.8, 0.6 Hz, 1H, $H_{7'}$), 7.24 (d, J = 2.1 Hz, 1H, $H_{2'}$), 6.98 (d, J = 2.4 Hz, 1H, $H_{4'}$), 6.77 (dd, J = 2.4, 1.0 Hz, 1H, H_4), 6.74 (ddd, J = 8.8, 2.4, 0.6 Hz, 1H, $H_{6'}$), 6.59 (dd, J = 8.3, 2.4 Hz, 1H, H_6), 6.55 (d, J = 8.3 Hz, 1H, H_7), 5.14 (t, J = 8.4 Hz, 1H, H_2), 4.77 (s, 1H, H_1), 3.70 (s, 3H, OCH_3), 3.68 (s, 3H, OCH_3'), 3.40 (ddd, J = 15.6, 9.0, 0.6 Hz, 1H, H_3), 3.05 (ddt, J = 15.5, 7.8, 1.0 Hz, 1H, H_3). ^{13}C NMR (126 MHz, Acetone-d_6) δ 154.7 ($C_{5'}$), 154.1 (C_5), 147.2 (C_{7a}), 133.5 ($C_{7a'}$), 131.3 (C_{3a}), 127.4 ($C_{3a'}$), 123.4 ($C_{2'}$), 120.1 ($C_{3'}$), 113.1 (C_6), 113.0 ($C_{7'}$), 112.6 ($C_{6'}$), 112.3 (C_4), 109.9 (C_7), 102.3 ($C_{4'}$), 58.0 (C_2), 56.2 (OCH_3), 55.9 (OCH_3'), 39.0 (C_3). HPLC-MS (15:95- g.t.5 min) ^{t}R 2.39 min, *m/z* = 295.16 $[M+H]^+$, calcd. for $[C_{18}H_{18}N_2O_2+H]^+$ 295.35. HRMS [ESI+] *m/z* = 294.13753 [M]+, calcd for $[C_{18}H_{18}N_2O_2]^+$ 294.13683.

Core Modification

Naphthalene and Dihydronaphthalene

6-Methoxy-4-methyl-1,2-dihydronaphthalene (1.33)

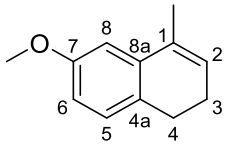

(Adaptation from Ref.[100]) To a solution of the commercial 7-methoxy-1-tetralone (200 mg, 1.13 mmol) in 5 mL of Et_2O, CH_3MgI was added dropwise at rt. The mixture was stirred for 3 h (alcohol formation), washed with a saturated solution of NH_4Cl and extracted with Et_2O (x3). Then, a 2 M HCl solution was added dropwise until pH 5. The mixture was heated at 40 ºC for 3 h. The layers were separated, and the organic layer was washed with a solution of $Na_2S_2O_3$, and brine; dried over $MgSO_4$, filtrated and the solvent was removed under reduced pressure. The crude was purified by flash chromatography in hexane. The alkene **1.33** was obtained as a colorless oil in 97% yield (191 mg, 1.10 mmol). ^{1}H NMR (400 MHz, $CDCl_3$) δ 7.05 (d, *J* = 8.1 Hz, 1H, H_5), 6.82 (d, *J* = 2.7 Hz, 1H, H_8), 6.70 (dd, *J* = 8.1, 2.7 Hz, 1H, H_6), 5.86 - 5.89 (m, 1H, H_2), 3.82 (s, 3H, OCH_3), 2.70 (t, *J* = 8.0 Hz, 2H, H_4), 2.27 – 2.19 (m, 2H, H_3), 2.06 – 2.03 (m, 3H, CH_3C=). ^{13}C NMR (101 MHz, $CDCl_3$) δ 158.5 (C_7), 137.1 (C_{8a}), 132.2 (C_1), 128.7 (C_{4a}), 128.0 (C_5), 126.3 (C_2), 111.0 (C_6), 109.8 (C_8), 55.5 (OCH_3), 27.5 (C_4), 23.7(C_3), 19.5 ($\underline{C}H_3C$=). HPLC-MS (50:95- g.t.10 min) ^{t}R 6.55 min, it does not ionize.

7-Methoxy-1-methylnaphthalene (1.34)

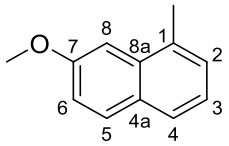

Naphthalene **1.34** was synthesized from dihydronaphthalene **1.33** (447 mg, 2.56 mmol) following general procedure of aromatization VIII in 95% yield as a waxy solid (418 mg, 2.42 mmol). Chromatography: hexane. Mp: 46 - 48 ºC (40 - 42 ºC)[101]. ^{1}H NMR (400 MHz, $CDCl_3$) δ 7.78 (d, *J* = 8.9 Hz, 1H, H_5), 7.66 (d, *J* = 8.0 Hz, 1H, H_4), 7.32 (d, *J* = 7.0 Hz, 1H, H_2), 7.29 – 7.24 (m, 2H, H_8, H_3), 7.18 (dd, *J* = 8.9, 2.6 Hz, 1H, H_6), 3.97 (s, 3H, OCH_3), 2.68 (s, 3H, CH_3Ar). ^{13}C NMR (101 MHz, $CDCl_3$) δ 157.7 (C_7), 133.8 (C_{8a}), 133.0 (C_1),

130.2 (C_5), 129.1 (C_{4a}), 127.2 (C_2), 126.2 (C_4), 123.4 (C_3), 118.0 (C_6), 102.9 (C_8), 55.4 (OCH_3), 19.7 (CH_3Ar). HPLC-MS (50:95- g.t.10 min) ^tR 5.72 min, it does not ionize.

7-Methoxynaphthalene-1-carbaldehyde (1.35)[102]

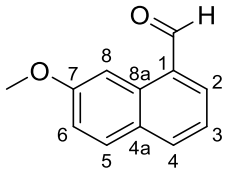

To methyl naphthalene **1.34** (40 mg, 0.23 mmol) a drop of Br_2 (2 µL, 0.023 mmol, 0.1 equiv) was added. The obtained mixture was stirred for 20 min and heated up to 120 ºC. DMSO (500 µL) was added and the heating was continued for 1.5 h, as no reaction was observed, same amounts of Br_2 and DMSO were added and it was left at 120 ºC overnight. The crude was extracted with EtOAc (x3), washed with a saturated solution of $NaHCO_3$ and brine, dried over $MgSO_4$, filtrated and the solvent was removed under reduced pressure. The crude was purified by preparative TLC in hexane to hexane:EtOAc 9:1, to obtain **1.35** as a colorless oil in 20% yield (8 mg, 0.05 mmol). ^{1}H NMR (500 MHz, MeOD) δ 10.30 (s, 1H, COH), 8.75 (d, *J* = 2.6 Hz, 1H, H_8), 8.11 (d, *J* = 8.1 Hz, 1H, H_4), 8.06 (dd, *J* = 7.1, 1.4 Hz, 1H, H_2), 7.89 (d, *J* = 9.0 Hz, 1H, H_5), 7.54 (dd, *J* = 8.1, 7.1 Hz, 1H, H_3), 7.25 (dd, *J* = 9.0, 2.6 Hz, 1H, H_6), 3.96 (s, 3H, CH_3). ^{13}C NMR (126 MHz, MeOD) δ 195.8 (COH), 162.1 (C_7), 139.5 (C_2), 136.3 (C_4), 133.3 (C_{8a}), 131.6 (C_1), 131.2 (C_5), 130.8 (C_{4a}), 123.8 (C_3), 120.5 (C_6), 104.4 (C_8), 55.9 (CH_3). HPLC-MS (50:95- g.t.10 min) ^tR 2.99 min, *m/z* = 187.39 $[M+H]^+$, calcd. for $[C_{12}H_{10}O_2+H]^+$ 187.21.

7-Methoxy-3,4-dihydronaphthalene-1-carbaldehyde (1.37)[103]

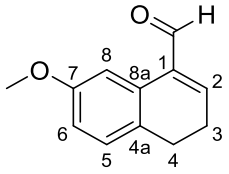

To a solution of **1.33** (238 mg, 1.37 mmol) in EtOH (5 mL), was added dropwise (35 min addition) a solution of SeO_2 (758 mg, 6.83 mmol) in EtOH:H_2O (15 mL, 10:1). The reaction mixture was heated at reflux overnight. The crude was extracted with EtOAc (x3) and washed with a saturated solution of $NaHCO_3$ and brine. The combined organic layers were dried over $MgSO_4$, filtered and concentrated under reduced pressure. It was purified

by chromatography, gradient hexane to hexane:EtOAc 6:4 to afford **1.37** in 25% yield (64 mg, 0.34 mmol) as a brown oil. ^{1}H NMR (400 MHz, $CDCl_3$) δ 9.68 (s, 1H, COH), 7.87 (d, *J* = 2.7 Hz, 1H, H_8), 7.10 (d, *J* = 8.5 Hz, 1H, H_5), 7.04 (t, *J* = 4.7 Hz, 1H, H_2), 6.80 (dd, *J* = 8.3, 2.7 Hz, 1H, H_6), 3.83 (s, 3H, CH_3), 2.76 (t, *J* = 7.9 Hz, 2H, H_4), 2.61 – 2.54 (m, 2H, H_3). ^{13}C NMR (101 MHz, $CDCl_3$) δ 192.7 (CO), 158.4 (C_7), 153.7 (C_2), 138.0 (C_1), 130.3 (C_{8a}), 128.4 (C_5), 127.8 (C_{4a}), 114.2 (C_6), 111.4 (C_8), 55.5 (CH_3), 26.3 (C_4), 24.8 (C_3). HPLC-MS (50:95- g.t.10 min) ^{t}R 2.46 min, *m/z* = 189.39 $[M+H]^+$, calcd. for $[C_{12}H_{12}O_2+H]^+$ 189.23.

9-Methoxy-2,4a,5,6-tetrahydro-3*H*-naphtho[2,1-*b*]pyran-3-one (1.39)

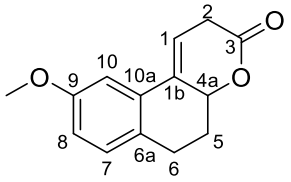

Lactone **1.39** was obtained from aldehyde **1.36** (280 mg, 1.49 mmol) by a *Knoevenagel-Doebner* reaction in 23% yield (79 mg, 0.34 mmol). Mp: 96 - 98 ºC. ^{1}H NMR (500 MHz, $CDCl_3$) δ 7.10 (d, *J* = 2.7 Hz, 1H, H_{10}), 7.07 (d, *J* = 8.4 Hz, 1H, H_7), 6.81 (dd, *J* = 8.4, 2.6 Hz, 1H, H_8), 6.37 (dt, *J* = 5.6, 2.7 Hz, 1H, H_1), 5.15 (dtd, *J* = 13.7, 4.4, 1.6 Hz, 1H, H_{4a}), 3.82 (s, 3H, CH_3), 3.36 (ddd, *J* = 20.6, 5.9, 1.5 Hz, 1H, H_2), 3.21 (ddd, *J* = 20.7, 4.4, 2.8 Hz, 1H, H_2), 2.91 – 2.75 (m, 2H, H_6), 2.42 (dq, *J* = 12.4, 4.3 Hz, 1H, H_5), 1.99 (tddd, *J* = 12.2, 11.4, 5.0, 0.6 Hz, 1H, H_5). ^{13}C NMR (126 MHz, $CDCl_3$) δ 170.2 (C_3), 158.5 (C_9), 134.5 (C_{1b}), 131.8 (C_{10a}), 130.0 (C_7), 128.7 (C_{6a}), 114.8 (C_8), 114.7 (C_1), 108.0 (C_{10}), 77.7 (C_{4a}), 55.5 (CH_3), 31.8 (C_2), 29.6 (C_5), 26.9 (C_6). HPLC-MS (50:95- g.t.10 min) ^{t}R 1.75 min, *m/z* = 231.17 $[M+H]^+$, calcd. for $[C_{14}H_{14}O_3+H]^+$ 231.26.

5-[(*E*)-2-(7-Methoxy-3,4-dihydronaphthalen-1-yl)ethenyl]-1,3,4-oxadiazol-2(3*H*)-one (1.40)

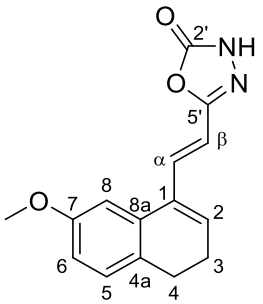

Lactone **1.39** (70 mg, 0.30 mmol) was transformed into the corresponding hydrazide without isolation following the general procedure IV, identified by HPLC-MS (50:95- g.t.10 min and 2:30- g.t.10 min), which appears in the injection point, *m/z* = 245.11 $[M+H]^+$, calcd. for $[C_{14}H_{16}N_2O_2+H]^+$ 245.29. Hydrazide was reacted with CDI following procedure V to obtain the oxadiazolone **1.40** in 15% yields (12 mg, 0.044 mmol). Chromatography: hexane to hexane:EtOAc 3:7. Mp: 133 - 136 ºC. ^{1}H NMR (400 MHz, MeOD) δ 7.11 (d, *J* = 8.4 Hz, 1H, H_5), 7.09 (dd, *J* = 16.2, 1.2 Hz, 1H, H_α), 6.91 (d, *J* = 2.6 Hz, 1H, H_8), 6.75 (dd, *J* = 8.2, 2.6 Hz, 1H, H_6), 6.50 (d, *J* = 16.2 Hz, 1H, H_β), 6.45 (t, *J* = 4.8 Hz, 1H, H_2), 3.78 (s, 3H, CH_3), 2.66 (t, *J* = 7.7 Hz, 2H, H_4), 2.35 – 2.27 (m, 2H, H_3). ^{13}C NMR (126 MHz, $CDCl_3$) δ 158.5 (C_7), 155.6 ($C_{5'}$), 153.9 ($C_{2'}$), 137.5 (C_α), 134.7 (C_1), 133.7 (C_{8a}), 133.1 (C_2), 128.9 (C_{4a}), 128.8 (C_5), 112.4 (C_6), 111.3 (C_β), 110.7 (C_8), 55.6 (CH_3), 27.1 (C_4), 24.1 (C_3). HPLC-MS (50:95- g.t.10 min) ^{t}R 4.72 min, *m/z* = 271.26 $[M+H]^+$, calcd. for $[C_{15}H_{14}N_2O_3+H]^+$ 271.29. HRMS [ESI$^+$] *m/z* = 270.10827 $[M]^+$, calcd. for $[C_{15}H_{14}N_2O_3]^+$ 270.10044.

7-Methoxy-3,4-dihydronaphthalen-1-yl trifluoromethanesulfonate (1.41)[104]

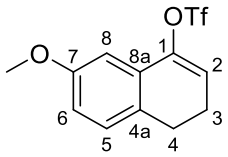

To a solution of commercial 7-methoxy-1-tetralone (507 mg, 2.88 mmol) in 7 mL of dry DCM were added Tf_2O (0.6 mL, 3.31 mmol) and 2-chloropyridine (0.3 mL, 3.31 mmol) at rt under inert atmosphere. The reaction was complete after 2 h, the solvent was evaporated and the crude was purified by flash chromatography on hexane, to obtain the triflate **1.41** as a colorless oil in 78% yield (697 mg, 2.26 mmol). ^{1}H NMR (400 MHz, MeOD) δ 7.16 (d, *J*

= 7.9 Hz, 1H, H_5), 6.90 – 6.83 (m, 2H, H_6, H_8), 6.12 (t, *J* = 4.8 Hz, 1H, H_2), 3.80 (s, 3H, CH_3), 2.80 (t, *J* = 8.1 Hz, 2H, H_4), 2.54 – 2.46 (m, 2H, H_3). ^{13}C NMR (101 MHz, MeOD) δ 160.1 (C_7), 147.6 (C_1), 130.7 (C_{8a}), 129.9 (C_5), 129.7 (C_{4a}), 120.3 (q, J_{C-F} = 320.1 Hz, C_{Tf}), 120.2 (C_2), 115.2 (C_6), 108.2 (C_8), 55.8 (CH_3), 26.8 (C_4), 23.7 (C_3). HPLC-MS (50:95-g.t.10 min) ^{t}R 6.08 min, *m/z* = 309.02 $[M+H]^+$, calcd. for $[C_{12}H_{11}F_3O_4S+H]^+$ 309.27.

Ethyl (2*E*)-3-(7-methoxy-3,4-dihydronaphthalen-1-yl)prop-2-enoate (1.42)

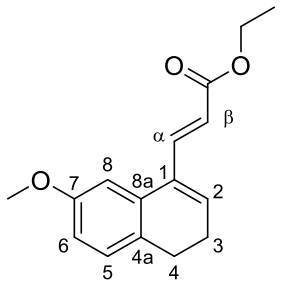

Triflate **1.41** (120 mg, 0.39 mmol) was solved in 1 mL of anhydrous DMF under N_2 atmosphere, a solution of ethyl acrylate (93 µL, 0.86 mmol, 2.2 equiv), TEA (189 µL, 1.36 mmol, 3.5 equiv) and $Pd(PPh_3)_2Cl_2$ (6 mg, 2.2 mol %) in 0.5 mL of DMF was added. The reaction was heated under mw irradiation at 105 ºC for 15 min. Ether was added and mixture was washed with H_2O (x3). Organic layer was dried over $MgSO_4$ and filtered. Crude was purified by preparative TLC in hexane:EtOAc 8:2 to afford unsaturated ester **1.42** in 50% yield (46 mg, 0.19 mmol) as white solid. Mp: 72 - 74 ºC. ^{1}H NMR (400 MHz, MeOD) δ 7.60 (d, *J* = 16.0 Hz, 1H, H_α), 7.12 (d, *J* = 8.3 Hz, 1H, H_5), 6.87 (d, *J* = 2.6 Hz, 1H, H_8), 6.77 (dd, *J* = 8.2, 2.7 Hz, 1H, H_6), 6.56 (t, *J* = 5.0 Hz, 1H, H_2), 6.26 (d, *J* = 15.9 Hz, 1H, H_β), 4.24 (q, *J* = 7.2 Hz, 2H, OCH_2), 3.78 (s, 3H, OCH_3), 2.66 (t, *J* = 7.8 Hz, 2H, H_4), 2.33 (td, *J* = 7.6, 4.7 Hz, 2H, H_3), 1.32 (t, *J* = 7.1 Hz, 3H, $CH_2C\underline{H}_3$). ^{13}C NMR (101 MHz, MeOD) δ 168.8 (CO), 159.9 (C_7), 144.7 (C_α), 135.7 (C_1), 135.1 (C_2), 134.8 (C_{8a}), 129.9 (C_{4a}), 129.6 (C_5), 120.0 (C_β), 113.3 (C_6), 111.4 (C_8), 61.7 (OCH_2), 55.8 (OCH_3), 27.9 (C_4), 25.0 (C_3), 14.6 ($CH_2\underline{C}H_3$). HPLC-MS (50:95- g.t.10 min) ^{t}R 5.38 min, *m/z* = 259.11 $[M+H]^+$, calcd. for $[C_{16}H_{18}O_3+H]^+$ 259.32.

2-Methoxynaphthalene (1.43)

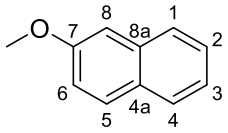

Naphthalene **1.43** was isolated as secondary product of previous reaction from **1.41** to obtain **1.42** in 35% yield (22 mg, 0.39 mmol) as a bright white flakes. Mp: 72 - 73 ºC (lit. 73.5 ºC). ^{1}H NMR (400 MHz, MeOD) δ 7.80 – 7.72 (m, 3H, H_1, H_5, H_4), 7.43 (ddd, *J* = 8.3, 6.9, 1.3 Hz, 1H, H_2), 7.32 (ddd, *J* = 8.0, 6.9, 1.2 Hz, 1H, H_3), 7.23 (d, *J* = 2.5 Hz, 1H, H_8), 7.14 (dd, *J* = 8.9, 2.6 Hz, 1H, H_6), 3.92 (s, 3H, CH_3). ^{13}C NMR (101 MHz, MeOD) ^{13}C NMR (101 MHz, MeOD) δ 159.1 (C_7), 136.2 (C_{8a}), 130.5 (C_{4a}), 130.3 (C_5), 128.5 (C_4), 127.8 (C_1), 127.3 (C_3), 124.5 (C_2), 119.6 (C_6), 106.7 (C_8), 55.7 (CH_3). HPLC-MS (50:95-g.t.10 min) ^{t}R 4.22 min, it does not ionize.

6,7-Dimethoxy-3,4-dihydronaphthalen-1-yl trifluoromethanesulfonate (1.44)

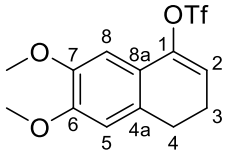

Triflate **1.44** was obtained following the same procedure as **1.41**, from commercial 6,7-dimethoxy-1-tetralone (550 mg, 2.67 mmol) in 33% yield (301 mg, 0.89 mmol) as a colorless oil. Chromatography: hexane to hexane:EtOAc 75:25. ^{1}H NMR (500 MHz, MeOD) δ 6.88 (s, 1H, H_5), 6.87 (s, 1H, H_8), 5.95 (t, *J* = 4.8 Hz, 1H, H_2), 3.85 (s, 3H, C_6OCH_3), 3.81 (s, 3H, C_7OCH_3), 2.80 (t, *J* = 8.3 Hz, 2H, H_4), 2.47 (td, *J* = 8.3, 4.8 Hz, 2H, H_3). ^{13}C NMR (126 MHz, MeOD) δ 151.3 (C_6), 149.1 (C_7), 147.6 (C_1), 131.3 (C_{4a}), 122.4 (C_{8a}), 120.0 (q, J_{C-F} = 319.2 Hz, C_{Tf}), 116.8 (C_2), 113.1 (C_5), 106.6 (C_8), 56.6 ($2CH_3$), 27.4 (C_4), 23.5 (C_3). HPLC-MS (50:95- g.t.10 min) ^{t}R 4.78 min, *m/z* = 339.16$[M+H]^+$, calcd. for $[C_{13}H_{13}F_3O_5S+H]^+$ 339.04.

7-Methoxynaphthalen-1-yl trifluoromethanesulfonate (1.45)

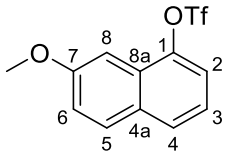

Naphthalene **1.45** was synthesized from dihydronaphthalene **1.41** (165 mg, 0.53 mmol) following general procedure VIII of aromatization in 88% yield (142 mg, 0.46 mmol) as a colorless oil. Chromatography: hexane. ^{1}H NMR (500 MHz, MeOD) δ 7.91 (d, *J* = 8.1 Hz, 1H, H_5), 7.89 (d, *J* = 7.6 Hz, 1H, H_4), 7.50 (d, *J* = 7.7 Hz, 1H, H_2), 7.40 (td, *J* = 8.4, 1.5 Hz, 1H, H_3), 7.30 (d, *J* = 3.0 Hz, 1H, H_8), 7.28 (dd, *J* = 8.9, 1.1 Hz, 1H, H_6), 3.95 (s, 3H, CH_3). ^{13}C NMR (126 MHz, MeOD) δ 160.7 (C_7), 146.2 (C_1), 132.0 (C_{4a}), 131.1 (C_5), 129.5 (C_4), 128.8 (C_{8a}), 123.9 (C_3), 121.5 (C_6), 120.2 (q, J_{C-F} = 319.2 Hz, C_{Tf}), 119.7 (C_2), 99.4 (C_8), 55.9 (CH_3). HPLC-MS (50:95- g.t.10 min) ^{t}R 6.42 min, *m/z* = 305.13 $[M-H]^-$, calcd. for $[C_{12}H_9F_3O_4S-H]^-$ 305.26.

6,7-Dimethoxynaphthalen-1-yl trifluoromethanesulfonate (1.46)

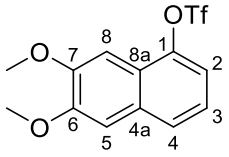

Naphthalene **1.46** was obtained following the same procedure as **1.45**, from dihydronaphthalene **1.44** (280 mg, 0.83 mmol) in 86% yield (240 mg, 0.71 mmol) as a colorless oil. Chromatography: hexane to hexane:EtOAc 9:1. ^{1}H NMR (500 MHz, MeOD) δ 7.82 (ddt, *J* = 7.8, 1.3, 0.6 Hz, 1H, H_4), 7.38 (s, 1H, H_5), 7.37 (t, *J* = 7.8 Hz, 1H, H_3), 7.35 (dd, *J* = 7.8, 1.5 Hz, 1H, H_2), 7.28 (s, 1H, H_8), 3.98 (s, 3H, CH_3), 3.98 (s, 3H, CH_3). ^{13}C NMR (126 MHz, MeOD) δ 152.7 (C_7), 152.1 (C_6), 146.1 (C_1), 132.8 (C_{4a}), 128.1 (C_4), 124.7 (C_3), 123.2 (C_{8a}), 120.2 (q, J_{C-F} = 319.2 Hz, C_{Tf}), 117.2 (C_2), 107.9 (C_5), 100.0 (C_8), 56.4 (CH_3), 56.3 (CH_3). HPLC-MS (50:95- g.t.10 min) tR 4.99 min, *m/z* = 335.11$[M-H]^-$, calcd. for $[C_{13}H_{11}F_3O_5S-H]^-$ 335.28.

Ethyl (2*E*)-3-(7-methoxynaphthalen-1-yl)prop-2-enoate (1.47)

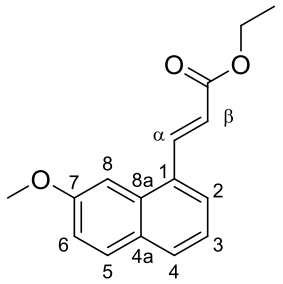

Ester **1.47** was synthesized from triflate **1.41** (520 mg, 1.70 mmol) following the general procedure IX in 90% yield (390 mg, 1.52 mmol). Chromatography: hexane to hexane:EtOAc 95:5. Mp: 76 - 78 ºC. ^{1}H NMR (500 MHz, MeOD) δ 8.42 (dd, *J* = 15.8, 3.9 Hz, 1H, H_{α}), 7.81 (d, *J* = 7.6 Hz, 1H, H_4), 7.78 – 7.72 (m, 2H, H_5, H_2), 7.39 (bs, 1H, H_8), 7.31 (t, *J* = 7.1 Hz, 1H, H_3), 7.16 (d, *J* = 8.9 Hz, 1H, H_6), 6.53 (d, *J* = 15.7 Hz, 1H, H_{β}), 4.28 (q, *J* = 7.1 Hz, 2H, CH_2), 3.93 (s, 3H, OCH_3), 1.35 (t, *J* = 7.1 Hz, 3H, $CH_2C\underline{H}_3$). ^{13}C NMR (126 MHz, MeOD) δ 168.9 (CO), 160.0 (C_7), 143.0 (C_{α}), 134.1 (C_{8a}), 131.6 (C_4), 131.4 (C_5), 131.3 (C_1), 130.7 (C_{4a}), 120.8 (C_{β}), 119.8 (C_6), 102.5 (C_8), 61.8 (CH_2), 55.8 (OCH_3), 14.6 ($CH_2\underline{C}H_3$). HPLC-MS (50:95- g.t.10 min) ^{t}R 6.61 min, *m/z* = 257.07 $[M+H]^+$, calcd. for $[C_{16}H_{16}O_3+H]^+$ 257.30.

Ethyl (2*E*)-3-(6,7-dimethoxynaphthalen-1-yl)prop-2-enoate (1.48)

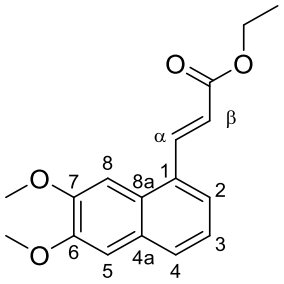

Ester **1.48** was synthesized from triflate **1.46** (230 mg, 0.68 mmol) following the general procedure IX in 81% yield (182 mg, 0.64 mmol). Chromatography: hexane to hexane:EtOAc 85:15. Mp: 89 - 90 ºC. ^{1}H NMR (400 MHz, $CDCl_3$) δ 8.44 (d, *J* = 15.7 Hz, 1H, H_{α}), 7.74 (d, *J* = 8.1 Hz, 1H, H_4), 7.62 (d, *J* = 7.4 Hz, 1H, H_2), 7.39 (s, 1H, H_8), 7.34 (t, *J* = 7.7 Hz, 1H, H_3), 7.14 (s, 1H, H_5), 6.52 (d, *J* = 15.7 Hz, 1H, H_{β}), 4.32 (q, *J* = 7.1 Hz, 2H, CH_2), 4.05 (s, 3H, CH_3OC_7), 4.01 (s, 3H, CH_3OC_6), 1.37 (t, *J* = 7.1 Hz, 3H, $CH_2C\underline{H}_3$). ^{13}C NMR (101 MHz, $CDCl_3$) δ 167.3 (CO), 150.4 (C_7), 149.7 (C_6), 142.1 (C_{α}), 130.4 (C_1), 129.9 (C_{4a}), 129.0 (C_4), 127.6 (C_{8a}), 124.1 (C_3), 123.6 (C_2), 120.5 (C_{β}), 107.1 (C_5), 102.4

(C_8), 60.7 (CH_2), 56.2 ($\underline{C}H_3OC_7$), 56.0 ($\underline{C}H_3OC_6$), 14.5 ($CH_2\underline{C}H_3$). HPLC-MS (50:95-g.t.10 min) ^tR 3.50 min, *m/z* = 287.27 $[M+H]^+$, calcd. for $[C_{17}H_{18}O_4+H]^+$ 287.33.

(2*E*)-3-(7-Methoxynaphthalen-1-yl)prop-2-enoic acid (1.49)

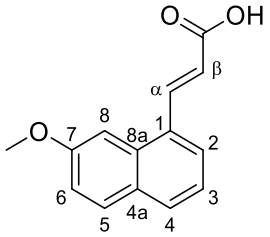

Acid **1.49** was obtained from ester **1.47** (100 mg, 0.39 mmol) following the hydrolysis procedure X in quantitative yield (89 mg, 0.39 mmol). Mp: 212 - 215 ºC. ^{1}H NMR (400 MHz, $CDCl_3$) δ 8.53 (d, *J* = 15.7 Hz, 1H, H_α), 7.84 (d, *J* = 8.1 Hz, 1H, H_4), 7.80 – 7.75 (m, 2H, H_5, H_2), 7.42 (d, *J* = 2.4 Hz, 1H, H8), 7.36 (t, *J* = 7.8 Hz, 1H, H_3), 7.20 (dd, *J* = 9.0, 2.4 Hz, 1H, H_6), 6.55 (d, *J* = 15.6 Hz, 1H, H_β), 3.97 (s, 3H, CH_3). ^{13}C NMR (101 MHz, $CDCl_3$) δ 169.2 (CO_2H), 158.5 (C_7), 143.2 (C_α), 132.8 (C_{8a}), 130.5 (C_4), 130.3 (C_5, C_1), 129.2 (C_{4a}), 125.9 (C_2), 123.2 (C_3), 120.0 (C_β), 118.9 (C_6), 101.9 (C_8), 55.5 (CH_3). HPLC-MS (50:95-g.t.10 min) ^tR 1.47 min, it does not ionize.

(2*E*)-3-(6,7-Dimethoxynaphthalen-1-yl)prop-2-enoic acid (1.50)

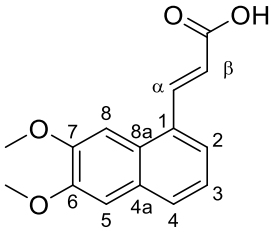

Acid **1.50** was obtained from ester **1.48** (150 mg, 0.52 mmol) following the hydrolysis procedure X in quantitative yield (134 mg, 0.52 mmol). Mp: 220 - 222 ºC. ^{1}H NMR (500 MHz, MeOD) δ 8.45 (d, *J* = 15.7 Hz, 1H, H_α), 7.84 (d, *J* = 8.1 Hz, 1H, H_4), 7.75 (d, *J* = 7.0 Hz, 1H, H_2), 7.53 (s, 1H, H_8), 7.38 (t, *J* = 7.9 Hz, 1H, H_3), 7.36 (s, 1H, H_5), 6.57 (d, *J* = 15.7 Hz, 1H, H_β), 4.02 (s, 3H, CH_3OC_7), 3.96 (s, 3H, CH_3OC_6). ^{13}C NMR (126 MHz, MeOD) δ 167.8 (CO_2H), 151.6 (C_7), 151.0 (C_6), 142.6 (C_α), 131.0 (C_1), 130.9 (C_{4a}), 129.8 (C_4), 128.3 (C_{8a}), 124.6 (C_3), 124.1 (C_2), 121.2 (C_β), 108.1 (C_5), 103.0 (C_8), 56.0 ($\underline{C}H_3OC_7$), 55.9 ($\underline{C}H_3OC_6$). HPLC-MS (50:95- g.t.10 min) ^tR 1.62 min, it does not ionize.

5-[(*E*)-2-(7-Methoxynaphthalen-1-yl)ethenyl]-1,3,4-oxadiazol-2(3*H*)-one (1.51)

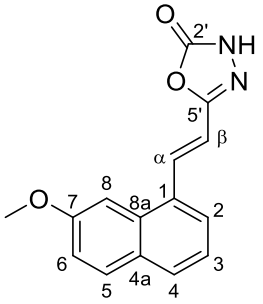

Acid **1.49** (230 mg, 1.01 mmol) was transformed into the corresponding hydrazide without isolation following the procedure IV, identified by HPLC-MS (50:95- g.t.10 min and 2:30- g.t.10 min), hydrazide appears in the injection point, *m/z* = 243.11 $[M+H]^+$, calcd. for $[C_{14}H_{14}N_2O_2+H]^+$ 243.28, which was reacted with CDI following procedure V to obtain the oxadiazolone **1.51** in 91% yield (245 mg, 0.91 mmol). Chromatography: hexane to hexane:EtOAc 6:4. Mp: 207 - 208 ºC. ^{1}H NMR (500 MHz, MeOD) δ 8.10 (d, *J* = 16.1 Hz, 1H, H_α), 7.84 (d, *J* = 8.4 Hz, 1H, H_4), 7.82 (d, *J* = 9.0 Hz, 2H, H_5, H_2), 7.45 (d, *J* = 2.5 Hz, 1H, H_8), 7.37 (dd, *J* = 8.0, 7.4 Hz, 1H, H_3), 7.20 (dd, *J* = 9.0, 2.4 Hz, 1H, H_6), 6.83 (d, *J* = 16.1 Hz, 1H, H_β), 3.98 (s, 3H, CH_3). ^{13}C NMR (126 MHz, MeOD) δ 160.0 (C_7), 156.6 ($C_{5'}$), 135.4 (C_α), 133.9 (C_{8a}), 132.1 (C_1), 131.4 (C_5), 131.0 (C_4), 130.8 (C_{4a}), 126.1 (C_2), 124.3 (C_3), 119.9 (C_6), 113.5 (C_β), 102.5 (C_8), 55.9 (CH_3). HPLC-MS (50:95- g.t.10 min) ^{t}R 1.83 min, *m/z* = 269.16 $[M+H]^+$, calcd. for $[C_{15}H_{12}N_2O_3+H]^+$ 269.27. HRMS [ESI^+] *m/z* = 268.08547 $[M]^+$, calcd. for $[C_{15}H_{12}N_2O_3]^+$ 268.08479.

5-[(*E*)-2-(6,7-Dimethoxynaphthalen-1-yl)ethenyl]-1,3,4-oxadiazol-2(3*H*)-one (1.52)

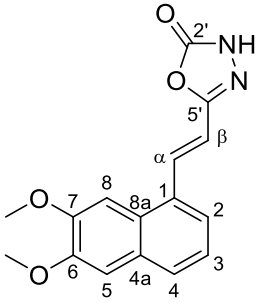

Acid **1.50** (100 mg, 0.39 mmol) was transformed into the corresponding hydrazide following procedure IV without isolation, identified by HPLC-MS (2:30- g.t.10 min), hydrazide appears in the injection point, *m/z* = 273.11 $[M+H]^+$, calcd. for $[C_{15}H_{16}N_2O_3+H]^+$ 273.30, which was reacted with CDI following procedure V to obtain the oxadiazolone **1.52**

in 85% yield (99 mg, 0.33 mmol), as a yellow pale solid. Chromatography: hexane to hexane:EtOAc 6:4. Mp: 232 – 234 ºC. ^{1}H NMR (400 MHz, DMSO-*d*$_6$) δ 8.04 (d, *J* = 16.1 Hz, 1H, H$_\alpha$), 7.82 (d, *J* = 8.1 Hz, 1H, H$_4$), 7.78 (d, *J* = 7.3 Hz, 1H, H$_2$), 7.46 (s, 1H, H$_8$), 7.41 – 7.32 (m, 2H, H$_5$, H$_3$), 6.93 (d, *J* = 16.1 Hz, 1H, H$_\beta$), 3.97 (s, 3H, C$_7$OCH$_3$), 3.90 (s, 3H, C$_6$OCH$_3$). ^{13}C NMR (101 MHz, DMSO-*d*$_6$) δ 154.4 (C$_{5'}$), 154.2 (C$_{2'}$), 149.9 (C$_7$), 149.3 (C$_6$), 133.7 (C$_\alpha$), 130.1 (C$_1$), 129.4 (C$_{4a}$), 128.4 (C$_4$), 126.6 (C$_{8a}$), 123.8 (C$_3$), 122.7 (C$_2$), 112.6 (C$_\beta$), 107.2 (C$_5$), 102.2 (C$_8$), 55.6 (C$_7$O<u>C</u>H$_3$), 55.4 (C$_6$O<u>C</u>H$_3$). HPLC-MS (50:95-g.t.10 min) ^{t}R 1.21 min, *m/z* = 299.18 [M+H]$^+$, calcd. for [C$_{16}$H$_{14}$N$_2$O$_4$+H]$^+$ 299.30. HRMS [ESI$^+$] *m/z* = 298.09568 [M]$^+$, calcd. for [C$_{16}$H$_{14}$N$_2$O$_4$]$^+$ 298.09536.

Resveratrol-like derivatives

(2*E*)-3-(3-Cyanophenyl)prop-2-enoic acid (1.53)

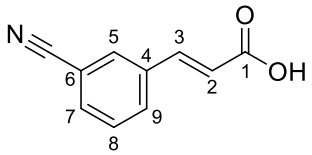

Following the *Knoevenagel-Doebner* reaction procedure II, acid **1.53** was obtained from the commercial 3-formylbenzonitrile (500 mg, 3.82 mmol), without further purification, in 99% yield (650 mg, 3.78 mmol). Mp: 234 - 235 ºC.(lit. 236 - 238 ºC)[153]. ^{1}H NMR (400 MHz, MeOD) δ 8.00 (t, *J* = 1.7 Hz, 1H, H$_5$), 7.92 (dt, *J* = 7.9, 1.4 Hz, 1H, H$_9$), 7.75 (dt, *J* = 8.1, 1.3 Hz, 1H, H$_7$), 7.68 (d, *J* = 16.0 Hz, 1H, H$_3$), 7.59 (t, *J* = 7.8 Hz, 1H, H$_8$), 6.61 (d, *J* = 16.1 Hz, 1H, H$_2$). ^{13}C NMR (101 MHz, MeOD) δ 169.5 (C$_1$), 143.5 (C$_3$), 137.4 (C$_4$), 134.3 (C$_7$), 133.3 (C$_9$), 132.7 (C$_5$), 131.1 (C$_8$), 122.3 (C$_2$), 119.2 (CN), 114.3 (C$_6$). HPLC-MS (5:95- g.t.10 min) ^{t}R 6.58 min, *m/z* = 172.27 [M-H]$^-$, calcd. for [C$_{10}$H$_7$NO$_2$-H]$^-$ 172.17.[154]

(2*E*)-3-(2*H*-1,3-Benzodioxol-5-yl)prop-2-enoic acid (1.54)

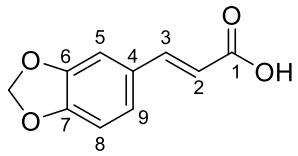

Following the general procedure II by a *Knoevenagel-Doebner* reaction from commercial piperonal (500 mg, 3.3 mmol), the corresponding acid was obtained in 92% yield (583.5 mg, 3.0 mmol). Mp: 222 - 224 ºC (lit. 245 - 246 ºC)[155]. ^{1}H NMR (400 MHz, MeOD) δ 7.61 (d, *J* = 15.9 Hz, 1H, H_3), 7.18 (d, *J* = 1.7 Hz, 1H, H_5), 7.10 (dd, *J* = 8.0, 1.8 Hz, 1H, H_9), 6.88 (d, *J* = 8.0 Hz, 1H, H_8), 6.34 (d, *J* = 15.9 Hz, 1H, H_2), 6.03 (s, 2H, CH_2). ^{13}C NMR (101 MHz, MeOD) δ 170.6 (C_1), 151.2 (C_7), 149.9 (C_6), 146.2 (C_3), 130.2 (C_4), 125.6 (C_9), 117.1 (C_2), 109.4 (C_8), 107.5 (C_5), 103.0 (CH_2). HPLC-MS (15:95- g.t.5 min) ^{t}R 3.58 min, *m/z* = 193.12 $[M+H]^+$, calcd. for $[C_{10}H_8O_4+H]^+$ 193.17.

(2*E*)-3-Phenylprop-2-enehydrazide (1.55)

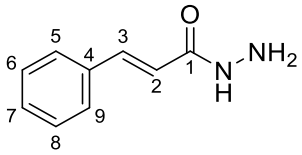

Following the general procedure IV, the hydrazide **1.55** was obtained from the commercial cinnamic acid (600 mg, 4.05 mmol), without further purification in 99% yield (650 mg, 4.01 mmol). Mp: 107 - 110 ºC (lit. 116 - 117 ºC)[146]. ^{1}H NMR (500 MHz, MeOD) δ 7.56 (d, *J* = 15.9 Hz, 1H, H_3), 7.54 (dd, *J* = 7.7, 1.7 Hz, 2H, H_5, H_9), 7.40 – 7.33 (m, 3H, H_6, H_7, H_8), 6.56 (d, *J* = 15.8 Hz, 1H, H_2). ^{13}C NMR (126 MHz, MeOD) δ 167.9 (C_1), 141.6 (C_3), 136.2 (C_4), 130.8 (C_7), 129.9 (C_6, C_8), 128.8 (C_5, C_9), 119.6 (C_2). HPLC-MS (15:95- g.t.10 min) ^{t}R 1.37 min, *m/z* = 163.17 $[M+H]^+$, calcd. for $[C_9H_{10}N_2O+H]^+$ 163.19.

(2*E*)-3-(3-Methoxyphenyl)prop-2-enehydrazide (1.58)

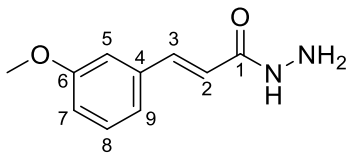

Following the general procedure IV, the hydrazide **1.58** was obtained from the commercial 3-methoxycinnamic acid (500 mg, 2.8 mmol), without further purification in 98% yield

(528 mg, 2.75 mmol). Mp: 131 - 134 ºC (lit. 130 °C)[156]. ^{1}H NMR (300 MHz, MeOD) δ 7.52 (d, *J* = 15.8 Hz, 1H, H_3), 7.30 (t, *J* = 7.9 Hz, 1H, H_8), 7.13 (d, *J* = 8.0 Hz, 1H, H_9), 7.09 (t, *J* = 2.1 Hz, 1H, H_5), 6.94 (dd, *J* = 7.9, 2.0 Hz, 1H, H_7), 6.54 (d, *J* = 15.8 Hz, 1H, H_2), 3.82 (s, 3H, CH_3). ^{13}C NMR (75 MHz, MeOD) δ 167.9 (C_1), 161.5 (C_6), 141.6 (C_3), 137.6 (C_4), 130.9 (C_8), 121.3 (C_9), 119.9 (C_2), 116.5 (C_7), 113.8 (C_5), 55.7 (CH_3). HPLC-MS (15:95- g.t.5 min) ^{t}R 2.51 min, *m/z* = 193.46 $[M+H]^+$, calcd. for $[C_{10}H_{12}N_2O_2 +H]^+$ 193.22.

(2*E*)-3-(4-Methoxyphenyl)prop-2-enehydrazide (1.59)

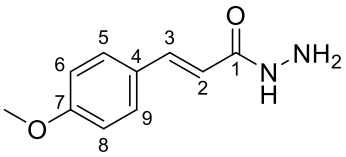

Following the general procedure IV, the hydrazide **1.59** was obtained from the commercial 4-methoxycinnamic acid (500 mg, 2.8 mmol), without further purification as a pale yellow solid, in 72% yield (386 mg, 2.00 mmol). Mp: 123 - 126 ºC (lit. 135 - 136 ºC)[93]. ^{1}H NMR (400 MHz, MeOD) δ 7.51 (d, *J* = 15.8 Hz, 1H, H_3), 7.49 (d, *J* = 8.5 Hz, 2H, H_5, H_9), 6.93 (d, *J* = 8.8 Hz, 2H, H_6, H_8), 6.41 (d, *J* = 15.7 Hz, 1H, H_2), 3.82 (s, 3H, CH_3). ^{13}C NMR (101 MHz, MeOD) δ 168.4 (C_1), 162.6 (C_7), 141.4 (C_3), 130.4 (C_5, C_9), 128.8 (C_4), 117.1 (C_6, C_8), 55.8 (CH_3). HPLC-MS (15:95- g.t.5 min) ^{t}R 2.28 min, *m/z* = 193.19 $[M+H]^+$, calcd. for $[C_{10}H_{12}N_2O_2 +H]^+$ 193.22.

(2*E*)-3-(2,4-Dimethoxyphenyl)prop-2-enehydrazide (1.60)

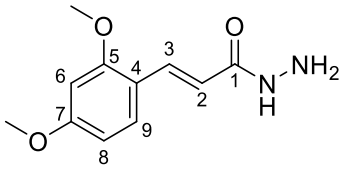

Following the general procedure IV, the hydrazide **1.60** was obtained from the commercial 2, 4-dimethoxycinnamic acid (500 mg, 2.40 mmol), without further purification, in 98% yield (524 mg, 2.36 mmol). Mp: 135 - 138 ºC (decomposition). ^{1}H NMR (400 MHz, MeOD) δ 7.80 (d, *J* = 15.9 Hz, 1H, H_3), 7.48 (d, *J* = 8.4 Hz, 1H, H_9), 6.63 – 6.57 (m, 2H, H_6, H_8), 6.54 (d, *J* = 15.9 Hz, 1H, H_2), 3.92 (s, 3H, C_5OCH_3), 3.86 (s, 3H, C_7OCH_3).^{13}C NMR (101 MHz, MeOD) δ 169.2 (C_1), 164.1 (C_7), 161.1 (C_5), 137.1 (C_3), 130.9 (C_9),

117.8 (C_4), 117.2 (C_2), 106.7 (C_6), 99.3 (C_8), 56.0 ($C_9O\underline{C}H_3$), 55.9 ($C_7O\underline{C}H_3$). HPLC-MS (15:95- g.t.5 min) ^tR 2.60 min, *m/z* = 223.23 $[M+H]^+$, calcd. for $[C_{11}H_{14}N_2O_3+H]^+$ 223.24.

(2*E*)-3-(2,5-Dimethoxyphenyl)prop-2-enehydrazide (1.61)

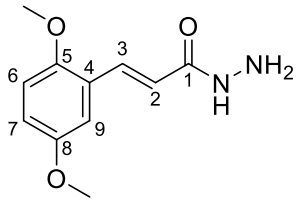

Following the general procedure IV, the hydrazide **1.61** was obtained from the commercial 2, 5-dimethoxycinnamic acid (500 mg, 2.40 mmol), without further purification, in 89% yield (475 mg, 2.14 mmol). Mp: 141 - 143 ºC (lit. 144 - 146 ºC)[157].^{1}H NMR (400 MHz, MeOD) δ 7.86 (d, *J* = 15.9 Hz, 1H, H_3), 7.11 (d, *J* = 2.7 Hz, 1H, H_9), 6.99 – 6.96 (m, 2H, H_6, H_7), 6.64 (d, *J* = 15.9 Hz, 1H, H_2), 3.87 (s, 3H, C_5OCH_3), 3.81 (s, 3H, C_8OCH_3). ^{13}C NMR (101 MHz, MeOD) δ 168.4 (C_1), 155.1 (C_8), 154.1 (C_5), 136.8 (C_3), 125.5 (C_4), 120.2 (C_2), 117.4 (C_7), 114.2 (C_9), 113.7 (C_6), 56.6 ($C_5O\underline{C}H_3$), 56.2 ($C_8O\underline{C}H_3$). HPLC-MS (15:95- g.t.5 min) ^tR 2.72 min, *m/z* = 223.15 $[M+H]^+$, calcd. for $[C_{11}H_{14}N_2O_3+H]^+$ 223.24.

(2*E*)-3-(3,4-Dimethoxyphenyl)prop-2-enehydrazide (1.62)

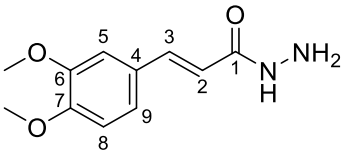

Following the general procedure IV, the hydrazide **1.62** was obtained from the commercial 3, 4-dimethoxycinnamic acid (500 mg, 2.40 mmol), without further purification, in 84% yield (448 mg, 2.02 mmol). Mp: 199 - 202 ºC (lit. 217 - 217.5 ºC)[146]. ^{1}H NMR (400 MHz, MeOD) δ 7.53 (d, *J* = 15.7 Hz, 1H, H_3), 7.19 (d, *J* = 2.0 Hz, 1H, H_5), 7.16 (dd, *J* = 8.3, 2.1 Hz, 1H, H_9), 7.00 (d, *J* = 8.2 Hz, 1H, H_8), 6.46 (d, *J* = 15.7 Hz, 1H, H_2), 3.90 (s, 3H, CH_3), 3.89 (s, 3H, CH_3). ^{13}C NMR (101 MHz, MeOD) δ 168.4 (C_1), 152.3 (C_7), 150.8 (C_6), 141.7 (C_3), 129.3 (C_4), 123.2 (C_9), 117.4 (C_2), 112.8 (C_8), 111.4 (C_5), 56.5 (CH_3), 56.4 (CH_3). HPLC-MS (15:95- g.t.5 min) ^tR 1.66 min, *m/z* = 223.23 $[M+H]^+$, calcd. for $[C_{11}H_{14}N_2O_3+H]^+$ 223.24.

(2*E*)-3-(2*H*-1,3-benzodioxol-5-yl)prop-2-enehydrazide (1.63)

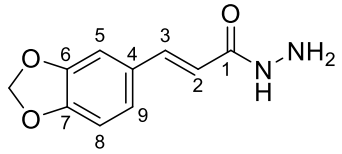

Following the general procedure IV, the hydrazide **1.63** was obtained from the acid **1.54** (150 mg, 0.78 mmol), without further purification, in 72% yield (116 mg, 0.56 mmol). Mp: 145 - 148 ºC (lit. 151 - 152 ºC)[158]. ^{1}H NMR (400 MHz, MeOD) δ 7.49 (d, *J* = 15.7 Hz, 1H, H_3), 7.12 (d, *J* = 1.7 Hz, 1H, H_5), 7.05 (dd, *J* = 8.0, 1.7 Hz, 1H, H_9), 6.86 (d, *J* = 8.0 Hz, 1H, H_8), 6.40 (d, *J* = 15.7 Hz, 1H, H_2), 6.01 (s, 2H, CH_2). ^{13}C NMR (101 MHz, MeOD) δ 168.2 (C_1), 150.7 (C_7), 149.9 (C_6), 141.5 (C_3), 130.6 (C_4), 125.0 (C_9), 117.5 (C_2), 109.4 (C_8), 107.1 (C_5), 102.9 (CH_2). HPLC-MS (15:95- g.t.5 min) ^{t}R 2.07 min, *m/z* = 207.28 $[M+H]^+$, calcd. for $[C_{10}H_{10}N_2O_3+H]^+$ 207.20.

(2*E*)-3-(3,4,5-Trimethoxyphenyl)prop-2-enehydrazide (1.65)

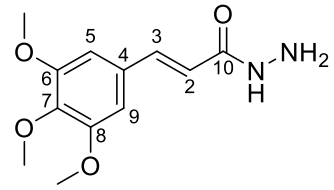

Following the general procedure IV, the hydrazide **1.65** was obtained from the commercial 3,4,5-trimethoxycinnamic acid (500 mg, 2.1 mmol), without further purification, in 86% yield (455 mg, 1.8 mmol). Mp: 153 - 156 ºC (lit. 153 - 154 °C)[159]. ^{1}H NMR (400 MHz, MeOD) δ 7.51 (d, *J* = 15.8 Hz, 1H, H_3), 6.90 (s, 2H, H_5, H_9), 6.51 (d, *J* = 15.7 Hz, 1H, H_2), 3.90 (s, 6H, C_6OCH_3, C_8OCH_3), 3.82 (s, 3H, C_7OCH_3). ^{13}C NMR (101 MHz, MeOD) δ 168.0 (C_1), 154.8 (C_6, C_8), 141.6 (C_3), 140.8 (C_7), 132.1 (C_4), 119.1 (C_2), 106.3 (C_5, C_9), 61.2 ($C_7O\underline{C}H_3$), 56.7 ($C_6O\underline{C}H_3$, $C_8O\underline{C}H_3$). HPLC-MS (15:95- g.t.5 min) ^{t}R 2.28 min, *m/z* = 253.20 $[M+H]^+$, calcd. for $[C_{12}H_{16}N_2O_4+H]^+$ 252.27.

5-[(*E*)-2-Phenylethenyl]-1,3,4-oxadiazol-2(3*H*)-one (1.66)

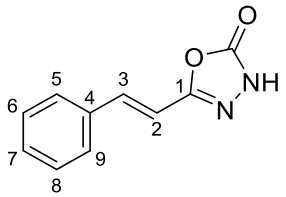

Following the general procedure V, the oxadiazolone **1.66** was obtained from hydrazide **1.55** (656 mg, 4.05 mmol) in 65% yield (495 mg, 2.63 mmol). Chromatography: hexane to hexane:EtOAc 80:20. Mp: 191 - 194 ºC (lit 191 - 193 ºC)[160]. ^{1}H NMR (500 MHz, MeOD) δ 7.61 – 7.58 (m, 2H, H_5, H_9), 7.43 – 7.37 (m, 3H, H_6, H_7, H_8), 7.34 (d, *J* = 16.5 Hz, 1H, H_3), 6.78 (d, *J* = 16.5 Hz, 1H, H_2). ^{13}C NMR (126 MHz, MeOD) δ 156.5 (CO), 156.5 (C_1), 138.7 (C_3), 136.2 (C_4), 130.8 (C_7), 130.0 (C_6, C_8), 128.5 (C_5, C_9), 111.5 (C_2). HPLC-MS (15:95- g.t.10 min) ^{t}R 6.41 min, *m/z* = 189.30 $[M+H]^+$, calcd. for $[C_{10}H_8N_2O_2+H]^+$ 189.19. HRMS $[ESI^+]$ *m/z* = 188.05822 $[M]^+$, calcd. for $[C_{10}H_8N_2O_2]^+$ 188.05858.

3-[(*E*)-2-(5-Oxo-4,5-dihydro-1,3,4-oxadiazol-2-yl)ethenyl]benzonitrile (1.67)

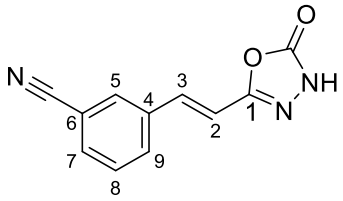

Acid **1.53** (50 mg, 0.29 mmol) was transformed into the hydrazide **1.56** without isolation following the general procedure IV, identified by HPLC-MS (15:95- g.t.5). Hydrazide appears at ^{t}R 1.27 min, *m/z* = 188.14 $[M+H]^+$, calcd. for $[C_{10}H_9N_3O-H]^-$ 188.20, which was reacted with CDI following V procedure to obtain the oxadiazolone **1.67** in 62% yield (38 mg, 0.18 mmol). Chromatography: hexane to hexane:EtOAc 75:25. Mp: 244 – 247 ºC. ^{1}H NMR (400 MHz, MeOD) δ 8.01 (s, 1H, H_5), 7.92 (d, *J* = 7.9 Hz, 1H, H_7), 7.71 (d, *J* = 7.7 Hz, 1H, H_9), 7.59 (t, *J* = 7.8 Hz, 1H, H_8), 7.37 (d, *J* = 16.4 Hz, 1H, H_3), 6.94 (d, *J* = 16.4 Hz, 1H, H_2). HPLC-MS (30:95- g.t.10 min) ^{t}R 2.22 min, *m/z* = 212.16 $[M-H]^-$, calcd. for $[C_{11}H_7N_3O_2-H]^-$ 212.20. HRMS $[ESI^+]$ *m/z* = 213.05295 $[M]^+$, calcd for $[C_{11}H_7N_3O_2]^+$ 213.05383.

5-[(*E*)-2-(3-Nitrophenyl)ethenyl]-1,3,4-oxadiazol-2(3*H*)-one (1.68)

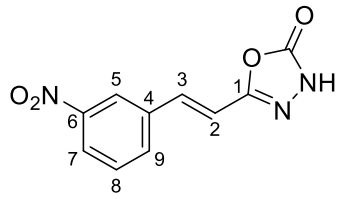

Commercial 3-nitrocinnamic acid (465 mg, 2.41 mmol) was transformed into the hydrazide **1.57** without isolation, identified by HPLC-MS (15:95- g.t.5), hydrazide appears in the

injection point, *m/z* = 208.05 $[M+H]^+$, calcd. for $[C_9H_9N_3O_3 +H]^+$ 208.19, which was reacted with CDI following V procedure to obtain the oxadiazolone **1.68** in 92% yield (515 mg, 2.21 mmol). Chromatography: hexane to hexane:EtOAc 60:40. Mp: 232 - 234 ºC. ^{1}H NMR (500 MHz, DMSO-d_6) δ 9.38 (t, *J* = 1.9 Hz, 1H, H_5), 9.04 – 8.98 (m, 2H, H_7, H_9), 8.51 (t, *J* = 8.0 Hz, 1H, H_8), 8.29 (d, *J* = 16.5 Hz, 1H, H_3), 8.03 (d, *J* = 16.5 Hz, 1H, H_2). ^{13}C NMR (126 MHz, DMSO-d_6) δ 163.5 (CO), 163.3 (C_1), 157.9 (C_6), 146.1 (C_4), 143.9 (C_3), 142.9 (C_9), 139.8 (C_8), 133.3 (C_7), 131.8 (C_5), 123.3 (C_2). HPLC-MS (15:95- g.t.10 min) ^{t}R 6.46 min, *m/z* = 232.23$[M-H]^-$, calcd. for $[C_{10}H_7N_3O_4 -H]^-$ 232.18. HRMS [ESI$^+$] *m/z* = 233.04337 $[M]^+$, calcd. for $[C_{10}H_7N_3O_4]^+$ 233.04366.

5-[(*E*)-2-(3-Methoxyphenyl)ethenyl]-1,3,4-oxadiazol-2(3*H*)-one (1.69)

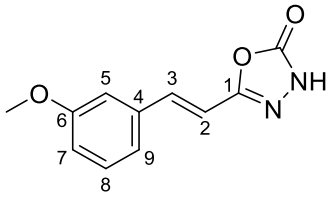

Following the general procedure *V*, the oxadiazolone **1.69** was obtained from **1.58** (350 mg, 1.8 mmol) in 96% yield (382 mg, 1.75 mmol). Chromatography: hexane to hexane:EtOAc 8:2. Mp: 178 - 180 ºC. ^{1}H NMR (500 MHz, MeOD) δ 7.32 (d, *J* = 16.5 Hz, 1H, H_3), 7.31 (t, *J* = 7.9 Hz, 1H, H_8), 7.17 (d, *J* = 7.6 Hz, 1H, H_9), 7.15 (bs, 1H, H_5), 6.94 (t, *J* = 8.1 Hz, 1H, H_7), 6.78 (d, *J* = 16.4 Hz, 1H, H_2), 3.83 (s, 3H, CH_3). ^{13}C NMR (126 MHz, MeOD) δ 161.6 (C_6), 156.6 (CO), 156.5 (C_1), 138.6 (C_3), 137.6 (C_4), 131.0 (C_8), 121.1 (C_9), 116.7 (C_7), 113.4 (C_5), 111.8 (C_2), 55.8 (CH_3). HPLC-MS (15:95- g.t.5 min) ^{t}R 4.07 min, *m/z* = 219.18 $[M+H]^+$, calcd. for $[C_{11}H_{10}N_2O_3 +H]^+$ 219.21. HRMS [ESI$^+$] *m/z* = 218.06887 $[M]^+$, calcd. for $[C_{11}H_{10}N_2O_3]^+$ 218.06914.

5-[(*E*)-2-(4-Methoxyphenyl)ethenyl]-1,3,4-oxadiazol-2(3*H*)-one (1.70)

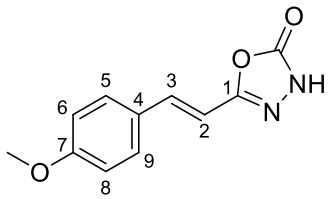

Following the general procedure V, the oxadiazolone **1.70** was obtained from hydrazide **1.59** (305 mg, 1.59 mmol) in 82% yield (284 mg, 1.30 mmol). Chromatography: hexane to

hexane:EtOAc 65:35. Mp: 191 - 193 ºC. ^{1}H NMR (400 MHz, MeOD) δ 7.53 (d, *J* = 8.8 Hz, 2H, H_5, H_9), 7.28 (d, *J* = 16.4 Hz, 1H, H_3), 6.94 (d, *J* = 8.8 Hz, 2H, H_6, H_8), 6.61 (d, *J* = 16.4 Hz, 1H, H_2), 3.82 (s, 3H, CH_3). ^{13}C NMR (101 MHz, MeOD) δ 162.6 (C_7), 156.8 (C_1), 156.6 (CO), 138.5 (C_3), 130.1 (C_5, C_9), 128.9 (C_4), 115.4 (C_6, C_8), 109.0 (C_2), 55.8 (CH_3). HPLC-MS (15:95- g.t.5 min) ^{t}R 3.59 min, *m/z* = 219.18 $[M+H]^+$, calcd. for $[C_{11}H_{10}N_2O_3+H]^+$ 219.21. HRMS [ESI$^+$] *m/z* = 218.06832 $[M]^+$, calcd. for $[C_{11}H_{10}N_2O_3]^+$ 218.06914.

5-[(*E*)-2-(2,4-Dimethoxyphenyl)ethenyl]-1,3,4-oxadiazol-2(3*H*)-one (1.71)

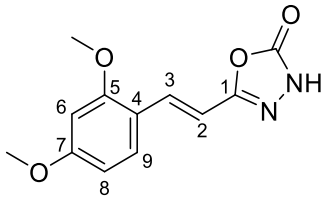

Following the general procedure V, the oxadiazolone **1.71** was obtained from hydrazide **1.60** (293 mg, 1.32 mmol) in 76% yield (248 mg, 1.00 mmol). Chromatography: hexane to hexane:EtOAc, 65:35. Mp: 220 - 222 ºC. ^{1}H NMR (500 MHz, MeOD) δ 7.49 (d, *J* = 16.4 Hz, 1H, H_3), 7.49 (d, *J* = 8.6 Hz, 1H, H_9), 6.69 (d, *J* = 16.5 Hz, 1H, H_2), 6.60 – 6.54 (m, 2H, H_6, H_8), 3.91 (s, 3H, C_5OCH_3), 3.84 (s, 3H, C_7OCH_3). ^{13}C NMR (126 MHz, MeOD) δ 164.1 (C_7), 160.8 (C_5), 157.4 (C_1), 156.8 (CO), 134.1 (C_3), 130.7 (C_9), 117.7 (C_4), 109.1 (C_2), 106.9 (C_6), 99.2 (C_8), 56.1($C_9O\underline{C}H_3$), 55.9 ($C_7O\underline{C}H_3$). HPLC-MS (15:95- g.t.5 min) ^{t}R 4.12 min, *m/z* = 249.15 $[M+H]^+$, calcd. for $[C_{12}H_{12}N_2O_4+H]^+$ 249.24. HRMS [ESI$^+$] *m/z* = 248.07922 $[M]^+$, calcd. for $[C_{12}H_{12}N_2O_4]^+$ 248.07971.

5-[(*E*)-2-(2,5-Dimethoxyphenyl)ethenyl]-1,3,4-oxadiazol-2(3*H*)-one (1.72)

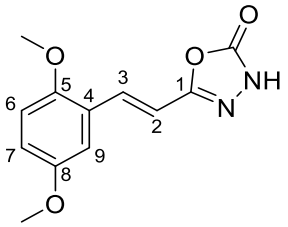

Following the general procedure *V*, the oxadiazolone **1.72** was obtained from hydrazide **1.61** (465 mg, 2.09 mmol) in 79% yield (410 mg, 1.65 mmol). Chromatography: hexane to hexane:EtOAc 65:35. Mp: 124 - 126 ºC. ^{1}H NMR (400 MHz, MeOD) δ 7.58 (d, *J* = 16.6 Hz, 1H, H_3), 7.15 (d, *J* = 2.9 Hz, 1H, H_9), 6.99 (d, *J* = 9.0 Hz, 1H, H_6), 6.95 (dd, *J* = 9.0,

2.9 Hz, 1H, H_7), 6.84 (d, *J* = 16.6 Hz, 1H, H_2), 3.88 (s, 3H, C_5OCH_3), 3.80 (s, 3H, C_8OCH_3). ^{13}C NMR (101 MHz, MeOD) δ 156.9 (C_1), 156.7 (CO), 155.2 (C_8), 153.8 (C_5), 133.8 (C_3), 125.3 (C_4), 117.7 (C_7), 113.8 (C_9), 113.7 (C_6), 112.0 (C_2), 56.6 ($C_5O\underline{C}H_3$), 56.2 ($C_8O\underline{C}H_3$). HPLC-MS (15:95- g.t.5 min) ^{t}R 4.11 min, *m/z* = 249.05 $[M+H]^+$, calcd. for $[C_{12}H_{12}N_2O_4+H]^+$ 249.24. HRMS $[ESI^+]$ *m/z* = 248.08094 $[M]^+$, calcd. for $[C_{12}H_{12}N_2O_4]^+$ 248.07971.

5-[(*E*)-2-(3,4-Dimethoxyphenyl)ethenyl]-1,3,4-oxadiazol-2(3*H*)-one (1.73)

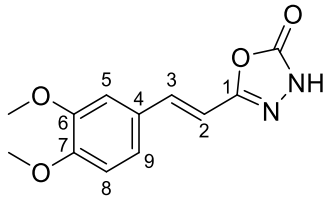

Following the general procedure V, the oxadiazolone **1.73** was obtained from hydrazide **1.62** (330 mg, 1.49 mmol) in 64% yield (165 mg, 0.66 mmol). Chromatography: hexane to hexane:EtOAc 65:35. Mp: 248 - 251 ºC. ^{1}H NMR (500 MHz, DMSO-d_6) δ 7.36 (d, *J* = 2.0 Hz, 1H, H_5), 7.23 (d, *J* = 16.5 Hz, 1H, H_3), 7.20 (dd, *J* = 8.5, 2.0 Hz, 1H, 12), 6.97 (d, *J* = 8.3 Hz, 1H, H_8), 6.87 (d, *J* = 16.4 Hz, 1H, H_2), 3.81 (s, 3H, C_6OCH_3), 3.78 (s, 3H, C_7OCH_3). ^{13}C NMR (126 MHz, DMSO-d_6) δ 154.6 (C_1), 154.1 (CO), 150.3(C_7), 149.0 (C_6), 136.9 (C_3), 127.6 (C_4), 122.0 (C_9), 111.5 (C_8), 109.7 (C_5), 108.5 (C_2), 55.6 ($C_6O\underline{C}H_3$), 55.5 ($C_7O\underline{C}H_3$). HPLC-MS (15:95- g.t.5 min) ^{t}R 3.62 min, *m/z* = 249.23 $[M+H]^+$, calcd. for $[C_{12}H_{12}N_2O_4+H]^+$ 249.24. HRMS $[ESI^+]$ *m/z* = 248.08081 $[M]^+$, calcd. for $[C_{12}H_{12}N_2O_4]^+$ 248.07971.

5-[(*E*)-2-(2*H*-1,3-Benzodioxol-5-yl)ethenyl]-1,3,4-oxadiazol-2(3*H*)-one (1.74)

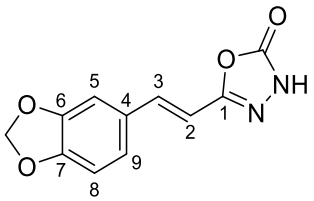

Following the general procedure V, the oxadiazolone **1.74** was obtained from hydrazide **1.63** (100 mg, 0.48 mmol) in 86% (95 mg, 0.46 mmol). Chromatography: hexane to hexane:EtOAc 65:35. Mp: 245 - 248 ºC. ^{1}H NMR (400 MHz, MeOD) δ 7.28 (d, *J* = 16.4 Hz, 1H, H_3), 7.19 (d, *J* = 1.8 Hz, 1H, H_5), 7.08 (dd, *J* = 8.0, 1.8 Hz, 1H, H_9), 6.86 (d, *J* =

8.0 Hz, 1H, H_8), 6.63 (d, *J* = 16.3 Hz, 1H, H_2), 6.02 (s, 2H, CH_2). ^{13}C NMR (101 MHz, MeOD) δ 156.7 (C_1), 156.6 (CO), 150.7 (C_7), 150.0 (C_6), 138.5 (C_3), 130.7 (C_4), 124.7 (C_9), 109.5 (C_2, C_8), 106.9 (C_5), 103.0 (CH_2). HPLC-MS (15:95- g.t.5 min) ^{t}R 3.89 min, *m/z* = 233.12 $[M+H]^+$, calcd. for $[C_{11}H_8N_2O_4+H]^+$ 232.20. HRMS $[ESI^+]$ *m/z* = 232.04873 $[M]^+$, calcd. for $[C_{11}H_8N_2O_4]^+$ 232.04841.

5-[(*E*)-2-(3,5-Dimethoxyphenyl)ethenyl]-1,3,4-oxadiazol-2(3*H*)-one (1.75)

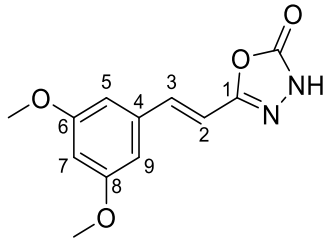

Commercial 3,5-dimethoxycinnamic acid (250 mg, 1.20 mmol) was transformed into the hydrazide **1.64** without isolation following the general procedure IV. The hydrazide was identified by HPLC-MS (15:95- g.t.5 min), appearing in the injection point and at 2.80 min, *m/z* = 223.14 $[M+H]^+$, calcd. for $[C_{11}H_{14}N_2O_3+H]^+$ 223.24, which was reacted with CDI following procedure V to obtain the oxadiazolone **1.75** in 74% yield (206 mg, 0.83 mmol). Chromatography: hexane to hexane:EtOAc 1:1. Mp: 156 - 159 ºC. ^{1}H NMR (400 MHz, MeOD) δ 7.29 (d, *J* = 16.4 Hz, 1H, H_3), 6.79 (d, *J* = 16.2 Hz, 1H, H_2), 6.78 (d, *J* = 2.3 Hz, 2H, H_5, H_9), 6.53 (t, *J* = 2.2 Hz, 1H, H_7), 3.83 (s, 6H, $2CH_3$). ^{13}C NMR (101 MHz, MeOD) δ 162.7 (C_6, C_8), 156.6 (CO), 156.4 (C_1), 138.8 (C_3), 138.1 (C_4), 112.0 (C_2), 106.4 (C_5, C_9), 103.0 (C_7), 55.9 ($2CH_3$). HPLC-MS (15:95- g.t.5 min) ^{t}R 4.16 min, *m/z* = 249.23 $[M+H]^+$, calcd. for $[C_{12}H_{12}N_2O_4+H]^+$ 249.24. HRMS $[ESI^+]$ *m/z* = 248.08033 $[M]^+$, calcd. for $[C_{12}H_{12}N_2O_4]^+$ 248.07971.

5-[(*E*)-2-(3,4,5-Trimethoxyphenyl)ethenyl]-1,3,4-oxadiazol-2(3*H*)-one (1.76)

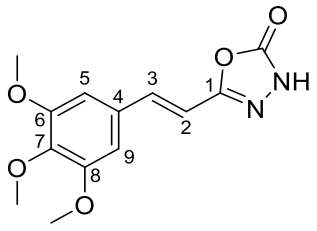

Following the general procedure V, the oxadiazolone **1.76** was obtained from hydrazide **1.65** (90 mg, 0.36 mmol) in 68% yield (189 mg, 0.68 mmol). Chromatography: hexane to

hexane:EtOAc 1:1. Mp: 214 - 217 ºC. ^{1}H NMR (500 MHz, MeOD) δ 7.43 (d, *J* = 16.3 Hz, 1H, H_3), 7.06 (s, 2H, H_5, H_9), 6.87 (d, *J* = 16.3 Hz, 1H, H_2), 4.03 (s, 6H, C_6OCH_3, C_8OCH_3), 3.94 (s, 3H, C_7OCH_3). ^{13}C NMR (126 MHz, MeOD) δ 156.7 (CO), 156.6 (C_1), 154.9 (C_6, C_8), 140.9 (C_7), 138.7 (C_3), 132.2 (C_4), 111.0 (C_2), 106.3 (C_5, C_9), 61.2 ($C_7O\underline{C}H_3$), 56.8 ($C_6O\underline{C}H_3$, $C_8O\underline{C}H_3$). HPLC-MS (15:95- g.t.5 min) ^{t}R 3.77 min, *m/z* = 279.12 $[M+H]^+$, calcd. for $[C_{10}H_8N_2O_4+H]^+$ 279.26. HRMS $[ESI^+]$ *m/z* = 278.09113 $[M]^+$, calcd. for $[C_{13}H_{14}N_2O_5]^+$ 278.09027.

3-(3-Methoxyphenyl)propanoic acid (1.77)

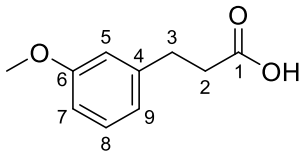

Following the general procedure for hydrogenation III, the acid **1.77** was obtained from the commercial 3-methoxycinnamic acid (500 mg, 2.8 mmol), without further purification in 98% yield (498 mg, 2.8 mmol) as an oil which slowly solidified. Mp: 41 - 43 ºC (lit. 40 ºC)[161]. ^{1}H NMR (400 MHz, MeOD) δ 7.18 (t, *J* = 8.1 Hz, 1H, H_8), 6.82 – 6.78 (m, 2H, H_9, H_5), 6.77 – 6.73 (m, 1H, H_7), 3.78 (s, 3H, CH_3), 2.89 (t, *J* = 7.7 Hz, 2H, H_3), 2.60 (t, *J* = 7.7 Hz, 2H, H_2). ^{13}C NMR (101 MHz, MeOD) δ 176.7 (C_1), 161.3 (C_6), 143.7 (C_4), 130.4 (C_8), 121.6 (C_9), 115.0 (C_5), 112.6 (C_7), 55.5 (CH_3), 36.7 (C_2), 32.1 (C_3). HPLC-MS (15:95- g.t.5 min) ^{t}R 3.64 min, *m/z* = 181.14 $[M+H]^+$, calcd. for $[C_{10}H_{12}O_3+H]^+$ 181.20.

3-(2,4-Dimethoxyphenyl)propanoic acid (1.78)

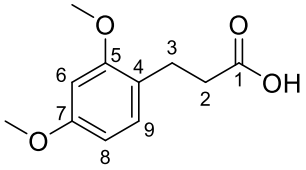

Following the general procedure for hydrogenation III, the saturated acid **1.78** was obtained from the commercial 2,4-dimethoxycinnamic acid (500 mg, 2.4 mmol), without further purification in 91% yield (438 mg, 2.1 mmol). Mp: 101 - 102 ºC (lit. 102.5 - 103.5 °C)[162]. ^{1}H NMR (300 MHz, MeOD) δ 7.03 (d, *J* = 8.2, 1H, H_9), 6.51 (d, *J* = 2.3 Hz, 1H, H_8), 6.43 (dd, *J* = 8.3, 2.4 Hz, 1H, H_6), 3.82 (s, 3H, C_7OCH_3), 3.78 (s, 3H, C_5OCH_3), 2.82 (t, *J* = 7.7 Hz, 2H, H_3), 2.58 – 2.44(m, 2H, H_2). ^{13}C NMR (75 MHz, MeOD) δ 177.3 (C_1), 161.2 (C_7),

159.7 (C_5), 131.1 (C_9), 122.3 (C_4), 105.2 (C_6), 99.3 (C_8), 55.7 ($2OCH_3$), 35.4 (C_2), 26.6 (C_3). HPLC-MS (15:95- g.t.5 min) ^tR 3.79 min, *m/z* = 211.17 $[M+H]^+$, calcd. for $[C_{11}H_{14}O_4 +H]^+$ 211.23.

3-(2,5-Dimethoxyphenyl)propanoic acid (1.79)

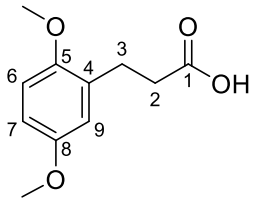

Following the general procedure of hydrogenation III the saturated acid **1.79** was obtained from the commercial 2,5-dimethoxycinnamic acid (500 mg, 2.4 mmol), without further purification in quantitative yield (504 mg, 2.4 mmol). Mp: 67 - 69 ºC (lit. 66 ºC)[163]. ^1H NMR (300 MHz, MeOD) δ 6.89 – 6.77 (m, 1H, H_6), 6.78 – 6.65 (m, 2H, H_7, H_9), 3.76 (s, 3H, C_5OCH_3), 3.70 (s, 3H, C_8OCH_3), 2.84 (t, *J* = 7.9 Hz, 2H, H_3), 2.52 (t, *J* = 7.7 Hz, 2H, H_2). ^{13}C NMR (75 MHz, MeOD) δ 177.1 (C_1), 154.9 (C_8), 153.1 (C_5), 131.2 (C_4), 117.3 (C_9), 112.6 (C_6), 112.3 (C_7), 56.2 ($C_5O\underline{C}H_3$), 56.0 ($C_8O\underline{C}H_3$), 35.2 (C_2), 27.3 (C_3). HPLC-MS (15:95- g.t.5 min) ^tR 3.73 min, *m/z* = 211.21 $[M+H]^+$, calcd. for $[C_{11}H_{14}O_4 +H]^+$ 211.23.

3-(2*H*-1,3-Benzodioxol-5-yl)propanoic acid (1.80)

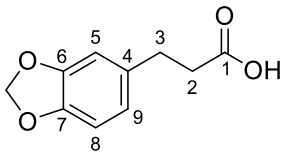

Following the general procedure of hydrogenation III, the saturated acid **1.80** was obtained from the acid **1.54** (150 mg, 0.78 mmol), without further purification in quantitative yield (152 mg, 0.78 mmol). Mp: 78.9 - 79.9 ºC (lit. 82 - 84 ºC)[164]. ^1H NMR (400 MHz, MeOD) δ 6.63 – 6.51 (m, 3H, H_5, H_8, H_9), 5.76 (s, 2H, OCH_2), 2.71 (t, *J* = 7.6 Hz, 2H, H_3), 2.43 (t, *J* = 7.6 Hz, 2H, H_2). ^{13}C NMR (101 MHz, MeOD) δ 176.7 (C_1), 149.0 (C_7), 147.3 (C_6), 136.0 (C_4), 122.2 (C_9), 109.7 (C_8), 109.0 (C_5), 102.0 (OCH_2), 37.0 (C_2), 31.7 (C_3). HPLC-MS (15:95- g.t.5 min) ^tR 3.55 min, *m/z* = 195.30 $[M+H]^+$, calcd. for $[C_{10}H_{10}O_4 +H]^+$ 195.19.

3-(3-Methoxyphenyl)propanehydrazide (1.81)

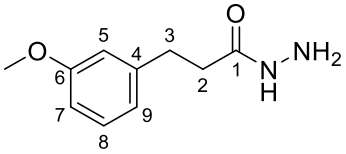

Following the general procedure IV, the hydrazide **1.81** was obtained from the acid **1.77** (480 mg, 2.7 mmol), without further purification in 79% yield (410 mg, 2.11 mmol). Mp: 79 - 82 ºC (lit. 88 - 89 ºC)[165]. ^{1}H NMR (400 MHz, MeOD) δ 7.18 (t, *J* = 8.1 Hz, 1H, H_8), 6.82 – 6.77 (m, 2H, H_5, H_9), 6.77 – 6.73 (m, 1H, H_7), 3.78 (s, 3H, CH_3), 2.89 (t, *J* = 7.7 Hz, 2H, H_3), 2.45 (dd, *J* = 7.7 Hz, 2H, H_2).^{13}C NMR (101 MHz, MeOD) δ 174.3 (C_1), 161.3 (C_6), 143.6 (C_4), 130.4 (C_8), 121.7 (C_9), 114.9 (C_5), 112.5 (C_7), 55.4 (CH_3), 36.8 (C_3), 32.7 (C_2). HPLC-MS (15:95- g.t.5 min) ^{t}R 2.03 min, *m/z* = 195.22 $[M+H]^+$, calcd. for $[C_{10}H_{14}N_2O_2+H]^+$ 195.23.

3-(2,4-Dimethoxyphenyl)propanehydrazide (1.82)

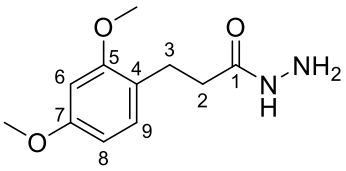

Following the general procedure IV, the hydrazide **1.82** was obtained from the acid **1.78** (435 mg, 2.07 mmol), without further purification, in quantitative yield (471 mg, 2.07 mmol). Mp: 110 - 113 ºC. ^{1}H NMR (500 MHz, MeOD) δ 7.00 (d, *J* = 8.2 Hz, 1H, H_9), 6.48 (d, *J* = 2.4 Hz, 1H, H_6), 6.40 (dd, *J* = 8.2, 2.4 Hz, 1H, H_8), 3.80 (s, 3H, C_5OCH_3), 3.76 (s, 3H, C_7OCH_3), 2.81 (dd, *J* = 8.5, 6.9 Hz, 2H, H_3), 2.36 (dd, *J* = 8.3, 7.1 Hz, 2H, H_2). ^{13}C NMR (126 MHz, MeOD) δ 174.9 (C_1), 161.2 (C_7), 159.7 (C_5), 131.1 (C_9), 122.2 (C_4), 105.2 (C_8), 99.3 (C_6), 55.7 ($2OCH_3$), 35.5 (C_2), 27.1 (C_3). HPLC-MS (15:95- g.t.5 min) ^{t}R 1.35 min, *m/z* = 225.18 $[M+H]^+$, calcd. for $[C_{11}H_{16}N_2O_3+H]^+$ 225.26.

3-(2,5-Dimethoxyphenyl)propanehydrazide (1.83)

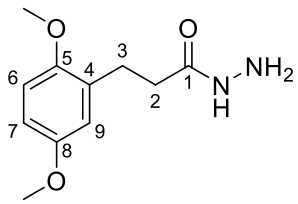

Following the general procedure IV, the hydrazide **1.83** was obtained from acid **1.79** (490 mg, 2.33 mmol), without further purification, in 82% yield (424 mg, 1.89 mmol). Mp: 90 - 92 ºC (lit. 94 - 95 ºC)[166]. ^{1}H NMR (400 MHz, MeOD) δ 6.86 (d, *J* = 9.3 Hz, 1H, H_6), 6.78 – 6.72 (m, 2H, H_7, H_9), 3.80 (s, 3H, C_5OCH_3), 3.75 (s, 3H, C_8OCH_3), 2.89 (dd, *J* = 8.1, 7.4 Hz, 2H, H_3), 2.43 (dd, *J* = 8.4, 7.1 Hz, 1H, H_2). ^{13}C NMR (101 MHz, MeOD) δ 174.7 (C_1), 155.0 (C_8), 153.0 (C_5), 131.2 (C_4), 117.3 (C_9), 112.7 (C_6), 112.3 (C_7), 56.2 ($C_5O\underline{C}H_3$), 56.0 ($C_8O\underline{C}H_3$), 35.2 (C_2), 27.7 (C_3). HPLC-MS (15:95- g.t.5 min) ^{t}R 3.73 min, *m/z* = 225.18 $[M+H]^+$, calcd. for $[C_{11}H_{16}N_2O_3+H]^+$ 225.26.

3-(2*H*-1,3-benzodioxol-5-yl)propanehydrazide (1.85)

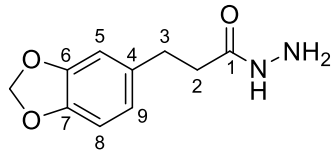

Following the general procedure IV, the hydrazide **1.85** was obtained from the corresponding acid **1.80** (145 mg, 0.75 mmol), without further purification, in 81% yield (126 mg, 0.60 mmol). Mp: 135 - 136 ºC (lit. 146 - 148 ºC)[158]. ^{1}H NMR (400 MHz, MeOD) δ 6.72 (d, *J* = 7.8 Hz, 1H, H_8), 6.72 (d, *J* = 1.6 Hz, 1H, H_5), 6.67 (d, *J* = 8.0, 1.6 Hz, 1H, H_9), 5.90 (s, 1H, OCH_2), 2.84 (t, *J* = 7.6 Hz, 1H, H_3), 2.41 (dd, *J* = 8.2, 7.0 Hz, 1H, H_2). ^{13}C NMR (101 MHz, MeOD) δ 174.2 (C_1), 135.8 (C_4), 122.3 (C_9), 109.7 (C_8), 109.1 (C_5), 102.1 (OCH_2), 37.2 (C_3), 32.5 (C_2). HPLC-MS (15:95- g.t.5 min) ^{t}R 1.58 min, *m/z* = 209.22 $[M+H]^+$, calcd. for $[C_{10}H_{12}N_2O_3+H]^+$ 209.22.

5-[2-(3-Methoxyphenyl)ethyl]-1,3,4-oxadiazol-2(3*H*)-one (1.86)

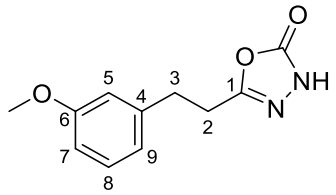

Following the general procedure V, the oxadiazolone **1.86** was obtained from hydrazide **1.81** (380 mg, 2.0 mmol) in 71% yield (304 mg, 1.39 mmol). Chromatography: hexane to hexane:EtOAc 6:4. Mp: 80 - 82 ºC. ^{1}H NMR (400 MHz, MeOD) δ 7.22 (t, *J* = 8.1 Hz, 1H, H_8), 6.85 – 6.75 (m, 3H, H_5, H_7, H_9), 3.80 (s, 3H, CH_3), 2.99 (t, *J* = 7.4 Hz, 2H, H_3), 2.89 (t, *J* = 7.5 Hz, 2H, H_2).^{13}C NMR (101 MHz, MeOD) δ 161.4 (C_6), 158.6 (C_1), 157.6 (CO),

142.5 (C_4), 130.6 (C_8), 121.6 (C_9), 115.0 (C_5), 113.0 (C_7), 55.6 (CH_3), 32.5 (C_3), 29.0 (C_2). HPLC-MS (15:95- g.t.5 min) ^tR 3.78 min, *m/z* = 221.13 $[M+H]^+$, calcd. for $[C_{11}H_{12}N_2O_3+H]^+$ 221.23. HRMS $[ESI^+]$ *m/z* = 220.08389 $[M]^+$, calcd. for $[C_{11}H_{12}N_2O_3]^+$ 220.08479.

5-[2-(2,4-Dimethoxyphenyl)ethyl]-1,3,4-oxadiazol-2(3*H*)-one (1.87)

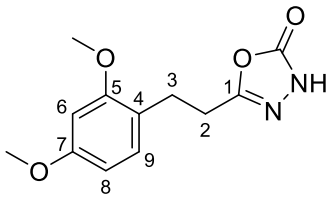

Following the general procedure V, the oxadiazolone **1.87** was obtained from hydrazide **1.82** (460 mg, 2.05 mmol) in 76% yield (389 mg, 1.55 mmol). Chromatography: hexane to hexane:EtOAc 65:35. Mp: 150 - 152 ºC. ^{1}H NMR (500 MHz, MeOD) δ 7.00 (d, *J* = 8.3 Hz, 1H, H_9), 6.49 (d, *J* = 2.4 Hz, 1H, H_6), 6.42 (dd, *J* = 8.2, 2.4 Hz, 1H, H_8), 3.79 (s, 3H, C_5OCH_3), 3.76 (s, 3H, C_7OCH_3), 2.88 (t, *J* = 7.3 Hz, 2H, H_3), 2.75 (t, *J* = 7.6 Hz, 2H, H_2). ^{13}C NMR (126 MHz, MeOD) δ 161.5 (C_7), 159.8 (C_5), 159.2 (C_1), 157.7 (CO), 131.4 (C_9), 121.1 (C_4), 105.4 (C_8), 99.3 (C_6), 55.7 ($2OCH_3$), 27.9 (C_2), 27.4 (C_3). HPLC-MS (30:95- g.t.10 min) ^tR 3.21 min, *m/z* = 251.17 $[M+H]^+$, calcd. for $[C_{12}H_{14}N_2O_4+H]^+$ 251.25. HRMS $[ESI^+]$ *m/z* = 250.09513 $[M]^+$, calcd. for $[C_{12}H_{14}N_2O_4]^+$ 250.09536.

5-[2-(2,5-Dimethoxyphenyl)ethyl]-1,3,4-oxadiazol-2(3*H*)-one (1.88)

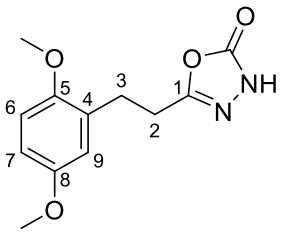

Following the general procedure V, the oxadiazolone **1.88** was obtained from hydrazide **1.83** (400 mg, 1.78 mmol) in 97% yield (434 mg, 1.73 mmol). Chromatography: hexane to hexane:EtOAc 60:40. Mp: 81 - 83 ºC. ^{1}H NMR (400 MHz, MeOD) δ 6.88 (d, *J* = 8.6 Hz, 1H, H_6), 6.78 (dd, *J* = 8.7, 3.0 Hz, 1H, H_7), 6.76 (d, *J* = 2.9 Hz, 2H, H_9), 3.80 (s, 3H, C_5OCH_3), 3.75 (s, 3H, C_8OCH_3), 2.97 (t, *J* = 7.5 Hz, 2H, H_3), 2.83 (t, *J* = 7.3 Hz, 2H, H_2). ^{13}C NMR (101 MHz, MeOD) δ 159.0 (C_1), 157.7 (CO), 155.0 (C_8), 153.1 (C_5), 130.0 (C_4),

117.4 (C_9), 113.2 (C_7), 112.4 (C_6), 56.2 ($C_5O\underline{C}H_3$), 56.1 ($C_8O\underline{C}H_3$), 28.0 (C_3), 27.6 (C_2). HPLC-MS (15:95- g.t.5 min) ^tR 3.89 min, *m/z* = 251.17 $[M+H]^+$, calcd. for $[C_{12}H_{14}N_2O_4 +H]^+$ 251.25. HRMS $[ESI^+]$ *m/z* = 250.0953 $[M]^+$, calcd. for $[C_{12}H_{14}N_2O_4]^+$ 250.09536.

5-[2-(3,4-Dimethoxyphenyl)ethyl]-1,3,4-oxadiazol-2(3*H*)-one (1.89)

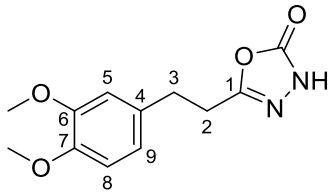

Commercial 3-(3,4-dimethoxyphenyl)propanoic acid (500 mg, 2.38 mmol) was transformed into the hydrazide **1.84** without isolation, identified by HPLC-MS (15:95- g.t.5 min), which appears in the injection point and at 1.24 min, *m/z* = 225.26 $[M+H]^+$, calcd. for $[C_{11}H_{16}N_2O_3 +H]^+$ 225.26, which was reacted with CDI following V procedure to afford the oxadiazolone **1.89** in 78% yield (428 mg, 1.71 mmol). Chromatography: hexane to hexane:EtOAc 60:40. Mp: 149 - 151 ºC. ^{1}H NMR (300 MHz, MeOD) δ 6.91 – 6.80 (m, 2H, H_8, H_5), 6.82 – 6.70 (m, 4.7, 2.0 Hz, 1H, H_9), 3.81 (s, 3H, C_6OCH_3), 3.79 (s, 3H, C_7OCH_3), 3.04 – 2.88 (m, 2H, H_3), 2.86 (t, *J* = 5.9 Hz, 2H, H_2). ^{13}C NMR (75 MHz, MeOD) δ 158.7 (C_1), 157.6 (CO), 150.5 (C_6), 149.2 (C_7), 133.9 (C_4), 121.7 (C_9), 113.3 (C_5), 113.1 (C_8), 56.5 (CH_3), 56.4 (CH_3), 32.1 (C_3), 29.3 (C_2). HPLC-MS (15:95- g.t.5 min) ^tR 3.35 min, *m/z* = 250.94 $[M+H]^+$, calcd. for $[C_{12}H_{14}N_2O_4 +H]^+$ 251.25. HRMS $[ESI^+]$ *m/z* = 250.09558 $[M]^+$, calcd. for $[C_{12}H_{14}N_2O_4]^+$ 250.09536.

5-[2-(2*H*-1,3-Benzodioxol-5-yl)ethyl]-1,3,4-oxadiazol-2(3*H*)-one (1.90)

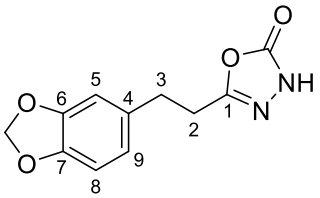

Following the general procedure V, the oxadiazolone **1.90** was obtained from hydrazide **1.85** (100 mg, 0.48 mmol) in 76% yield (85 mg, 0.36 mmol). Chromatography: hexane to hexane:EtOAc 9:1. Mp: 148 - 150 ºC. ^{1}H NMR (500 MHz, MeOD) δ 6.74 (d, *J* = 1.1 Hz, 1H, H_5), 6.73 (d, *J* = 8.1 Hz, 2H, H_8), 6.67 (dd, *J* = 7.9, 1.7 Hz, 1H, H_9), 5.90 (s, 2H, OCH_2), 2.91 (t, *J* = 7.6 Hz, 2H, H_3), 2.82 (ddd, *J* = 8.3, 7.1, 1.2 Hz, 2H, H_2). ^{13}C NMR (126

MHz, MeOD) δ 158.6 (C_1), 157.7 (CO), 149.2 (C_6), 147.7 (C_7), 134.8 (C_4), 122.4 (C_9), 109.7 (C_5), 109.2 (C_8), 102.2 (OCH_2), 32.2 (C_3), 29.4 (C_2). HPLC-MS (15:95- g.t.5 min) ^tR 3.70 min, *m/z* = 235.14 $[M+H]^+$, calcd. for $[C_{11}H_{10}N_2O_4+H]^+$ 209.22. HRMS $[ESI^+]$ *m/z* = 234.06465 $[M]^+$, calcd. for $[C_{11}H_{10}N_2O_4]^+$ 234.06406.

5-[(*E*)-2-(3-Hydroxyphenyl)ethenyl]-1,3,4-oxadiazol-2(3*H*)-one (1.91)

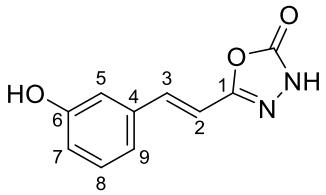

Following the general procedure VII, **1.91** was obtained from methoxylated **1.69** (132 mg, 0.60 mmol) in 91% yield (112 mg, 0.55 mmol) Chromatography: hexane to hexane:EtOAc 1:1. Mp: 230 - 233 ºC. ^1H NMR (400 MHz, MeOD) δ 7.29 (d, *J* = 16.5 Hz, 1H, H_3), 7.24 (t, *J* = 8.0 Hz, 1H, H_8), 7.08 (d, *J* = 7.7 Hz, 1H, H_9), 7.02 (t, *J* = 2.0 Hz, 1H, H_5), 6.83 (dd, *J* = 8.2, 2.5 Hz, 1H, H_7), 6.72 (d, *J* = 16.4 Hz, 1H, H_2). ^{13}C NMR (101 MHz, MeOD) δ 159.1 (C_6), 156.5 (CO), 156.5 (C_1), 138.9 (C_3), 137.5 (C_4), 131.0 (C_8), 120.1 (C_9), 118.0 (C_7), 114.6 (C_5), 111.3 (C_2). HPLC-MS (15:95- g.t.5 min) ^tR 3.21 min, *m/z* = 205.26 $[M+H]^+$, calcd. for $[C_{10}H_8N_2O_3+H]^+$ 205.19. HRMS $[ESI^+]$ *m/z* = 204.05432 $[M]^+$, calcd. for $[C_{10}H_8N_2O_3]^+$ 204.05349.

5-[(*E*)-2-(4-Hydroxyphenyl)ethenyl]-1,3,4-oxadiazol-2(3*H*)-one (1.92)

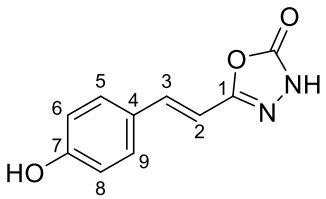

Following the general procedure VII, phenol **1.92** was obtained from **1.70** (75 mg, 0.34 mmol) in 91% yield (63 mg, 0.31 mmol). The final compound was washed with MeOH. Mp: 255 - 258 ºC. ^1H NMR (500 MHz, MeOD) δ 7.44 (d, *J* = 8.4 Hz, 2H, H_5, H_9), 7.25 (d, *J* = 16.3 Hz, 1H, H_3), 6.80 (d, *J* = 8.6 Hz, 2H, H_6, H_8), 6.56 (d, *J* = 16.4 Hz, 1H, H_2). ^{13}C NMR (126 MHz, MeOD) δ 160.6 (C_7), 157.0 (C_1), 156.7 (CO), 138.9 (C_3), 130.3 (C_5, C_9), 127.7 (C_4), 116.8 (C_6, C_8), 108.1 (C_2). HPLC-MS (15:95- g.t.5 min) ^tR 3.12 min, *m/z* =

205.18 $[M+H]^+$, calcd. for $[C_{10}H_8N_2O_3+H]^+$ 205.19. HRMS $[ESI^+]$ *m/z* = 204.05403 $[M]^+$, calcd. for $[C_{10}H_8N_2O_3]^+$ 204.05349.

5-[(*E*)-2-(3,4-Dihydroxyphenyl)ethenyl]-1,3,4-oxadiazol-2(3*H*)-one (1.93)

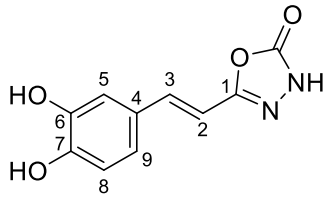

Following the general procedure VII, **1.93** was obtained from **1.73** (100 mg, 0.40 mmol) in 89% yield (78 mg, 0.36 mmol). Chromatography: hexane to hexane:EtOAc 1:1. Mp: 253 - 256 ºC. ^{1}H NMR (500 MHz, MeOD) δ 7.20 (d, *J* = 16.3 Hz, 1H, H_3), 7.03 (d, *J* = 2.1 Hz, 1H, H_5), 6.93 (dd, *J* = 8.2, 2.1 Hz, 1H, H_9), 6.78 (d, *J* = 8.1 Hz, 1H, H_8), 6.50 (d, *J* = 16.3 Hz, 1H, H_2).^{13}C NMR (126 MHz, MeOD) δ 157.0 (C_1), 156.7 (CO), 148.9 (C_7), 146.8 (C_6), 139.2 (C_3), 128.3 (C_4), 121.9 (C_9), 116.5 (C_8), 114.5 (C_5), 108.0 (C_2). HPLC-MS (15:95-g.t.5 min) ^{t}R 2.70 min, *m/z* = 221.13 $[M+H]^+$, calcd. for $[C_{10}H_8N_2O_4+H]^+$ 221.18. HRMS $[ESI^+]$ *m/z* = 220.04861 $[M]^+$, calcd. for $[C_{10}H_8N_2O_4]^+$ 220.04841.

5-[(*E*)-2-(3,5-Dihydroxyphenyl)ethenyl]-1,3,4-oxadiazol-2(3*H*)-one (1.94)

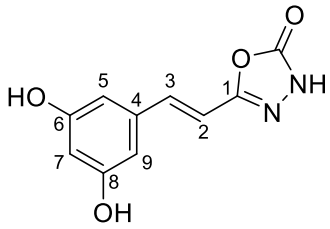

Following the general procedure VII, **1.94** was obtained from dimethoxy **1.75** (75 mg, 0.30 mmol) in 66% yield (44 mg, 0.20 mmol). Chromatography: hexane to EtOAc. Mp: 264 - 267 ºC. ^{1}H NMR (400 MHz, MeOD) δ 7.19 (d, *J* = 16.3 Hz, 1H, H_3), 6.64 (d, *J* = 16.3 Hz, 1H, H_2), 6.52 (d, *J* = 2.2 Hz, 2H, H_5, H_9), 6.31 (t, *J* = 2.2 Hz, 1H, H_7). ^{13}C NMR (101 MHz, MeOD) δ 160.1 (C_6, C_8), 156.7 (CO), 156.5 (C_1), 139.1 (C_3), 138.0 (C_4), 111.2 (C_2), 106.9 (C_5, C_9). HPLC-MS (15:95- g.t.5 min) ^{t}R 2.44 min, *m/z* = 221.21 $[M+H]^+$, calcd. for $[C_{10}H_8N_2O_4+H]^+$ 221.18. HRMS $[ESI^+]$ *m/z* = 220.04837 $[M]^+$, calcd. for $[C_{10}H_8N_2O_4]^+$ 220.04841.

5-[2-(3-Hydroxyphenyl)ethyl]-1,3,4-oxadiazol-2(3*H*)-one (1.95)

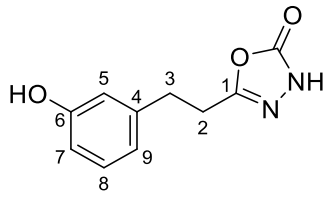

Following the general procedure VII, **1.95** was obtained from **1.86** (100 mg, 0.45 mmol) in 96% yield (90 mg, 0.44 mmol). Chromatography: hexane to hexane:EtOAc 35:65. Mp: 160 - 162 ºC. ^{1}H NMR (400 MHz, MeOD) δ 7.12 (t, *J* = 7.7 Hz, 1H, H_8), 6.71 (d, *J* = 7.8 Hz, 1H, H_9), 6.69 – 6.63 (m, 2H, H_5, H_7), 2.98 – 2.91 (m, 2H, H_3), 2.89 – 2.83 (m, 2H, H_2). ^{13}C NMR (101 MHz, MeOD) δ 158.6 (C_1, C_6), 157.6 (CO), 142.5 (C_4), 130.6 (C_8), 120.5 (C_9), 116.2 (C_5), 114.5 (C_7), 32.4 (C_3), 29.0 (C_2). HPLC-MS (15:95- g.t.5 min) ^{t}R 2.96 min, *m/z* = 207.20 $[M+H]^+$, calcd. for $[C_{10}H_{10}N_2O_3+H]^+$ 207.20. HRMS [ESI$^+$] *m/z* = 206.06906 $[M]^+$, calcd. for $[C_{10}H_{10}N_2O_3]^+$ 206.06914.

5-[2-(2,5-Dihydroxyphenyl)ethyl]-1,3,4-oxadiazol-2(3*H*)-one (1.96)

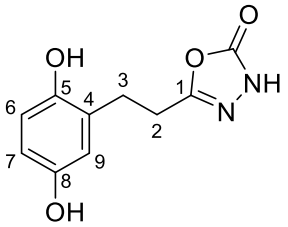

Following the general procedure VII, **1.96** was obtained from **1.88** (194 mg, 0.78 mmol) in 16% yield (27 mg, 0.16 mmol). The final compound was purified by semi-preparative HPLC-MS (10:20- g.t.30 min). Mp: 144 - 147 ºC. ^{1}H NMR (500 MHz, MeOD) δ 6.60 (d, *J* = 8.5 Hz, 1H, H_6), 6.55 (d, *J* = 2.9 Hz, 1H, H_9), 6.50 (dd, *J* = 8.5, 3.0 Hz, 1H, H_7), 2.91 – 2.87 (m, 2H, H_3), 2.85 – 2.81 (m, 2H, H_2). ^{13}C NMR (126 MHz, MeOD) δ 159.1 (C_1), 157.7 (CO), 151.1 (C_8), 149.4 (C_5), 128.0 (C_4), 117.7 (C_9), 116.7 (C_6), 115.1 (C_7), 28.0 (C_3), 27.5 (C_2). HPLC-MS (15:95- g.t.5 min) ^{t}R 1.55 min, *m/z* = 223.15 $[M+H]^+$, calcd. for $[C_{10}H_{10}N_2O_4+H]^+$ 223.20. HRMS [ESI$^+$] *m/z* = 222.06457$[M]^+$, calcd. for $[C_{10}H_{10}N_2O_4]^+$ 222.06406.

5-[2-(3,4-Dihydroxyphenyl)ethyl]-1,3,4-oxadiazol-2(3*H*)-one (1.97)

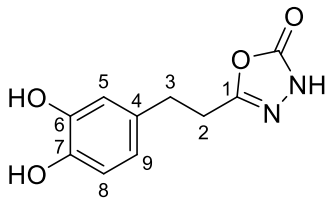

Following the general procedure VII, **1.97** was obtained from **1.89** (250 mg, 1.0 mmol) in 63% yield (139 mg, 0.63 mmol). Chromatography: hexane to EtOAc. Mp: 170 - 172 ºC. ^{1}H NMR (400 MHz, MeOD) δ 6.71 (d, *J* = 8.0 Hz, 1H, H_8), 6.67 (d, *J* = 2.1 Hz, 1H, H_5), 6.55 (dd, *J* = 8.1, 2.1 Hz, 1H, H_9), 2.90 – 2.76 (m, 4H, H_2, H_3). ^{13}C NMR (101 MHz, MeOD) δ 158.8 (C_1), 157.6 (CO), 146.3 (C_6), 144.9 (C_7), 132.5 (C_4), 120.6 (C_9), 116.4 (C_5, C_8), 32.0 (C_3), 29.4 (C_2). HPLC-MS (15:95- g.t.5 min) ^{t}R 2.29 min, *m/z* = 223.09 $[M+H]^+$, calcd. for $[C_{10}H_{10}N_2O_4 +H]^+$ 223.20. HRMS $[ESI^+]$ *m/z* = 222.06385 $[M]^+$, calcd. for $[C_{10}H_{10}N_2O_4]^+$ 222.06406.

5-[(*E*)-2-(3-Aminophenyl)ethenyl]-1,3,4-oxadiazol-2(3*H*)-one (1.98)[167]

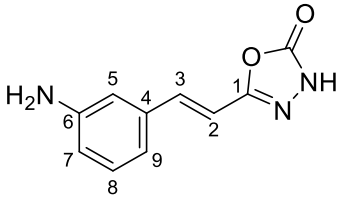

To a solution of nitro compound **1.68** (50 mg, 0.21 mmol) in EtOH (1 mL), a saturated solution of ammonium chloride (NH_4Cl, 0.5 mL) and iron powder (56 mg, 1.0 mmol) were added. The mixture was refluxed for 1 h, cooled at rt and filtered through Celite. The crude was extracted with EtOAc (x3). The organic layer was concentrated under reduced pressure and precipitated in hexane: EtOAc to obtain the aniline **1.98** in 87% yield (37 mg, 0.18 mmol). Mp: 255 ºC (decomposition). ^{1}H NMR (400 MHz, $CDCl_3$) δ 6.85 (d, *J* = 16.6 Hz, 1H, H_3), 6.80 (t, *J* = 7.8 Hz, 1H, H_8), 6.52 (d, *J* = 7.8 Hz, 1H, H_9), 6.48 (s, 1H, H_5), 6.36 (dd, *J* = 7.9, 2.3 Hz, 1H, H_7), 6.23 (d, *J* = 16.4 Hz, 1H, H_2). ^{13}C NMR (101 MHz, $CDCl_3$) δ 154.3 (CO), 154.3 (C_1), 146.9 (C_6), 137.3 (C_3), 135.1 (C_4), 129.3 (C_8), 116.9 (C_9), 116.2 (C_7), 112.9 (C_5), 109.8 (C_2).

3-[(Prop-2-en-1-yl)oxy]benzaldehyde (1.99)

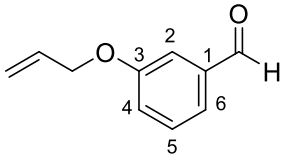

To a solution of commercial 3-hydroxybenzaldehyde (500 mg, 4.09 mmol) in dry acetone (5 mL/mmol), K_2CO_3 (677 mg, 4.9 mmol) was added at rt and the mixture was stirred for 10 min. Allyl bromide (425 µL, 4.9 mmol) was then added and the reaction was heated at 140 ºC for 20 min under mw irradiation. As starting material remained in the reaction, was heated 20 min more at 140 °C. The reaction was stopped without total conversion. H_2O was added and the mixture was extracted with EtOAc (x2), washed with brine, dried over $MgSO_4$, filtered, and evaporated under reduced pressure. The crude was purified by chromatography (hexane to hexane:EtOAc 7:3) to obtain **1.99** as a colorless oil in 49% yield (325 mg, 2.0 mmol). ^{1}H NMR (400 MHz, $CDCl_3$) δ 9.97 (s, 1H, CHO), 7.49 – 7.41 (m, 2H, H_5, H_6), 7.40 (d, *J* = 2.0 Hz, 1H, H_2), 7.20 (dt, *J* = 6.8, 2.5 Hz, 1H, H_4), 6.06 (ddt, *J* = 17.1, 10.5, 5.3 Hz, 1H, CH=), 5.43 (dd, *J* = 17.2, 1.6 Hz, 1H, CH_2=), 5.31 (dd, *J* = 10.5, 1.5 Hz, 1H, CH_2=), 4.60 (dt, *J* = 5.0, 1.2 Hz, 2H, C$\underline{H}_2$CH=). ^{13}C NMR (101 MHz, $CDCl_3$) δ 192.2 (CHO), 159.3 (C_3), 138.0 (C_1), 132.8 (CH=), 130.2 (C_5), 123.7 (C_6), 122.2 (C_4), 118.2 (CH_2=), 113.3 (C_2), 69.1 ($\underline{C}H_2$CH=). HPLC-MS (15:95- g.t.10 min) ^{t}R 7.57 min, *m/z* = 163.17 $[M+H]^+$, calcd. for $[C_{10}H_{10}O_2 -H]^-$ 163.19.

(3*E*)-4-(3-Hydroxyphenyl)but-3-en-2-one (1.100)

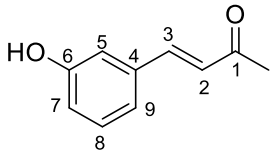

Ketone **1.100** was isolated as undesirable from reaction to prepare **1.99**, resulted of aldol condensation between 3-hydroxybenzaldehyde and acetone (the solvent) in 4% yield (25 mg, 0.15 mmol). Mp: 89 - 90 ºC. ^{1}H NMR (400 MHz, $CDCl_3$) δ 7.45 (d, *J* = 16.3 Hz, 1H, H_3), 7.28 (t, *J* = 7.9 Hz, 1H, H_8), 7.1 (d, *J* = 7.6 Hz, 1H, H_9), 7.02 (t, *J* = 2.0 Hz, 1H, H_5), 6.88 (dd, *J* = 8.2, 2.4 Hz, 1H, H_7), 6.68 (d, *J* = 16.3 Hz, 1H, H_2), 2.38 (s, 3H, CH_3). ^{13}C NMR (126 MHz, $CDCl_3$) δ 198.5 (C_1), 156.1 (C_6), 143.1 (C_3), 136.2 (C_4), 130.4 (C_8), 127.7

(C_2), 121.4 (C_9), 117.8 (C_7), 114.6 (C_5), 27.7 (CH_3). HPLC-MS (15:95- g.t.10 min) ^tR 4.67 min, *m/z* = 163.24 $[M+H]^+$, calcd. for $[C_{10}H_{10}O_2+H]^+$ 163.19.

(3*E*)-4-{3-[(Prop-2-en-1-yl)oxy]phenyl}but-3-en-2-one (1.101)

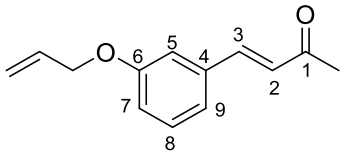

Ketone **1.101** was isolated as undesirable from reaction to prepare **1.99**, resulted of aldol condensation between **1.99** and acetone (the solvent), as oil in 6% yield (46 mg, 0.23 mmol). ^{1}H NMR (400 MHz, $CDCl_3$) δ 7.47 (d, *J* = 16.3 Hz, 1H, H_3), 7.31 (t, *J* = 7.9 Hz, 1H, H_8), 7.14 (d, *J* = 7.6 Hz, 1H, H_9), 7.08 (t, *J* = 2.0 Hz, 1H, H_5), 6.96 (dd, *J* = 8.2, 1.8 Hz, 1H, H_7), 6.69 (d, *J* = 16.3 Hz, 1H, H_2), 6.06 (ddt, *J* = 17.2, 10.5, 5.3 Hz, 1H, CH=), 5.43 (dd, *J* = 17.2, 1.6 Hz, 1H, CH_2=), 5.31 (dd, *J* = 10.5, 1.5 Hz, 1H, CH_2=), 4.57 (dt, *J* = 5.3, 1.5 Hz, 2H, C$\underline{H}_2$CH=), 2.38 (s, 3H, CH_3). ^{13}C NMR (101 MHz, $CDCl_3$) δ 198.5 (C_1), 159.1 (C_6), 143.5 (C_3), 136.0 (C_4), 133.1 (CH=), 130.1 (C_8), 127.6 (C_2), 121.3 (C_9), 118.0 (CH_2=), 117.3 (C_7), 114.1 (C_5), 69.0 ($\underline{C}H_2$CH=), 27.7 (CH_3). HPLC-MS (15:95- g.t.10 min) ^tR 8.18 min, *m/z* = 203.23 $[M+H]^+$, calcd. for $[C_{13}H_{14}O_2+H]^+$ 203.25. HRMS [ESI$^+$] *m/z* = 202.09966 $[M]^+$, calcd. for $[C_{13}H_{14}O_2]^+$ 202.09938.

(2*E*)-3-{3-[(Prop-2-en-1-yl)oxy]phenyl}prop-2-enoic acid (1.102)

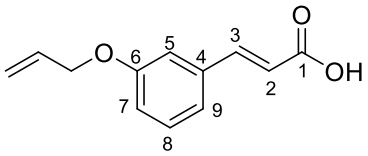

Following the *Knoevenagel-Doebner* reaction procedure II, acid **1.102** was obtained from the aldehyde **1.99** (320 mg, 1.97 mmol), without further purification, in 96% yield (386 mg, 1.89 mmol). Mp: 110 - 113 ºC. ^{1}H NMR (400 MHz, $CDCl_3$) δ 7.75 (d, *J* = 15.9 Hz, 1H, H_3), 7.32 (t, *J* = 7.9 Hz, 1H, H_8), 7.15 (d, *J* = 7.6 Hz, 1H, H_9), 7.09 (bs, 1H, H_5), 6.98 (dd, *J* = 8.1, 2.1 Hz, 1H, H_7), 6.43 (d, *J* = 15.9 Hz, 1H, H_2), 6.06 (ddt, *J* = 17.2, 10.5, 5.3 Hz, 1H, CH=), 5.43 (dd, *J* = 17.3, 1.6 Hz, 1H, 1/2CH_2=), 5.31 (dd, *J* = 10.5, 1.4 Hz, 1H, 1/2CH_2=), 4.58 (d, *J* = 5.4 Hz, 2H, C$\underline{H}_2$CH=). ^{13}C NMR (101 MHz, $CDCl_3$) δ 172.0 (C_1), 159.1 (C_6), 147.1 (C_3), 135.5 (C_4), 133.1 (CH=), 130.1 (C_8), 121.4 (C_9), 118.1 (CH_2=), 117.7 (C_2),

117.6 (C_7), 114.2 (C_5), 69.1 ($\underline{C}H_2CH$=). HPLC-MS (15:95- g.t.10 min) ^tR 7.40 min, *m/z* = 205.26 $[M+H]^+$, calcd. for $[C_{12}H_{12}O_3+H]^+$ 205.23.

(2*E*)-3-{3-[(Prop-2-en-1-yl)oxy]phenyl}prop-2-enehydrazide (1.103)

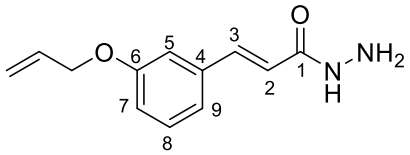

Following the general procedure IV, the hydrazide **1.104** was obtained from acid **1.102** (330 mg, 1.62 mmol), without further purification, in 99% yield (350 mg, 1.60 mmol). Mp: 73 - 76 ºC. ^{1}H NMR (400 MHz, $CDCl_3$) δ 7.64 (d, *J* = 15.6 Hz, 1H, H_3), 7.29 (t, *J* = 7.9 Hz, 1H, H_8), 7.11 (d, *J* = 7.7 Hz, 1H, H_9), 7.05 (bs, 1H, H_5), 6.93 (dd, *J* = 8.2, 2.6 Hz, 1H, H_7), 6.87 (bs, 1H, NH), 6.32 (d, *J* = 15.6 Hz, 1H, H_2), 6.06 (ddt, *J* = 17.2, 10.5, 5.3 Hz, 1H, CH=), 5.42 (dd, *J* = 17.3, 1.5 Hz, 1H, CH_2=), 5.30 (dd, *J* = 10.5, 1.3 Hz, 1H, CH_2=), 4.56 (d, *J* = 5.3 Hz, 2H, $C\underline{H}_2CH$=). ^{13}C NMR (101 MHz, $CDCl_3$) δ 167.1 (C_1), 159.1 (C_6), 142.0 (C_3), 136.1 (C_4), 133.1 (CH=), 130.0 (C_8), 120.8 (C_9), 118.2 (C_2), 118.0 (CH_2=), 116.6 (C_7), 114.1 (C_5), 69.0 ($\underline{C}H_2CH$=). HPLC-MS (15:95- g.t.10 min) ^tR 5.03 min, *m/z* = 219.18 $[M+H]^+$, calcd. for $[C_{12}H_{14}N_2O_2+H]^+$ 219.26.

5-[(*E*)-2-{3-[(prop-2-en-1-yl)oxy]phenyl}ethenyl]-1,3,4-oxadiazol-2(3*H*)-one (1.104)

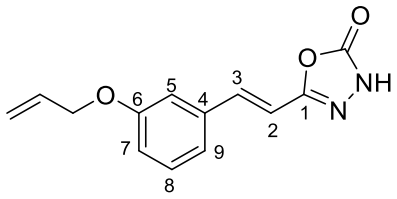

Following the general procedure V, the oxadiazolone **1.103** was obtained from the hydrazide **1.103** (350 mg, 1.6 mmol) in 78% yield (276 mg, 1.26 mmol). Chromatography: hexane to hexane:EtOAc 65:35. Mp: 151 - 154 ºC. ^{1}H NMR (500 MHz, MeOD) δ 7.30 (t, *J* = 7.9 Hz, 1H, H_8), 7.28 (d, *J* = 16.4 Hz, 1H, H_3), 7.16 (d, *J* = 7.7 Hz, 1H, H_9), 7.14 (bs, 1H, H_5), 6.94 (dd, *J* = 8.3, 2.6 Hz, 1H, H_7), 6.74 (d, *J* = 16.4 Hz, 1H, H_2), 6.07 (ddt, *J* = 17.3, 10.5, 5.2 Hz, 1H, CH=), 5.41 (dq, *J* = 17.3, 1.7 Hz, 1H, CH_2=), 5.26 (dq, *J* = 10.6, 1.5 Hz, 1H, CH_2=), 4.58 (dt, *J* = 5.2, 1.7 Hz, 2H, $C\underline{H}_2CH$=). ^{13}C NMR (126 MHz, MeOD) δ 160.5 (C_1), 156.5 (CO), 156.4 (C_6), 138.6 (C_3), 137.6 (C_4), 134.8 (CH=), 131.0 (C_8), 121.3 (C_9), 117.6 (CH_2=), 117.4 (C_7), 114.3 (C_5), 111.7 (C_2), 69.8 ($\underline{C}H_2CH$=). HPLC-MS (15:95-

g.t.10 min) ^{t}R 7.87 min, *m/z* = 245.18 $[M+H]^+$, calcd. for $[C_{13}H_{12}N_2O_3+H]^+$ 245.25. HRMS $[ESI^+]$ *m/z* = 244.08436 $[M]^+$, calcd. for $[C_{13}H_{12}N_2O_3]^+$ 244.08479.

SUBSTITUITED

All following substituted derivatives were obtained from the corresponding oxadiazolone derivative and propargyl bromide following the general procedure VI for *N-alkylation of 1,3,4-oxadiazol-2(3H)-one.*

5-[(*E*)-2-Phenylethenyl]-3-(prop-2-yn-1-yl)-1,3,4-oxadiazol-2(3*H*)-one (1.105)

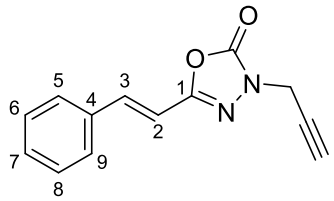

Final compound **1.105** was obtained from the oxadiazolone **1.66** in 87% yield (83 mg, 0.36 mmol). Chromatography: hexane to hexane:EtOAc 77:23. Mp: 138 - 140 ºC. ^{1}H NMR (500 MHz, DMSO-d_6) δ 7.73 (dd, *J* = 8.1, 1.4 Hz, 1H, H_5, H_9), 7.45 – 7.40 (m, 3H, H_6, H_7, H_8), 7.38 (d, *J* = 16.5 Hz, 1H, H_3), 7.01 (d, *J* = 16.5 Hz, 1H, H_2), 4.61 (d, *J* = 2.5 Hz, 2H, CH_2), 3.48 (t, *J* = 2.5 Hz, 1H, CH). ^{13}C NMR (126 MHz, DMSO-d_6) δ 153.1 (C_1), 151.9 (CO), 137.8 (C_3), 134.5 (C_4), 129.9 (C_7), 128.9 (C_6, C_8), 127.8 (C_5, C_9), 110.2 (C_2), 77.1 (≡C), 76.2 (≡CH), 35.4 (CH_2). HPLC-MS (15:95- g.t.10 min) ^{t}R 8.01 min, *m/z* = 227.20 $[M+H]^+$, calcd. for $[C_{13}H_{10}N_2O_2+H]^+$ 227.24.HRMS $[ESI^+]$ *m/z* = 226.07401 $[M]^+$, calcd. for $[C_{13}H_{10}N_2O_2]^+$ 226.07423.

5-[(*E*)-2-(3-Methoxyphenyl)ethenyl]-3-(prop-2-yn-1-yl)-1,3,4-oxadiazol-2(3*H*)-one (1.106)

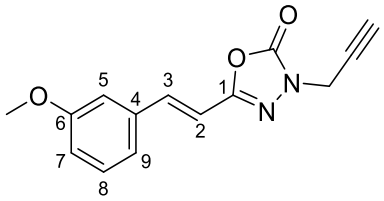

Final compound **1.106** was obtained from the oxadiazolone **1.69** (100 mg, 0.446 mmol) in 68% yield (80.2 mg, 0.31 mmol). Chromatography: hexane to hexane:EtOAc 85:15. Mp: 92 - 94 ºC. ^{1}H NMR (500 MHz, MeOD) δ 7.34 (d, *J* = 16.5 Hz, 1H, H_3), 7.30 (t, *J* = 8.0 Hz,

1H, H_8), 7.17 (d, *J* = 7.7 Hz, 1H, H_9), 7.15 (bs, 1H, H_5), 6.95 (dd, *J* = 8.3, 2.5 Hz, 1H, H_7), 6.79 (d, *J* = 16.4 Hz, 1H, H_2), 4.57 (d, *J* = 2.3 Hz, 2H, CH_2), 3.83 (s, 3H, CH_3), 2.86 (t, *J* = 2.5 Hz, 1H, ≡CH). ^{13}C NMR (126 MHz, MeOD) δ 161.6 (C_6), 155.1 (C_1), 154.0 (CO), 139.5 (C_3), 137.4 (C_4), 131.0 (C_8), 121.3 (C_9), 116.9 (C_7), 113.5 (C_5), 111.2 (C_2), 77.1 (≡C), 74.9 (≡CH), 55.8 (CH_3), 36.4 (CH_2). HPLC-MS (15:95- g.t.10 min) ^{t}R 8.37 min, *m/z* = 257.26 $[M+H]^+$, calcd. for $[C_{14}H_{12}N_2O_3+H]^+$ 257.26. HRMS [ESI$^+$] *m/z* = 256.08539 $[M]^+$, calcd. for $[C_{14}H_{12}N_2O_3]^+$ 256.08479.

5-[(*E*)-2-(4-Methoxyphenyl)ethenyl]-3-(prop-2-yn-1-yl)-1,3,4-oxadiazol-2(3*H*)-one (1.107)

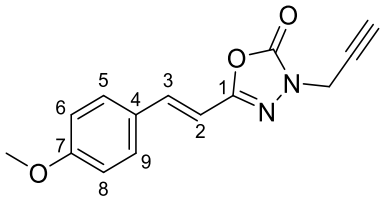

Final compound **1.107** was obtained from **1.70** (50 mg, 0.23 mmol) in 56% yield (33 mg, 0.13 mmol). Chromatography: hexane to hexane:EtOAc 85:15. Mp: 140 - 142 ºC. ^{1}H NMR (500 MHz, DMSO-d_6) δ 7.68 (d, *J* = 8.8 Hz, 2H, H_5, H_9), 7.32 (d, *J* = 16.4 Hz, 1H, H_3), 6.98 (d, *J* = 8.7 Hz, 2H, H_6, H_8), 6.84 (d, *J* = 16.4 Hz, 1H, H_2), 4.60 (d, *J* = 2.5 Hz, 1H, CH_2), 3.80 (s, 3H, CH_3), 3.47 (t, *J* = 2.5 Hz, 1H, ≡CH).^{13}C NMR (126 MHz, DMSO-d_6) δ 160.7 (C_7), 153.4 (C_1), 151.9 (CO), 137.6 (C_3), 129.5 (C_5, C_9), 127.2 (C_4), 114.4 (C_6, C_8), 107.6 (C_2), 77.1 (≡C), 76.1 (≡CH), 55.3 (CH_3), 35.3 (CH_2). HPLC-MS (15:95- g.t.10 min) ^{t}R 8.08 min, *m/z* = 257.17 $[M+H]^+$, calcd. for $[C_{14}H_{12}N_2O_3+H]^+$ 257.26. HRMS [ESI$^+$] *m/z* = 256.08363 $[M]^+$, calcd. for $[C_{14}H_{12}N_2O_3]^+$ 256.08479.

5-[(*E*)-2-(3-Hydroxyphenyl)ethenyl]-3-(prop-2-yn-1-yl)-1,3,4-oxadiazol-2(3*H*)-one (1.108)

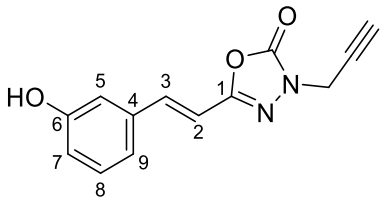

Final phenol **1.108** was obtained from **1.91** (55 mg, 0.27 mmol) in 44% yield (28 mg, 0.12 mmol). Chromatography: hexane to hexane:EtOAc 75:25. Mp: 166 - 168 ºC. ^{1}H NMR (500

MHz, MeOD) δ 7.30 (d, *J* = 16.4 Hz, 1H, H_3), 7.22 (t, *J* = 7.9 Hz, 1H, H_8), 7.06 (dt, *J* = 7.7, 1.2 Hz, 1H, H_9), 7.00 (t, *J* = 2.1 Hz, 1H, H_5), 6.81 (ddd, *J* = 8.1, 2.5, 0.9 Hz, 1H, H_7), 6.72 (d, *J* = 16.4 Hz, 1H, H_2), 4.57 (s, 2H, CH_2). ^{13}C NMR (126 MHz, MeOD) δ 159.1 (C_6), 155.1 (C_1), 154.0 (CO), 139.7 (C_3), 137.3 (C_4), 131.0 (C_8), 120.2 (C_9), 118.2 (C_7), 114.8 (C_5), 110.7 (C_2), 76.7(≡C), 74.6 (≡CH), 36.4 (CH_2). HPLC-MS (15:95- g.t.10 min) ^{t}R 6.61 min, *m/z* = 241.29 $[M-H]^-$, calcd. for $[C_{13}H_{10}N_2O_3 -H]^-$ 241.23. HRMS $[ESI^+]$ *m/z* = 242.06867 $[M]^+$, calcd. for $[C_{13}H_{10}N_2O_3]^+$ 242.06914.

5-[(*E*)-2-(5-Methoxy-1*H*-indol-3-yl)ethenyl]-3-(prop-2-yn-1-yl)-1,3,4-oxadiazol-2(3*H*)-one (1.109)

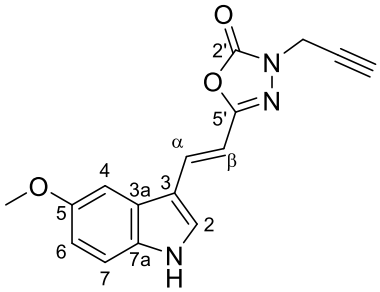

Final indole **1.109** was obtained from **1.27** (60 mg, 0.23 mmol), the crude was purified by semipreparative HPLC (gradient 35:40- g.t.30 min) and lyophilized to give **1.109** in 17% yield (12 mg, 0.039 mmol). Mp: 201 - 203 ºC. ^{1}H NMR (400 MHz, DMSO-d_6) δ 11.59 (s, 1H, NH), 7.88 (d, *J* = 2.5 Hz, 1H, H_2), 7.56 (d, *J* = 16.4 Hz, 1H, $H_α$), 7.37 (d, *J* = 2.4 Hz, 1H, H_4), 7.35 (d, *J* = 8.8 Hz, 1H, H_7), 6.83 (dd, *J* = 8.7, 2.4 Hz, 1H, H_6), 6.63 (d, *J* = 16.4 Hz, 1H, $H_β$), 4.58 (d, *J* = 2.6 Hz, 2H, CH_2), 3.83 (s, 3H, CH_3), 3.45 (t, *J* = 2.5 Hz, 1H, ≡CH). ^{13}C NMR (101 MHz, DMSO-d_6) δ 154.7 (C_5), 154.3 ($C_{5'}$), 152.1 ($C_{2'}$), 132.3 ($C_α$), 132.1 (C_{7a}), 130.4 (C_2), 125.4 (C_{3a}), 113.0 (C_7), 112.5 (C_6), 111.9 (C_3), 102.9 ($C_β$), 101.6 (C_4), 77.3 (≡C), 76.0 (≡CH), 55.5 (CH_3), 35.2 (CH_2). HPLC-MS (15:95- g.t.10 min) ^{t}R 7.62 min, *m/z* = 296.25 $[M+H]^+$, calcd. for $[C_{16}H_{13}N_3O_3+H]^+$ 296.30. HRMS $[ESI^+]$ *m/z* = 270.10827 $[M]^+$, calcd. for $[C_{16}H_{13}N_3O_3]^+$ 270.10044.

AMIDES

All following amides derivatives were obtained from the corresponding acid and either propargyl or allyl bromide following the general procedure IV (Synthesis of amides and hydrazides from acids).

(2*E*)-3-(3-Cyanophenyl)-*N*-(prop-2-yn-1-yl)prop-2-enamide (1.110)

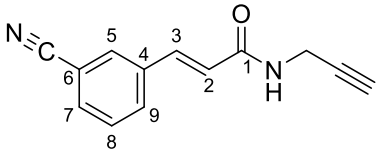

Final compound **1.110** was afforded from acid **1.53** (250 mg, 1.44 mmol) in 57% yield (173 mg, 0.82 mmol). Chromatography: hexane to hexane:EtOAc 1:1. Mp: 172 - 173 ºC. ^{1}H NMR (500 MHz, MeOD) δ 7.96 (t, *J* = 1.7 Hz, 1H, H_5), 7.87 (dt, *J* = 7.9, 1.4 Hz, 1H, H_9), 7.73 (dt, *J* = 7.8, 1.4 Hz, 1H, H_7), 7.60 (t, *J* = 7.9 Hz, 1H, H_8), 7.57 (d, *J* = 15.9 Hz, 1H, H_3), 6.69 (d, *J* = 15.8 Hz, 1H, H_2), 4.09 (d, *J* = 2.5 Hz, 2H, CH_2), 2.64 (t, *J* = 2.6 Hz, 1H, ≡CH). ^{13}C NMR (126 MHz, MeOD) δ 167.3 (C_1), 139.8 (C_3), 137.7 (C_4), 134.0 (C_7), 133.2 (C_9), 132.2 (C_5), 131.1 (C_8), 124.0 (C_2), 119.2 (CN), 114.3 (C_6), 80.3 (≡C), 72.5 (≡CH), 29.7 (CH_2). HPLC-MS (15:95- g.t.10 min) ^{t}R 5.38 min, *m/z* = 211.25 $[M+H]^+$, calcd. for $[C_{13}H_{10}N_2O+H]^+$ 211.24. HRMS $[ESI^+]$ *m/z* = 210.07991 $[M]^+$, calcd. for $[C_{13}H_{10}N_2O]^+$ 210.07931.

(2*E*)-3-(3-Methoxyphenyl)-*N*-(prop-2-yn-1-yl)prop-2-enamide (1.111)

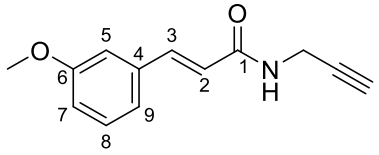

Final compound **1.111** was obtained from commercial 3-methoxycinnamic acid (500 mg, 2.81 mmol) in 83% yield (503 mg, 2.34 mmol). Chromatography: hexane to hexane:EtOAc 6:4. Mp: 105 - 106 ºC. ^{1}H NMR (500 MHz, MeOD) δ 7.52 (d, *J* = 15.8 Hz, 1H, H_3), 7.29 (t, *J* = 7.9 Hz, 1H, H_8), 7.13 (d, *J* = 7.6 Hz, 1H, H_9), 7.09 (dd, *J* = 2.6, 1.6 Hz, 1H, H_5), 6.94 (ddd, *J* = 8.3, 2.6, 1.0 Hz, 1H, H_7), 6.58 (d, *J* = 15.8 Hz, 1H, H_2), 4.08 (d, *J* = 2.6 Hz, 2H, CH_2), 3.81 (s, 3H, CH_3), 2.62 (t, *J* = 2.6 Hz, 1H, ≡CH). ^{13}C NMR (126 MHz, MeOD) δ 168.1 (C_1), 161.5 (C_6), 142.3 (C_3), 137.5 (C_4), 130.9 (C_8), 121.5 (C_2), 121.4 (C_9), 116.6 (C_7), 113.9 (C_5), 80.4 (≡C), 72.4 (≡CH), 55.7 (CH_3), 29.6 (CH_2). HPLC-MS (15:95- g.t.10 min) ^{t}R 6.10 min, *m/z* = 216.23 $[M+H]^+$, calcd. for $[C_{13}H_{13}NO_2+H]^+$ 216.25. HRMS $[ESI^+]$ *m/z* = 215.09483 $[M]^+$, calcd. for $[C_{13}H_{13}NO_2]^+$ 215.09463.

(2*E*)-3-(4-Methoxyphenyl)-*N*-(prop-2-yn-1-yl)prop-2-enamide (1.112)

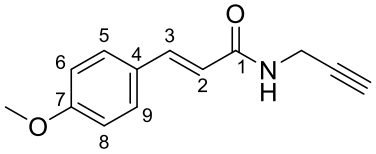

Propargyl amide **1.112** was afforded from commercial 4-methoxycinnamic acid (500 mg, 2.81 mmol) in 79% yield (418 mg, 1.94 mmol). Chromatography: hexane to hexane:EtOAc 6:4. Mp: 123 - 125 (lit. 122.6 - 123.5 °C)[168]. ^{1}H NMR (500 MHz, MeOD) δ 7.53 – 7.49 (m, 3H, H_3, H_9, H_5), 6.94 (d, *J* = 8.8 Hz, 2H, H_6, H_8), 6.45 (d, *J* = 15.8 Hz, 1H, H_2), 4.07 (d, *J* = 2.6 Hz, 2H, CH_2), 3.82 (s, 3H, CH_3), 2.61 (t, *J* = 2.6 Hz, 1H, ≡CH). ^{13}C NMR (126 MHz, MeOD) δ 168.6 (C_1), 162.7 (C_7), 142.1 (C_3), 130.5 (C_9, C_5), 128.7 (C_4), 118.6 (C_2), 115.3 (C_6, C_8), 80.6 (≡C), 72.3 (≡CH), 55.8 (CH_3), 29.6 (CH_2). HPLC-MS (15:95- g.t.10 min) ^{t}R 5.91 min, *m/z* = 216.23 $[M+H]^+$, calcd. for $[C_{13}H_{13}NO_2+H]^+$ 216.25. HRMS [ESI$^+$] *m/z* = 215.0946 $[M]^+$, calcd. for $[C_{13}H_{13}NO_2]^+$ 215.09463.

(2*E*)-3-(3-Methoxyphenyl)-*N*-methyl-*N*-(prop-2-yn-1-yl)prop-2-enamide (1.113)[168]

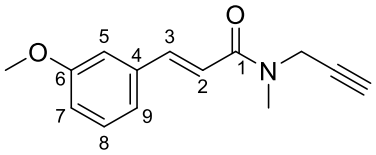

To a cooled (0 °C) suspension of NaH (60 mg, 60% in oil, 1.48 mmol) in THF (2 mL), a solution of amide **1.111** (250 mg, 1.16 mmol) in of dry THF (2 mL) was slowly added. The reaction mixture was stirred at rt for 1 h. Then, CH_3I (180 µL, 2.88 mmol) was added at 0 °C and the mixture was stirred at rt overnight and quenched with H_2O. The organic layer was washed with H_2O (x3) and brine. The aqueous layer was extracted with Et_2O (x3), and the combined organic layers were dried over $MgSO_4$, filtered, and concentrated in vacuum. The residue was purified by flash chromatography (hexane to hexane:EtOAc 55:45) to yield **1.113** as a yellow oil (162 mg, mmol, 61%). ^{1}H NMR (500 MHz, MeOD) mixture of rotamers [1(M):0.70 (m)] δ 7.55 (d, *J* = 15.4 Hz, 1H, H_3), 7.30 (t, *J* = 7.9 Hz, 1H, H_8), 7.19 (d, *J* = 7.8 Hz, 1H, H_9), 7.16 (bs, 1H, H_5), 7.10 (d, *J* = 15.6 Hz, 1H, H_2m) 7.07 (d, *J* = 15.3 Hz, 1H, H_2M), 6.94 (ddd, *J* = 8.2, 2.6, 1.0 Hz, 1H, H_7), 4.37 (s, 2H, CH_2m), 4.30 (s, 2H, CH_2M), 3.82 (s, 3H, OCH_3), 3.27 (s, 3H, NCH_3M), 3.08 (s, 3H, NCH_3m). ^{13}C NMR (126 MHz, MeOD) mixture of rotamers (1:0.70) δ 169.0 (C_1m), 168.5 (C_1M), 161.5 (C_6), 144.6

(C_3M), 144.4 (C_3m), 137.7 (C_4), 130.9 (C_8), 121.7 (C_9M), 121.6 (C_9m), 118.4 (C_2Mm), 116.8 (C_7), 114.1 (C_5M), 114.1 (C_5m), 78.9 (≡CM), 78.9 (≡Cm), 74.2 (≡CHm), 73.0 (≡CHM), 55.8 (OCH_3), 40.3 (CH_2m), 37.5 (CH_2M), 35.2 (NCH_3M), 34.3 (NCH_3m). HPLC-MS (15:95- g.t.10 min) ^{t}R 7.04 min, *m/z* = 230.16 $[M+H]^+$, calcd. for $[C_{14}H_{15}NO_2 +H]^+$ 230.28. HRMS $[ESI^+]$ *m/z* = 229.11024 $[M]^+$, calcd. for $[C_{14}H_{15}NO_2]^+$ 229.11028.

(2*E*)-3-(3-Cyanophenyl)-*N*-(prop-2-en-1-yl)prop-2-enamide (1.114)

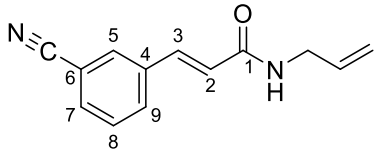

Allyl amide **1.114** was afforded from acid **1.53** (250 mg, 1.44 mmol) in 65% yield (200 mg, 0.94 mmol). Chromatography: hexane to hexane:EtOAc 1:1. Mp: 105 - 106 ºC. ^{1}H NMR (400 MHz, MeOD) δ 7.95 (dd, *J* = 1.7, 1.1 Hz, 1H, H_5), 7.86 (dt, *J* = 7.9, 1.2 Hz, 1H, H_9), 7.72 (dt, *J* = 7.7, 1.4 Hz, 1H, H_7), 7.58 (t, *J* = 7.9 Hz, 1H, H_8), 7.55 (d, *J* = 15.8 Hz, 1H, H_3), 6.72 (d, *J* = 15.8 Hz, 1H, H_2), 5.90 (ddt, *J* = 17.2, 10.3, 5.5 Hz, 1H, CH=), 5.23 (dq, *J* = 17.2, 1.7 Hz, 1H, CH_2=), 5.15 (dq, *J* = 10.3, 1.5 Hz, 1H, CH_2=), 3.93 (dt, *J* = 5.5, 1.6 Hz, 2H, C$\underline{H}_2$CH=). ^{13}C NMR (101 MHz, MeOD) δ 167.6 (C_1), 139.4 (C_3), 137.8 (C_4), 135.2 (CH=), 133.9 (C_7), 133.2 (C_9), 132.2 (C_5), 131.1 (C_8), 124.5 (C_2), 119.3 (CN), 116.5 (CH_2=), 114.3 (C_6), 43.0 ($\underline{C}H_2$CH=). HPLC-MS (15:95- g.t.10 min) ^{t}R 5.76 min, *m/z* = 213.19 $[M+H]^+$, calcd. for $[C_{13}H_{12}N_2O_2 +H]^+$ 213.25. HRMS $[ESI^+]$ *m/z* = 212.0951 $[M]^+$, calcd. for $[C_{13}H_{12}N_2O]^+$ 212.09496.

(2*E*)-3-(3-Methoxyphenyl)-*N*-(prop-2-en-1-yl)prop-2-enamide (1.115)

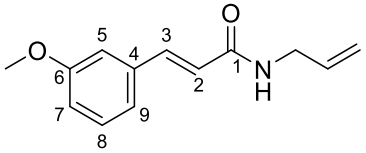

Final compound **1.15** was obtained from commercial 3-methoxycinnamic acid (500 mg, 2.81 mmol) in 81% yield (495 mg, 2.28 mmol). Chromatography: hexane to hexane:EtOAc 1:1. Mp: 86 - 87 ºC. ^{1}H NMR (500 MHz, MeOD) δ 7.51 (d, *J* = 15.7 Hz, 1H, H_3), 7.29 (t, *J* = 7.9 Hz, 1H, H_8), 7.13 (d, *J* = 7.6 Hz, 1H, H_9), 7.09 (bs, 1H, H_5), 6.94 (dd, *J* = 8.1, 2.4 Hz, 1H, H_7), 6.62 (d, *J* = 15.7 Hz, 1H, H_2), 5.90 (ddt, *J* = 17.1, 10.2, 5.5 Hz, 1H, CH=), 5.23 (dd, *J* = 17.2, 1.6 Hz, 1H, 1/2CH_2), 5.14 (dd, *J* = 10.3, 1.5 Hz, 1H, 1/2CH_2), 3.92 (d, *J* = 5.5

Hz, 1H, C<u>H</u>$_2$CH=), 3.81 (s, 3H, CH_3). ^{13}C NMR (126 MHz, MeOD) δ 168.4 (C_1), 161.5 (C_6), 141.8 (C_3), 137.6 (C_4), 135.4 (CH=), 130.9 (C_8), 121.9 (C_2), 121.4 (C_9), 116.5 (C_7), 116.4 (CH_2=), 113.9 (C_5), 55.7 (CH_3), 42.9 (<u>C</u>H$_2$CH=). HPLC-MS (15:95- g.t.10 min) ^{t}R 6.40 min, *m/z* = 218.25 $[M+H]^+$, calcd. for $[C_{13}H_{15}NO_2 + H]^+$ 218.27. HRMS [ESI$^+$] *m/z* = 217.11117 $[M]^+$, calcd. for $[C_{13}H_{15}NO_2]^+$ 217.11028.

(2*E*)-3-(4-Methoxyphenyl)-*N*-(prop-2-en-1-yl)prop-2-enamide (1.116)

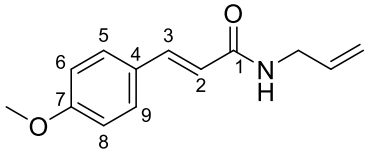

Allyl amide **1.116** was given from commercial 4-methoxycinnamic acid (500 mg, 2.81 mmol) in 88% yield (534 mg, 2.46 mmol). Chromatography: hexane to hexane:EtOAc 1:1. Mp: 121 - 123 ºC. ^{1}H NMR (500 MHz, MeOD) δ 7.50 (d, *J* = 8.7 Hz, 2H, H_5, H_9), 7.50 (d, *J* = 15.9 Hz, 1H, H_3), 6.94 (d, *J* = 8.7 Hz, 2H, H_6, H_8), 6.49 (d, *J* = 15.7 Hz, 1H, H_2), 5.98 (ddt, *J* = 17.2, 10.3, 5.5 Hz, 1H, CH=), 5.22 (dd, *J* = 17.2, 1.7 Hz, 1H, 1/2CH_2=), 5.13 (dd, *J* = 10.3, 1.6 Hz, 1H, 1/2CH_2=), 3.92 (d, *J* = 5.5 Hz, 1H, C<u>H</u>$_2$CH=), 3.82 (s, 3H, CH_3). ^{13}C NMR (126 MHz, MeOD) δ 168.9 (C_1), 162.6 (C_7), 141.7 (C_3), 135.5 (CH=), 130.4 (C_5, C_9), 128.8 (C_4), 119.1 (C_2), 116.3 (CH_2=), 115.3 (C_6, C_8), 55.8 (CH_3), 42.9 (<u>C</u>H$_2$CH=). HPLC-MS (15:95- g.t.10 min) ^{t}R 6.12 min, *m/z* = 218.25 $[M+H]^+$, calcd. for $[C_{13}H_{15}NO_2 + H]^+$ 218.27. HRMS [ESI$^+$] *m/z* = 217.11104 $[M]^+$, calcd. for $[C_{13}H_{15}NO_2]^+$ 217.11028.

(2*E*)-3-(5-Methoxy-1*H*-indol-3-yl)-*N*-(prop-2-yn-1-yl)prop-2-enamide (1.117)

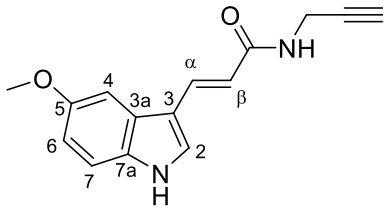

Amide **1.117** was obtained from acid **1.5** (100 mg, 0.46 mmol) in 51% yield (60 mg, 0.23 mmol). Chromatography: hexane to hexane:EtOAc 1:1. ^{1}H NMR (500 MHz, DMSO-*d*$_6$) δ 11.44 (s, 1H, NH_{indole}), 8.29 (t, *J* = 5.5 Hz, 1H, NH_{amide}), 7.72 (d, *J* = 2.9 Hz, 1H, H_2), 7.62 (d, *J* = 15.8 Hz, 1H, H_α), 7.34 (d, *J* = 8.8 Hz, 1H, H_7), 7.34 (d, *J* = 1.9 Hz, 1H, H_4), 6.85 (dd, *J* = 8.7, 2.5 Hz, 1H, H_6), 6.53 (d, *J* = 15.8 Hz, 1H, H_β), 4.01 (dd, *J* = 5.5, 2.5 Hz, 2H, CH_2), 3.84 (s, 3H, CH_3), 3.16 (t, *J* = 2.6 Hz, 1H, ≡CH). ^{13}C NMR (126 MHz, DMSO-*d*$_6$) δ

166.1 (CO), 154.5 (C_5), 133.9 (C_α), 132.3 (C_{7a}), 131.0 (C_2), 125.3 (C_{3a}), 114.7 (C_β), 112.8 (C_7), 111.8 (C_6), 109.5 (C_3), 102.5 (C_4), 81.5 (≡C), 73.1 (≡CH), 55.5 (CH_3), 27.8 (CH_2). HPLC-MS (15:95- g.t.10 min) ^tR 5.80 min, *m/z* = 255.07 $[M+H]^+$, calcd. for $[C_{15}H_{14}N_2O_2+H]^+$ 255.29. HRMS $[ESI^+]$ *m/z* = 254.10667 $[M]^+$, calcd. for $[C_{15}H_{14}N_2O_2]^+$ 254.10553.

(2*E*)-3-(5-Methoxy-1*H*-indol-3-yl)-*N*-(prop-2-en-1-yl)prop-2-enamide (1.118)

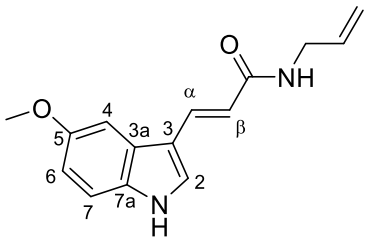

Amide **1.118** was obtained from acid **1.5** (100 mg, 0.46 mmol) in 72% yield (84 mg, 0.33 mmol). Chromatography: hexane to hexane:EtOAc 3:7. Mp: 124 - 126 ºC. ^{1}H NMR (500 MHz, $CDCl_3$) δ 8.77 (s, 1H, NH_{indole}), 7.87 (d, *J* = 15.5 Hz, 1H, H_α), 7.40 (d, *J* = 2.8 Hz, 1H, H_2), 7.30 (d, *J* = 2.6 Hz, 1H, H_4), 7.30 (d, *J* = 8.7 Hz, 1H, H_7), 6.90 (dd, *J* = 8.9, 2.3 Hz, 1H, H_6), 6.35 (d, *J* = 15.6 Hz, 1H, H_β), 5.92 (ddt, *J* = 17.1, 10.1, 5.6 Hz, 1H, CH=), 5.72 (t, *J* = 6.4 Hz, 1H, CONH), 5.25 (dd, *J* = 17.2, 1.5 Hz, 1H, CH_{2trans}=), 5.17 (dd, *J* = 10.3, 1.5 Hz, 1H, CH_{2cis}=), 4.05 (tt, *J* = 5.8, 1.6 Hz, 2H, CH_2), 3.87 (s, 3H, CH_3). ^{13}C NMR (126 MHz, $CDCl_3$) δ 167.3 (CO), 155.3 (C_5), 135.1 (C_α), 134.6 (CH=), 132.2 (C_{7a}), 128.7 (C_2), 126.2 (C_{3a}), 116.6 (=CH_2), 115.2 (C_β), 113.3 (C_3), 112.9 (C_6), 112.6 (C_7), 102.8 (C_4), 56.2 (CH_3), 42.3 (CH_2). HPLC-MS (15:95- g.t.10 min) ^tR 6.12 min, *m/z* = 257.23 $[M+H]^+$, calcd. for $[C_{15}H_{16}N_2O_2+H]^+$ 257.31. HRMS $[ESI^+]$ *m/z* = 256.12237 $[M]^+$, calcd. for $[C_{15}H_{16}N_2O_2]^+$ 256.12118.

(2*E*)-3-(3-Hydroxyphenyl)-*N*-(prop-2-en-1-yl)prop-2-enamide (1.119)

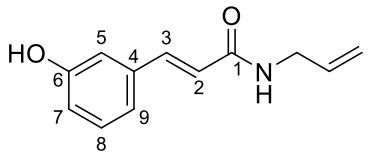

Phenol **1.119** was obtained from methoxylated compound **1.115** (150 mg, 0.69 mmol) following procedure VII, in 66% yield (92 mg, 0.45 mmol). Chromatography: hexane to hexane:EtOAc 1:1. Mp: 115 - 118 ºC. ^{1}H NMR (400 MHz, MeOD) δ 7.47 (d, *J* = 15.8 Hz,

1H, H_3), 7.20 (t, *J* = 7.9 Hz, 1H, H_8), 7.02 (dd, *J* = 7.8, 1.4 Hz, 1H, H_9), 6.97 (bs, 1H, H_5), 6.80 (dd, *J* = 8.1, 2.5 Hz, 1H, H_7), 6.57 (d, *J* = 15.7 Hz, 1H, H_2), 5.90 (ddt, *J* = 17.2, 10.2, 5.5 Hz, 1H, CH=), 5.22 (dd, *J* = 17.2, 1.7 Hz, 1H, 1/2CH_2), 5.14 (dq, *J* = 10.3, 1.5 Hz, 1H, 1/2CH_2), 3.92 (d, *J* = 5.5 Hz, 1H, C$\underline{H}_2$CH=). ^{13}C NMR (101 MHz, MeOD) δ 168.5 (C_1), 159.0 (C_6), 142.1 (C_3), 137.6 (C_4), 135.4 (CH=), 130.9 (C_8), 121.5 (C_2), 120.3 (C_9), 117.9 (C_7), 116.4 (CH_2=), 115.1 (C_5), 42.9 ($\underline{C}H_2$CH=). HPLC-MS (15:95- g.t.10 min) ^{t}R 4.11 min, *m/z* = 204.24$[M+H]^+$, calcd. for $[C_{12}H_{13}NO_2 + H]^+$ 204.24. HRMS [ESI$^+$] *m/z* = 203.09457 $[M]^+$, calcd. for $[C_{12}H_{13}NO_2]^+$ 203.09463.

(2*E*)-3-(4-Hydroxyphenyl)-*N*-(prop-2-en-1-yl)prop-2-enamide(1.120)

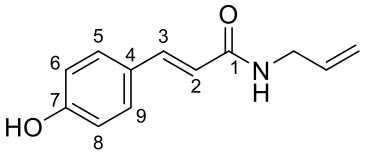

Phenol **1.120** was obtained from methoxylated compound **1.116** (150 mg, 0.69 mmol) following procedure *VII*, in 72% yield (101 mg, 0.50 mmol). Chromatography: hexane to hexane:EtOAc 1:1. Mp: 118.1 - 120 ºC. ^{1}H NMR (400 MHz, MeOD) δ 7.47 (d, *J* = 15.7 Hz, 1H, H_3), 7.41 (d, *J* = 8.6 Hz, 2H, H_5, H_9), 6.79 (d, *J* = 8.6 Hz, 2H, H_6, H_8), 6.44 (d, *J* = 15.7 Hz, 1H, H_2), 5.89 (ddt, *J* = 17.2, 10.7, 5.5 Hz, 1H, CH=), 5.21 (dd, *J* = 17.2, 1.7 Hz, 1H, 1/2CH_2=), 5.12 (dd, *J* = 10.3, 1.6 Hz, 1H, 1/2CH_2=), 3.91 (d, *J* = 5.5 Hz, 1H, C$\underline{H}_2$CH=). ^{13}C NMR (101 MHz, MeOD) δ 169.1 (C_1), 160.5 (C_7), 142.0 (C_3), 135.5 (CH=), 130.6 (C_5, C_9), 127.7 (C_4), 118.2 (C_2), 116.7 (C_6, C_8), 116.3 (CH_2=), 42.9 ($\underline{C}H_2$CH=). HPLC-MS (15:95- g.t.10 min) ^{t}R 3.45 min, *m/z* = 204.24 $[M+H]^+$, calcd. for $[C_{12}H_{13}NO_2 + H]^+$ 204.24. HRMS [ESI$^+$] *m/z* = 203.09463 $[M]^+$, calcd. for $[C_{12}H_{13}NO_2]^+$ 203.09463.

(2*E*)-3-(3-Hydroxyphenyl)-*N*-(prop-2-yn-1-yl)prop-2-enamide (1.121)

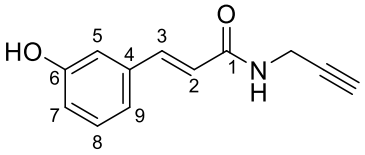

Propargyl amide **1.121** was afforded from commercial 3-hydroxycinnamic acid (400 mg, 2.43 mmol) following procedure IV, in 80% yield (392 mg, 1.95 mmol). Chromatography: hexane to hexane:EtOAc 1:1. Mp: 158 - 160 ºC. ^{1}H NMR (500 MHz, DMSO-d_6) δ 9.58 (s, 1H, OH), 8.53 (t, *J* = 5.5 Hz, 1H, NH), 7.36 (d, *J* = 15.8 Hz, 1H, H_3), 7.20 (t, *J* = 7.8 Hz,

1H, H_8), 6.98 (d, *J* = 7.7 Hz, 1H, H_9), 6.93 (t, *J* = 2.0 Hz, 1H, H_5), 6.78 (dd, *J* = 8.1, 1.7 Hz, 1H, H_7), 6.53 (d, *J* = 15.8 Hz, 1H, H_2), 3.98 (dd, *J* = 5.5, 2.6 Hz, 2H, CH_2), 3.15 (t, *J* = 2.5 Hz, 1H, ≡CH). ^{13}C NMR (126 MHz, DMSO-d_6) δ 164.7 (C_1), 157.7 (C_6), 139.5 (C_3), 136.0 (C_4), 129.9 (C_8), 121.2 (C_2), 118.8 (C_9), 116.8 (C_7), 113.7 (C_5), 81.0 (≡C), 73.2 (≡CH), 28.0 (CH_2). HPLC-MS (15:95- g.t.10 min) ^{t}R 3.55 min, *m/z* = 202.22 $[M+H]^+$, calcd. for $[C_{12}H_{11}NO_2+H]^+$ 202.23. HRMS $[ESI^+]$ *m/z* = 201.07982 $[M]^+$, calcd. for $_{[}C_{12}H_{11}NO_2]^+$ 201.07898.

(2*E*)-3-(4-Hydroxyphenyl)-*N*-(prop-2-yn-1-yl)prop-2-enamide (1.122)

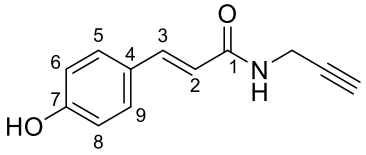

Phenol **1.122** was afforded from commercial 3-hydroxycinnamic acid (100 mg, 0.61 mmol) following procedure *IV*, in 76% yield (93 mg, 0.46 mmol). Chromatography: hexane to hexane:EtOAc 7:3. Mp: 125 - 128 ºC. ^{1}H NMR (500 MHz, MeOD) δ 7.48 (d, *J* = 15.7 Hz, 1H, H_3), 7.42 (d, *J* = 8.7 Hz, 2H, H_5, H_9), 6.79 (d, *J* = 8.6 Hz, 2H, H_6, H_8), 6.40 (d, *J* = 15.7 Hz, 1H, H_2), 4.07 (d, *J* = 2.6 Hz, 2H, CH_2), 2.61 (t, *J* = 2.6 Hz, 1H, ≡CH). ^{13}C NMR (126 MHz, MeOD) δ 168.8 (C_1), 160.7 (C_7), 142.5 (C_3), 130.7 (C_5, C_9), 127.6 (C_4), 117.7 (C_2), 116.7 (C_6, C_8), 80.6 (≡C), 72.2 (≡CH), 29.5 (CH_2). HPLC-MS (15:95- g.t.10 min) ^{t}R 2.38 min, *m/z* = 202.22 $[M+H]^+$, calcd. for $[C_{12}H_{11}NO_2+H]^+$ 202.23. HRMS $[ESI^+]$ *m/z* = 201.07891 $[M]^+$, calcd. for $[C_{12}H_{11}NO_2]^+$ 201.07898.

(2*E*)-3-(4-Hydroxy-3-methoxyphenyl)-*N*-(prop-2-yn-1-yl)prop-2-enamide (1.123)

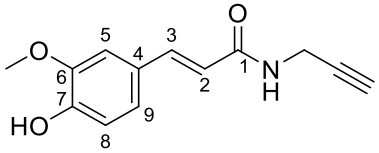

Propargyl amide **1.123** was obtained from commercial 4-hydroxy-3-methoxycinnamic acid (ferulic acid) (300 mg, 1.54 mmol) following procedure IV, in 86% yield (308 mg, 1.33 mmol). Chromatography: hexane to hexane:EtOAc 1:1. Mp: 131 - 132 ºC (lit 128 - 129 ºC)[33]. ^{1}H NMR (500 MHz, DMSO-d_6) δ 9.47 (bs, 1H, OH), 8.38 (bs, 1H, NH), 7.35 (d, *J* = 15.7 Hz, 1H, H_3), 7.12 (s, 1H, H_5), 7.00 (d, *J* = 8.2 Hz, 1H, H_9), 6.79 (d, *J* = 8.1 Hz, 1H, H_8), 6.44 (d, *J* = 15.7 Hz, 1H, H_2), 3.97 (bs, 2H, CH_2), 3.80 (s, 3H, CH_3), 3.12 (bs, 1H,

≡CH). ^{13}C NMR (126 MHz, DMSO-d_6) δ 165.2 (C_1), 148.4 (C_7), 147.8 (C_6), 139.8 (C_3), 126.2 (C_4), 121.6 (C_9), 118.1 (C_2), 115.7 (C_8), 111.0 (C_5), 81.2 (≡C), 73.0 (≡CH), 55.6 (CH_3), 28.0 (CH_2). HPLC-MS (15:95- g.t.10 min) ^{t}R 3.00 min, *m/z* = 232.10 $[M+H]^+$, calcd. for $[C_{13}H_{13}NO_3+H]^+$ 232.25. HRMS [ESI$^+$] *m/z* = 231.08981 $[M]^+$, calcd. for $[C_{13}H_{13}NO_2]^+$ 231.08954.

(2*E*)-3-(3,4-dihydroxyphenyl)-*N*-(prop-2-yn-1-yl)prop-2-enamide (1.124)

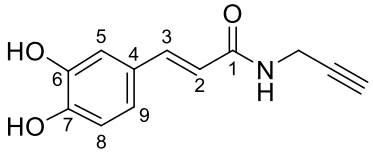

Catechol **1.124** was afforded from commercial 3,4-dihydroxycinnamic acid (caffeic acid) (400 mg, 2.22 mmol) following procedure *IV*, in 56% yield (269 mg, 0.91 mmol). Chromatography: hexane to hexane:EtOAc 55:45. Mp: 169 - 171 ºC (lit. 169 - 170 ºC)[34]. ^{1}H NMR (500 MHz, MeOD) δ 7.42 (d, *J* = 15.7 Hz, 1H, H_3), 7.01 (d, *J* = 2.1 Hz, 1H, H_5), 6.91 (dd, *J* = 8.2, 2.1 Hz, 1H, H_9), 6.77 (d, *J* = 8.2 Hz, 1H, H_8), 6.36 (d, *J* = 15.7 Hz, 1H, H_2), 4.06 (d, *J* = 2.6 Hz, 2H, CH_2), 2.59 (t, *J* = 2.6 Hz, 1H, ≡CH). ^{13}C NMR (126 MHz, MeOD) δ 168.8 (C_1), 148.8 (C_7), 146.7 (C_6), 142.9 (C_3), 128.1 (C_4), 122.2 (C_9), 117.7 (C_2), 116.4 (C_8), 115.1 (C_5), 80.6 (≡C), 72.2 (≡CH), 29.5 (CH_2). HPLC-MS (5:95- g.t.10 min) ^{t}R 4.93 min, *m/z* = 218.17 $[M+H]^+$, calcd. for $[C_{12}H_{11}NO_3+H]^+$ 218.22. HRMS [ESI$^+$] *m/z* = 217.07318 $[M]^+$, calcd. for $[C_{12}H_{11}NO_3]^+$ 217.07389.

AMINE

2-methoxy-4-{(1*E*)-3-[(prop-2-yn-1-yl)amino]prop-1-en-1-yl}phenol (1.125)

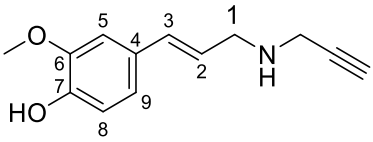

To a solution of commercial ferulic aldehyde (100 mg, 0.56 mmol) and molecular sieves 4 Å in 3 mL (6 mL/mmol) of dry THF, propargylamine (179 µL, 2.81 mmol, 5 equiv) was added. The reaction was stirred at rt overnight. The mixture was filtered, washed with THF several times and evaporated (imine formation). The crude was resolved in 3.5 mL of MeOH and $NaBH_4$ was added (23 mg, 0.62, 1.1 equiv) at 0 ºC. The reaction was stirred at

rt for 30 min. The solvent was removed and residue was solved in EtOAc, extracted, washed with H_2O and brine, dried over $MgSO_4$, filtered and evaporated.[118] The crude was purified by flash chromatography in EtOAc:TEA 95:5 to obtained **1.125** as a yellow pale solid in 62% yield (76 mg, 0.35 mmol). Mp: 76 - 78 ºC. ^{1}H NMR (500 MHz, DMSO-d_6) δ 8.98 (bs, 1H), 7.63 (bs, 1H), 6.99 (d, J = 2.0 Hz, 1H, H_5), 6.78 (dd, J = 8.1, 2.0 Hz, 1H, H_9), 6.70 (d, J = 8.1 Hz, 1H, H_8), 6.39 (d, J = 16.0 Hz, 1H, H_3), 6.08 (dt, J = 15.9, 6.3 Hz, 1H, H_2), 3.77 (s, 3H, CH_3), 3.32 – 3.29 (m, 4H, H_1, $CH_2C\equiv$), 3.06 (t, J = 2.4 Hz, 1H, ≡CH). ^{13}C NMR (126 MHz, DMSO-d_6) δ 147.7 (C_6), 146.1 (C_7), 130.7 (C_3), 128.5 (C_4), 125.3 (C_2), 119.3 (C_9), 115.4 (C_8), 109.6 (C_5), 83.0 (≡C), 73.6 (≡CH), 55.5 (CH_3), 49.6 (C_1), 36.6 ($\underline{C}H_2C\equiv$). HPLC-MS (2:30- g.t.10 min) ^{t}R 1.57 min, *m/z* = 218.10 $[M+H]^+$, calcd. for $[C_{13}H_{15}NO_2+H]^+$ 218.27. HRMS $[ESI^+]$ *m/z* = 217.11067 $[M]^+$, calcd. for $[C_{13}H_{15}NO_2]^+$ 217.11028.

Conformational studies

Conformational studies were carried out by Dr. Federico Gago from University of Alcalá de Henares (Madrid, Spain) in order to know the optimal dihedral angles between either indole or naphthalene and the corresponding oxadiazolone ring, which is defined by carbons 1-2-3-4 (Figure 1.8). This dihedral parametrization was done using Gaussian following the protocol described in Ref.[169]

Thus, the dihedral angle was rotated from 0 to 360 degrees (72 steps with a step size of 5 degrees) and the rest of the structure was minimized, obtaining energy values expressed in Hartrees, which were converted to kcal/mol by multiplying by 627.51 (1Hartree = 627.51 kcal/mol). Finally, the minimum value was calculated and subtracted to the rest to obtain relative energies. The resulting energies were plotted to visualize the energy profile (energy (kcal/mol) *vs* dihedral angle degrees).

Biological Studies

Human melatonin receptors MT_1R and MT_2R and hamster MT_3R

Radioligand displacement and functional studies were performed at *Eurofins-Cerep SA.*

The results are expressed as a percent inhibition of the control radioligand specific binding. The standard reference compound (MT) was tested in each experiment at several concentrations to obtain a competition curve from which its IC_{50} is calculated.

MT_1R

The affinity of compounds for *h*MT_1R in transfected CHO cells was determined in a radioligand binding assay. Cell membrane homogenates (about 80 µg protein) were incubated at 22 °C for 240 min with 0.01 nM [^{125}I]iodomelatonin in the absence or presence of the test compound in a buffer containing 50 mM Tris-HCl (pH 7.4), 5 mM $MgCl_2$ and 0.1% BSA. Nonspecific binding was determined in the presence of 1 µM MT.

Following incubation, the samples were filtered rapidly under vacuum through glass fiber filters (GF/B, Packard) presoaked with 0.3% PEI and rinsed several times with ice-cold 50 mM Tris-HCl using a 96-sample cell harvester (Unifilter, Packard). The filters were dried then counted for radioactivity in a scintillation counter (Topcount, Packard) using a scintillation cocktail (Microscint 0, Packard).[120-122]

MT_2R

The affinity of compounds for *h*MT_2R in transfected CHO cells was determined in a radioligand binding assay. Cell membrane homogenates (6 µg protein) were incubated for 120 min at 37°C with 0.05 nM [^{125}I]iodomelatonin in the absence or presence of the test compound in a buffer containing 50 mM Tris-HCl (pH 7.4) and 5 mM $MgCl_2$. Nonspecific binding was determined in the presence of 1 µM MT. Following incubation, the samples were filtered rapidly under vacuum through glass fiber filters (GF/B, Packard) presoaked with 0.3% PEI and rinsed several times with ice-cold 50 mM Tris-HCl using a 96-sample cell harvester (Unifilter, Packard). The filters were dried then counted for radioactivity in a

scintillation counter (Topcount, Packard) using a scintillation cocktail (Microscint 0, Packard).[120-122]

Functional characterization in MT_2R

Functional characterization of **1.51** at *h*MT_2R was determined by measuring its effects on cyclic adenosine monophosphate (cAMP) modulation using the homogeneous time resolved fluorescence (HTRF) detection method. CHO cells expressing *h*MT_2R were suspended in Hanks' balanced salt solution (HBSS) buffer (Invitrogen) complemented with 20 mM HEPES (pH 7.4) and 500 µM IBMX, then distributed in microplates at a density of 7.103 cells/well in the presence of either of the following: HBSS (basal control), the reference agonist at 10 nM (stimulated control) or various concentrations (EC_{50} determination), or the test compounds.

Thereafter, the adenylyl cyclase activator NKH 477 was added at a final concentration of 5 µM. Following 10 min incubation at 37°C, the cells are lysed and the fluorescence acceptor (D2-labeled cAMP) and fluorescence donor (anti-cAMP antibody labeled with europium cryptate) were added. After 60 min at rt, the fluorescence transfer was measured at λ_{ex} = 337 nm and λ_{em} = 620 and 665 nm using a microplate reader (Envison, Perkin Elmer). The cAMP concentration was determined by dividing the signal measured at 665 nm by that measured at 620 nm (ratio).[121]

The results are expressed as a percent of the control response to MT (10 nM). The standard reference (MT) was tested in each experiment at several concentrations to generate a concentration-response curve from which its EC_{50} value is calculated.

Hamster MT_3R

Affinity of compounds toward MT_3R in the hamster brain was determined by radioligand binding assay. Membrane homogenates of brain (750 µg protein) were incubated for 60 min at 4 °C with 0.1 nM [^{125}I]iodomelatonin in the absence or presence of the test compound in a buffer containing 50 mM Tris-HCl (pH 7.4) and 4 mM $CaCl_2$. Nonspecific binding was determined in the presence of MT (30 µM). Following incubation, the samples were filtered rapidly under vacuum through glass fiber filters (Filtermat B, Wallac)

presoaked with 0.5% PEI (pH 7.4) and rinsed several times with an ice-cold buffer containing 50 mM Tris-HCl and 2 M NaCl using a 48-sample cell harvester (Mach II, Tomtec). The filters were dried then counted for radioactivity in a scintillation counter (Betaplate 1204, Wallac) using a solid scintillator (Meltilex B/HS, Wallac).[122]

Oxygen radical absorbance capacity assay (ORAC)

The ORAC method was followed, using a Polarstar Galaxy plate reader (BMG Labtechnologies GmbH, Offenburg, Germany) with 485-P excitation and 520-P emission filters.[125,170] The equipment was controlled by the Fluorostar Galaxy software (version 4.11-0) for fluorescence measurement. 2,2'-Azobis-(amidinopropane) dihydrochloride (AAPH), trolox and fluorescein (FL) were purchased from Sigma-Aldrich. The reaction was carried out in 75 mM phosphate buffer (pH 7.4) and the final reaction mixture was 200 μL. Antioxidant (20 μL) and FL (120 μL; 70 mM, final concentration) solutions were placed in a black 96-well microplate (96F untreated, Nunc). The mixture was pre-incubated for 15 min at 37 ºC and then, AAPH solution (60 μL, 12 mM, final concentration) was added rapidly using a multichannel pipette. The microplate was immediately placed in the reader and the fluorescence recorded every min for 80 min. The microplate was automatically shaken prior each reading. Samples were measured at eight different concentrations (0.1-1μM). A blank (FL + AAPH in phosphate buffer) instead of the sample solution and eight calibration solutions using trolox (1-8 μM) were also carried out in each assay. All the reaction mixtures were prepared in duplicate, and at least three independent assays were performed for each sample. Raw data were exported from the Fluostar Galaxy Software to an Excel sheet for further calculations. Antioxidant curves (fluorescence *vs.* time) were first normalized to the curve of the blank corresponding to the same assay, and the area under the fluorescence decay curve (AUC) was calculated. The net AUC corresponding to a sample was calculated by subtracting the AUC corresponding to the blank. Regression equations between net AUC and antioxidant concentration were calculated for all the samples. ORAC-FL values were expressed as trolox equivalents by

using the standard curve calculated for each assay, where the ORAC-FL value of trolox was taken as 1.0.

Inhibition of human monoamine oxidases (hMAO-A and hMAO-B)

MAO inhibition measurements were carried out following the general procedure previously described.[171] Briefly, test drugs and adequate amounts of recombinant *h*MAO-A or *h*MAO-B (Sigma-Aldrich Chemistry S.A., Alcobendas, Spain) required and adjusted to oxidize 165 pmol of *p*-tyramine/min in the control group, were incubated at 37 ºC for 15 min in a flat-black-bottom 96-well microtest plate (BD Biosciences, Franklin Lakes, NJ) placed in the dark fluorimeter chamber. The reaction was started by adding 200 mM Amplex Red reagent (Molecular Probes, Inc., Eugene, OR), 1 U/mL horseradish peroxidase, and 1 mM *p*-tyramine and the production of resorufin, was quantified at 37 ºC in a multidetection microplate fluorescence reader (FLX800, Bio-Tek Instruments, Inc., Winooski, VT) based on the fluorescence generated (excitation, 545 nm; emission, 590 nm). The specific fluorescence emission was calculated after subtraction of the background activity, which was determined from wells containing all components except the *h*MAO isoforms, which were replaced by PBS.

Inhibition of human lipoxygenase-5 (hLOX-5)

The fluorescence-based enzyme method previously described by Pufahl *et al.* was followed, in 96-well microtiter plates.[172] The assay solution consists of Tris buffer (50 mM, pH 7.5), ethylenediaminetetraacetic acid (EDTA, 2 mM), $CaCl_2$ (2 mM), AA (3 μM), ATP (10 μM), 2',7'-dichlorodihydrofluorescein diacetate (H_2DCFDA, 10 μM), *h*LOX-5 (100 mU/well), bovine glutathione peroxidase (GPx, 25 mU/well) and reduced glutathione (1 mM). Compounds were added to the test solution prior to AA and ATP, and preincubated for 10 min at rt. Then, the AA and ATP substrates were added; the enzymatic reaction allowed to progress for 20 min and followed by the addition of 40 μL of ACN. The fluorescence measurements (excitation: 485 nm; emission: 520 nm) were performed on a FLUOstar OPTIMA (BMG LABTECH, Offenburg, Germany). IC_{50} is defined as the

concentration of compound that inhibits enzymatic activity by 50% over the control of untreated enzyme.

Luciferase activity: Nrf2 induction

These experiments were performed in the Intituto Teófilo Hernando (Madrid). Thus, AREc32 cells were plated in 96-well white plates (2×10^4 cells/well). After 24 h, cells were incubated with increasing concentrations of each compound in duplicate for 24 h. AREc32 cells express constitutively the plasmid pGL-8xARE that implements 8 copies of the EpRE sequences followed by luciferase reporter gen. Therefore, Nrf2 induction is related to the activation of EpRE sequences, expressing luciferase at the same extent as EpRE sequences are activated. The Luciferase Assay System (Promega E1500) was used according to provider protocol and luminescence was quantified in an Orion II microplate luminometer (Berthold, Germany). Fold induction of luciferase activity was normalized to basal conditions. Data are expressed as CD values, expressing the concentration required to double the luciferase activity. CD values were calculated from dose-response curves generated from fold induction of control conditions *vs.* inducer concentration and fitted by non-linear regression and data interpolated to 2-fold induction concentration.[133]

In vitro blood–brain barrier permeation assay (PAMPA-BBB)

Prediction of the brain penetration was evaluated using the PAMPA-BBB assay, in a similar manner as previously described.[111,135,173,174] Pipetting was performed with a semi-automatic robot (CyBi®-SELMA) and UV reading with a microplate spectrophotometer (Multiskan Spectrum, Thermo Electron Co.). Commercial drugs, phosphate buffered saline solution at pH 7.4 (PBS), and dodecane were purchased from Sigma, Aldrich, Acros, and Fluka. Millex filter units (PVDF membrane, diameter 25 mm, pore size 0.45 μm) were acquired from Millipore. The porcine brain lipid (PBL) was obtained from Avanti Polar Lipids. The donor microplate was a 96-well filter plate (PVDF membrane, pore size 0.45 μm) and the acceptor microplate was an indented 96-well plate, both from Millipore. The

acceptor 96-well microplate was filled with 200 μL of PBS: EtOH (70:30) and the filter surface of the donor microplate was impregnated with 4 μL of PBL in dodecane (20 mg mL^{-1}). Compounds were dissolved in PBS: EtOH (70:30) at 100 μg mL^{-1}, filtered through a Millex filter, and then added to the donor wells (200 μL). The donor filter plate was carefully put on the acceptor plate to form a sandwich, which was left undisturbed for 240 min at 25 ºC. After incubation, the donor plate is carefully removed and the concentration of compounds in the acceptor wells was determined by UV-Vis spectroscopy. Every sample is analyzed at five wavelengths, in four wells and at least in three independent runs, and the results are given as the mean ± SD. In each experiment, 11 quality control standards of known BBB permeability were included to validate the analysis set.

Neurogenic assays

These studies were performed by Drs. José A Morales-García and Ana Pérez Castillo at the Instituto de Investigaciones Biomédicas "Alberto Sols". Thus, adult male C57BL/6 mice (3 months old) were used in order to determine neurogenesis activity. All animal experimental procedures were previously approved by the Ethics Committee for Animal Experimentation of CSIC following national normative (1201/2005) and international recommendations (Directive 2010/63 from the European Communities Council). Special care was taken to minimize animal suffering. NSC were isolated from the SGZ of the dentate gyrus of the hippocampus of adult mice and cultured as NS as previously described.[140,175] After treatment of NS with the corresponding compounds at 10 μM, the expression of neuronal markers was analyzed by immunocytochemistry according to published protocols,[140] using two well-known neurogenesis-associated markers: Tuj1 to early stages of neurogenesis and MAP-2 to late neuronal maturation. A rabbit anti-β-III-tubulin (TuJ clone; Abcam) polyclonal antibody coupled to an Alexa-488-fluor-labeled secondary antibody (Molecular Probes) and a mouse anti-MAP-2 (Sigma) monoclonal antibody coupled to an Alexa-546-fluor-labeled secondary antibody (Molecular Probes) were used. DAPI staining was used as a nuclear marker. Fluorescent representative images were acquired with a Nikon fluorescence microscope 90i coupled to a digital camera Qi. The microscope configuration was adjusted to produce the optimum signal-to-noise ratio.

Neuroprotection studies

These assays were performed in the Instituto Teófilo Hernando. Substances used were purchased from Sigma-Aldrich (OA) and Invitrogen (DCFDA, PI, Hoechst 33342). C57BL/6 (WT) mice from the laboratory's colony were used between 3 - 4 months old for acute OA protocol. The embryos for pregnant Sprague Dawley rats were used for the primary cultures of cortical neurons. The European Directives that controls the scientific use and care of animals were strictly followed. Animals were housed in standard cages with a 12 /12 h light/dark cycle and fed *ad libitum*.

Human neuroblastoma SH-SY5Y cell line culture

SH-SY5Y cells were maintained in flasks with supplemented medium in incubators with standard conditions (37 ^{o}C, 5% CO_2, 95% H_2O). The culture medium was MEM-F12 (9.53 g MEM, 2.5% non-essential amino acids, 4 g $NaHCO_3$, 0.05% sodium pyruvate, penicillin 100 U/mL, streptomycin 100 U/mL) supplemented with 10% Fetal Bovine Serum (FBS). Subcultures were performed once or twice a week when confluent. They were seeded in 96-well plates at a density of 60000 cells/well for posterior pharmacological evaluation.

Enriched primary neuron cultures

Cortical neurons were cultured from rat embryos obtained from an 18-day pregnant rat. For this purpose, a cesarean section was made to take out the embryos. Immediately after, they were beheaded and submerged in saline phosphate buffer containing (in mM): 137 NaCl, 3 KCl, 10 Na_2HPO_4, 2 KH_2PO_4, 4 BSA, 1.5 glucose; pH 7.4. Next, their brain cortices were extracted, unbundled mechanically and centrifuged at 800 rpm (Kubota 5100, PACISA) for 10 min. Finally, they were suspended in DMEM/F-12 (Gibco) supplemented with 20% FBS and 0.005% penicillin/streptomycin. Their seeding process required well plates with poly-d-lysine (PDL; Sigma-Aldrich) pretreatment for a minimum of 2 h under UV light. Once the PDL was dry and washed twice with sterile H_2O, primary cortical neurons were seeded at a density of 60.000 cells/well in 96-well plates. After 2 h of incubation, a medium

replacement was performed with NB (Gibco) supplemented with 10% FBS, 0.005% penicillin/streptomycin and B-27 (Invitrogen). Cells were cultured for 7 - 10 days (37 ºC, 5% CO_2, 95% H_2O) before pharmacological assays took place, which were performed using NB medium supplemented with B-27 minus antioxidants (Invitrogen).

Pharmacological evaluation of cell cultures

SH-SY5Y and neurons were seeded in 96-well plates and pre-treated with the selected compounds (1 µM). After 24 h, the cells were co-treated with the compounds (1 µM) and OA (10 nM) in their respective culture mediums (1% FBS). Lastly, cell viability was measured 24 h after the co-treatment by MTT assay.

Acute OA protocol in hippocampal slices

Hippocampal slices were obtained in the same way as before from 3 - 4 months old mice. However, after slice individualization, they were transferred to a small cup and stabilized for 45 min in pre-incubation solution containing (in mM): 120 NaCl, 2 KCl, 26 $NaHCO_3$, 2 $CaCl_2$, 1.18 KH_2PO_4, 1.19 $MgSO_4$ and 11 glucose, using a water bath set at 34 ºC in constant bubbling conditions (5% CO_2, 95% O_2). Next, 3 - 5 slices were introduced in each well of a 48-well plate containing a 1:1 mixture of DMEM medium and control solution containing (in mM): 120 NaCl, 2 KCl, 26 $NaHCO_3$, 2 $CaCl_2$, 1.18 KH_2PO_4, 1.19 $MgSO_4$ and 11 glucose. Each well was treated differently, using OA (1 µM) as toxic and the corresponding compounds (1 µM), and the plate was maintained under culture conditions (37 ºC, 5% CO_2, 95% O_2) for 6 h. The cell viability was measured by MTT, cell death by PI, oxidative stress by DCFDA.

MTT assay

MTT reduction rate is an indicator of the functional integrity of the mitochondria and, hence, of cellular viability.[176,177] This test consists of the internalization of thiazolyl blue tetrazolium bromide (Sigma-Aldrich) inside the cell. This soluble yellow molecule is metabolized by the mitochondrial dehydrogenase of living cells into formazan, an insoluble purple salt. Then, DMSO (VWR Chemicals) was used for solved these purple deposits. In cell cultures, tetrazolium (0.5 mg/mL in culture medium) was added for 2 h, after which DMSO was added and absorbance measured. In hippocampal slices, after the 6 h-incubation period, each slice was transferred to an individual well containing 100 µL of MTT (0.5 mg/mL in control solution) and incubated under culture conditions (37 ºC, 5% CO_2, 95% O_2) for 45 min. Later, MTT solution was removed and DMSO was added for 45 min shaking. Finally, cell viability was measured in microplate reader in the presence and absence of the hippocampal slices. The absorbance was measured at 540 nm using a microplate reader (Labsystems iEMS). Data were normalized against the basal condition.

Fluorescence measurements in hippocampal slices

Propidium iodide (PI)a fluorescent intercalating agent, measures cell death. DCFDA, a fluorogenic compound used to measure ROS activity, spreads into the cell, where esterases transform it into a non-fluorescent substance. ROS oxidize this probe into 2',7'-dichlorofluorescein (DCF), an intensive fluorescent molecule. The probes PI (1 µL/mL; $\lambda_{Ex/Em}$ = 535/617 nm) and DCFDA (10 µl/mL; $\lambda_{Ex/Em}$ = 495/529 nm) were added 1 h before the 6 h-incubation period for the slices of the OA-acute protocol. Hoechst dye (2 µL/mL; $\lambda_{Ex/Em}$ = 350/461 nm) identifies and quantifies cell nuclei. Fluorescence was then measured in the CA1 region of the hippocampal slices using a fluorescence microscope Eclipse TE300 (Nikon) attached to an EM-CCD digital camera C9100 (Hamamatsu). The data obtained for PI and DCFDA were normalized against Hoechst.

Statistical analysis

Data was analyzed with GraphPad Prism 5.0 software. Each compound has been analyzed independently from the others, although they have been represented in the same graph. The results are represented as mean ± SD from the mean, employing one-way ANOVA test and the Newman-Keuls post-test correction. The threshold of statistical significance was stablished at $\alpha < 0.05$.

CHAPTER II

Photoswitchable muscular nicotinic receptor ligands

INTRODUCTION

INTRODUCTION

Nicotinic acetylcholine receptors

ACh (Figure 2.1A) is a neurotransmitter produced, stored and released by cholinergic neurons at neuromuscular junctions, at synapses in the ganglia of the visceral and motor system, and at a variety of sites within the CNS. ACh is involved in many neuronal functions, acting through the ACh receptors (AChRs).[178] These receptors have been sorted according to their affinities for different molecules into two main classes, muscarinic and nicotinic subtypes, with different pharmacological properties. The metabotropic muscarinic receptors are membrane bound GPCRs activated by muscarine, whereas the ionotropic nicotinic receptors (nAChRs) are stimulated by nicotine (Figure 2.1A).

nAChRs are widely distributed in both CNS and peripheral nervous system (PNS) and belong to the ligand-gated ion-channel superfamily. They are crucially involved in electrical signaling in brain and skeletal muscles. They are composed by the assembly of five transmembrane subunits organized around a central pore, resulting by combinations of alpha (α1-10, ligand-binding site), beta (β1-4), gamma (γ), delta (δ), and epsilon (ε) subunits, which define different tissue-specific nAChR subtypes.[179] They can be broadly classified into two classes, neuronal and muscular receptors. Neuronal nAChRs consist of α and β combinations (α2-α10 and β2-β4) with variable stoichiometry or as alpha homo-pentamers (α7-α9), mainly found in CNS, PNS, and non-neuronal tissues.[180] In the mammalian brain, the most common neuronal subtypes are α7 and α4β2 nAChRs and, as a result, they are considered remarkable therapeutic targets for the treatment of neurodegenerative diseases.[181]

Muscular nAChRs are found in the electrical organs of fish and in the post-junctional folds of the motor endplate of the neuromuscular junction in vertebrates, and mediate all fast synaptic excitation on voluntary muscle contraction.[182] There are five classes of muscular-type AChR subunits (α1, β1, γ, ε and δ) that form a circle around the central channel.[183,184] In embryonic muscle nAChRs consist of $(\alpha1)_2\beta1\gamma\delta$, whereas in adult muscle, the γ subunit is replaced by an ε subunit, being its composition $(\alpha1)_2\beta1\varepsilon\delta$.[185,186] Muscle-type nAChR channels have two ligand-binding sites for ACh, a common location in the α-δ protein

interface, and another place in either α-γ (in fetal status) or α-ε (in adults) interfaces (Figure 2.1B).[187] In these binding-sites there are several aromatic amino acids (tryptophan and tyrosine), which provide a negative electrostatic environment for stabilizing the quaternary ammonium group [-$N^+(CH_3)_3$] of ACh by cation-π interactions[188-190] (Figure 2.1B).

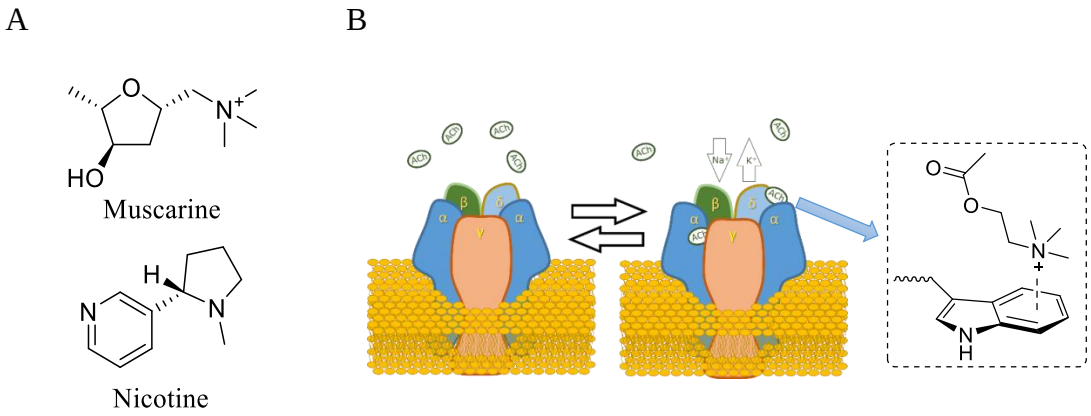

Figure 2.1. (**A**) Chemical structures of muscarine and nicotine; (**B**) Embryonic muscular nAChR in resting and active state, being activated by ACh; cation-π interaction between a tryptophan residue (Trp-149) and the neurotransmitter ACh (reproduced from Ref.[188]).

When ACh binds to the two binding sites of the muscle-type nAChR, it causes a conformational change of the ion channel, producing its opening (Figure 2.1B). In the open state, Na^+ influxes across the plasma membrane of post-junctional endplate, which has low permeability for these ions, causing electrical impulse and consequently, depolarization of the motor endplate membrane. Immediately K^+ exits, producing the repolarization and the return to the negative membrane potential. The electrical impulse is propagated through diverse receptor channels triggering muscle contraction.[191]

Neuromuscular blocking drugs

Neuromuscular blocking agents (NMBAs) inhibit muscle contraction by blocking nAChRs at the neuromuscular junction.[192,193] Natural extracts containing NMBAs have been used for centuries for a variety of applications, ranging from hunting to surgical procedures. South American indigenous tribes used to coat the tip of arrows or blow-pipe darts with curare alkaloids from different plants, in which tubocurarine is the main active ingredient (Figure 2.2). Since the early 1940s, NMBAs are used as muscle relaxants to facilitate endotracheal intubation. Due to several adverse effects observed in these drugs, in the last years several synthetic or semi-synthetic NMBAs have been developed.[194,195] As a common feature, NMBAs have at least one positively charged quaternary ammonium group or a tertiary ammonium group protonated at physiological pH, through which they bind to muscle-type nAChRs in a similar way as ACh does (Figure 2.1B).[179]

According to their mechanism of action, NMBAs can be classified into two groups: depolarizing and non-depolarizing drugs. Depolarizing NMBAs act as agonists, causing a prolonged depolarization of the plasma membrane of the muscle fiber, because they are more resistant to degradation by AChE than the neurotransmitter itself. As a result, they stay longer in the receptor, desensitizing the ion channel and triggering paralysis. This behavior can be differentiated in two phases: in phase I the opening of the channel allows the entry of Na^+ and the output of K^+ and consequently, the beginning of depolarization; in phase II, the desensitization of the nicotinic receptor takes place and therefore, muscular relaxation occurs. Examples of depolarizing agents that mimic two molecules of ACh are decamethonium (prolonged action) and suxamethonium, the latter (also known as succinylcholine) in current clinical use (shorter action time because is easily hydrolyzed by esterases) (Figure 2.2).

The non-depolarizing agents are competitive antagonists that challenge ACh for nicotinic binding sites, preventing the effect of the neurotransmitter on the receptor. Therefore, they do not induce the channel opening, avoiding depolarization of the muscle cell membrane, and consequently, producing direct paralysis. Their effects can be reversed by increasing ACh levels or by the action of an AChE inhibitor. Non-depolarizing NMBAs in clinic use can be categorized into two main groups according to their structure,

benzylisoquinoliniums and aminosteroids. Structurally derived from tubocurarine, the first family has quaternary ammonium groups linked by a long and flexible hydrocarbon chain, facilitating enzymatic degradation. Examples of the benzylisoquinoliniums' group are atracurium and mivacurium (Figure 2.2), with a short duration of action (30 and 18 min, respectively). The aminosteroid family is composed of molecules with bulkier structures, where the quaternary ammonium groups are anchored to a steroid nucleus that makes enzymatic degradation more difficult. Some examples are vecuronium, rocuronium, and pancuronium, with increasing duration of action (40, 70 and >180 min, respectively) (Figure 2.2).

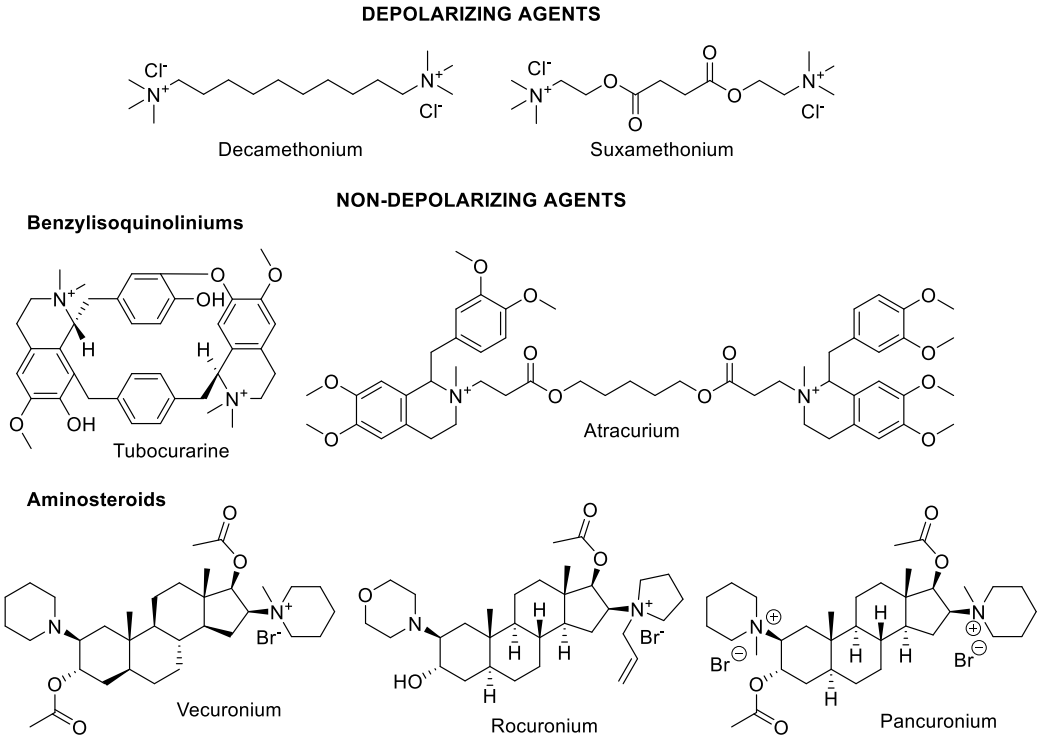

Figure 2.2. Examples of depolarizing and non-depolarizing NMBAs

Azobenzenes

Azobenzenes are compounds that contain an azo group (-N=N-) linking two benzenes, which in turn can carry several substituents. They exist in two isomeric forms, (*E*) and (*Z*), which can be reversibly exchanged thermally or by light irradiation at characteristic wavelengths, which depend on the nature of the aromatic substituents (Figure 2.3). In 1937, Hartley identified both isomers from a solution of azobenzene exposed to light.[196] In general, the (*E*)-isomer is the thermodynamically favored form that can be changed to the (*Z*)-isomer by irradiation with UV light (320-350 nm). The metastable (*Z*)-isomer can be also isomerized to the more stable (*E*)-isomer with light of higher wavelength (400-450 nm) or by thermal relaxation in the darkness (Figure 2.3). In addition to the fact that both isomers adopt different three-dimensional dispositions, the isomerization of the (*E*) to the (*Z*)-form shortens the molecule about 0.6 nm, affecting the physical, chemical and biological properties, as explained along this work.

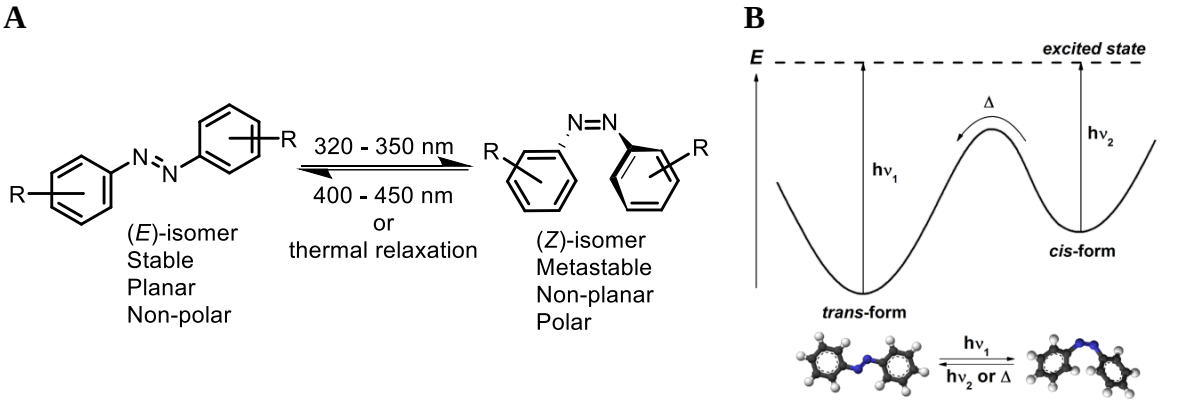

Figure 2.3. (**A**) Photo- and thermal isomerization of the (*E, Z*)-isomers of azobenzene. (**B**) Energetic profile for the switching process of azobenzene isomers (reproduced from Ref.[197])

For a long time, azobenzenes have been developed for many applications in the chemical industry of dyes and pigments,[198] radical reaction initiators,[199] supramolecular devices,[200] ionic liquids,[201] etc. More recently, and due to their light-dependent properties, other attractive uses are disclosed in relation to this PhD thesis, such as their application in biological systems.

Photopharmacology and photoswitchable drugs

Photopharmacology has grown impressively in the last decade and recent findings in areas as diverse as chemistry, biology and pharmacy continue to provide new evidence of their therapeutic potential. This area is based on the use of drugs that can be selectively activated and deactivated with light irradiation at different wavelengths (Figure 2.4A). The use of light provides a fine adjustment in the control of the administration of these drugs, with high spatial and temporal resolution,[202] being able to avoid the systemic side effects of conventional drugs. Photo-activation/deactivation can be achieved inside the organism by activated fluorescent compounds, or from the outside using minimally invasive optical fibers for the delivery of photon excitation in specific tissues.[203,204]

Photoswitchable drugs are compounds that consist of at least one biological active fragment (e.g. agonist, antagonist or ion channel blocker) and a photoisomerizable group (azobenzene in this work). In recent years, photoswitches have been applied to a wide range of biological targets, such as enzymes,[205] transmembrane proteins (ionic channels,[206-208] GPCRs,[209] etc.), nucleic acids,[204] etc. Therapeutic efficacy of these drugs has been demonstrated at the cellular level and some studies have progressed to live animals, with the restoration of vision in degenerative retinal diseases at the vanguard of these efforts (Figure 2.4B).[210,211]

A

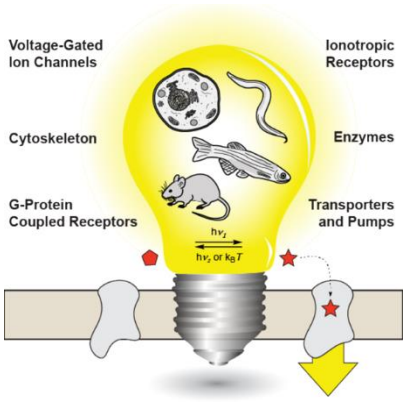

B

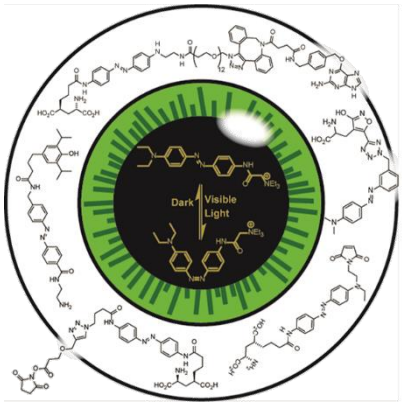

Figure 2.4. (**A**) Applications of photopharmacology to biological targets (taken from Ref.[204]). (**B**) Chemical photoswitches for restoring vision of the blind (taken from Ref.[210]).

From the pioneer studies of the application of photoswitchable drugs on the cholinergic system described around the 1970's,[212,213] several photoisomerizable ligands have been developed seeking the modulation of nAChRs with light.[214-216] Firstly, the Erlanger's group published two photochromic modulators of nAChRs, with *meta*-substitutions in both benzene rings: 3-(α-bromomethyl)-3'-[α-(trimethylammonium)methyl]azobenzene bromide (*m*-QBr, Figure 2.5A), which binds covalently to nAChR by reduction of the disulfide (S-S) bonds of the membrane with dithiothreitol;[217] and 3,3'-bis[α-(trimethylammonium)methyl]azobenzene dibromide (*m*-bisQ, Figure 2.5A), bearing two quaternary ammonium groups (Q) on the side of azobenzene, which binds reversibly to nAChRs. In the (*E*)-conformation both compounds are potent activators of nAChR, but (*Z*)-isomers result practically inactive in the electrogenic membrane of the electroplax of *Electrophorus electricus*.[218-220] Later, Lester characterized *m*-bisQ as a light-dependent nicotinic agonist in the electric eel,[221,222] and in an additional study on rat myoballs this group determined a Hill coefficient of approximately 2, concluding that more than one *m*-bisQ molecule binds to receptor in a cooperative process.[223]

A study about the preferred interactions of *m*-bisQ and its *ortho*- and *para*-analogues with muscular nAChRs revealed that *m*-bisQ displayed the optimized arrangement to interact

with the two binding sites of the receptor.[224,225] Hydrophobic areas (benzene) of *m*-bisQ mimics the methylene groups of ACh, in the planar hydrophobic area of the receptor, where also exits a site that interact with the carbonyl oxygen of ACh. There is also an anionic site located out of this plane that interacts with quaternary methyl groups (Figure 2.5B).[224]

A B

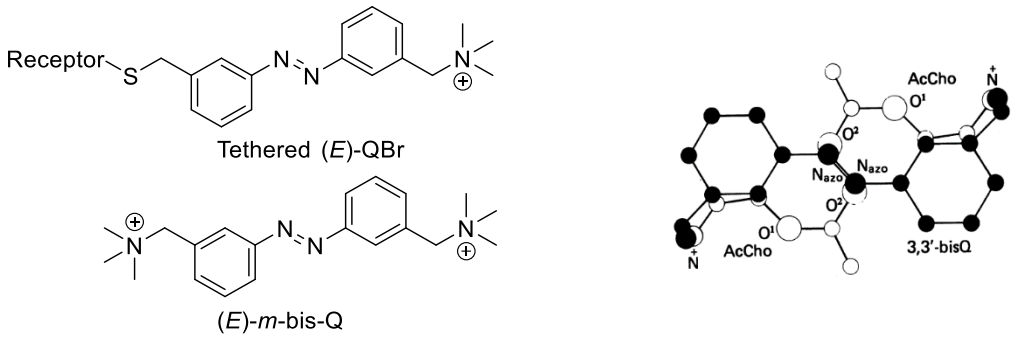

Figure 2.5. (**A**) Chemical structures of QBr and *m*-bisQ. (**B**) Diagram of two ACh molecules (open circles) and (*E*)-*m*-bisQ (solid circles) showing overlapping of critical functional groups (reproduced from Ref.[224]).

In 2015 Trauner´s group reviewed the light-dependent properties of *m*-bisQ using modern methods of channel electrophysiology.[214] In HEK293T cells, they found that the (*E*)-isomer is an agonist, which preferably acts on muscle-type nAChRs compared to the neuronal subtypes.

OBJECTIVES AND WORK PLAN

Taking into account all of the above mentioned, in this chapter, we propose to design, synthesize and evaluate novel ligands for the muscular nAChR, with lower affinity toward neuronal receptors and with the ability to be activated/deactivated with light.

As mentioned earlier, the most commonly used NMBAs have two positively charged amino groups linked in order to stablish cation-π interactions in the aromatic binding sites. Focusing now our attention on these quaternary ammonium groups of ligands of muscular nAChRs, we noticed that compounds with less sterically hindered amino groups tend to be agonists, such as *m*-bisQ, suxamethonium and carbachol. In contrast, compounds with larger substitutions in the amino group, including *N*-carbocycles are likely to be antagonists, such as the case of benzylisoquinoliniums (e.g., atracurium, mivacurium and cisatracurium) or aminosteroids (e.g., pancuronium, rocuronium and vecuronium).[192,193] Following this notion, we rationalized that we could generate photoswitchable antagonists for muscular nAChR by an *N*-cycle replacement of two methyl groups of each quaternary amine group of *m*-bisQ. As proof of principle, here we have designed, synthesized and tested a first generation of novel muscular nAChR ligands, named azocuroniums (**2.1**), which can be modulated *ad libitum* by light and consequently allow the finely tuned study of nAChR (Figure 2.6).

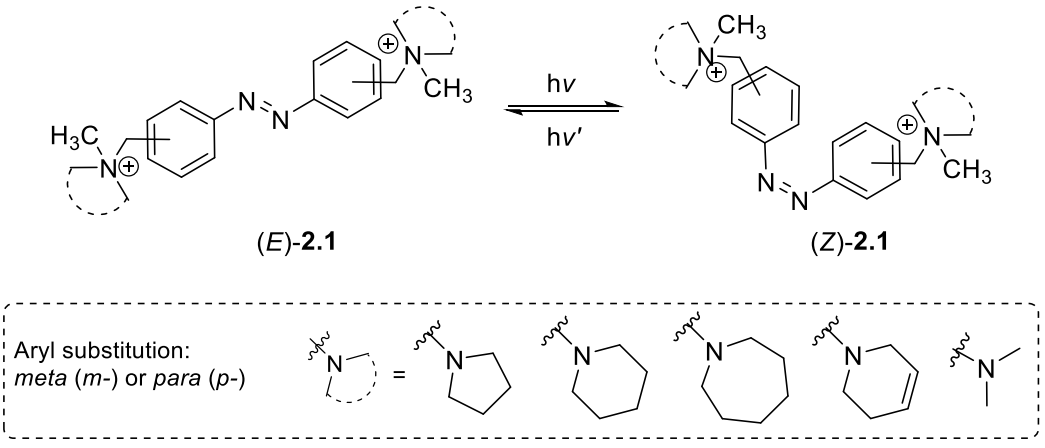

Figure 2.6. General structure of target (*E*)-(*Z*)-azocuroniums **2.1** and their putative photoisomerization

To achieve this general goal, we proposed the following work plan: (1) Synthesis of new photoswitchable compounds named as *meta*-azocuroniums (*m*-**2.1**) by replacement of the dimethylamino moiety of *m*-bisQ by different *N*-heterocycles (i.e. pyrrolidine, piperidine, azepane, and 1,2,3,6-tetrahydropyridine), which are present in non-depolarizing aminosteroids, such as *pancuronium*. For comparative purposes, we also plan the synthesis of the corresponding *para*-azocuroniums (*p*-**2.1**), as well as *m*- and *p*-bisQ (Figure 2.6). (2) Study of their photoisomerizable behavior by spectrometry UV-Vis and NMR, for stablishing the optimal wavelength for the (*E*)-(*Z*) interconversion. (3) Evaluation of physical-chemical properties, such as water solubility, pKas, and passive permeation into the CNS. (4) Assessment of their biological activities through the determination of binding constants in muscle and neuronal nAChRs by radioligand displacement. (5) Finally, evaluation of the functional character of the most active compounds by electrophysiology in muscular nAChRs expressed in *Xenopus laevis* oocytes.

The synthesis of target azocuroniums of general formula **2.1** was planned by quaternization of tertiary amines **2.2** bearing the azo group, which can be obtained from the corresponding nitrobenzenes **2.3** or anilines **2.4** (Scheme 2.1). In this strategy, the critical step is the formation of the corresponding azo derivative of general formula **2.2**, which could be achieved using different methodologies according to the bibliographic precedents, as explained below.

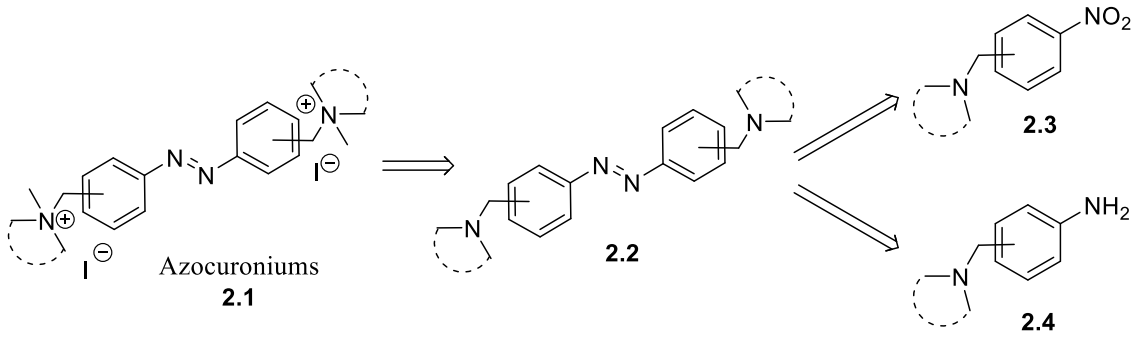

Scheme 2.1. General retrosynthetic plan of desired azocuroniums

The most used synthetic strategies for obtaining azobenzenes can be grouped in the following classical methods:[226,227]

1. Azo coupling reaction (diazonium salts with activated aromatic compounds). Many azobenzenes are formed by this electrophilic reaction, which starts with the diazotization reaction of the corresponding aniline at low temperature. Given that diazonium salts are weak electrophiles, they must react with an electron rich aromatic nucleophile (containing electron donating groups (EDG), such as amine, hydroxyl, or alkoxy groups) to obtain the corresponding azobenzene.[228-230] Since activating groups direct to *para*- and *ortho*-positions, the resulting azobenzenes will be mainly *para*-substituted, because the steric hindrance hampers the formation of *ortho*-derivatives (Scheme 2.2). Taking into account these limitations, this methodology cannot be employed to obtain the desired *meta*-azobenzenes bearing not activated substituents, as planned in this work.

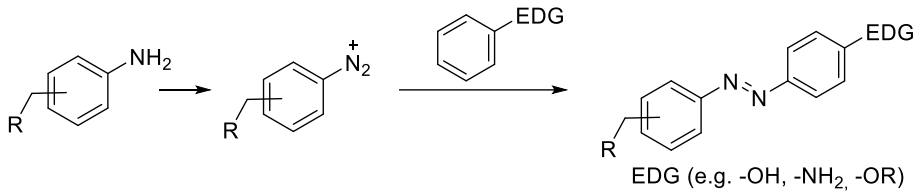

Scheme 2.2. Synthesis of azo compounds by coupling of diazonium salts with activated aromatic derivatives

The following methods use nitrobenzene or aniline derivatives as starting material, involving all the oxidation-reduction states showed in scheme 2.3 in the generation of the azo functionality. Azobenzenes **2.2** can be obtained by direct reduction of azoxybenzenes **2.5**, which could be obtained from the reaction of nitroso compounds **2.6** and hydroxylamines **2.7**.[231] However, an over reduction of azoxybenzenes **2.5** may lead to hydrazine derivatives **2.8**, instead of the desired azobenzenes **2.2**.[232] An alternative pathway is the reaction of nitro compounds **2.3** with hydroxylamines **2.7**. Finally, reaction of amines **2.4** with nitroso derivatives **2.6** may also produce the desired azobenzenes **2.2** (Mills reaction), although and as depicted in scheme 2.3, the involvement of different species in equilibrium may complicate the synthetic procedures. Thus, driving the reaction towards a

unique product is a complex task, because undesired products **2.5**-**2.8** are generally obtained, depending on the experimental conditions.

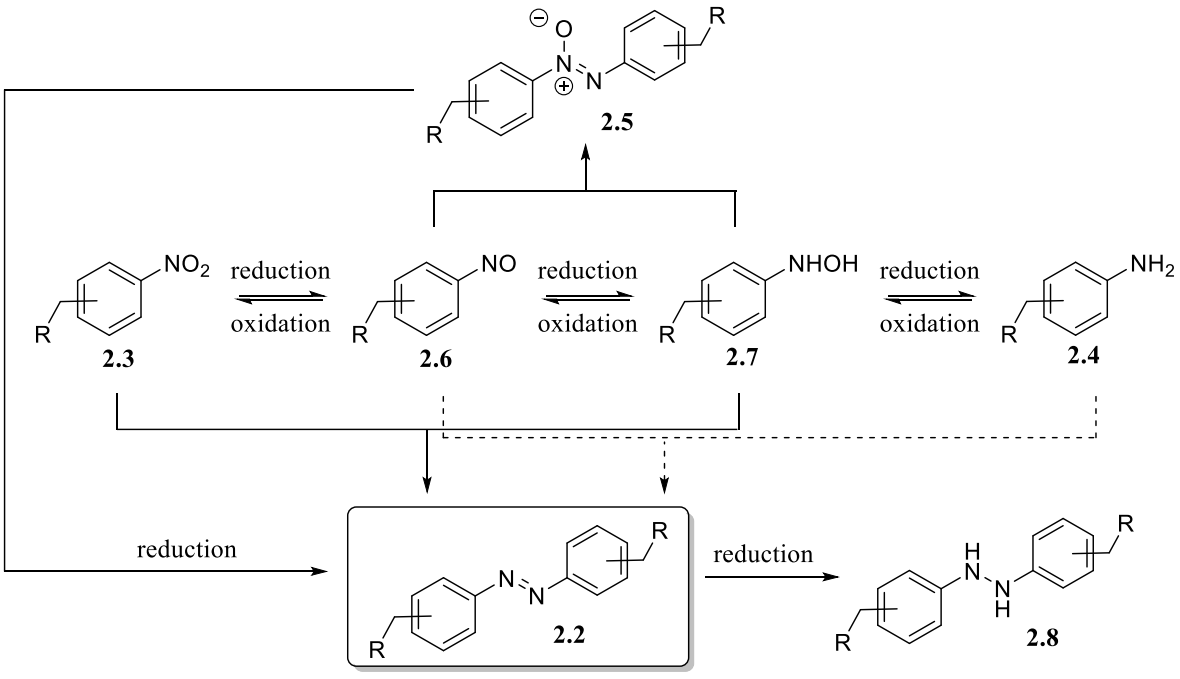

Scheme 2.3. Main species involved in the synthesis of azobenzene derivatives

2. Mills reaction (coupling of nitrosobenzenes and anilines). This methodology takes place between anilines and nitroso compounds in acidic media, making possible the synthesis of asymmetric azobenzene derivatives with substitution in all possible benzene positions and in the presence of deactivated rings (with electron-withdrawing groups). However, the isolation of nitroso derivative is a difficult task due to its high reactivity and its great tendency to oxidation, dimerizing rapidly to azodioxides (Scheme 2.4).[233,234] Furthermore, different side-products might be obtained because of the easy overoxidation of nitroso group.

Nitrosobenzenes can be obtained by the oxidation of anilines using several reagents and methodologies, such as the Caro's acid (H_2SO_5), peracetic acid, 3-chloroperoxybenzoic acid,[235] hydrogen peroxide in the presence of rhenium,[236] etc. However, biphasic

heterogeneous system with Oxone® [$(KHSO_5)_2 \cdot KHSO_4 \cdot K_2SO_4$] in H_2O:DCM has become one of the most employed, since it is inexpensive and environmentally friendly.[237-239]

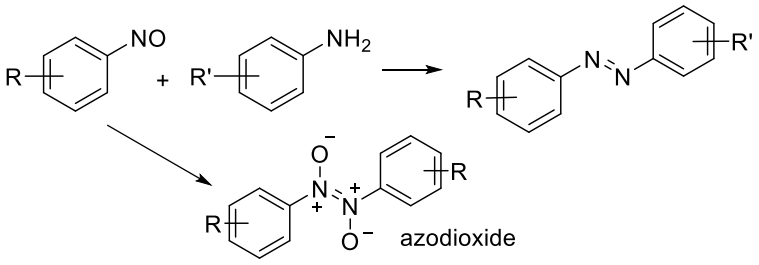

Scheme 2.4. Synthesis of azodioxide derivative from nitrosobenzene.

3. Oxidation of anilines. This methodology leads to symmetric azo compounds. Partial oxidation of anilines has been described by electrolytic oxidation,[240] chemical oxidants (sodium perborate/acetic acid (AcOH), potassium permanganate,[241] copper,[242] etc.) or by solvent-free oxidation.[243]

4. Reductive coupling of nitro compounds. This method is used to prepare symmetric azobenzenes, by the reaction of nitro derivatives with different reducing reagents ($NaBH_4$,[244] $LiAlH_4$,[245] $SnCl_2$/NaOH,[246,247] etc.) or by using H_2/Pd nanoclusters under basic conditions.[248] The disadvantage of the reductive coupling is that an excess of reducing agents have to be employed, giving environmentally unfriendly by-products.

RESULTS AND DISCUSSION

RESULTS AND DISCUSSION

Chemistry results

According to the bibliographic precedents, in this work the synthesis of azobenzenes **2.2** was explored using five methodologies, either from nitrobenzenes **2.3** or anilines **2.4**, which were obtained as described below.

*Synthesis of nitro- and amino- intermediates (**2.3** and **2.4**)*. The treatment of commercially available *meta*- or *para*-nitrobenzyl bromide with the corresponding amine (pyrrolidine, piperidine, azepane, 1,2,3,6-tetrahydropyridine, or dimethylamine) under basic conditions and mw irradiation at 120 ºC for 10 min, gave the corresponding nitro derivatives **2.3** in excellent yields. Some of these nitro derivatives were subjected to a subsequent Pd-C catalyzed hydrogenation to afford anilines **2.4** in high yields (Scheme 2.5).

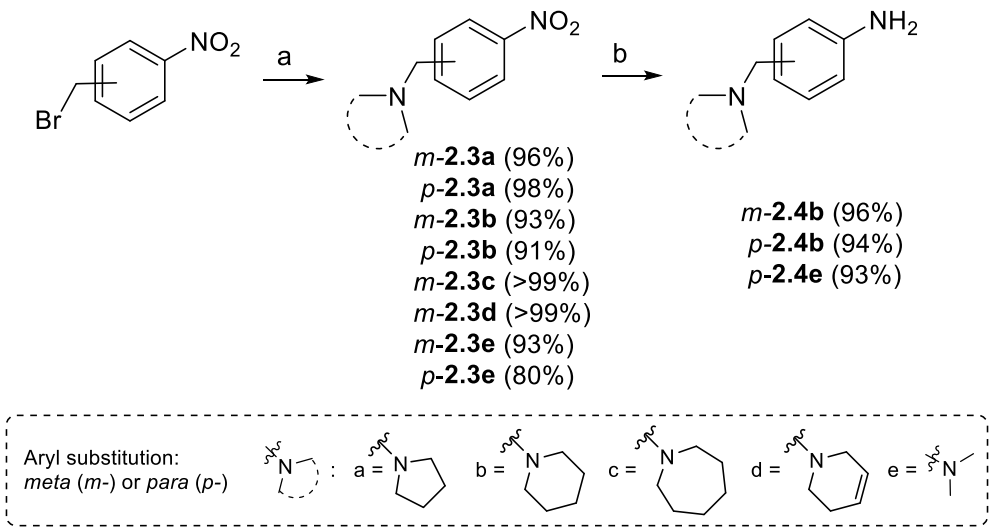

Scheme 2.5. Reagents and conditions. (a) K_2CO_3, corresponding amine, acetone, mw, 120 ºC, 10 min, (b) H_2, Pd/C (5%), EtOH, overnight.

Generation of the azo group. This critical step was explored using different methodologies along this chapter, according to the literature precedents described above. We tried to use similar synthetic strategies for both *meta*- and *para*- symmetric derivatives to facilitate the synthesis. Thus, coupling of diazonium salts could not be carried out because, as previously mentioned, this methodology is just used for activated rings leading to azobenzenes with *para*- or *orto*- substituents. The methodologies applied in this work have been classified according to the starting material, to facilitate the understanding of the results.

Symmetric azobenzenes

1. From anilines **2.4**
    1.1. Mills reaction catalyzed by Oxone®[237]
    1.2. Aerobic oxidation of anilines catalyzed by copper[242]
2. From nitrobenzenes **2.3**
    2.1. Hydrogenation catalyzed by Pd over charcoal 5% (Pd/C) at low pressure
    2.2. Hydrogenation catalyzed by Pd nanoclusters under basic conditions[248]
    2.3. Reduction with $LiAlH_{4rea}$[245]

Asymmetric azobenzene *m*-**2.13**: Mills reaction

Methodology 1.1. Mills reaction by oxidation of anilines catalyzed by Oxone®

The classical Mills reaction for obtaining azobenzenes involves the attack of anilines to aromatic nitroso derivatives in acidic media. In turn, nitroso compounds can be obtained by amine oxidation. Thus, our first attempt to obtain azobenzenes was the oxidation of the aniline *p*-**2.4b** with Oxone® at rt, following the method described by Priewisch and Rück-Braun.[237] Under these conditions, the aniline oxidation affords the corresponding nitroso derivative, which reacts with another molecule of aniline leading to the corresponding azo derivative. However, the treatment of the aniline *p*-**2.4b** with Oxone® produced a complex mixture (Scheme 2.6), depending on the reaction conditions listed in Table 2.1.

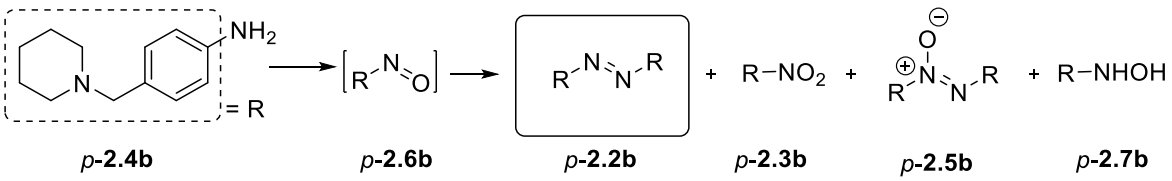

Scheme 2.6. Reagents and conditions. Oxone®.

According to the experimental conditions previously described for these transformations,[237] aniline *p*-**2.4b** was oxidized with 1.5 equiv of Oxone® in a mixture of H_2O:DCM in proportion 2:3 at rt (Table 2.1, first row). By HPLC-MS it was observed that the intermediate nitrosarene *p*-**2.6b** was immediately formed at the very beginning of the reaction, giving the desired azobenzene *p*-**2.2b**, together with the azoxy- and nitro-derivatives (*p*-**2.5b** and *p*-**2.3b**), as the result of the oxidation of azobenzene *p*-**2.2b** and aniline *p*-**2.4b**, respectively. After 30 min, we observed that the major product formed was the azoxy derivative *p*-**2.5b** and not the required azobenzene *p*-**2.2b**. Variations in the speed of addition led to similar results.

Table 2.1. Different conditions used for the oxidation of *p*-**2.4b** catalyzed by Oxone®

Conditions		Products (%)			
Oxone® (equiv)	Solvent	Azo derivative (*p*-**2.2b**)	Nitro derivative (*p*-**2.3b**)	Azoxybenzene (*p*-**2.5b**)	*N*-hydroxylamine (*p*-**2.7b**)
1.5	H_2O:DCM (2:3)	40[a]	8[a]	52[a]	n.d.
0.6	H_2O:MeOH (1:1)	n.d.	n.d.	n.d.	100[a]
1.2	H_2O	30[b]	n.d.	12[b]	n.d.

[a] Conversion by HPLC-MS; [b] Yield of isolated product; n.d.: not detected

As previously reported, the biphasic system assures the separation of the generally less water-soluble nitroso compound *p*-**2.6b** from the *N*-arylhydroxylamine intermediate (*p*-**2.7b**) and aniline precursor (*p*-**2.4b**), avoiding undesirable condensation reactions. However, in our case the basic character of the piperidine fragment made difficult this separation and all oxidative products coexisted in both phases and thus, products were not isolated.

Since the desired azobenzene *p*-**2.2b** was obtained in lower proportion (40% conv.) than its overoxidized product (*p*-**2.5b**, 52% conv.), the reaction was repeated with less equivalents of Oxone® (0.6 equiv), using a homogeneous solvent system composed by H_2O and MeOH in proportion 1:1 (Table 2.1, second row). Nevertheless, the reaction proceeded very slowly and only hydroxylamine *p*-**2.7b** was detected.

In the light of these results, we decided to use 1.2 equiv of Oxone® and H_2O as solvent. In these conditions, the oxidation of aniline *p*-**2.4b** afforded the corresponding azo- and azoxy-benzenes *p*-**2.2b** and *p*-**2.5b**, which were isolated in low yields (30% and 12%,

respectively). These low yields in both products were due to the fact they have a very similar R_f.

Methodology 1.2. Copper catalyzed oxidation of anilines

Another synthetic route was tried in order to avoid the formation of azoxy derivatives. It was based on a dehydrogenative coupling of anilines using a copper salt (CuBr) and pyridine at 60 ºC during 24 h (Scheme 2.7).[242] However, from aniline *p*-**2.4e** the expected azo derivative *p*-**2.2e** was not obtained and we only detected by HPLC-MS two azo compounds as the result of the loss of one or two dimethylamine moieties (*p*-**2.9e** and *p*-**2.10**, respectively). From these results we can conclude that the azobenzene was formed but the conditions were too drastic and consequently, the dimethylamine moiety tends to be lost. With the intention of avoiding the loss of the dimethylamino groups the reaction was repeated at rt, but it did not take place in these conditions.

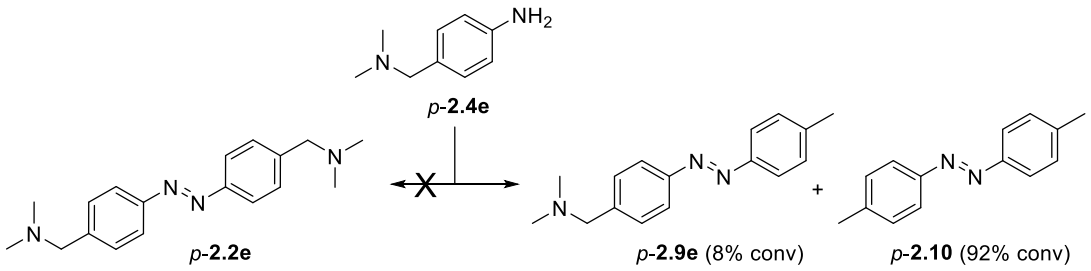

Scheme 2.7. Reagents and conditions. CuBr (0.1 equiv), pyridine (0.3 equiv), toluene, 60 ºC, 24 h.

To overcome the loss of amino moieties that occurs in the precedent reactions, we proposed another synthetic route based on the previously reported by Zhang and Jiao.[242] It consisted of the formation of azo compound from *p*-toluidine, followed by the bromination of benzylic positions with *N*-bromosuccinimide (NBS) and finally, a bimolecular nucleophilic substitution (S_N2) with the appropriate amine.[249]

Thus, dehydrogenative coupling of the commercially available *p*-toluidine using CuBr and pyridine afforded azo compound *p*-**2.10** with moderate yield (63%) (Scheme 2.8). However, the subsequent radical bromination in benzylic positions was not completed after refluxing for 10 days. In the HPLC-MS chromatogram of the reaction mixture, a combination of mono- and dibromide compounds with similar retention time was detected (*p*-**2.11** and *p*-**2.12**, respectively). Thus, this route was abandoned.

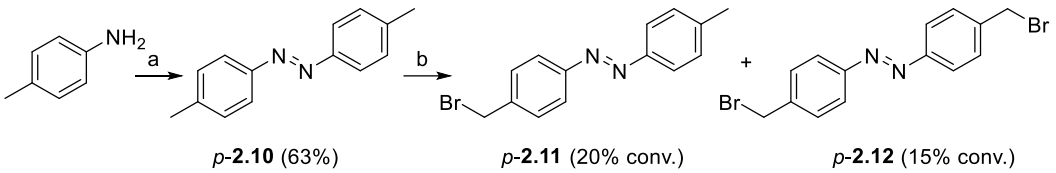

Scheme 2.8. Reagents and conditions. (a) CuBr (0.1 equiv), pyridine (0.3 equiv), toluene, 60 ºC, 24 h.; (b) NBS (3 equiv), benzoyl peroxide (0.06 equiv), $CHCl_3$, reflux, 10 days.

Methodology 2.1. Hydrogenation catalyzed by Pd/C 5% at low pressure

Starting from 1-(4-nitrobenzyl)piperidine *p*-**2.3b**, low pressure hydrogenation catalyzed by Pd/C in dry EtOH was attempted. However, after 48 hours at rt, aniline *p*-**2.4b** was the main isolated product (53%) along with the undesired azoxy compound *p*-**2.5b** in low yield (17%) (Scheme 2.9).

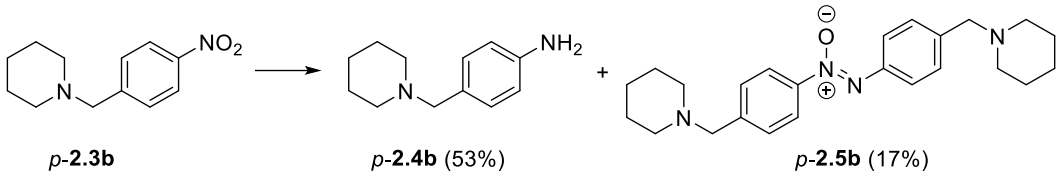

Scheme 2.9. Reagents and conditions. H_2 (low pressure), Pd/C (5%), dry EtOH, rt, 48 h.

When this reaction was repeated with the *meta*-nitro derivative *m*-**2.3b** as starting material and by increasing the reaction time until 7 days, the desired azo compound *m*-**2.2b** was obtained in a very low yield (9%). Moreover, were also isolated aniline *m*-**2.4b** and

undesired products *m*-**2.9b** and *m*-**2.10**, resulting from the loss of one or two piperidine fragments (Scheme 2.10).

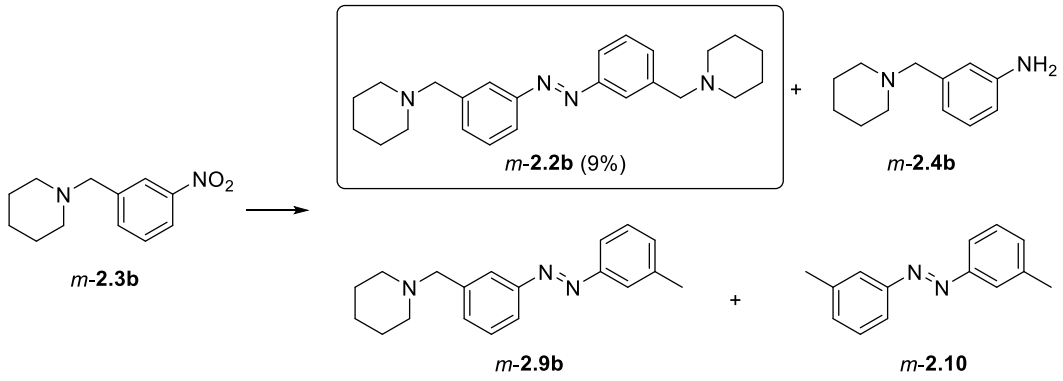

Scheme 2.10. Reagents and conditions. H_2 (low pressure), Pd/C (5%), dry EtOH, rt, 7 days.

Methodology 2.2. Hydrogenation catalyzed by Pd nanoclusters under basic conditions

The next attempt to get the desired azocompound consisted of the hydrogenation of the corresponding nitroaromatic compound catalyzed by Pd nanoclusters, generated *in situ* from palladium (II) acetylacetonate [$Pd(acac)_2$] under mild reaction conditions. According to the mechanism proposed by Wang *et al.*, $Pd(acac)_2$ is reduced *in situ* to Pd nanoclusters of an average diameter of 1 nm. These nanoparticles take part in the reaction yielding azoderivatives.[248] However, when we applied these reaction conditions to *p*-piperidine- and *p*-dimethylamine- nitrobenzenes (*p*-**2.3b** and *p*-**2.3e**) the expected azo compounds *p*-**2.2b** and *p*-**2.2e** were not obtained and only anilines *p*-**2.4b** and *p*-**2.4e** were identified in the HPLC-MS chromatograms.

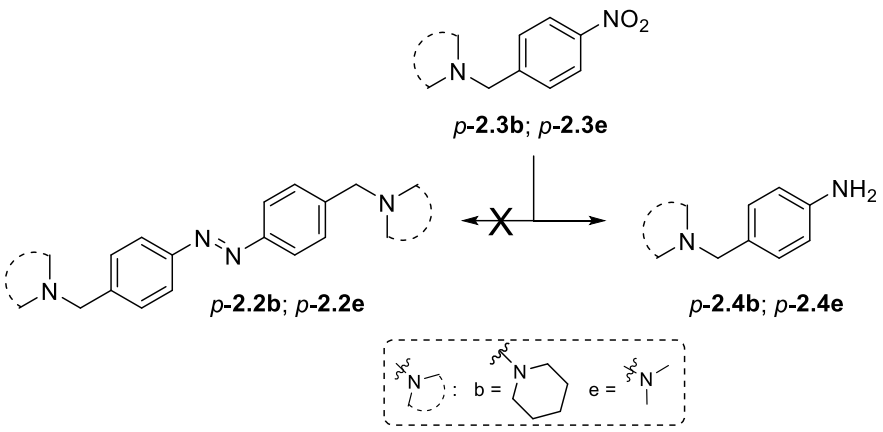

Scheme 2.11. Reagents and conditions. H_2, $Pd(acac)_2$ (5%), KOH, dry EtOH, 70 ºC.

Methodology 2.3. Reduction with $LiAlH_4$

Finally, we found the most appropriate synthetic route for obtaining the desired symmetric azobenzenes of general formula **2.2**. It was based on the reduction of nitro compounds **2.3** with $LiAlH_4$ in one step, as described by Di Gioia *et al.*[169] Thus the treatment of nitro derivatives *m*-**2.3(a-e)** and *p*-**2.3(a,b,e)** with $LiAlH_4$ in diethyl ether afforded the required azobenzenes *m*-**2.2(a-e)** and *p*-**2.2(a,b,e)** in moderate to excellent yields (49-95%) (Scheme 2.12).

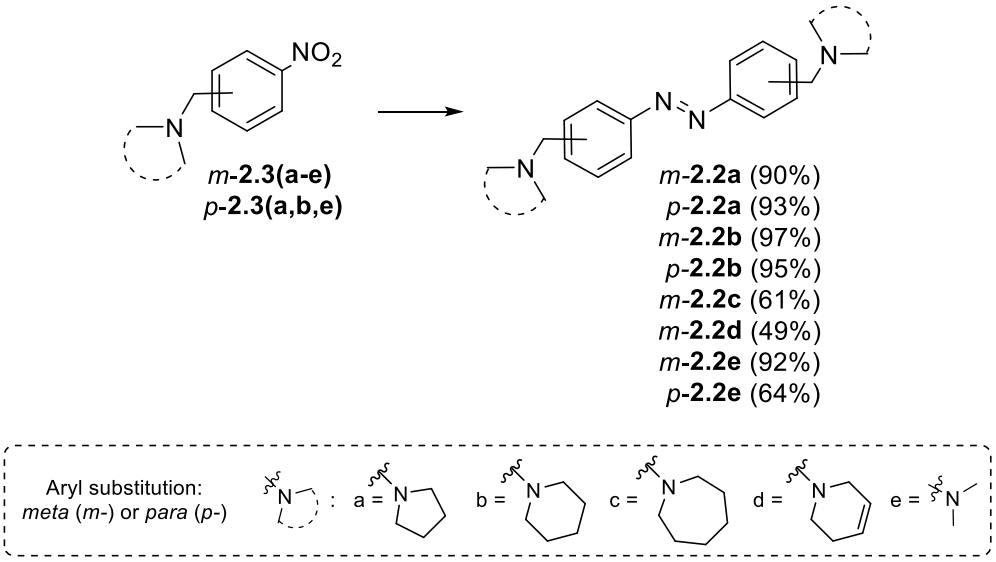

Scheme 2.12. Reagents and conditions. $LiAlH_4$, Et_2O, N_2, -78 ºC to rt.

The reaction probably proceeds through an electron transfer from hydride to the nitro group with the formation of a radical intermediate that dimerizes providing the desired azobenzene (Scheme 2.13).[169]

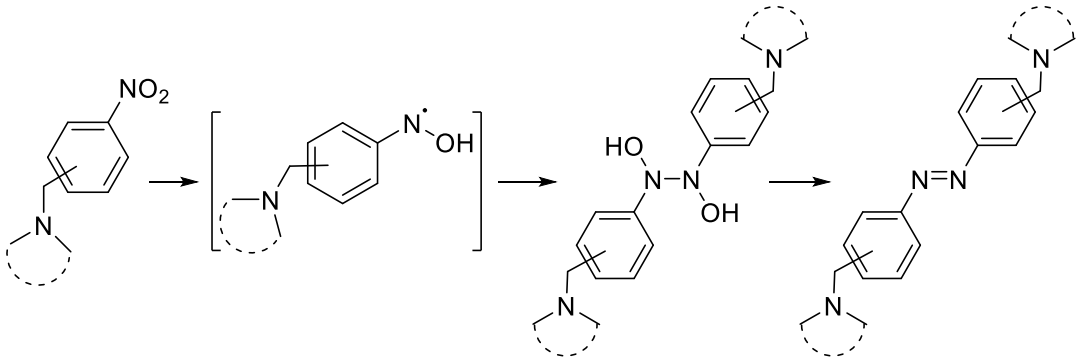

Scheme 2.13. Probable mechanism of formation of azo compounds from reduction of nitro derivatives with $LiAlH_4$ (adapted from Di Gioia *et al.*[169])

Otherwise, asymmetric azocompound *m*-**2.13b** was synthesized from 3-(piperidin-1-ylmethyl)aniline *m*-**2.4b** and commercial nitrosobenzene in high yield (93%) by a Mills reaction[250] (Scheme 2.14).

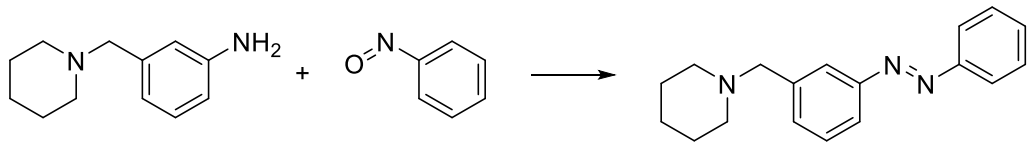

m-**2.4b** *m*-**2.13b** (93%)

Scheme 2.14. Reagents and conditions. AcOH, toluene, 60 ºC, overnight.

It is worth to mention that a very high purity of azoderivatives is crucial, because minimum impurities with similar nature will suffer equal reaction in the next step of amine quaternization, making purification much more difficult or even impossible. Given that, azobenzenes *m*-**2.2(a-e)**, *p*-**2.2(a,b,e)**, and *m*-**2.13b** were subjected to a preparative TLC followed by a recrystallization, to assure maximum purity of each azoderivative.

Synthesis of azocuronium salts. Finally, the azobenzenes with a tertiary amino group were methylated with methyl iodide (CH_3I) at 120 ºC for 12 min in mw, obtaining the desired azocuroniums (Scheme 2.15). Symmetric azocuroniums *m*-**2.1(a-e)** and *p*-**2.1(a,b,e)** were obtained in good to excellent yields (78-99%), whereas the yield of the asymmetric derivative *m*-**2.14b** was lower (58%). This yield could be due to the low melting point of this compound that made difficult its purification by precipitation.

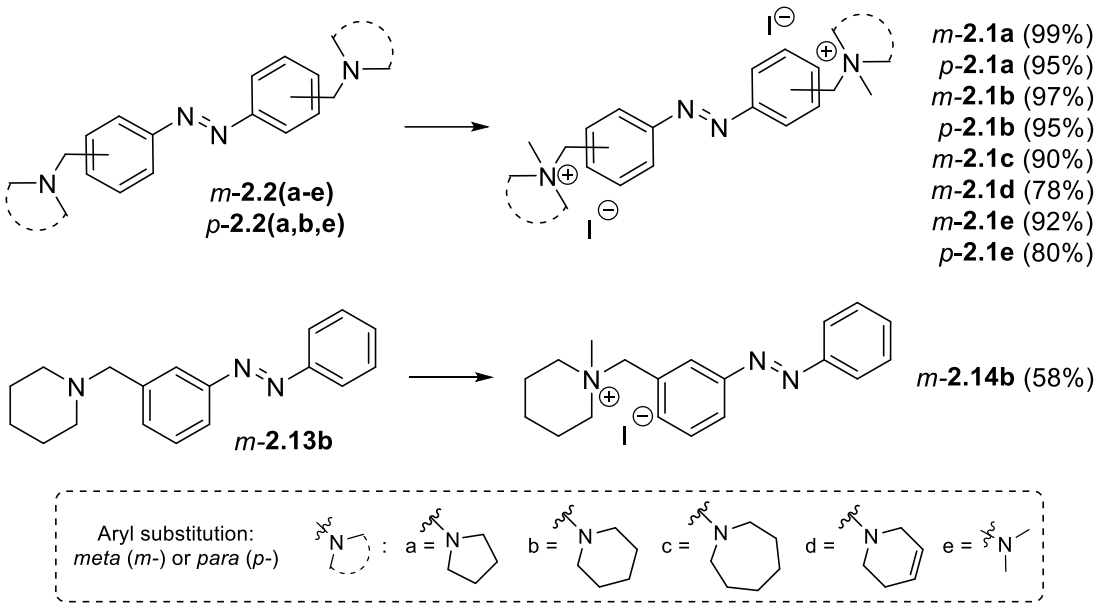

Scheme 2.15. Reagents and conditions. CH_3I, DMF, mw, 120 ºC, 12 min.

Thermodynamic solubility studies

The thermodynamic solubility of azocuronium *m*-**2.1**(**a**-**d**), *p*-**2.1**(**a**,**b**) and *m*-**2.14b** was determined by UV spectroscopy, using a Sirius T3 equipment in phosphate buffer (45 mM) at pH 7.4, following described protocols.[251] Results are gathered in Table 2.2. As expected, all azocuronium showed high solubility values in aqueous solution at physiologic pH (5.5 – 38.4 mM). All *meta*- derivatives were found to be more soluble than their *para*-counterparts, probably due to the higher polarity of the first. Salts bearing *meta*-pyrrolidine (*m*-**2.1a**) and *meta*-piperidine fragments (*m*-**2.1b**) showed similar values (36 and 38 mM, respectively), whereas the *meta*-azepane derivative (*m*-**2.1c**) displayed a lower solubility according to its higher lipophilicity. Nevertheless, not so drastic decrease was observed when a double bond was introduced in the piperidine fragment (*m*-**2.1d**). Otherwise, the loss of one ammonium group in derivative *m*-**2.14b** remarkably decreased the solubility in water with respect to the analogue *m*-**2.1b** with two piperidines.

Table 2.2. Thermodynamic solubility (mM) in water at pH 7.4 of azocuroniums *m*-**2.1**(**a**-**d**), *p*-**2.1**(**a**,**b**) and *m*-**2.14b**, measured at the indicated wavelengths.

	Solubility at pH 7.4 (mM)[a]	λ (nm)
m-**2.1a**	36.3 ± 3.1	340
p-**2.1a**	14.8 ± 1.2	340
m-**2.1b**	38.4 ± 3.5	320
p-**2.1b**	34.9 ± 3.2	320
m-**2.1c**	5.9 ± 0.5	290
m-**2.1d**	16.3 ± 0.1	290
m-**2.14b**	5.5 ± 0.1	290

[a]Results are the mean ± SD of three independent experiments.

Therefore, new azocuronium *m*-**2.1**(**a**-**d**) and *p*-**2.1**(**a**,**b**) show good solubility in physiologic media.

Calculation of pKa values

Aiming to know if tertiary amines are charged at physiologic pH (7.4), pKa values were calculated in a Sirius equipment, using the Yasuda-Shedlovsky extrapolation[252] for the azobenzene *p*-**2.2b** and azoxybenzene *p*-**2.5b**, both bearing two protonatable *para*-piperidine fragments. Despite the symmetry of the molecule, in the azobenzene *p*-**2.2b** one piperidine is protonated before the other, although the pKas are very close: pKa(1) = 7.11 ± 0.07 and pKa(2) = 7.67 ± 0.03. From these data we can conclude that at physiologic pH the azobenzene *p*-**2.2b** shows one protonated piperidine fragment.

Otherwise in azoxybenzene *p*-**2.5b**, a higher difference between pKas was observed, obtaining 7.03 ± 0.01 and 8.92 ± 0.06 values. As expected, the higher value was assigned to the piperidine conjugated with oxygen of azoxy group, due to the oxygen is giving charge to the benzene for resonant effect; while benzene closer to nitrogen is affected by inductive effect, making that this pKa decreases. This means that at physiologic pH more than 50% of one of piperidine can be found as a quaternary amine in the azoxybenzene *p*-**2.5b**.

Given that at physiological pH only one piperidine is protonated, and cationic charge is necessary for the cation-π interaction with the receptor, amine quaternization is required to improve the affinity toward muscle nAChRs.

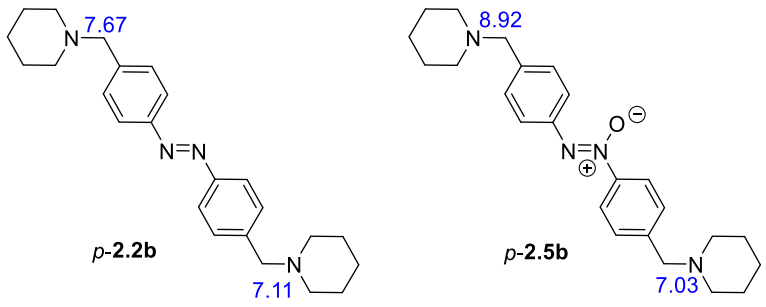

Figure 2.7. pKa values for azocuroniums *p*-**2.2b** and *p*-**2.5b**

In vitro evaluation of the CNS-penetration (PAMPA-BBB assay)

To check if new azocuroniums *m*-**2.1**(**a**-**d**), *p*-**2.1**(**a**,**b**) and *m*-**2.14b** could be able to reach the CNS, we used the *in vitro* parallel artificial membrane permeability assay for the blood-brain barrier (PAMPA-BBB) described by Di *et al.*,[135] and partially modified and validated by us.[70,111,128,173] The passive CNS-permeation of *m*- and *p*-azocuroniums through a lipid extract of porcine brain was measured at rt. In each experiment, 11 commercial drugs of known brain permeability were also tested and their permeability values normalized to the reported PAMPA-BBB data. According to P_e values previously described by Di *et al.*,[135] compounds with P_e values exceeding $4 \cdot 10^{-6}$ cm s^{-1} would be able to cross the BBB (cns+), whereas those displaying P_e less than $2 \cdot 10^{-6}$ cm s^{-1} would not reach the CNS (cns-). Between these two values the prediction is uncertain (cns +/-).

Table 2.3. *In vitro* CNS permeability data of azocuroniums *m*-**2.1**(**a**-**d**), *p*-**2.1**(**a**,**b**) and *m*-**2.14b**, and their predictive CNS penetration.[a]

	PAMPA-BBB (P_e, 10^{-6} cm s^{-1})	CNS-Penetration Prediction
m-**2.1a**	< 1.0	cns -
p-**2.1a**	< 1.0	cns -
m-**2.1b**	< 1.0	cns -
p-**2.1b**	< 1.0	cns -
m-**2.1c**	< 1.0	cns -
m-**2.1d**	< 1.0	cns -
m-**2.14b**	2.0 ± 0.2	cns +/-

[a]Results are the mean ± SD of three independent experiments. [b]Predictive CNS penetration: cns- denotes compounds that could not be able to penetrate into the CNS; cns +/- denotes uncertainty in CNS penetration prediction.

Whereas the asymmetric derivative *m*-**2.14b** with only one positive charge displayed an uncertainty in CNS penetration, the rest of azocuronium with two positive charges, *m*-**2.1**(**a-d**) and *p*-**2.1**(**a**,**b**), were predicted would not cross the BBB (Table 2.3).

From these data we can conclude that, as expected, new *m*- and *p*-azocuroniums *m*-**2.1**(**a-d**) and *p*-**2.1**(**a**,**b**) will not penetrate the CNS and will not interact with CNS-receptors.

Photochemical characterization

UV-vis spectra under irradiation

As discussed in the introduction, the (*E*)-isomer of azocuronium is the most abundant species in the darkness because it is the most thermodynamically stable geometry. This (*E*)-isomer can be reversibly photoisomerized under irradiation to the (*Z*)-form. Both isomers have three possible excited singlet states, resulting three absorption bands in UV-vis. The molecular orbital diagram for azobenzene consists of three highest unoccupied and three lowest occupied orbitals and the non-bonding atomic orbitals of the azo-nitrogen atoms (n_a and n_b) (Figure 2.8).[253] The lowest transition, $S_0 \rightarrow S_1$, occurs in the visible region (around 440 nm and 430 nm, (*E*) and (*Z*), respectively), due to the forbidden process of excitation of an electron from the non-bonding n orbital of an *N* atom of azo group to an antibonding π* orbital (n→π*). The second transition, in UV region, $S_0 \rightarrow S_2$ (around 314 nm and 280 nm, (*E*) and (*Z*), respectively) is associated with a symmetry-allowed π-π* transition. This notable difference is due to the non-planar configuration of (*Z*)-isomer.[253,254] The highest transition is due to $\phi \rightarrow \phi^*$ process (230 – 240 nm for both isomers), due to close association of ϕ orbital with benzene ring.

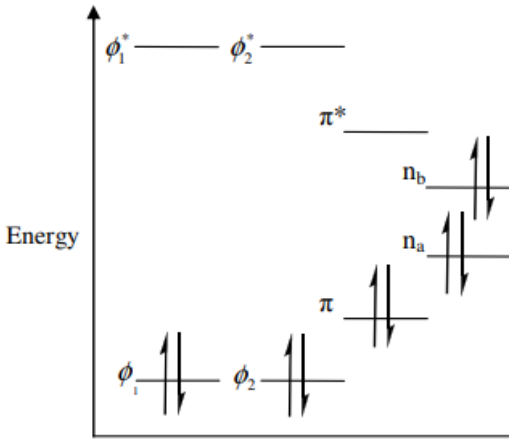

Figure 2.8. Molecular orbital diagram for azobenzene system.[253]

UV/vis spectra of *m*- and *p*-azocuroniums *m*-**2.1**(**a**-**d**), *p*-**2.1**(**a**,**b**) and *m*-**2.14b** were recorded in aqueous solutions (50 µM) at rt, as a qualitative measure of their isomerization. All of them had a similar spectrum, thus photochemical characterizations of *m*-**2.1**(**a**-**d**) are given as examples (Figure 2.9). As typical azobenzene derivatives, the thermally equilibrated spectrum of both compounds (black line Figure 2.9B) showed two absorption bands, corresponding to the (*E*)-isomer. The most intense one was centered on 315 nm, attributed to the π-π *electronic transition of the (*E*)-azobenzene moiety, and the other around 425 nm is due to the forbidden n-π*. After irradiation with 335 nm light using a LED-based source, the amplitude of the 315 nm band decreased while increasing irradiation time, whereas the amplitude of the 425 nm peak increased (red line). As known, this spectral change is due to the (*E*)-to-(*Z*) isomerization of azobenzene molecules.[255] This effect was reverted by irradiating with light of 400 nm (blue line). The recovery of the initial spectra indicated that both compounds are found in the (*E*)-isomer, most likely due to thermal relaxation. The insets show details of the spectra between 375 nm and 525 nm.

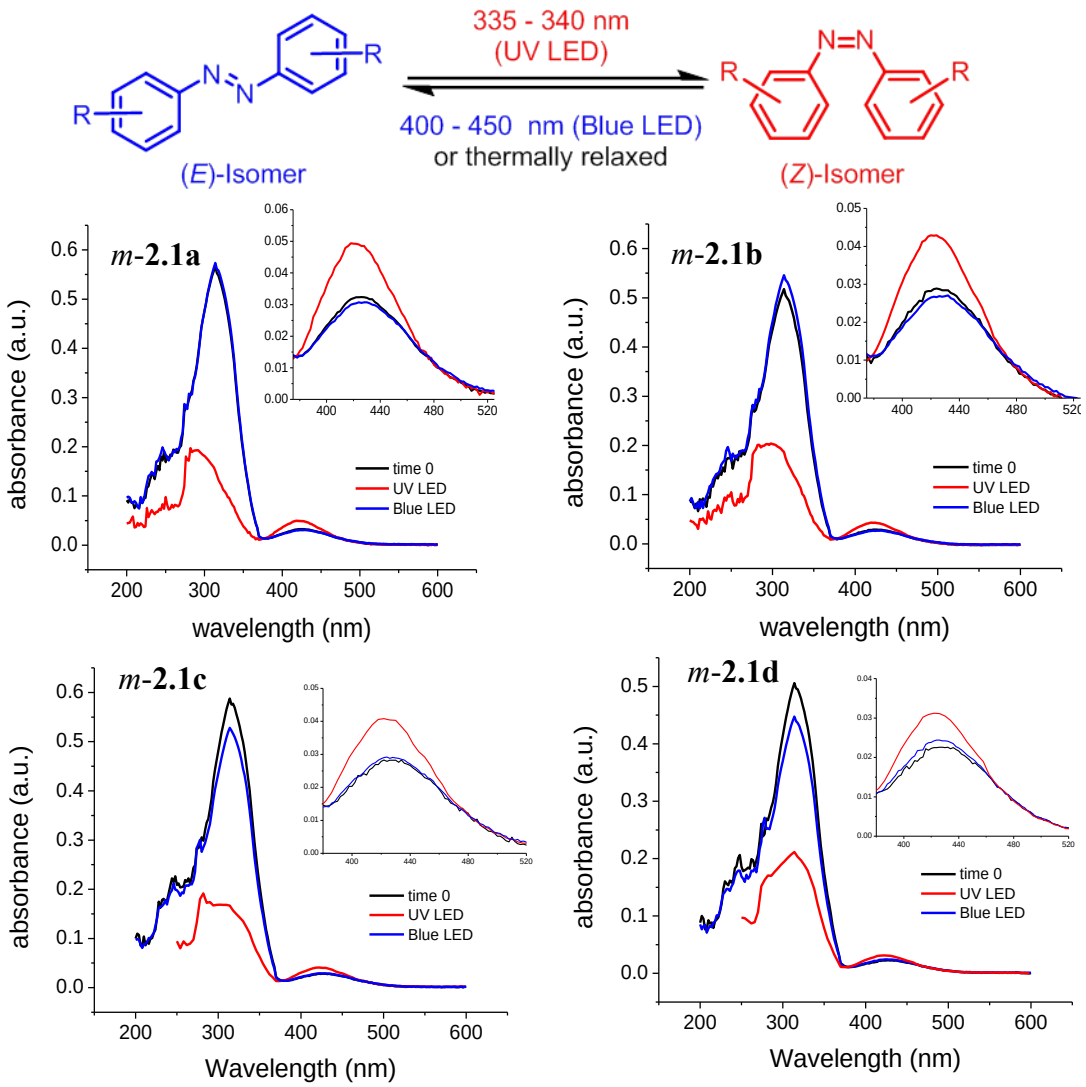

Figure 2.9. (*E*)-(*Z*)-isomerization of azobenzene scaffold (Upper); UV absorption spectra of *m*-**2.1**(**a-d**) (Lower).

NMR spectra under irradiation

The (*E*)-(*Z*) conversion can be also quantified by conventional ^{1}H-NMR technique.[256,257] When azobenzenes are irradiated with UV light (around 335 nm), the intensities of signals of (*E*)-isomer decrease and the signals belonging to (*Z*)-isomer grow simultaneously. This effect is usually reverted irradiating at 400 nm [(*E*)-isomer formation], demonstrating reversible isomerization.

In situ laser irradiation by an optical fiber has been reported in several works to study photoisomerization.[258,259] Because we do not have access to this apparatus, an array of light emitting diodes (LEDs) was used. Thus, azocuroniums *m*-**2.1b** and *m*-**2.1d** were dissolved in deuterium oxide (D_2O) and their NMR spectra were recorded. Solutions were irradiated with LED-light (335 or 400 nm) in a round-bottom flask for different exposure times and then transferred to a NMR tube for registering the spectrum. The ratio between isomers was calculated from the integration values of some characteristic common protons.

Firstly, the NMR spectrum of the freshly synthesized *m*-**2.1b** (not-irradiated sample) showed two groups of aromatic signals, integrating for 8 protons and which were assigned to (*E*)-azobenzene isomer (upper spectrum Figure 2.10). After 15 min of LED irradiation under 335 nm, the (*Z*)-isomer was formed in an approximate percentage of 71% [(*Z*):(*E*) ratio 1.0:0.4] that was increased to 83% [(*Z*):(*E*) ratio 1.0:0.2] when irradiation was continued until 30 min. Aiming to explore the maximum conversion of the (*Z*)-isomer of *m*-**2.1b**, sample was irradiated under 335 nm for 1 and 4 h, obtaining a percentage of (*Z*)-isomer of 84 and 87%, respectively. In order to recover the (*E*)-isomer, the solution was irradiated at 400 nm for 1 h, obtaining a percentage of (*E*)-*m*-**2.1b** of 77% [(*Z*):(*E*) ratio 0.3:1.0]. After leaving the solution in the darkness at rt overnight, no changes were observed, pointing out that the complete thermally relaxation at rt needs a longer time.

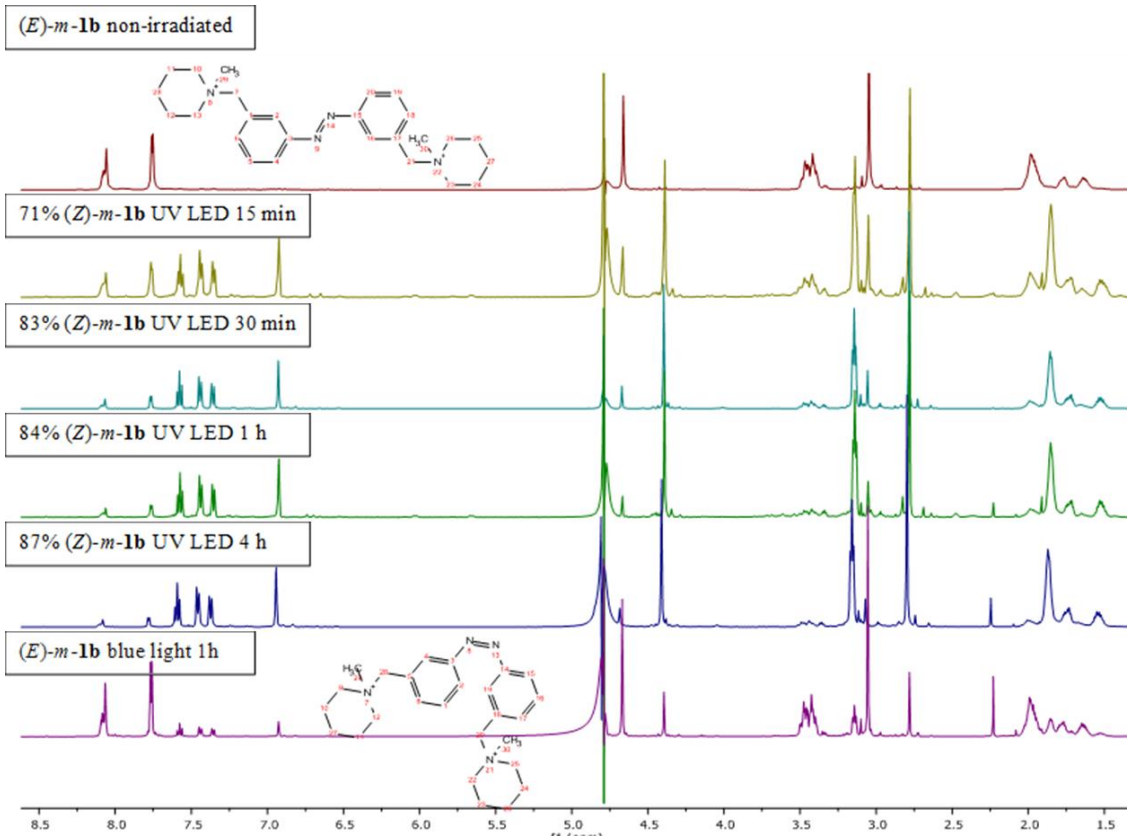

Figure 2.10. ^{1}H-NMR spectra of azocuronium *m*-**2.1b** irradiated with a UV LED (335-340 nm) or blue LED (400-450 nm) during the indicated times.

On the other hand, azocuronium *m*-**2.1d** has a double bond that gives characteristic signals between 5.5 and 6 ppm, which make the differences between the (*Z*)- and (*E*)- spectra more appreciable. Thus, ^{1}H-NMR of *m*-**2.1d** was recorded in D_2O at daylight and rt (Figure 2.11, upper spectrum), observing an (*E*):(*Z*) ratio of 1:0.2. Then, the solution was irradiated with UV LED (335-340 nm) for 2.5 h, to maximize the conversion (Figure 2.11, lower spectrum). Although total conversion to the (*Z*)-isomer was not achieved, the ratio (*E*):(*Z*) was almost reverted as it can be seen in the graphic. When the solution containing mainly the (*Z*)-isomer was irradiated with the blue LED (400-450 nm) for 1 h the (*E*)-isomer was recovered almost totally (spectrum not shown).

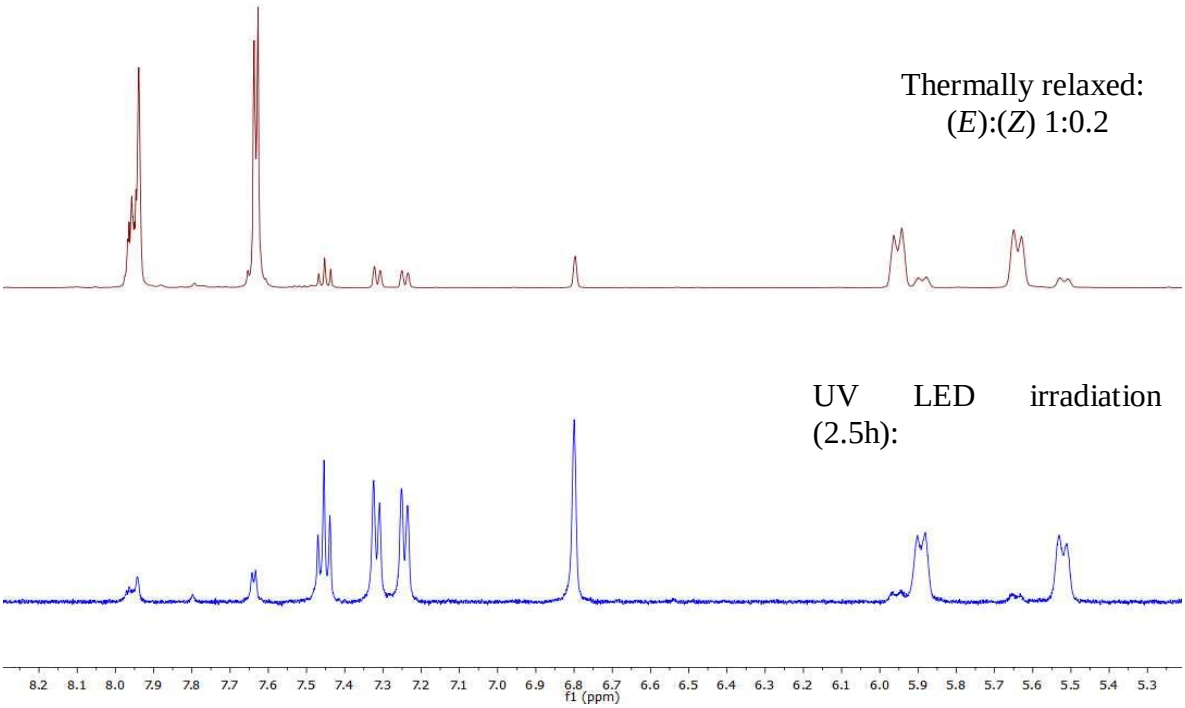

Figure 2.11. Expansion of ^{1}H-NMR spectra of *m*-**2.1d**. Upper spectrum was recorded without irradiation and lower spectrum was registered after UV LED irradiation (335-400 nm) for 2.5h.

As expected, signals of the (*E*)-isomer are more deshielded than those of the (*Z*)-form.[260] This can be explained by the change in the geometry of the minimum energy structures of both isomers (Figure 2.12). In (*E*)-isomers, the two benzenes are far away from each other and consequently protons are deshielded by their 'own' aromatic ring. Otherwise, in the (*Z*)-isomer aromatic rings are nearer and perpendicular between them and thus, their protons are more shielded by the π -clouds.

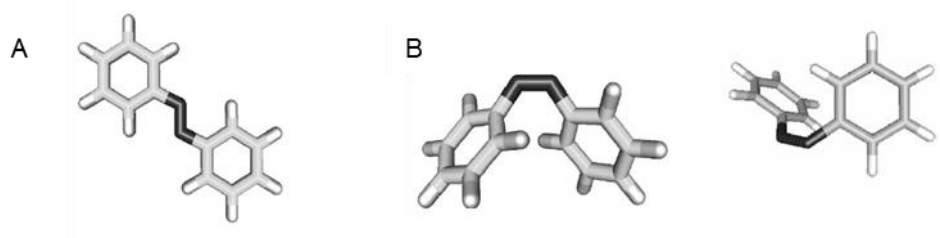

Figure 2.12. The calculated minimum energy structures of (**A**) (*E*)-azobenzene and (**B**) (*Z*)-azobenzene. Two views of the (*Z*)-isomer are shown, to illustrate the relative orientation of the phenyl rings. Reproduced from Ref.[33]

Biological results

Radioligand binding assays at nAChRs

In order to characterize the action of our compounds at nicotinic receptors, a selection of azoderivatives [*m*-**2.2(a,b**) and *p*-**2.2(a,b**)] and all azocuronium [*m*-**2.1(a-d)**, *p*-**2.1(a,b)** and *m*-**2.14b**] were tested in radioligand-displacement experiments, using muscular nAChRs and two neuronal-type nAChRs (α7 and α4β2) (Eurofins Cerep SA, France). BisQ (compound *m*-**2.1e**) was also assayed for comparative purposes.

Firstly, the percentage of radioligand displacement of compounds at a single concentration (10 µM) was calculated for each receptor type, using the appropriate radioligand ([^{125}I]-α-bungarotoxine for muscle-type and α7 nAChRs, and [^{3}H]-cytisine for α4β2 nAChR). As shown in Table 2.4, the majority of azoderivatives [*m*-**2.2(a,b**) and *p*-**2.2(a,b**)] and azocuroniums [*m*-**2.1(a-d)**, *p*-**2.1(a,b)** and *m*-**2.14b**] showed selectivity towards muscular nAChRs compared with neuronal ones. In all cases, azocuronium *m*-**2.1(a,b**) and *p*-**2.1(a,b**) exhibited higher radioligand displacement values at 10 µM than their respective azoderivatives *m*-**2.2(a,b**) and *p*-**2.2(a,b**).

Table 2.4. Radioligand displacement (%) of azoderivatives and azocuronium salts at 10 μM.

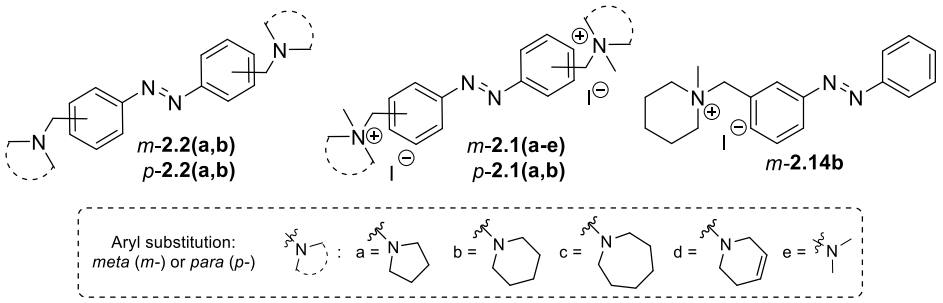

Compd.	Radioligand displacement at 10 μM (%)		
	Muscle-type	Neuronal α7	Neuronal α4β2
***m*-2.2a**	88	57	9
***p*-2.2a**	66	14	0
***m*-2.2b**	79	75	6
***p*-2.2b**	49	5	0
***m*-2.1a**	87	64	31
***p*-2.1a**	89	95	51
***m*-2.1b**	98	77	7
***p*-2.1b**	85	16	71
***m*-2.1c**	87	78	29
***m*-2.1d**	92	88	32
***m*-2.1e**	93	12	26
***m*-2.14b**	45	48	39

Then, binding constants (K_i) were calculated for azocuroniums that had a displacement percentage above 60% (Table 2.5). Standard reference compounds were α-bungarotoxin (muscle-type nAChR), epibatidine (α7 nAChR) and nicotine bitartrate (α4β2 nAChR), which were tested in each experiment at several concentrations to obtain competition curves from which K_is were calculated.

Table 2.5. Affinity constants of azocuroniums *m*-**2.1**(**a**-**d**), *p*-**2.1**(**a**,**b**) and *m*-**14b** in human nAChRs of muscular and neuronal-type (α7 and α4β2).[a]

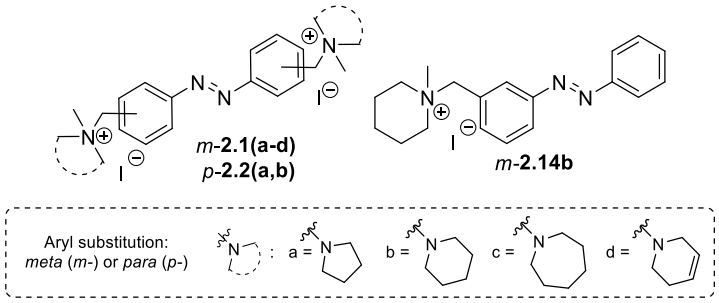

Compd.	K_i (nM)		
	Muscle-type	Neuronal α7	Neuronal α4β2
m-**2.1a**	42 ± 4	2500 ± 210	>10,000
p-**2.1a**	200 ± 20	930 ± 80	>10,000
m-**2.1b**	35 ± 3	910 ± 90	>10,000
p-**2.1b**	1,100 ± 100	>10,000	1,500 ± 130
m-**2.1c**	220 ± 20	1,900 ± 180	>10,000
m-**2.1d**	100 ± 9	730 ± 70	>10,000
m-**2.14b**	>10,000	>10,000	>10,000
α-bungarotoxin	1.0 ± 0.1	n.d.	n.d.
epibatidine	n.d.	120 ± 10	n.d.
nicotine	n.d.	n.d.	1.5 ± 0.1

[a]Results are the mean ± SEM of three independent experiments. N.d.: not determined.

In general, *meta*-substitution in azocuroniums favors the interactions with muscle-type nicotinic receptors ($K_i = 10^{-8}$ M) compared to subtypes α7 ($K_i = 10^{-6} – 10^{-7}$ M) and α4β2 ($K_i > 10^{-5}$ M). Azocuroniums bearing *para*-substitutions were less active in all nAChRs and showed no selectivity towards the muscular type. For instance, the pyrrolidine derivative *p*-**2.1a** that was the most active *para*-azocuronium compound in muscular nAChR (K_i = 200 nM) showed α7-nAChR affinity in the same order of magnitude (K_i = 930 nM). Moreover, *para*-piperidine azocuronium *p*-**2.1b** was not selective either, this time between muscle-type and neuronal α4β2, as its binding constants were in the same range (K_i = 1,100 and 1,400 nM, respectively).

In muscle-type nAChRs, the most potent ligands were the *meta*-pyrrolidine *m*-**2.1a** and the *meta*-piperidine *m*-**2.1b** azocuroniums, with binding affinities in the nanomolar range (K_is = 42 nM and 35 nM, respectively), whereas they presented worse affinities for α7 (K_is = 2,500 and 910 nM, respectively) and were almost inactive in α4β2 (K_is >10,000 nM). Thus, *m*-**2.1a** and *m*-**2.1b** displayed interesting selectivity ratios towards muscle-type nAChRs compared to the neuronal subtypes α7 (60- and 26-fold) and α4β2 (>240- and >290-fold).

From *m*-**2.1b**, both the enlargement of the piperidine fragment to give the *meta*-azepane derivative *m*-**2.1c** or the introduction of a double bond to provide the *meta*-1,2,3,6-tetrahydropyridine derivative *m*-**2.1d**, clearly decreased the binding constants in muscle-type nAChR (K_is= 220 and 100 nM, respectively) and also diminished selectivity indexes between muscular and neuronal nAChRs. Finally, asymmetric derivative *m*-**2.14b** resulted poorly active in all nicotinic receptors assayed (Table 2.5), pointing out the importance of the presence of two cationic heads for a successful nAChRs binding.

Functional characterization in muscular nAChRs

To evaluate the effect of *meta*-azocuroniums *m*-**2.1(a-d)**, we expressed embryonic mouse muscular nAChR in *Xenopus laevis* oocytes, which were previously extracted from frogs and transfected with the corresponding messenger RNA (mRNA). The two-electrode voltage-clamp (TEVC) technique was used to measure the nAChR-mediated ionic currents through the plasma membrane. To activate nAChR receptors, the neurotransmitter ACh (2.3-18.4 nL, 50 μM) was delivered on the surface of the oocytes using a nano-injector (Figure 2.13). This small volume of ACh ("puff") was washed from the oocyte vicinity by recirculation of the solution used in the experiment (recording solution) propelled by a pump attached to the chamber (perfusion). Above the oocyte, two LEDs were placed to irradiate the oocyte membrane and to drive the photo-isomerization. These LEDs hereafter referred to as "UV LED" and "blue LED", had their emission spectra adjusted at 335-340 nm and 400-450 nm, respectively. For current recordings, the membrane potential was held at -60 mV. Thus, nAChR opening will result in a downward deflection of the current trace as result of the net inward current mediated by the activation of nAChR.

Under voltage-clamp, oocytes have a basal conductance, yielding a relatively small current in the order of 0.2 μA or lesser. Oocytes displaying higher currents were discarded. An ACh puff was applied after the recirculation pump was turned off. This allowed ACh to reach the membrane, activating the nAChR and resulting in an increase of the membrane conductance. Then, the pump was turned on, washing ACh from the oocyte's vicinity, deactivating nAChR. This was made apparent by the decrease of the inward current amplitude (Figure 2.13). Using this approach, we proceeded to evaluate the functional effect of *meta*-azocuroniums *m*-**2.1(a-d)** and *m*-**2.14b** in muscle-type nAChRs.

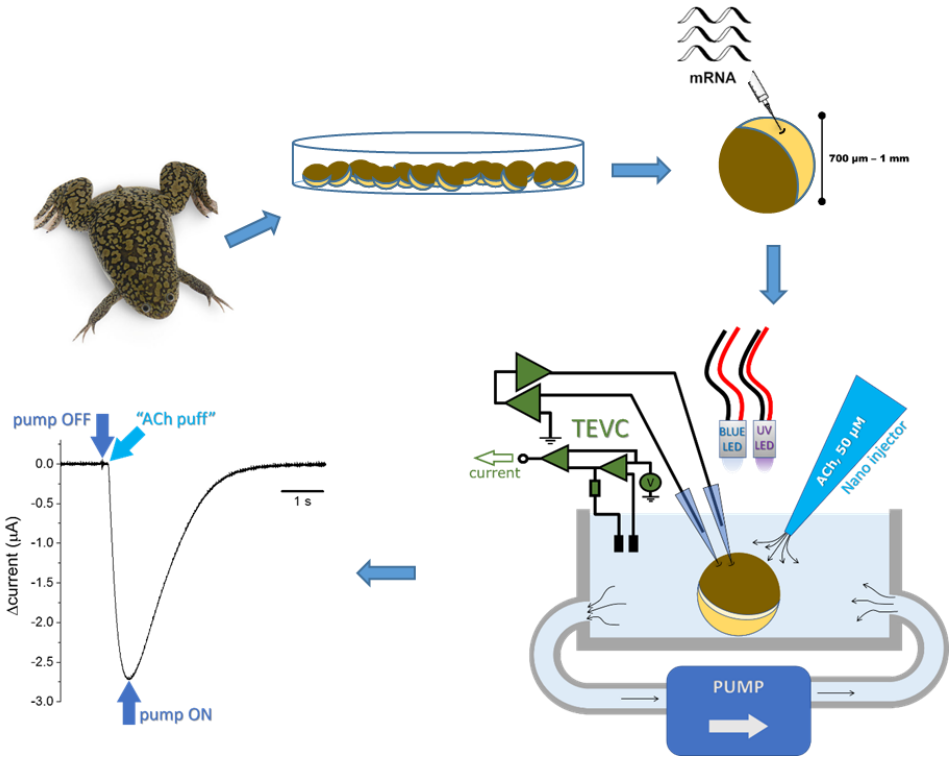

Figure 2.13. Schematic experimental procedure for functional characterization: *Xenopus* oocytes extraction, mRNA injection, measuring ionic currents from oocytes expressing embryonic mouse muscular nAChR using the TEVC technique.

*Pyrrolidine-based azocuronium m-**2.1a** acts as a muscular nAChR agonist*. Firstly, the functional character of pyrrolidine derivative *m-**2.1a*** was evaluated. We observed that exposing the oocytes to thermally relaxed *m*-**2.1a** [(*E*)-isomer] produced the activation of the nAChR current (without ACh). Voltage-clamped oocytes were exposed to *m*-**2.1a** under constant UV irradiation to keep the compound as (*Z*)-isomer (purple area in Figure 2.14A). To test the effect of the (*E*)-isomer, a 5-second pulse of blue radiation was applied while turning off the UV LED (blue area). After 5 seconds, the UV LED was turned back on [(*Z*)-isomer] (purple area). Turning on the blue LED activated nAChRs as a robust inwards current was detected (Figure 2.14A). This was observed at different concentrations of *m*-**2.1a**, ranging from 0.5 to 10 µM. Activation of the current concentration-dependent with an apparent half-maximum binding constant of 4.2 ± 0.4 µM (n = 4) (Figure 2.14B). From

these results we can conclude that (*E*)-*m*-**2.1a** acts as an agonist, in the same way as *m*-bisQ, whereas the (*Z*)-isomer resulted completely inactive, even at high concentration.

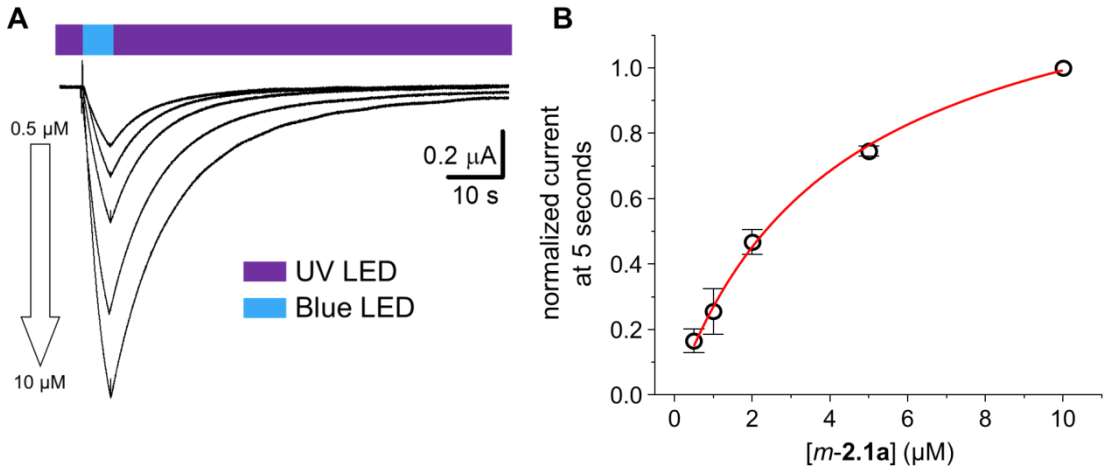

Figure 2.14. Azocuronium *m*-2.1a is a light-dependent agonist of the nAChR. (**A**) Current recordings in the presence of *m*-**2.1a** (0.5-10 µM). Constant irradiation with the UV LED made *m*-**2.1a** inactive as agonist [(*Z*)-isomer]. Inducing the isomerization to the (*E*)-isomer with the blue LED resulted in a robust increase of the nAChR current. This activation was readily reverted by turning back to irradiation with the UV LED. (**B**) Average normalized current measure following 5 seconds of activation showed a clear concentration-dependence for activation.

*Piperidine-derived azocuronium m-**2.1b** inhibits muscular nAChR.* Compound *m*-**2.1b** containing a quaternary piperidine instead of the pyrrolidine present in *m*-**2.1a**, was evaluated subsequently. Initially the same conditions for compound *m*-**2.1a** were used. Unlike the case of *m*-**2.1a**, irradiating the oocytes (both UV and blue light) in the presence of increasing concentrations of only *m*-**2.1b**, did not exert any effect on the receptor; thus, we concluded that *m*-**2.1b** does not act as an agonist.

Afterwards, azocuronium *m*-**2.1b** was evaluated in presence of ACh. Under voltage-clamp, inward currents were observed in oocytes expressing muscle-type nAChR upon application of an ACh puff (control recording, Figure 2.15A, green trace). ACh was immediately washed away by perfusion. Then, adding the *meta*-piperidine azocuronium *m*-**2.1b** (5 μM) (thermally relaxed, (*E*)-isomer) to the recording solution inhibited such response as shown by a decrease in the maximum amplitude of the currents (Figure 2.15A, black trace). This effect of *m*-**2.1b** on current amplitude was partially reverted when oocytes and the surrounding solution were irradiated with the UV LED for 5 min [(*Z*)-isomer, Figure 2.15A, red trace]. This inhibitory effect of (*E*)-*m*-**2.1b** was recovered by irradiating with the blue LED. These observations suggested that *m*-**2.1b** acted on the deactivated (closed) receptors.

To understand whether azocuronium *m*-**2.1b** could also act on the activated (open) receptors, nAChR currents were recorded in the presence of *m*-**2.1b** (0.5 μM). We performed this assay with no perfusion to prolong the activating effect of ACh on the receptor. Firstly, *m*-**2.1b** was held in its (*Z*)-isomer by constant irradiation with the UV LED, then a puff of ACh was applied to open the channel and finally blue LED was changed by UV light [isomerization (*Z*) to (*E*)] (Figure 2.15, red trace). When UV light was kept on, the current reached a peak and slowly decayed for several seconds, this was likely due to receptor desensitization (Figure 2.15, black trace).

Thus, swapping the UV LED for the blue LED radiation [(*E*)-isomer] caused a faster decrease in the current amplitude (Figure 2.15, red trace), indicating *m*-**2.1b** was like affecting receptors in any conformation.

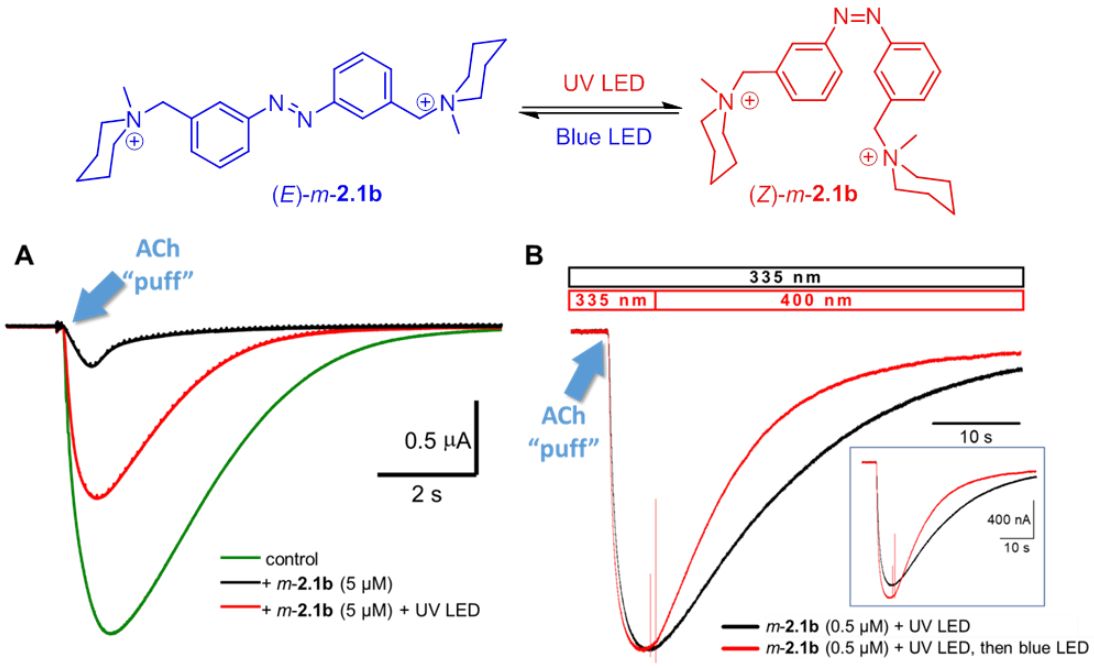

Figure 2.15. Inhibitory effect of azocuronium *m*-**2.1b. (A**) An ACh puff (50 µM, 9.2 nL, 46 nL/s, green trace) evoked currents in oocytes. Adding (*E*)-*m*-**2.1b** (5 µM) decreased the current, resulting from inhibition of the receptors (black trace). Excitation under UV LED partially reverted the effect of *m*-**2.1b** [(*Z*)-isomer, red trace]. (**B**) Normalized recording of *m*-**2.1b** (0.5 µM), applying a puff of ACh. In the first register (black trace) in the presence of (*Z*)-isomer (under UV light), an ACh puff (50 µM, 9.2 nL) evoked a current. The slow deactivation was presumably due to the ACh diffusion and nAChR desensitization (black trace). A second recording was made switching to blue LED 5 s from activation with Ach (red trace). Irradiation with blue LED, decrease the current amplitude at a higher rate. Insert: non-normalized currents.

To further characterize the action of *m*-**2.1b** on nAChR, we evaluate the relationship between drug concentration and receptor inhibition. Thus, the response to ACh in the presence of thermally relaxed *m*-**2.1b** [(*E*)-isomer] was recorded. As the concentration of *m*-**2.1b** increased, the response to ACh puff decreased (Figure 2.16A, left). This inhibitory

effect was partially reverted upon irradiation with UV LED for 5 min [(*Z*)-isomer] (Figure 2.16A, right). To assess the inhibitory effect of *m*-**2.1b** in detail, the recordings were performed in the presence of a range of concentrations of *m*-**2.1b** (0.05-20 μM) thermally relaxed [(*E*)-isomer] (Figure 2.16B, black trace) and under UV radiation [(*Z*)-isomer] (Figure 2.16B, red trace) and the average of current amplitude normalized was plotted with respect to recording in the absence of the drug. The current-*vs*-dose plots were fitted to a simple one-site binding model, yielding apparent half-maximum inhibitory constant (K_i) of 0.46 ± 0.06 μM (n = 24) for the thermally relaxed *m*-**2.1b** (Figure 2.16B, black trace) and 2.6 ± 0.5 μM (n = 24) for the UV-irradiated *m*-**1b** (Figure 2.16B, red trace).

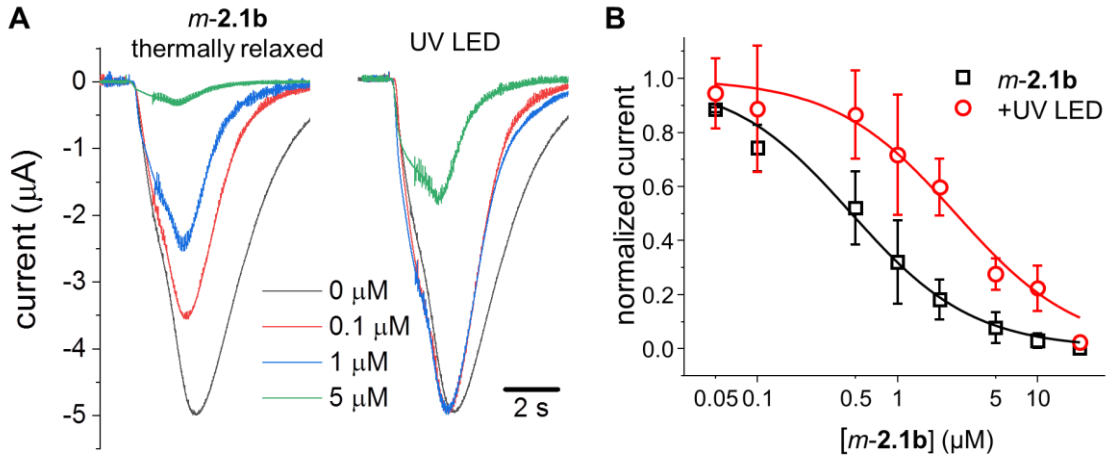

Figure 2.16. Compound *m*-2.1b is a light-dependent antagonist. (**A**) nAChR currents recorded upon application of an ACh puff (50 μM, 9.2 nL) in the absence (green trace) and presence of *m*-**2.1b** (0.1-5 μM) thermally relaxed (left) or while irradiating with the UV LED. (**B**) The maximum amplitude of the currents was normalized with respect to the maximal amplitude observed in the absence of *m*-**2.1b** when it was thermally relaxed (black symbols) or after irradiation under UV LED (red symbols).

We noticed that the variability in current amplitude for the UV-irradiated drugs was slightly higher than for their thermally relaxed counterparts. Although we consider this issue to be

beyond the scope of the present study, we argue that such increase in variability could be attributed to variations in the effective intensities of the UV radiation that reached oocytes. We did not evaluate this issue systematically, yet we notice that it depended on the angle of the incidence of the LED beam and the recording chamber. For this reason, we opted to skip to further analyzing the (*E*)-to-(*Z*) isomerization time course for this study.

Per our initial hypothesis, the hydrophobic character of the molecule's quaternary amine seems to determine the character agonist or antagonist of the molecule. To this point, the pyrrolidine-based *m*-**2.1a** functions as an agonist of nAChR, while the piperidine–based *m*-**2.1b**, behaves as an antagonist. From here, we proceeded to evaluate *m*-**2.1c** which is an azepane-based compound.

*Azepane-derived azocuronium m-**2.1c** behaves as a muscle-type nAChR inhibitor*. Consistent with our initial hypothesis, *m*-**2.1c** which has a larger hydrophobic moiety (azepane fragment) associated to the quaternary amine was able to inhibit ACh-induced current in oocytes expressing nAChR. Fitting the normalized current-*vs*-dose plots to a one-site binding model for the thermally relaxed *m*-**2.1c** [(*E*)-isomer] yielded a K_i of 0.33 ± 0.04 μM (n = 26) (not shown). However, the plot for the UV-irradiated drug [(*Z*)-isomer] was not properly fitted to the model. Therefore, given that nAChR have two distinct binding sites for ACh which are coupled, we chose to fit the plot to a Hill equation. Fitting both curves to this equation yielded a K_i of 0.30 ± 0.02 μM and 2.6 ± 0.5 μM for the (*E*) and (*Z*)-isomer, respectively (Figure 2.17). As expected, the Hill coefficient for the thermally relaxed *m*-**2.1c** was near one, particularly, 0.97 ± 0.05. This suggested that the inhibition by (*E*)-*m*-**2.1c** was not cooperative. In contrast the Hill coefficient for the UV-irradiated *m*-**2.1c** [(*Z*)-isomer] was 0.56 ± 0.07. Accordingly, this strongly suggests that there was negative cooperativity in the binding of the drug. This proposed that there were at least two *m*-**2.1c** molecules bind the nAChR, with the first molecule decreasing the affinity of the receptor for the second one. ACh binding and activation of the muscular nAChR is highly cooperative, where the binding of one ACh leads to an increase in affinity for the second ACh molecule.[187,261] Accordingly, the (*E*)-*m*-**2.1c** (and *m*-**2.1b**) seems to occupy one of the ACh binding sites, blocking further steps in the activation of the receptor. Whereas, the (*Z*)-

m-**2.1c** seems to be competed out by ACh in such a way that the binding of ACh allosterically decreases the affinity of the receptor for *m*-**2.1c**.

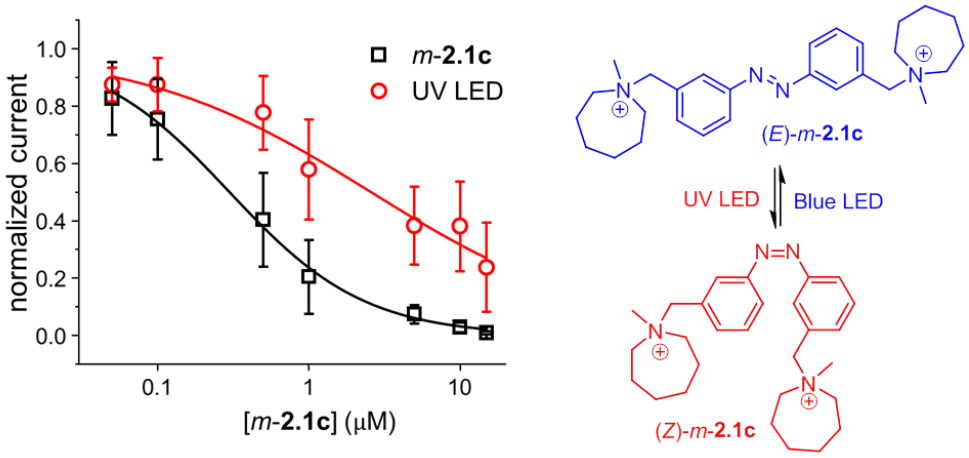

Figure 2.17. Light dependent inhibition of azocuronium *m*-**2.1c.** Inhibition of nAChR current by *m*-**2.1c** when thermally relaxed (black) and under irradiation with UV LED (red). The current-*vs*-[*m*-**2.1c**] plots were fitted to a Hill equation, yielding a K_i of 0.30 ± 0.02 μM and 2.6 ± 0.5 μM, respectively. The corresponding Hill coefficients were 0.97 ± 0.05 and 0.56 ± 0.07 (n = 26).

The rigidity of the N-cycle is important for activity. Next, we explored the effect of the rigidity of the *N*-cycle on the action of the drug. For this, we used *m*-**2.1b** as reference and compared it with *m*-**2.1d**. This latter compound has 1,2,3,6-tetrahydropyridine instead of a piperidine associated to the quaternary ammonium. This *N*-cycle has a lesser flexible, more planar geometry than the one of *m*-**2.1b**. Like this compound, *m*-**2.1d** behaved as an inhibitor of nAChR. Both, the thermally relaxed and UV-irradiated *m*-**2.1d** showed very similar K_i values of 0.84 ± 0.09 μM and 0.88 ± 0.11 μM (n = 15) (Figure 2.18), respectively. In spite of the similarity in the receptor's affinity for both isomers, the efficacy for drug action was isomer-dependent. Per the fitting analysis, the fractions of active receptors at saturating concentration of *m*-**2.1d** were 0.11 ± 0.04 and 0.35 ± 0.03 for

the thermally relaxed and UV-irradiated *m*-**2.1d**, respectively (Figure 2.18). This indicated that this drug was likely operated with a distinct mechanism that the ones described above. Furthermore, it is noteworthy, that Hill coefficients fitted for both isomers were similar, 3.5 ± 1.3 and 2.9 ± 1.1, and higher than those of the drugs tested here. These values indicated the inhibition by *m*-**2.1d** was underlying by a highly cooperative process. Understanding the nature of this process was beyond the scope of this study.

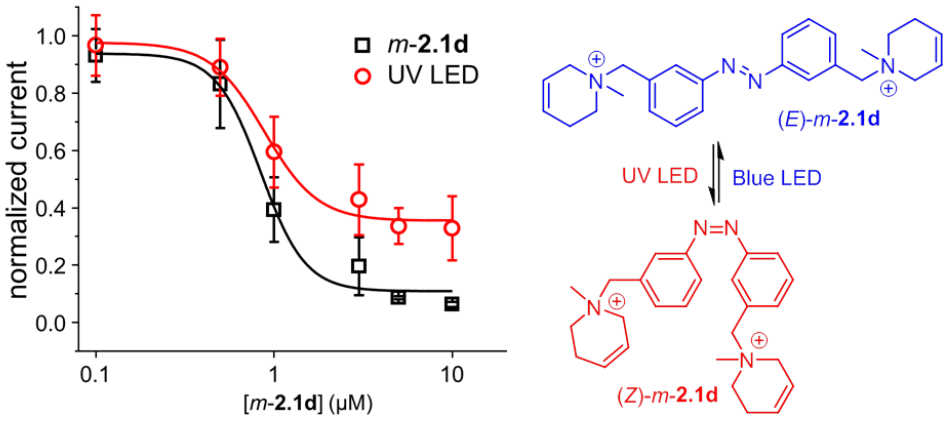

Figure 2.18. Inhibition of nAChR current by thermally relaxed *m*-**2.1d** (black squares) and under irradiation with UV LED (red square). Fitting to a Hill equation, yielded a K_i of 0.84 ± 0.09 μM and 0.88 ± 0.11 μM, respectively. The current fraction at maximum inhibition was 0.11 ± 0.04 and 0.35 ± 0.03 for the thermally relaxed and UV-irradiated *m*-**2.1d**, respectively. The corresponding Hill coefficients were 3.5 ± 1.3 and 2.9 ± 1.1 (n = 15).

The two ammonium groups are required for photo-switchable activity. Thus far, we have established that *m*-**2.1a**, *m*-**2.1b**, and *m*-**2.1c** have different photo-switchable activity in muscular nAChRs. Given that one of the differences between the (*E*)- and (*Z*)-isomers is their geometry, we argue that the photo-switchable character of these compounds emerges from the proximity of the ammonium groups from one another in the (*Z*)-isomer hindering the binding to the receptor. If so, removing one of the ammonium groups should make the molecule able to inhibit the nAChR independently of the geometry. To test this hypothesis, we evaluated the effect of the piperidine-based compound *m*-**2.14b** on the activity of nAChR. Derivative *m*-**2.14b** is like *m*-**2.1b** but lacking one of the *N*-cycle groups. As predicted, the thermally-relaxed *m*-**2.14b** [(*E*)-isomer] was able to inhibit the activation of nAChR by ACh with a K_i of 5.0 ± 0.2 μM, while the UV-irradiated *m*-**2.14b** [(*Z*)-isomer] displayed a K_i of 6.4 ± 0.4 μM (n = 5) (Figure 2.19). Noteworthy, the Hill coefficients were 1.6 ± 0.1 and 1.2 ± 0.1, suggesting a weak positive allosteric interaction for binding. From these observations, we conclude that steric hindrance is a critical factor conferring photo-switchable activity to these azocuroniums.

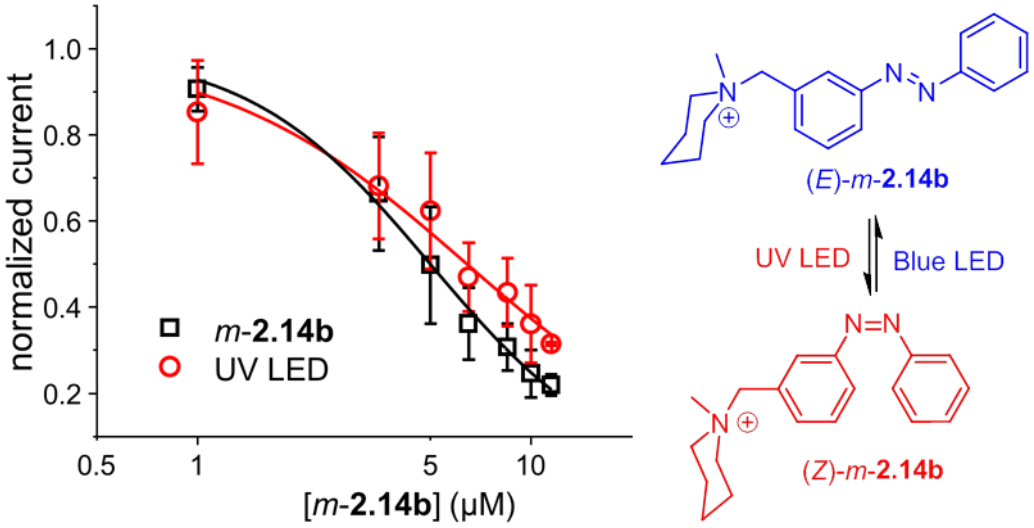

Figure 2.19. Inhibition of nAChR current by thermally relaxed *m*-**2.14b** (black) and under irradiation with UV LED (red). Fitting to a Hill equation, yielded a K_i of 5.0 ± 0.2 μM and 6.4 ± 0.4 μM, respectively. The corresponding Hill coefficients were 1.6 ± 0.1 and 1.2 ± 0.1 (n = 5).

Cell viability assay

Finally, cytotoxicity of azocuroniums salts *m*-**2.1(a-d)**, *p*-**2.1(a,b)** and ***m*-2.14b** was determined in Raw 264.7 macrophages, using the quantitative colorimetric assay MTT.[262,263] Compounds at a concentration of 10 μM were incubated with the cell line at 37 ºC during 24 h and then, the mitochondrial activity of living cells was measured by the absorbance change at 540 nm. All tested compounds showed cell viabilities in the same range than the basal experiment, pointing out that none of them showed any significant cytotoxic effect

CONCLUSIONS

CONCLUSIONS

In this chapter, the design, synthesis and characterization of selective ligands toward muscle nAChRs, azocuroniums, has been accomplished. These compounds are based on the structure of steroid non-depolarizing drugs and bisQ (*meta* substituted azobenzene). They present an azobenzene scaffold bearing diverse *N*-methyl-*N*-carbocyclic quaternary ammonium group, allowing the reversible (*E*)-(*Z*) isomerization by irradiation at 400-450 nm (blue LED) and 335-340 nm (UV LED), respectively. As expected, these azocuroniums showed good solubility in physiological media, negligible toxicity and they would not penetrate into the CNS.

The optimized azo group formation was based on reductive coupling of nitrobenzenes with $LiAlH_4$, in symmetric azobenzenes (**2.2**) and a Mills reaction in the asymmetric derivative *m*-**2.13b.** Quaternization of these compounds gave the azocuroniums salts *m*-**2.1(a-e)**, *p*-**2.1(a,b,e)** and *m*-**2.14b** in good yields.

The ability of (*E*)-azocuroniums to bind muscular and neuronal nAChRs (α7 and α4β2) were determined by radioligand displacement assays. *Meta*-azocuroniums were more potent and selective towards neuromuscular receptors than their *para*-substituted counterparts. Derivatives with smaller cationic heads, namely the *m*-pyrrolidine *m*-**2.1a** and the *m*-piperidine *m*-**2.1b** emerged as the most potent and selective ligands in muscle-type nAChRs, with binding affinities in the nanomolar range (K_is = 42 and 35 nM, respectively). Moreover, they presented worse affinities for α7 (K_is = 2,500 and 910 nM, respectively) and were almost inactive in α4β2 (K_is >10,000 nM), showing thus interesting selectivity. In contrast, azocuroniums with increased volume or rigidity in the *N*-carbocycle (*m*-**2.1c** and *m*-**2.1d**), showed worse binding constants in muscle-type nAChR (K_is = 220 and 100 nM, respectively) with diminished selectivity indexes between muscular and neuronal nAChRs. The asymmetric derivative *m*-**2.14b** with only one cationic head displayed poor radioligand displacement in muscular and neuronal nAChRs, pointed out the importance of the presence of two cationic heads for a successful nAChRs binding.

Meta azocuroniums (*m*-**2.1(a-d)** and *m*-**2.14b**) were functionally characterized by TEVC technique in *Xenopus* oocytes expressing embryonic muscle nAChR. By irradiation with

either blue LED or UV LED while recording electrical currents, in all cases the (*E*)-isomer was found to be more potent than the corresponding (*Z*)-isomer. The volume and hydrophobic character of the ammonium groups seemed to determine whether these azocuroniums would block or activate the receptor. All *meta*-azocuroniums behaved as antagonists of muscular nAChR, with the exception of the smallest pyrrolidine derivative *m*-**2.1a**, which resulted to be a potent agonist in (*E)*-isomer (apparent half-maximum binding constant of 4.2 ± 0.4 μM, thermally stable or under blue light), whereas it was completely inactive in (*Z*)-form (under UV light), as it was proposed in the initial hypothesis. In contrast, the character changed toward antagonist when the *N*-cycle increased its size by one carbon member (piperidine). Thus, *m*-**2.1b** acted as an antagonist in (*E*)-isomer, while in (*Z)*-form resulted less active. The same functional character was observed when either piperidine is increased one carbon (azepane, *m*-**2.1c**) or a double bond was introduced in the ring (1,2,3,6-tetrahydropyridine, *m*-**2.1d**).

m-**2.1a-b** curves were fitted to one binging site plot. In contrast, azocuronium *m*-**2.1c** plot fitted to a Hill equation, where (*E*)-*m*-**2.1c** resulted more active than (*Z*)-*m*-**2.1c**. Moreover, (*E*)-isomer acts by a no cooperative inhibition (Hill coefficient around 1), while (Z)-isomer inhibition was a negative process (Hill coefficient <1). Otherwise, *m*-**2.1d** plot fitted to a Hill equation as well, but in this case, both isomers had similar affinity constants and a highly cooperative inhibition. However, the efficacy for (*Z*)-isomer was minor.

It is expected that the different behavior observed in these new azocuroniums, depending on the nature of the *N*-methyl-*N*-carbocyclic quaternary ammonium group and the wavelength of the irradiated light, could greatly contribute to the biological and electrophysiological study of muscle-type nAChRs.

EXPERIMENTAL SECTION

EXPERIMENTAL SECTION

Synthesis

General procedures

I. Symmetric azo group formation

A $LiAlH_4$ solution in Et_2O (1 or 2 M, 5 equiv) was added dropwise to the stirred mixture of nitrobenzene (1 equiv) in dry Et_2O at -78 ºC. After 15 min, the mixture was allowed to warm to rt and stirred overnight. The excess of hydride was carefully destroyed with H_2O. The crude of reaction was filtered and washed with cold H_2O several times. The mixture was acidified with a solution of citric acid (10%) and the organic layer was separated and evaporated under reduced pressure. The residue was purified by preparative TLC in the corresponding gradient.

II. Methylation of amino moiety.

A solution of the corresponding amino derivative (1 equiv) and CH_3I (1.25 equiv per amine) in anhydrous DMF (1.5 mL/mmol) was heated under mw irradiation at 120 ºC for 12 min. The mixture was evaporated under reduced pressure, dissolved in H_2O and washed with EtOAc. The aqueous layer was lyophilized to give the desired compound. In some cases, it was necessary recrystallizing in MeOH.

Given amines can form salts in the HPLC-MS column, most of them appears in the injection point and in different peaks along the spectrum.

Nitro compounds. Obtained following the general procedure VI of Chapter II without further purification.

1-[(3-Nitrophenyl)methyl]pyrrolidine (*m*-2.3a)[264]

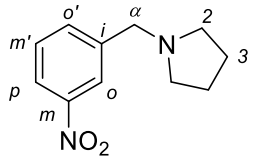

Nitrobenzene *m*-**2.3a** was prepared from 1-(bromomethyl)-3-nitrobenzene (250 mg, 1.16 mmol) and pyrrolidine (105 µL, 1.27 mmol) as brown oil in 96% yield (230 mg, 1.11 mmol). ^{1}H NMR (300 MHz, $CDCl_3$) δ 8.24 – 8.16 (m, 1H, H_o), 8.10 (dt, *J* = 8.2, 1.6 Hz, 1H, H_p), 7.68 (dt, *J* = 7.8, 1.4 Hz, 1H, $H_{o'}$), 7.47 (t, *J* = 7.9 Hz, 1H, $H_{m'}$), 3.70 (s, 2H, H_α), 2.52 (ddd, *J* = 6.7, 4.2, 1.5 Hz, 4H, H_2), 1.84 – 1.75 (m, 4H, H_3). ^{13}C NMR (75 MHz, $CDCl_3$) δ 148.5 (C_m), 142.0 (C_i), 134.9 ($C_{o'}$), 129.2 ($C_{m'}$), 123.7 (C_p), 122.1 (C_o), 59.9 (C_α), 54.3 (C_2), 23.7 (C_3). HPLC-MS (2:30- g.t.5 min) ^{t}R 0.68 min, *m/z* = 207.22 $[M+H]^+$, calcd. for $[C_{11}H_{14}N_2O_2+H]^+$ 207.25.

1-[(4-Nitrophenyl)methyl]pyrrolidine (*p*-2.3a)[265]

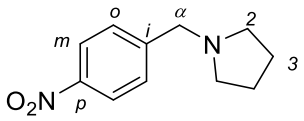

Nitrobenzene *p*-**2.3a** was obtained from 1-(bromomethyl)-4-nitrobenzene (250 mg, 1.16 mmol) and pyrrolidine (105 µL, 1.27 mmol) as a brown oil in 98% yield (234 mg, 1.13 mmol). ^{1}H NMR (300 MHz, $CDCl_3$) δ 8.09 (dd, *J* = 8.8, 2.2 Hz, 2H, H_m), 7.44 (d, *J* = 8.6 Hz, 2H, H_o), 3.63 (s, 2H H_α), 2.44 (dt, *J* = 4.1, 2.2 Hz, 4H, H_2), 1.72 (q, *J* = 3.4 Hz, 4H, H_3). ^{13}C NMR (75 MHz, $CDCl_3$) δ 147.6 (C_p), 147.1 (C_i), 129.4 (C_o), 123.6 (C_m), 60.0 (C_α), 54.3 (C_2), 23.7 (C_3). HPLC-MS (2:30- g.t.5 min) ^{t}R 0.74 min, *m/z* = 207.30 $[M+H]^+$, calcd. for $[C_{11}H_{14}N_2O_2+H]^+$ 207.25.

1-[(3-Nitrophenyl)methyl]piperidine (*m*-2.3b)[266]

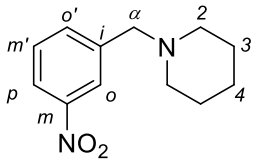

Nitrobenzene *m*-**2.3b** was prepared from 1-(bromomethyl)-3-nitrobenzene (3080 mg, 13.61 mmol) and piperidine (1.4 mL, 14.10 mmol) as an orange oil in 93% (2780 mg, 12.58 mmol). ^{1}H NMR (300 MHz, $CDCl_3$) δ 8.19 (s, 1H, H_o), 8.09 (d, *J* = 7.7 Hz, 1H, H_p), 7.67

(d, J = 7.6 Hz, 1H, $H_{o'}$), 7.46 (t, J = 7.9 Hz, 1H, $H_{m'}$), 3.54 (s, 2H, H_{α}), 2.42 (m, 4H, H_2), 1.59 (p, J = 5.5 Hz, 4H, H_3), 1.49-1.38 (m, 2H, H_4). ^{13}C NMR (75 MHz, $CDCl_3$) δ 148.5 (C_m), 141.6 (C_i), 135.1 ($C_{o'}$), 129.1 ($C_{m'}$), 123.9 (C_o), 122.1 (C_p), 63.0 (C_{α}), 54.7 (C_2), 26.1 (C_3), 24.4 (C_4). HPLC-MS (2:30- g.t.5 min) ^{t}R injection point and 2.30 min, *m/z* = 221.15 $[M+H]^+$, calcd. for $[C_{12}H_{16}N_2O_2+H]^+$ 221.17.

1-[(4-Nitrophenyl)methyl]piperidine (*p*-2.3b)[267]

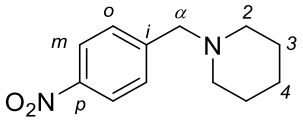

Compound ***p*-2.3b** was prepared from 1-(bromomethyl)-4-nitrobenzene (3000 mg, 13.61 mmol) and piperidine (1.4 mL, 14.09 mmol) as an orange oil in 91% yield (2780 mg, 12.58 mmol). ^{1}H NMR (400 MHz, $CDCl_3$) δ 8.16 (d, J = 8.7 Hz, 2H, H_m), 7.50 (d, J = 8.8 Hz, 2H, H_o), 3.54 (s, 2H, H_{α}), 2.37 (t, J = 5.2 Hz, 4H, H_2), 1.58 (p, J = 5.6 Hz, 4H, H_3), 1.44 (p, J = 6.1 Hz, 2H, H_4). ^{13}C NMR (75 MHz, $CDCl_3$): δ 147.2 (C_i, C_p), 129.6 (C_o), 123.6 (C_m), 63.1 (C_{α}), 54.8 (C_2), 26.1 (C_3), 24.3 (C_4). HPLC-MS (2:30- g.t.5 min) ^{t}R injection point and 2.82 min, *m/z* = 221.05 $[M+H]^+$, calcd. for $[C_{12}H_{16}N_2O_2+H]^+$ 221.17.

1-[(3-Nitrophenyl)methyl]azepane (*m*-2.3c)[268]

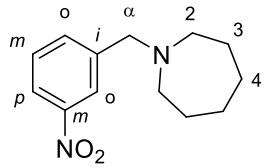

Nitro compound ***m*-2.3c** was prepared from 1-(bromomethyl)-4-nitrobenzene (500 mg, 2.31 mmol) and azepane (286 µL, 2.54 mmol) as a yellow-brown oil in quantitative yield (541 mg, 2.31 mmol). ^{1}H NMR (400 MHz, $CDCl_3$) δ 8.16 (s, 1H, H_o), 8.01 (dd, J = 8.3, 2.3 Hz, 1H, H_p), 7.62 (d, J = 7.6 Hz, 1H, $H_{o'}$), 7.39 (t, J = 7.9 Hz, 1H, $H_{m'}$), 3.65 (s, 2H, H_{α}), 2.56 (t, J = 4.6 Hz, 4H, H_2), 1.56 (s, 8H, H_3, H_4). ^{13}C NMR (101 MHz, $CDCl_3$) δ 148.4 (C_m), 142.7 (C_i), 134.7 ($C_{o'}$), 129.0 ($C_{m'}$), 123.4 (C_p), 121.9 (C_o), 61.9 (C_{α}), 55.7 (C_2), 28.3 (C_3), 27.0 (C_4). HPLC-MS (2:30- g.t.5 min) ^{t}R 4.34 min, *m/z* = 235.20 $[M+H]^+$, calcd. for $[C_{13}H_{18}N_2O_2+H]^+$ 235.30.

1-[(3-Nitrophenyl)methyl]-1,2,3,6-tetrahydropyridine (*m*-2.3d)

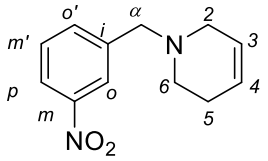

Nitrobenzene ***m*-2.3d** was obtained from 1-(bromomethyl)-4-nitrobenzene (500 mg, 2.31 mmol) and 1,2,3,6-tetrahydropyridine (253 µL, 2.77 mmol) as a yellow-brown solid (504 mg, quantitative yield). Mp: 90 - 93 ºC. ^{1}H NMR (400 MHz, $CDCl_3$) δ 8.22 (bs, 1H, H_o), 8.11 (d, *J* = 8.2 Hz, 1H, H_p), 7.71 (d, *J* = 7.6 Hz, 1H, $H_{o'}$), 7.48 (t, *J* = 7.9 Hz, 1H, $H_{m'}$), 5.80 – 5.74 (m, 1H, H_4), 5.69 – 5.63 (m, 1H, H_3), 3.66 (s, 2H, H□), 3.02 – 2.96 (m, 2H, H_2), 2.57 (t, *J* = 5.7 Hz, 2H, H_6), 2.20 – 2.15 (m, 1H, H_5). ^{13}C NMR (101 MHz, $CDCl_3$) δ 148.5 (C_m), 141.2 (C_i), 135.1 ($C_{o'}$), 129.3 ($C_{m'}$), 125.4 (C_4), 125.2 (C_3), 123.9 (C_o), 122.3 (C_p), 62.1 (C_α), 52.9 (C_2), 49.9 (C_6), 26.2 (C_5). HPLC-MS (2:30- g.t.5 min) ^{t}R 1.47 min, *m/z* = 219.28 $[M+H]^+$, calcd. for $[C_{12}H_{14}N_2O_2+H]^+$ 219.26.

***N*,*N*-dimethyl-1-(3-nitrophenyl)methanamine (*m*-2.3e)**[269,270]

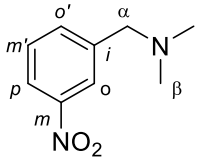

Nitro ***m*-2.3e** was synthetized from 1-(bromomethyl)-3-nitrobenzene (500 mg, 2.31 mmol) and 2 M solution of dimethylamine (1.15 mL, 2.31 mmol) as an orange oil in 93% yield (387 mg, 2.14 mmol). ^{1}H NMR (500 MHz, MeOD) δ 8.19 (t, *J* = 2.0 Hz, 1H, H_o), 8.12 (dt, *J* = 8.0, 1.8 Hz, 1H, H_p), 7.66 (d, *J* = 7.6 Hz, 1H, $H_{o'}$), 7.48 (t, *J* = 7.8 Hz, 1H, $H_{m'}$), 3.51 (s, 2H, H_α), 2.25 (s, 6H, H_β). ^{13}C NMR (75 MHz, $CDCl_3$) δ 1 48.5 (C_m), 141.5(C_i), 135.1 ($C_{o'}$), 129.3 ($C_{m'}$), 123.9 (C_p), 122.3 (C_o), 63.6 (C_α), 45.5 (C_β). HPLC-MS (2:30- g.t.5 min) ^{t}R 0.73 – 0.80 min, *m/z* = 181.01 $[M+H]^+$, calcd. for $[C_9H_{12}N_2O_2+H]^+$ 181.21.

***N*,*N*-dimethyl-1-(4-nitrophenyl)methanamine (*p*-2.3e)**[269,271]

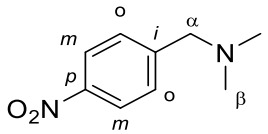

Nitro *p*-**2.3e** was prepared from 1-(bromomethyl)-4-nitrobenzene (2000 mg, 9.25 mmol) and 2 M solution of dimethylamine (4.63 mL, 9.25 mmol) as a brown oil in 80% yield (1320 mg, 7.29 mmol). ^{1}H NMR (300 MHz, $CDCl_3$) δ 8.19 (d, *J* = 8.7 Hz, 2H, H_m), 7.56 (d, *J* = 8.7 Hz, 2H, H_m), 3.59 (s, 2H, H_α), 2.27 (s, 9H, H_β).^{13}C NMR (75 MHz, $CDCl_3$) δ 148.7 (C_p), 146.9 (C_i), 131.4 (C_o), 124.4 (C_m), 64.0 (C_α), 45.4 (C_β). HPLC-MS (2:30- g.t.5 min) ^{t}R 0.73 – 0.80 min and 1.05 min, *m/z* = 181.11 $[M+H]^+$, calcd. for $[C_9H_{12}N_2O_2+H]^+$ 181.21.

Amines. Obtained following the general procedure III of hydrogenation of Chapter I without further purification.

3-(Piperidin-1-ylmethyl)aniline (*m*-2.4b)[264]

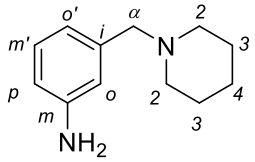

Aniline *m*-**2.4b** was obtained from the nitro *m*-**2.3b** (500 mg, 2.26 mmol) as pale brown crystals in 96% yield (441 mg, 2.18 mmol), mp: 104 - 106 ºC (lit. 96.7 - 97.8 ºC).[264] ^{1}H NMR (300 MHz, MeOD) δ 7.04 (t, *J* = 7.8 Hz, 1H, $H_{m'}$), 6.69 (s, 1H, H_o), 6.67 – 6.53 (m, 2H, $H_{o'}$, H_p), 3.38 (s, 1H, H_α), 2.40 (t, *J* = 5.4 Hz, 4H, H_2), 1.58 (p, *J* = 5.5 Hz, 4H, H_3), 1.45 (q, *J* = 6.0 Hz, 2H, H_4). ^{13}C NMR (75 MHz, MeOD) δ 148.6 (C_m), 138.9 (C_i), 129.9 ($C_{m'}$), 120.8 ($C_{o'}$), 118.0 (C_o), 115.6 (C_p), 65.0 (C_α), 55.3 (C_2), 26.4 (C_3), 25.2 (C_4). HPLC-MS (2:30- g.t.5 min) ^{t}R in the injection point, *m/z* = 191.25 $[M+H]^+$, calcd. for $[C_{12}H_{18}N_2+H]^+$ 191.29.

4-(Piperidin-1-ylmethyl)aniline (*p*-2.4b)[272]

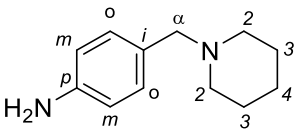

Compound *p*-**2.4b** was prepared from nitro *p*-**2.3b** (1.55 g, 7.04 mmol) as pale yellow crystals (1.34 g, 94%), mp: 80 - 83 ºC (lit. 87 - 88 ºC).[272] ^{1}H NMR (400 MHz, $CDCl_3$) δ 7.09 (d, *J* = 8.3 Hz, 2H, H_o), 6.63 (d, *J* = 8.4 Hz, 2H, H_m), 3.61 (bs, 2H, NH_2), 3.38 (s, 2H, H_α), 2.36 (t, *J* = 5.5 Hz, 4H, H_2), 1.57 (p, *J* = 5.6 Hz, 4H, H_3), 1.42 (p, J=5.6 Hz, 2H, H_4). ^{13}C NMR (75 MHz, $CDCl_3$) δ 145.7 (C_p), 130.9 (C_o), 128.5 (C_i), 115.2 (C_m), 63.8 (C_α), 54.6

(C_2), 26.3 (C_3), 24.8 (C_4). HPLC-MS (2:30- g.t.5 min) ^{t}R 0.60 min, *m/z* = 191.02 $[M+H]^+$, calcd. for $[C_{12}H_{18}N_2+H]^+$ 191.29.

4-((Dimethylamino)methyl)aniline (*p*-2.4e)[273]

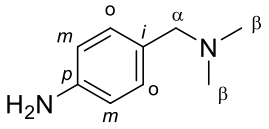

Aniline *p*-**2.4e** was obtained from nitro *p*-**2.3e** (1.30 g, 7.21 mmol) as an orange oil (1.85 g, 12.3 mmol, 93%). ^{1}H NMR (300 MHz, $CDCl_3$) δ 7.04 (d, *J* = 8.3 Hz, 2H, H_o), 6.92 (d, *J* = 8.1 Hz, 2H, H_m), 3.31 (s, 2H, H_α), 2.18 (s, 6H, H_β). ^{13}C NMR (75 MHz, $CDCl_3$) δ 148.2 (C_p), 131.6 (C_o), 127.3 (C_i), 116.1 (C_m), 64.3 (C_α), 44.8 (C_β). HPLC-MS (2:30- g.t.5 min) ^{t}R in the injection point, *m/z* = 151.11 $[M+H]^+$, calcd. for $[C_9H_{14}N_2+H]^+$ 151.23.

Intermediate products

(*Z*)-1,2-Bis(4-(piperidin-1-ylmethyl)phenyl)diazene 1-oxide (*p*-2.5b)

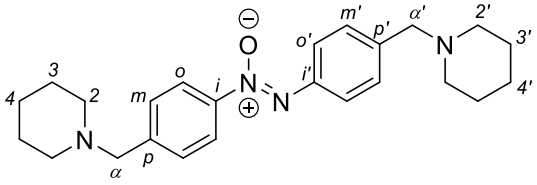

Azoxy *p*-**2.5b** was synthesized from nitro *p*-**2.3b** (2.15 g, 9.76 mmol) following the general procedure of hydrogenation of chapter I. The reaction mixture was stirred for 48 h. After filtration, the crude was purified by a flash chromatography (hexane to EtOAc) to *p*-**2.5b** obtain as brown oil (450 mg, 17%). ^{1}H NMR (500 MHz, MeOD) δ 9.82 (d, *J* = 8.6 Hz, 2H, H_o), 9.71 (d, *J* = 8.6 Hz, 2H, $H_{o'}$), 9.10 (d, *J* = 8.6 Hz, 2H, H_m), 9.04 (d, *J* = 8.6 Hz, 2H, $H_{m'}$), 5.16 (s, 2H, H_α), 5.12 (s, 2H, $H_{\alpha'}$), 2.64 – 2.38 (m, 8H, H_2, $H_{2'}$), 3.18 (p, *J* = 5.5 Hz, 8H, H_3, $H_{3'}$), 3.10 – 2.91 (m, 4H, H_4, $H_{4'}$). ^{13}C NMR (75 MHz, MeOD) δ 148.8 (C_i), 144.6 ($C_{i'}$), 143.3 (C_p), 140.7 ($C_{p'}$), 131.1 (C_m), 131.1 ($C_{m'}$), 126.5 ($C_{o'}$), 123.1 (C_o), 64.3 ($C_{\alpha'}$), 63.9 (C_α), 55.5 (C_2), 55.4 ($C_{2'}$), 26.6 (C_3), 26.6 ($C_{3'}$), 25.2 (C_4, $C_{4'}$). HPLC-MS (2:30- g.t.5 min) ^{t}R in the injection point and 4.23 min, *m/z* = 393.42 $[M+H]^+$, calcd. for $[C_{24}H_{32}N_4O+H]^+$ 393.55.

(*E*,*Z*)-Bis(4-methylphenyl)diazene (*p*-2.10)[243]

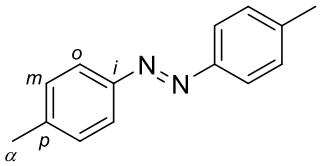

To a stirred solution of aniline *p*-**2.4e** (1.00 g, 9.33 mmol) and pyridine (0.23 mL, 2.80 mmol) in toluene, a solution of CuBr (0.14 g, 0.93 mmol) in toluene was added. The reaction was stirred at 60 ºC overnight. The mixture was evaporated under reduced pressure and the residue was purified by column chromatography (hexane) to afford azo compound *p*-**2.10** as orange crystals (620 mg, 63%), mp: 142 - 145 ºC (lit. 144 - 145 ºC).[274] ^{1}H NMR (500 MHz, MeOD): mixture of isomers (*Z*):(*E*) (0.7:0.3), δ 7.82 (d, *J* = 8.2 Hz, 4H, H_o *E*), 7.38 (d, *J* = 8.1 Hz, 4H, H_m *E*), 7.13 (d, *J* = 8.0 Hz, 4H, H_o *Z*), 6.79 (d, *J* = 8.2 Hz, 4H, H_m *Z*), 2.46 (s, 6H, H_α *E*), 2.32 (s, 6H, H_α *Z*). ^{13}C NMR (101 MHz, MeOD) δ 152.2 (C_i), 142.8 (C_p), 130.8 (C_m *E*), 130.4 (C_m *Z*), 123.7 (C_o *E*), 121.7 (C_o *Z*), 21.4 (C_α *E*), 21.1 (C_α *Z*).[22] HPLC-MS (30:95- g.t.10 min) ^{t}R 6.70 min (*Z*) and 9.66 min (*E*), *m/z* = 211.41 $[M+H]^+$, calcd. for $[C_{14}H_{14}N_2+H]^+$ 211.28.

1-({3-[(*E*,*Z*)-(3-methylphenyl)diazenyl]phenyl}methyl)piperidine (*m*-2.9b)

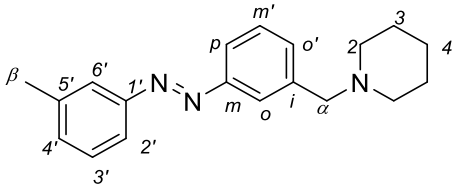

This azo derivative was obtained as a subproduct of the reaction to obtain azo *m*-**2.2b** by hydrogenation with Pd-C as catalysis, as an orange oil (55 mg, %m/m 5). ^{1}H NMR (400 MHz, $CDCl_3$): mixture of isomers (*Z*):(*E*) (0.2:0.8), (only (*E*) has been characterized) δ 7.88 (s, 1H, H_o), 7.82 (dt, *J* = 6.9, 2.1 Hz, 1H, H_p), 7.73 (s, 1H, $H_{6'}$), 7.69 (m, 1H, $H_{2'}$), 7.56 – 7.47 (m, 2H, $H_{m'}$, $H_{o'}$), 7.42 (t, *J* = 7.6 Hz, 1H, $H_{3'}$), 7.34 (d, *J* = 7.4 Hz, 1H, $H_{4'}$), 3.61 (s, 2H, H_α), 2.56 – 2.38 (m, 7H, H_β, H_2), 1.61 (p, *J* = 5.6 Hz, 4H, H_3), 1.53 – 1.41 (m, 2H, H_4). ^{13}C NMR (75 MHz, $CDCl_3$) δ 154.1 (C_m, $C_{1'}$), 140.4 ($C_{5'}$), 140.0 (C_i), 133.5 ($C_{o'}$), 133.0 ($C_{4'}$), 130.1 ($C_{3'}$, $C_{m'}$), 124.8 (C_o), 124.1 ($C_{6'}$), 123.0 (C_p), 121.2 ($C_{2'}$), 64.4 (C_α), 55.4 (C_2), 26.5 (C_3), 25.2 (C_4), 21.4(C_β). HPLC-MS (15:95- g.t.10 min) ^{t}R 6.02 min, *m/z* = 294.38 $[M+H]^+$, calcd. for $[C_{19}H_{23}N_3+H]^+$ 294.41.

(*E*,*Z*)-bis(3-methylphenyl)diazene (*m*-2.10)[243]

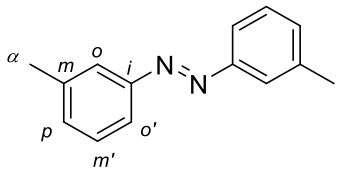

Azobenzene *m*-**2.10** was also obtained as subproduct of the previous reaction as yellow crystals (457 mg, 63%), mp: 53 - 55 ºC (lit. 55 ºC)[275]. ^{1}H NMR (500 MHz, MeOD, δ): mixture of isomers (*Z*):(*E*) (0.1:0.9), 7.72 – 7.64 (m, 4H, H_o, $H_{o'}$ *E*), 7.38 (t, *J* = 7.8 Hz, 2H, $H_{m'}$ *E*), 7.29 (d, *J* = 7.5 Hz, 2H, H_p *E*), 7.09 (t, *J* = 7.7 Hz, 2H, $H_{m'}$ *Z*), 6.96 (d, *J* = 7.5 Hz, 2H, $H_{o'}$ *Z*), 6.71 (s, 2H, H_o *Z*), 6.54 (d, *J* = 7.8 Hz, 2H, H_p *Z*), 2.41 (s, 6H, H_α *E*), 2.21 (s, 6H, H_α *Z*).[22] HPLC-MS (30:95- g.t.10 min) ^{t}R 6.81 min (*Z*) and 9.74 min (*E*), *m/z* = 211.33 $[M+H]^+$, calcd. for $[C_{14}H_{14}N_2+H]^+$ 211.28.

Diazene derivatives *m*-2.2 (a-e), *p*-2.2(a,b) and *m*-2.13b

(*E*,*Z*)-1,2-bis(3-(pyrrolidin-1-ylmethyl)phenyl)diazene (*m*-2.2a)

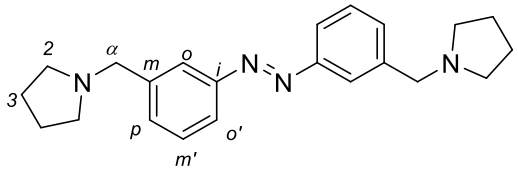

Compound *m*-**2.2a** was prepared from nitro *m*-**2.3a** (159 mg, 0.77 mmol) and a $LiAlH_4$ solution in Et_2O (1.93 mL, 3.85 mmol) following the general procedure I. After a purification by TLC (EtOAc:MeOH, 90:10), a mixture of (*E*):(*Z*)-isomers (80:20) of *m*-**2.3a** was obtained as orange crystals (121 mg, 90%), mp: 62 – 64 ºC. Each isomer is reported separately. ^{1}H NMR (500 MHz, MeOD) δ (*E*) 7.92 (s, 2H, H_o), 7.86 – 7.83 (m, 2H, $H_{o'}$), 7.55 – 7.50 (m, 4H, $H_{m'}$, H_p), 3.76 (s, 4H, H_α), 2.62 – 2.57 (m, 8H, H_2), 1.84 (tt, *J* = 3.8, 1.9 Hz, 8H, H_3). (*Z*) 7.29 (t, *J* = 7.8 Hz, 2H, $H_{m'}$), 7.14 (dt, *J* = 6.6, 1.0 Hz, 2H, H_p), 6.88 (d, *J* = 7.9 Hz, 2H, $H_{o'}$), 6.72 (s, 2H, H_o), 3.49 (s, 4H, H_α), 2.32 – 2.30 (m, 8H, H_2), 1.74 – 1.71 (m, 8H, H_3). ^{13}C NMR (126 MHz, MeOD) δ (*E*) 154.1 (C_i), 140.9 (C_m), 133.2 (C_p), 130.3 ($C_{m'}$), 124.4 (C_o), 123.10 ($C_{o'}$), 61.15 (C_α), 54.98 (C_2), 24.15 (C_3). (*Z*) 155.3 (C_i), 140.3 (C_m), 130.0 (C_p), 129.3 ($C_{m'}$),121.60 (C_o), 121.03 ($C_{o'}$), 60.70 (C_α), 54.62 (C_2), 24.04 (C_3). HPLC-MS (2:30 - g.t.10 min) ^{t}R in the injection and 5.96 min, m/z = 349.47 $[M+H]^+$,

calcd. for $[C_{22}H_{28}N_4+H]^+$ 349.49. HRMS [ESI+] m/z = 348.23092 [M], calcd for $[C_{22}H_{28}N_4]$ 348.2314.

(*E,Z*)-1,2-bis(4-(pyrrolidin-1-ylmethyl)phenyl)diazene (*p*-2.2a)

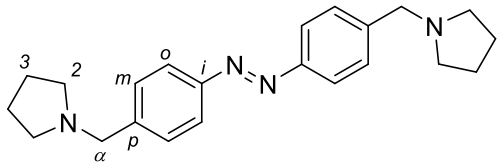

Azobenzene *p*-**2.2a** was prepared from nitro *p*-**2.3a** (138 mg, 0.67 mmol) and a $LiAlH_4$ solution (1.67 mL, 3.34 mmol) following the general procedure I of this chapter. After a preparative TLC using EtOAc:MeOH (95:5) as eluent, compound *p*-**3a** was obtained as brown oil (108 mg, 93%). NMR spectra was recorded in (*E*):(*Z*) 9:1 proportion. Each isomer is reported separately.^{1}H NMR (500 MHz, MeOD) δ (*E*) 8.27 (d, *J* = 8.4 Hz, 4H, H_o), 7.92 (d, *J* = 8.4 Hz, 4H, H_m), , 4.12 (s, 4H, H_α), 2.99 (m, 8H, H_2), 2.25 – 2.20 (m, 8H, H_3). (*Z*) 7.65 (d, *J* = 8.3 Hz, 4H, H_o), 7.21 (d, *J* = 8.3 Hz, 4H, H_m) 3.57 (s, 4H, H_α), 2.51 – 2.47 (m, 8H, H_2), 1.80 – 1.77 (m, 8H, H_3).^{13}C NMR (126 MHz, MeOD) δ (*E*) 153.3 (C_i), 143.0 (C_p), 131.2 (C_m), 123.8 (C_o), 61.06 (C_α), 55.0 (C_2), 24.2 (C_3). HPLC-MS (2:30 - g.t.10 min) ^{t}R in the injection and 6.22 min, m/z = 349.21 $[M+H]^+$, calcd. for $[C_{22}H_{28}N_4+H]^+$ 349.49. HRMS [ESI+] m/z = 348.23157 [M], calcd for $[C_{22}H_{28}N_4]$ 348.2314.

(*E,Z*)-1,2-bis(3-(piperidin-1-ylmethyl)phenyl)diazene (*m*-2.2b)

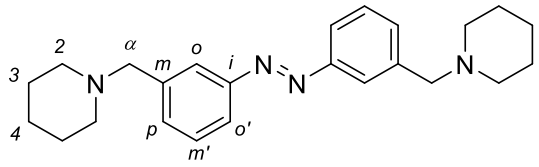

Diazene *m*-**2.2b** was obtained from hydrogenation of nitro *m*-**2.3b** (1.50 g, 6.81 mmol) catalyzed by Pd/C (5%) under H_2 atmosphere for 7 days following the general procedure. After purification by preparative TLC (EtOAc:MeOH 90:10), *m*-**2.2b** was isolated as orange crystals (110 mg, 15%), mp: 89 - 92 ºC. ^{1}H NMR (500 MHz, MeOD): mixture of isomers (*Z*):(*E*) (0.24:0.76), δ 7.91(bs, 2H, H_o *E*), 7.85 (dt, *J* = 7.3, 1.9 Hz, 2H, $H_{o'}$ *E*), 7.52 (t, *J* = 5 Hz, 2H, $H_{m'}$ *E*), 7.50 (dt, *J* = 10, 2 Hz, 2H, H_p *E*), 7.30 (t, *J* = 7.7 Hz, 2H, $H_{m'}$ *Z*), 7.13 (ddd, *J* = 7.6, 1.7, 1.1 Hz, 2H, $H_{o'}$ *Z*), 6.94 (ddd, *J* = 7.9, 2.1, 1.1 Hz, 2H, H_p *Z*), 6.64

(m, 2H, H_o *Z*), 3.63 (s, 4H, H_α *E*), 3.35 (s, 4H, H_α *Z*), 2.49 (s, 8H, H_2), 1.63 (p, *J* = 5.7 Hz, 8H, H_3), 1.50 (m, 4 H, H_4). ^{13}C NMR (126 MHz, MeOD, δ) [(*E*)-isomer]: 154.0 (C_i), 133.7 (C_m), 130.2 ($C_{m'}$), 124.9 (C_p), 123.1 (C_o), 121.8 ($C_{o'}$), 64.4 (C_α), 55.4 (C_2), 26.5 (C_3), 25.2 (C_4). HPLC-MS (2:30 - g.t.10 min) ^{t}R in the injection and 6.22 min, m/z = 377.47 $[M+H]^+$, calcd. for $[C_{24}H_{32}N_4+H]^+$ 377.26.

(*E*,*Z*)-1,2-Bis(4-(piperidin-1-ylmethyl)phenyl)diazene (*p*-2.2b)

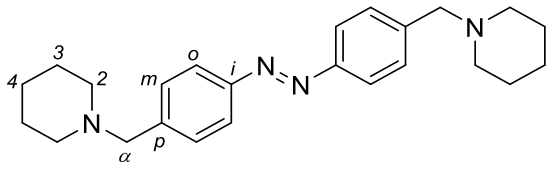

Oxone® (1.94 g, 6.30 mmol) was solved in H_2O and was added to a solution of amino *p*-**2.4b** (1.00 g, 5.26 mmol) in H_2O. The mixture was stirred for 15 min. Then, more amino compound was added (1.00 g, 3.25 mmol), previously solved in H_2O with few drops of AcOH and the reaction was stirred overnight at rt. Then, it was evaporated under reduced pressure, solved in EtOAc, washed with $NaHCO_3$ and brine, dried over $MgSO_4$, filtered, and evaporated under reduced pressure. The residue was purified by column chromatography (hexane) and a preparative TLC (EtOAc:MeOH, 95:5) to afford azo *p*-**2.2b**. Orange crystals (150 mg, 30%), mp: 141 - 142 ºC. ^{1}H NMR (300 MHz, MeOD, δ): mixture of isomers *Z:E* (0.1:0.9), only (*E*)-isomer has been characterized, 7.88 (d, *J* = 8.3 Hz, 4H, H_o), 7.52 (d, *J* = 8.2 Hz, 4H, H_m), 3.58 (s, 4H, H_α), 2.47 (s, 8H, H_2), 1.62 (s, 8H, H_3), 1.48 (s, 4H, H_4).^{13}C NMR (75 MHz, MeOD, δ): 53.3 (C_i), 139.9 (C_p), 131.6 (C_m), 123.6 (C_o), 64.3 (C_α), 55.5 (C_2), 26.6 (C_3), 25.2 (C_4). HPLC-MS (2:30 - g.t.10 min) ^{t}R in the injection and 6.15 min, m/z = 377.18 $[M+H]^+$, calcd. for $[C_{24}H_{32}N_4+H]^+$ 377.26.

(*E*,*Z*)-1,2-bis(3-(azepan-1-ylmethyl)phenyl)diazene (*m*-2.2c)

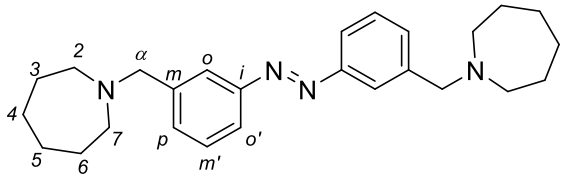

Diazene *m*-**2.2c** was prepared from nitro *m*-**2.3c** (540 mg, 2.31 mmol) and a $LiAlH_4$ solution (11.55 mL, 11.55 mmol) following the general procedure I of this chapter to yield *m*-**2.2c** as an orange oil (283 mg, 61%), after purification by preparative TLC

(EtOAc:MeOH 70:30). ^{1}H NMR (500 MHz, DMSO, δ) 7.84 (s, 2H, H_o), 7.76 (dt, *J* = 7.1, 2.0 Hz, 2H, $H_{o'}$), 7.55 (t, *J* = 7.5 Hz, 2H, $H_{m'}$), 7.53 – 7.50 (m, 2H, H_p), 3.73 (s, 4H, H_α), 2.63 – 2.59 (m, 8H, H_2, H_7), 1.65 – 1.54 (m, 16H, H_3, H_4, H_5, H_6). ^{13}C NMR (126 MHz, DMSO) δ 152.0 (C_i), 141.5 (C_m), 131.5 (C_p), 129.2 ($C_{m'}$), 122.1 (C_o), 121.3 ($C_{o'}$), 61.4 (C_α), 55.0 (C_2, C_7), 27.9 (CH_2), 26.5 (CH_2). HPLC-MS (2:30- g.t.10 min) ^{t}R 9.66 min, *m/z* = 405.38 $[M+H]^+$, calcd. for $[C_{26}H_{36}N_4+H]^+$ 405.60. λ_{max} = 320 nm [(*E*)-isomer]. HRMS [ESI$^+$] m/z = 404.29324 $[M]^+$, calcd for $[C_{26}H_{36}N_4]^+$ 404.2940.

(*E,Z*)-1,2-bis(3-((3,6-dihydropyridin-1(2*H*)-yl)methyl)phenyl)diazene (*m*-2.2d)

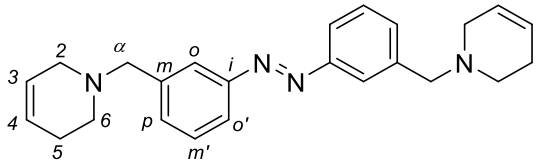

Azobenzene *m*-**2.2d** was prepared from nitro *m*-**2.3d** (300 mg, 1.37 mmol) and a $LiAlH_4$ solution (6.87 mL, 6.87 mmol) following the general procedure I of this chapter. After a preparative TLC (EtOAc:MeOH 95:5) a mixture of (*E*):(*Z*)-isomers (9:1) of diazene *m*-**3d** was obtained as orange crystals (126 mg, 49%), mp: 90 - 93 ºC. Each isomer is reported separately. ^{1}H NMR (500 MHz, $CDCl_3$, δ) (*E*) 7.89 (t, *J* = 1.9 Hz, 2H, H_o), 7.81 (dt, *J* = 7.5, 1.7 Hz, 2H, $H_{o'}$), 7.50 (dt, *J* = 7.6, 1.6 Hz, 2H, H_p), 7.46 (t, *J* = 7.6 Hz, 2H, $H_{m'}$), 5.77 (dtt, *J* = 9.4, 3.7, 2.1 Hz, 2H, H_4), 5.68 (dtt, *J* = 10.1, 3.3, 1.8 Hz, 2H, H_3), 3.68 (s, 4H, H_α), 3.02 (p, *J* = 2.8 Hz, 4H, H_2), 2.61 (t, *J* = 5.7 Hz, 4H, H_6), 2.19 (tp, *J* = 5.7, 2.8 Hz, 4H, H_5). (*Z*) δ 7.21 (t, *J* = 7.7 Hz, 2H, $H_{m'}$), 7.12 (d, *J* = 7.7 Hz, 2H, H_p), 6.83 (dt, *J* = 7.9, 1.5 Hz, 2H, $H_{o'}$), 6.72 (s, 2H, H_o), 5.73 – 5.70 (m, 2H, =CH) 5.58 (dtd, *J* = 10.0, 3.4, 1.7 Hz, 2H, =CH), 3.42 (s, 4H, H_α), 2.75 (dt, *J* = 5.3, 2.6 Hz, 4H, H_2), 2.35 (t, *J* = 5.7 Hz, 4H, H_6), 2.06 (dt, *J* = 5.7, 2.8 Hz, 4H, H_5). ^{13}C NMR (126 MHz, $CDCl_3$, δ) (*E*) 152.9 (C_i), 139.8 (C_m), 131.8 (C_p), 129.1 ($C_{m'}$), 125.5 (C_4), 125.4 (C_3), 123.6 (C_o), 121.8 ($C_{o'}$), 62.8 (C_α), 53.0 (C_2), 49.9 (C_6), 26.3 (C_5). (*Z*) 154.7 (C_i), 139.3 (C_m), 128.7 ($C_{m'}$), 128.0 (C_p), 125.3 (2 =CH), 120.7 (C_o), 119.8 ($C_{o'}$), 62.5 (C_α), 52.6 (C_2), 49.6 (C_6), 26.2 (C_5). HPLC-MS (2:30- g.t.10 min) ^{t}R 7.63 min, *m/z* = 373.28 $[M+H]^+$, calcd. for $[C_{24}H_{28}N_4+H]^+$ 373.52. λ_{max} = 319 nm [(*E*)-isomer]. HRMS [ESI$^+$] m/z = 372.23053 $[M]^+$, calcd for $[C_{24}H_{28}N_4]^+$ 372.2314.

(*E*,*Z*)-1,1'-(Diazene-1,2-diylbis(3,1-phenylene))bis(*N*,*N*-dimethylmethanamine) (*m*-2.2e)[276]

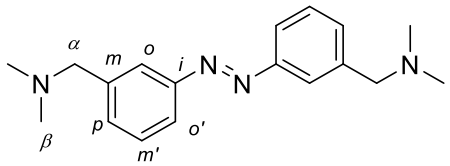

Azo derivative *m*-**2.2e** was synthetized from nitro *m*-**2.3e** (340 mg, 1.89 mmol) in dry Et_2O and $LiAlH_4$ (9.43 mL, 9.43 mmol) following the general procedure, orange oil (257 mg, 92%). ^{1}H NMR (300 MHz, MeOD, δ): mixture of isomers (*Z*):(*E*) (0.2:0.8), 7.90 (s, 2H, H_o *E*), 7.86 (d, *J* = 7.4 Hz, 2H, $H_{o'}$ *E*), 7.54 (t, *J* = 7.5 Hz, 2H, $H_{m'}$ *E*), 7.49 (d, *J* = 7.5 Hz, 2H, H_p *E*), 7.09 (t, *J* = 7.8 Hz, 2H, $H_{m'}$ *Z*), 6.78 (s, 2H, H_o *Z*), 6.75 (dd, *J* = 2.4, 1.0 Hz, 2H, $H_{o'}$ *Z*), 6.66 (d, *J* = 7.4 Hz, 2H, H_p *Z*), 3.36 (s, 4H, H_β), 2.19 (s, 12H, H_α). ^{13}C NMR (126 MHz, MeOD, δ): 154.1 (C_i), 140.2 (C_m), 133.5 ($C_{m'}$), 130.3 (C_p), 124.7 (C_o), 123.3 ($C_{o'}$), 64.5 (C_α), 45.2 (C_β). HPLC-MS (2:30 - g.t.10 min) ^{t}R in the injection both isomers, m/z = 297.39 $[M+H]^+$, calcd. for $[C_{18}H_{24}N_4+H]^+$ 297.42.

***N*,*N'*-{(*E*,*Z*)-Diazenediylbis[(4,1-phenylene)methylene]}bis(*N*-methylmethanamine) (*p*-2.2e)**

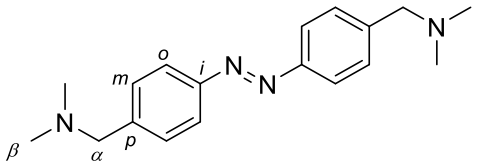

Azo derivative *p*-**2.2e** was synthetized from nitro *p*-**2.3e** (400 mg, 2.22 mmol) and $LiAlH_4$ (11.09 mL, 2.77 mmol) following the general procedure I of this chapter. Orange crystals (211 mg, 64%), mp: decomposes before melting. NMR spectra was recorded in (*E*)*:*(*Z*) 8:2 proportion. Each isomer is reported separately. ^{1}H NMR (500 MHz, MeOD, δ): (*E*) 7.90 (d, *J* = 8.4 Hz, 4H, H_o), 7.51 (d, *J* = 8.7 Hz, 4H, H_m), 3.57 (s, 4H, H_α), 2.29 (s, 12H, H_β). (*Z*) 7.24 (d, *J* = 8.6 Hz, 4H, H_o), 6.83 (d, *J* = 8.4 Hz, 4H, H_m), 3.40 (s, 4H, H_α), 2.18 (s, 12H, H_β). ^{13}C NMR (126 MHz, MeOD, δ): (*E*) 153.4 (C_i), 142.4 (C_p), 131.5 (C_m), 123.8 (C_o), 64.5 (C_α), 45.3 (C_β). (*Z*) 153.4 (C_i), 142.4 (C_p), 131.1 (C_m), 121.6 (C_o), 64.2 (C_α), 45.1 (C_β). HPLC-MS (2:30- g.t.10 min) ^{t}R in the injection both isomers, m/z = 297.38 $[M+H]^+$, calcd. for $[C_{18}H_{24}N_4+H]^+$ 297.42. HRMS [ESI+] m/z = 296.20084 [M] calcs for $[C_{18}H_{24}N_4]$ 296.2001.

(*E*)-1-(3-(Phenyldiazenyl)benzyl)piperidine (*m*-2.13b)[250]

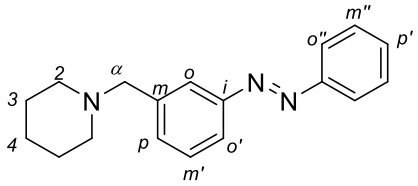

Commercial nitrosobenzene (100 mg, 0.93 mmol) was solved in anhydrous toluene (5 mL), amine *m*-**2.4b** (178 mg, 0.93 mmol) and AcOH (21 µL, 3.75 mmol) were added orderly under N_2. The reaction was stirred at 60 ºC overnight. The mixture was extracted with EtOAc, washed with water and brine, dried with $MgSO_4$, filtered and concentrated under reduced pressure. The residue was purified by reverse phase flash chromatography (H_2O to ACN). After lyophilization of the appropriate fractions diazene *m*-**4b** was obtained as orange oil in 93% yield (241 mg, 0.86 mmol). ^{1}H NMR (500 MHz, DMSO, δ): 7.90 (dd, *J* = 6.6, 1.5 Hz, 2H, $H_{m''}$), 7.80 (t, *J* = 1.5 Hz, 1H, H_o), 7.78 (dt, *J* = 7.7, 1.8 Hz, 1H, $H_{o'}$), 7.63 – 7.57 (m, 3H, $H_{o''}$, $H_{p'}$), 7.54 (t, *J* = 7.6 Hz, 1H, $H_{m'}$), 7.49 (dt, *J* = 7.6, 1.4 Hz, 1H, H_p), 3.53 (s, 2H, $H_α$), 2.39 – 2.31 (m, 4H, H_2, H_6), 1.50 (p, *J* = 5.6 Hz, 4H, H_3, H_5), 1.40 (q, *J* = 6.0 Hz, 2H, H_4).^{13}C NMR (126 MHz, DMSO, δ) 152.0 ($C_{i'}$), 151.9 (C_i), 140.4 (C_m), 131.9 (C_p), 131.5 ($C_{p'}$), 129.5 ($C_{o''}$), 129.3 ($C_{m'}$), 122.5 ($C_{m''}$), 122.4 (C_o), 121.5 ($C_{o'}$), 62.4 ($C_α$), 53.9 (C_2), 25.6 (C_3), 24.0 (C_4). HPLC-MS (15:95- g.t.10 min) ^{t}R 1.44 min, *m/z* = 280.28 $[M+H]^+$ (*Z*)-isomer; 4.97 min, *m/z* = 280.21 $[M+H]^+$ (*E*)-isomer, calcd. for $[C_{18}H_{21}N_3+H]^+$ 280.39. $λ_{max}$ = 285, 425 nm [(*Z*)-isomer]; 319 nm [(*E*)-isomer]. HRMS [ESI$^+$] m/z = 279.17353 $[M]^+$, calcd for $[C_{18}H_{21}N_3]^+$ 279.17355.

Azocuronium salts *m*-2.1(a-e), *p*-2.1(a,b) and *m*-2.14b

Salts with two positive charges were analyzed by HPLC-MS, however all of them appeared in the injection point, although different gradients were tried. Thus, the mass was verified and the characteristic UV spectrum of azobenzene. As expected, iodide ion ionized in negative mode. All of them were obtained following the general procedure II of this chapter.

(*E*,*Z*)-1,1'-((Diazene-1,2-diylbis(3,1-phenylene))bis(methylene))bis(1-methylpyrrolidin-1-ium) iodide (*m*-2.1a)

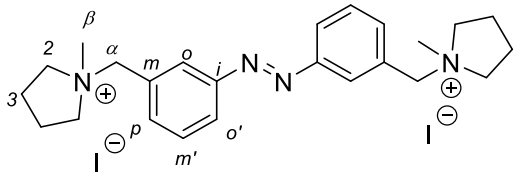

Azocuronium ***m*-2.1a** was obtained from azobenzene ***m*-2.2a** (50 mg, 0.14 mmol) and CH_3I (26 μL, 0.40 mmol) as orange solid (52 mg, 99%), mp: 53 - 55 ºC. ^{1}H NMR (500 MHz, MeOD, δ): mixture of isomers (*Z*):(*E*) (0.15:0.85), only (*E*)-isomer was characterized. 8.24 (d, *J* = 1.6 Hz, 2H, H_o), 8.13 (dd, *J* = 7.9, 1.6 Hz, 2H, $H_{o'}$), 7.81 (dd, *J* = 7.6, 1.5 Hz, 2H, H_p), 7.75 (t, *J* = 7.7 Hz, 2H, $H_{m'}$), 4.77 (s, 4H, H_α), 3.79 (dt, *J* = 12.5, 7.0 Hz, 4H, H_{2eq}), 3.60 – 3.52 (m, 4H, H_{2ax}), 3.09 (s, 6H, H_β), 2.39 – 2.24 (m, 8H, H_3). ^{13}C NMR (126 MHz, MeOD, δ) 154.2 (C_i), 136.5 (C_p), 131.5 ($C_{m'}$), 131.3 (C_m), 128.2 (C_o), 125.8 ($C_{o'}$), 67.4 (C_α), 65.0 (C_2), 48.8 (C_β), 22.3 (C_3). λ_{max} = 319 nm [(*E*)-isomer]. HRMS [ESI+] m/z = 378.27912 $[M]^{+2}$, calcd for $[C_{24}H_{34}N_4]^{+2}$ 378.27835.

(*E*,*Z*)-1,1'-((Diazene-1,2-diylbis(4,1-phenylene))bis(methylene))bis(1-methylpyrrolidin-1-ium) iodide (*p*-2.1a)

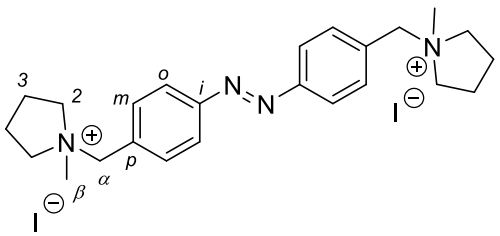

Azocuronium *p*-**2.1a** was synthetized from azobenzene *p*-**2.2a** (50 mg, 0.14 mmol) and CH_3I (26 μL, 0.40 mmol) as an orange solid (50 mg, 95%), mp: 153 – 156 ºC. ^{1}H NMR (400 MHz, MeOD, δ) (*E*) 8.08 (d, *J* = 8.4 Hz, 4H, H_o), 7.85 (d, *J* = 8.4 Hz, 4H, H_m), 4.74 (s, 4H, H_α), 3.81 – 3.70 (m, 4H, H_{2eq}), 3.60 – 3.51 (m, 4H, H_{2ax}), 3.07 (s, 6H, H_β), 2.38 – 2.24 (m, 8H, H_3). ^{13}C NMR (101 MHz, MeOD, δ) 154.8 (C_i), 134.9 (C_m), 133.1 (C_p), 124.6 (C_o), 67.1 (C_α), 64.9 (C_2), 48.6 (C_β), 22.3 (C_3). λ_{max} = 322 nm [(*E*)-isomer]. HRMS [ESI+] m/z = 378.27817 $[M]^{+2}$, calcd for $[C_{24}H_{34}N_4]^{+2}$ 378.27835.

(*E*,*Z*)-1,1'-((Diazene-1,2-diylbis(3,1-phenylene))bis(methylene))bis(1-methylpiperidin-1-ium) iodide (*m*-2.1b)

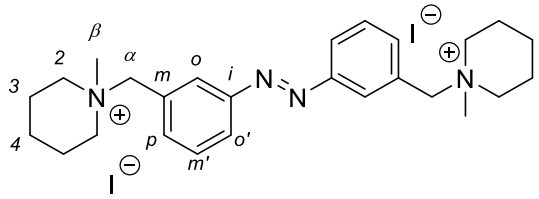

Salt *m*-**2.1b** was synthetized from *m*-**2.2b** (45 mg, 0.12 mmol) and CH_3I (17.9 μL, 0.49 mmol) as an orange solid (77 mg, 97%), mp: 174 - 176 ºC. NMR spectra was recorded in (*E*):(*Z*) 85:15 proportion. Each isomer is reported separately. ^{1}H NMR (500 MHz, MeOD, δ): (*E*) 8.24 (bs, 2H, H_o), 8.14 (dt, *J* = 7.6, 1.7 Hz, 2H, $H_{o'}$), 7.79 (dt, *J* = 7.7, 1.6 Hz, 2H, H_p), 7.75 (t, *J* = 7.6 Hz, 2H, $H_{m'}$), 4.78 (s, 4H, H_α), 3.55 (m, 4H, H_{2eq}), 3.50 – 3.42 (m, 4H, H_{2ax}), 3.10 (s, 6H, H_β), 2.08 – 1.93 (m, 8H, H_3), 1.87 – 1.76 (m, 2H, H_{4eq}), 1.76 – 1.61 (m, 2H, H_{4ax}). (*Z*) 7.57 (d, *J* = 7.8 Hz, 2H, $H_{m'}$), 7.45 – 7.43 (d, *J* = 7.8 Hz, 2H, H_p), 7.36 (d, *J* = 8.1 Hz, 2H, $H_{o'}$), 6.93 (s, 2H, H_o), 4.39 (s, 4H, H_α), 3.14 (t, *J* = 5.8 Hz, 8H, H_2), 2.78 (s, 6H, H_β), 1.89 – 1.82 (m, 8H, H_3), 1.77 – 1.69 (m, 2H, H_{4eq}), 1.57 – 1.46 (m, 2H, H_{4ax}). ^{13}C NMR (126 MHz, MeOD, δ): (*E*) 154.0 (C_i), 137.1 (C_p), 131.4 ($C_{m'}$), 130.0 (C_m), 129.0 (C_o), 125.8 ($C_{o'}$), 68.6 (C_α), 62.1 (C_2), 47.2 (C_β), 22.2 (C_4), 21.1 (C_3). (*Z*) 152.5 (C_i), 132.6 (C_p), 130.1 ($C_{m'}$), 127.8 (C_m), 123.8 (C_o), 123.7 ($C_{o'}$), 67.0 (C_α), 60.6 (C_2), 46.1 (C_β), 30.1, 20.4 (C_4), 19.4 (C_3). λ_{max} = 320 nm (*E*-isomer). HRMS [ESI+] m/z = 406.31014 $[M]^{+2}$, calcd for $[C_{26}H_{38}N_4]^{+2}$ 406.30965.

(*E*,*Z*)-1,1'-((Diazene-1,2-diylbis(4,1-phenylene))bis(methylene))bis(1-methylpiperidin-1-ium) iodide (*p*-2.1b)

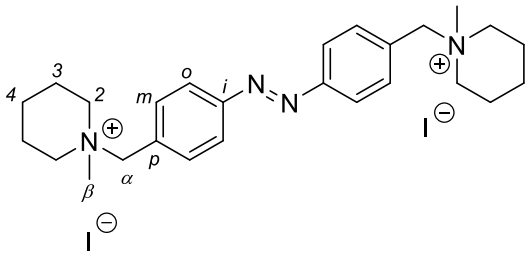

Azocuronium *p*-**2.1b** was prepared from *p*-**2.2b** (31 mg, 0.08 mmol) and CH_3I (14.35 μL, 0.23 mmol) in DMF as an orange solid (50 mg, 95%), mp: 291 - 231 ºC. ^{1}H NMR (300 MHz, MeOD, δ): mixture of isomers *Z*-*E* (0.1:0.9), only (*E*)-isomer was characterized. 8.09 (d, *J* = 8.4 Hz, 4H, H_o), 7.82 (d, *J* = 8.4 Hz, 4H, H_m), 4.72 (s, 4H, H_α), 3.58 – 3.47 (m, 4H, $H_{2\,eq}$), 3.46 – 3.36 (m, 4H, H_{2ax}), 3.08 (s, 6H, H_β), 2.08 – 1.94 (m, 8H, H_3), 1.87 – 1.75 (m, 2H, $H_{4\,eq}$), 1.75 – 1.64 (m, 2H, $H_{4\,ax}$). ^{13}C NMR (75 MHz, MeOD, δ): 54.8 (C_i), 135.5 (C_o), 131.8 (C_p), 124.5 (C_m), 68.4 (C_α), 62.2 (C_2), 55.9 (C_β), 22.2 (C_4), 21.1 (C_3). λ_{max} = 321 nm [(*E*)-isomer]. HRMS [ESI+] m/z = 406.30984 $[M]^{+2}$, calcd for $[C_{26}H_{38}N_4]^{+2}$ 406.30965.

(*E*,*Z*)-1,1'-((Diazene-1,2-diylbis(3,1-phenylene))bis(methylene))bis(1-methylazepan-1-ium) iodide (*m*-2.1c)

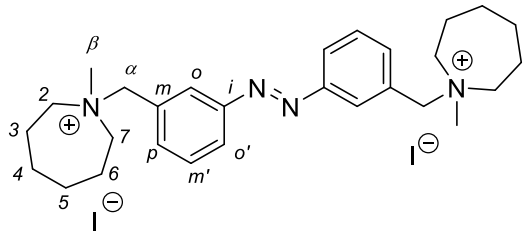

Azocuronium *m*-**2.1c** was obtained from *m*-**2.2c** (80 mg, 0.20 mmol) as yellow-orange crystals (115 mg, 0.17 mmol). Mp: 145 ºC (decompose) NMR spectra was recorded in (*E*):(*Z*) 8:2 proportion. Each isomer is reported separately. ^{1}H NMR (500 MHz, D_2O, δ) (*E*) 8.09 – 8.06 (m, 2H, $H_{o'}$), 8.06 (bs, 2H, H_o), 7.76 – 7.73 (m, 4H, $H_{m'}$, H_p), 4.63 (s, 4H, H_α), 3.62 (dt, *J* = 14.2, 5.0 Hz, 4H, H_{2eq}, H_{7eq}), 3.39 (dt, *J* = 14.0, 4.8 Hz, 4H, H_{2ax}, H_{7ax}), 3.03 (s, 6H, CH_3), 1.99 – 1.90 (m, 8H, H_3, H_6), 1.75 – 1.68 (m, 8H, H_4, H_5). (*Z*) δ 7.55 (t, *J* = 7.9 Hz, 2H, $H_{m'}$), 7.43 (d, *J* = 7.7 Hz, 2H, H_p), 7.30 (d, *J* = 8.0, 1.9 Hz, 2H, $H_{o'}$), 6.97 (s, 2H, H_o), 4.36 (s, 4H, H_α), 3.30 (dt, *J* = 14.0, 5.0 Hz, 4H, H_{2eq}, H_{7eq}), 3.16 (dt, *J* = 14.0, 4.8 Hz, 4H, H_{2ax}, H_{7ax}), 2.76 (s, 6H, CH_3), 1.85 – 1.78 (m, 8H, H_3, H_6), 1.67 – 1.61 (m, 8H, H_4,

H_5). ^{13}C NMR (126 MHz, D_2O, δ) (*E*) 152.9 (C_i), 136.7 (C_p), 131.0 ($C_{m'}$), 129.5 (C_m), 127.6 (C_o), 125.1 ($C_{o'}$), 68.5 (C_α), 64.7 (C_2, C_7), 50.6 (CH_3), 28.0 (C_4, C_5), 21.8 (C_3, C_6). (*Z*) δ 153.3 (C_i), 133.3 (C_p), 130.8 ($C_{m'}$), 129.5 (C_m), 124.7 (C_o), 124.2 ($C_{o'}$), 64.6 (C_2, C_7), 50.3 (CH_3), 27.9 (C_4, C_5), 21.7 (C_3, C_6). λ_{max} = 319 nm [(*E*)-isomer]. HRMS [ESI^+] m/z = 434.34076 $[M]^+$, calcd for $[C_{28}H_{42}N_4]^{2+}$ 434.34095.

(*E*,*Z*)-1,1'-((Diazene-1,2-diylbis(3,1-phenylene))bis(methylene))bis(1-methyl-1,2,3,6-tetrahydropyridin-1-ium) iodide (*m*-2.1d)

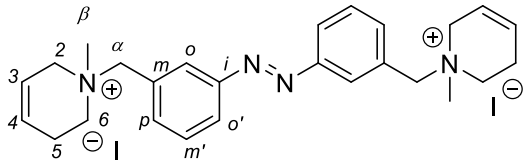

Azocuronium ***m*-2.1d** was obtained from azo ***m*-2.2c** (60 mg, 0.16 mmol) as yellow-orange solid (82 mg, 78%). Mp: 200 ºC (decompose). NMR spectra was recorded in (*E*):(*Z*) 8:2 proportion. Each isomer is reported separately. ^1H NMR (500 MHz, D_2O, δ) 8.12 – 8.09 (m, 2H, H_o), 8.08 (bs, 2H, $H_{o'}$), 7.79 – 7.76 (m, 4H, H_p, $H_{m'}$), 6.10 (d, *J* = 10.2 Hz, 2H, H_4), 5.78 (d, *J* = 10.0 Hz, 2H, H_3), 4.75 (d, *J* = 13.2 Hz, 4H, $1H_\alpha$), 4.63 (d, *J* = 13.2 Hz, 2H, $1H_\alpha$), 4.10 (d, *J* = 16.5 Hz, 2H, H_{2eq}), 3.78 (d, *J* = 16.4 Hz, 2H, H_{2ax}), 3.67 – 3.56 (m, 4H, H_6), 3.09 (s, 6H, H_β), 2.65 – 2.56 (m, 4H, H_5). (*Z*) 7.60 (t, *J* = 7.9 Hz, 2H, $H_{m'}$), 7.46 (d, *J* = 7.8 Hz, 2H, H_p), 7.39 (d, *J* = 8.2 Hz, 2H, $H_{o'}$), 6.94 (s, 2H, H_o), 6.03 (d, *J* = 10.4 Hz, 2H, H_4), 5.66 (d, *J* = 10.6 Hz, 2H, H_3), 4.47 (d, *J* = 13.2 Hz, 2H, $1H_\alpha$), 4.37 (d, *J* = 13.1 Hz, 2H, $1H_\alpha$), 3.71 (d, *J* = 16.5 Hz, 2H, H_{2eq}), 3.53 (d, *J* = 16.5 Hz, 2H, H_{2ax}), 3.39 – 3.32 (m, 2H, H_6), 3.22 (dt, *J* = 12.9, 6.2 Hz, 2H, H_6), 2.83 (s, 6H, H_β), 2.48 (s, 4H, H_5) ^{13}C NMR (126 MHz, D_2O, δ) (*E*) 153.0 (C_i), 136.7 (C_p), 131.0 ($C_{m'}$), 128.8 (C_m), 127.6 (C_o), 125.6 (C_4), 125.3 ($C_{o'}$), 118.9 (C_3), 67.5 (C_α), 58.7 (C_2), 57.8 (C_6), 47.4 (C_β), 21.6 (C_5). (*Z*) 153.3 (C_i), 133.3 (C_p), 130.9 ($C_{m'}$), 128.3 (C_m), 125.5 (C_4), 124.6 ($C_{o'}$), 124.5 (C_o), 118.6 (C_3), 67.2 (C_α), 58.4 (C_2), 57.4 (C_6), 47.2 (C_β), 21.5 (C_5). λ_{max} = 321 nm [(*E*)isomer]. HRMS [ESI^+] m/z = 402.27886 $[M]^{2+}$, calcd for $[C_{26}H_{34}N_4]^{2+}$ 402.27835.

(*E,Z*)-1,1'-(Diazene-1,2-diylbis(3,1-phenylene))bis(*N,N,N*-trimethylmethanaminium) iodide (bisQ, *m*-2.1e)[218]

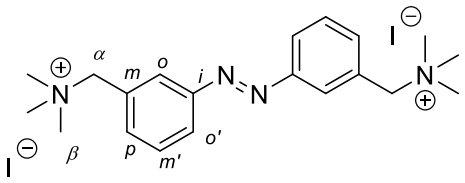

m-**2.1e** was obtained from *m*-**2.2e** (50 mg, 0.17 mmol) and CH_3I (30.5 μL, 0.49 mmol) as orange crystals (84 mg, 85%), mp: 191 ºC (decompose). NMR spectra was recorded in (*E*):(*Z*) 0.1:0.9 proportion. Each isomer is reported separately ^{1}H NMR (500 MHz, MeOD, δ): (*E*) 8.25 (s, 2H, H_o), 8.16 (dt, *J* = 7.6, 1.7 Hz, 2H, $H_{o'}$), 7.80 (tt, *J* = 10 Hz, 1.8 Hz, 2H, H_p), 7.76 (t, *J* = 7.6 Hz, 2H, $H_{m'}$), 4.75 (s, 4H, H_α), 3.22 (s, 18H, H_β). (*Z*) 7.30 (td, *J* = 7.7, 0.7 Hz, 2H, $H_{m'}$), 7.02 – 6.99 (m, 2H, H_o), 7.00 – 6.97 (m, 2H, $H_{o'}$), 6.89 (d, *J* = 7.6 Hz, 2H, H_p), 4.46 (s, 4H, H_α), 3.09 (s, 18H, H_β). ^{13}C NMR (126 MHz, MeOD, δ): (*E*) 154.1 (C_i), 151.6 (C_m), 136.9 (C_p), 131.5 ($C_{m'}$), 128.6 (C_o), 126.0 ($C_{o'}$), 70.8 (C_α), 53.3 (C_β). (*Z*) 154.1 (C_i), 151.6 (C_m), 131.0 ($C_{m'}$), 123.9 (C_p), 117.1 (C_o), 115.7 ($C_{o'}$), 69.8 (C_α), 53.3 (C_β). HRMS [ESI+] m/z = 326.24705 $[M]^{+2}$, calcd for $[C_{20}H_{30}N_4]^{+2}$ 326.2472.

(*E,Z*)-1,1'-(Diazene-1,2-diylbis(4,1-phenylene))bis(*N,N,N*-trimethylmethanaminium) iodide (*p*-2.1e)

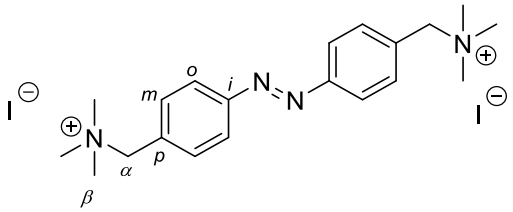

Azocuronium *p*-**2.1e** was obtained from azo derivative *p*-**2.2e** (46.2 mg, 0.16 mmol) and CH_3I (23.3 μL, 0.37 mmol) as orange crystals (74 mg, 80%), mp: decompose before melting. NMR spectra was recorded in (*E*):(*Z*) 0.1:0.9 proportion. ^{1}H of each isomer is reported separately.^{1}H NMR (500 MHz, MeOD, δ): (*E*) 8.10 (d, *J* = 8.4 Hz, 4H, H_o), 7.82 (d, *J* = 8.4 Hz, 4H, H_m), 4.68 (s, 4H, H_α), 3.19 (s, 18H, H_β). (*Z*) 7.53 (d, *J* = 8.7 Hz, 4H, H_o), 7.03 (d, *J* = 8.4 Hz, 4H, H_m), 4.50 (s, 4H, H_α), 3.09 (s, 18H, H_β). ^{13}C NMR (126 MHz, MeOD, δ) (*E*): 154.9 (C_i), 135.3 (C_m), 132.4 (C_p), 124.6 (C_o), 69.8 (C_α), 53.4 (C_β). HRMS [ESI+] m/z = 326.24743 $[M]^{+2}$, calcd for $[C_{20}H_{30}N_4]^{+2}$ 326.24705.

(*E,Z*)-1-Methyl-1-(3-(phenyldiazenyl)benzyl)piperidin-1-ium iodide (*m*-2.14b)

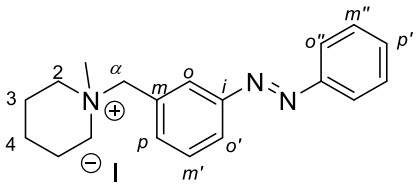

Azocuronium ***m*-2.14b** was obtained from ***m*-2.13b** (125 mg, 0.45 mmol) as a brown oil (110 mg, 58%). (*E*)-isomer was characterized. ^{1}H NMR (500 MHz, MeOD, δ): 8.09 (t, *J* = 1.8 Hz, 1H, H_o), 8.07 (d, *J* = 7.8 Hz, 2H, $H_{o'}$), 7.97 – 7.93 (m, 2H, $H_{o''}$), 7.71 (t, *J* = 7.6 Hz, 1H, $H_{m'}$), 7.70 – 7.64 (m, 1H, H_p), 7.59 – 7.54 (m, 3H, $H_{m'}$, $H_{p'}$), 4.44 (s, 2H, H_α), 3.54 – 3.49 (m, 2H, H_{2eq}), 3.03 (dd, *J* = 12.0, 2.6 Hz, 2H, H_{2eq}), 2.70 (s, 3H, CH_3), 1.97 (dt, *J* = 15.4, 2.6 Hz, 2H, H_{3eq}), 1.85 (dt, *J* = 13.1, 3.8 Hz, 1H, H_{4eq}), 1.79 – 1.73 (m, 2H, H_{3ax}), 1.54 (dt, *J* = 12.7, 3.8 Hz, 1H, H_{4ax}). ^{13}C NMR (126 MHz, MeOD, δ): 154.4 (C_i), 153.8 ($C_{i'}$), 134.8 (C_p), 132.9 ($C_{p'}$), 131.7 (C_m), 131.4 ($C_{m'}$), 130.4 ($C_{m''}$), 126.0 (C_o), 125.8 ($C_{o'}$), 123.9 ($C_{o''}$), 61.4 (C_α), 54.2 (C_2), 35.4 (CH_3), 24.1 (C_3). HPLC-MS (15:95- g.t.10 min) ^{t}R 4.79 min, *m/z* = 294.07 $[M+H]^+$, calcd. for $[C_{19}H_{24}N_3]^+$ 294.42; ^{t}R 0.92 min, *m/z* = 127 $[I]^-$. λ_{max} = 318 nm [(*E*)-isomer]. HRMS [ESI^+] m/z = 294.19714 $[M]^+$, calcd for $[C_{19}H_{24}N_3]^+$ 294.19702.

Photochemical properties by UV and NMR

A solution of the corresponding azocuronium in H_2O (100 μM) was placed in a 1 mL quartz cuvette (10 mm diameter) and absorption spectrum was recorded in a diode-array UV-vis spectrophotometer (DH2000) under thermal relaxed conditions. Then, the solution was irradiated under either UV or blue light with a LED and the UV-vis spectrum was registered again.

A Varian Unity-500 NMR spectrometer operating at 500 MHz was employed to quantified the (*E*)-(*Z*) isomerization of azobenzenes, using D_2O as solvent. Samples were irradiating with a LED light (either 335 or 400 nm) between records during different periods of time.

Thermodynamic solubility determination

The solubility experiments were performed at IQM-CSIC facilities by its analytical service following described protocols.[277,278] UV maximums were extracted from recorded UV-spectra of the compounds in the 270 - 400 nm range. A 10 mM stock solution of the corresponding compound in DMSO was prepared. A calibration line was built by measuring the absorbance at the corresponding maximum wavelength of sequential dilutions of the stock solution in buffer:ACN (80:20) mixture in a 96-well plate containing 200 µL per point. The buffers employed were: pH 1.2 KCl 45 mM buffer, pH 7.4 phosphate 45 mM buffer and pH 9.4 NH_4Cl buffer. In order to validate the calibration line, and exclude interferences due to the presence of 5% DMSO, a quality control standard of known concentrations was employed. The calibration line was accepted if $R^2>0.990$, the residual value of each point <15% and the relative error of the quality control standard <15%. The solubility determination was made as follows: 200 µL of buffer solution were added over 1 mg accurately weighted of the corresponding compound in order to achieve a saturated solution. The mixture was kept at rt in an orbital stirrer at 320 rpm for 24h and then centrifuged at 135 rpm for 15 min. 160 µL of the supernatant were transferred to a 96-well plate and diluted with 40 µL of a buffer:ACN (80:20) solution. The solubility was determined by extrapolation to the calibration line within the linearity range and expressed in mol/L. The experiments were run in triplicates.

Potentiometric pK_a determination

The solubility experiments were performed at IQM-CSIC by its analytical service. Thus, titrations were carried out at 25 ºC in 0.15 M KCl solution (aq) in a SiriusT3 equipment (Sirius Analytical Instruments Ltd, East Sussex, Britain) equipped with an Ag/AgCl double junction reference pH electrode, a Peltier temperature system and a turbidity sensor. Standardized 0.5 M KOH and 0.5 M HCl were used as titration reagents. KOH solution was standardized by potassium phthalate. The pK_a values are the mean of 3 titrations ± SD.[279]

Biological Studies

Radioligand binding assays at muscle-type nAChRs expressed in TE671 cells

All radioligand binding assays were performed in Eurofins Cerep SA (France). Cell membrane homogenates (60 µg protein) were incubated for 120 min at 22 °C with 0.5 nM [^{125}I]α-bungarotoxin in the absence or presence of the tested compound in a buffer solution containing 20 mM HEPES/NaOH (pH 7.3), 118 mM NaCl, 4.8 mM KCl, 2.5 mM $CaCl_2$, 1.2 mM $MgSO_4$ and 0.1% BSA. Nonspecific binding was determined in the presence of 5 µM α-bungarotoxin. Following incubation, the samples were filtered rapidly under vacuum through glass fiber filters (GF/B, Packard) presoaked with 0.3% PEI and rinsed several times with an ice-cold buffer containing 50 mM Tris-HCl, 500 mM NaCl and 0.1% BSA using a 96-sample cell harvester (Unifilter, Packard). The filters were dried then counted for radioactivity in a scintillation counter (Topcount, Packard) using a scintillation cocktail (Microscint 0, Packard). The results are expressed as a percent inhibition of the control radioligand specific binding. The standard reference compound is α-bungarotoxin, which is tested in each experiment at several concentrations to obtain a competition curve from which its IC_{50} is calculated.[280]

Radioligand binding assays at α7 neuronal nAChRs expressed in transfected SH-SY5Y cells

Cell membrane homogenates (20 µg protein) were incubated for 120 min at 37 °C with 0.05 nM [^{125}I]±-bungarotoxin in the absence or presence of the tested compound in a buffer solution containing 50 mM K_2HPO_4/KH_2PO_4 (pH 7.4), 10 mM $MgCl_2$ and 0.1% BSA. Nonspecific binding was determined in the presence of 1 µM α-bungarotoxin. After incubation, the samples are filtered rapidly under vacuum through glass fiber filters (GF/B, Packard) presoaked with 0.3% PEI and rinsed several times with ice-cold 50 mM Tris-HCl and 150 mM NaCl using a 96-sample cell harvester (Unifilter, Packard). The filters were dried then counted for radioactivity in a scintillation counter (Topcount, Packard) using a scintillation cocktail (Microscint 0, Packard). The results are expressed as a percent inhibition of the control radioligand specific binding. The standard reference compound is

(+/-)-epibatidine, which is tested in each experiment at several concentrations to obtain a competition curve from which its IC_{50} is calculated.[281]

Radioligand binding assays at α4β2 neuronal nAChRs expressed in transfected SH-SY5Y cells

Cell membrane homogenates (60 µg protein) were incubated for 120 min at 22 °C with 0.5 nM [^{125}I]α-bungarotoxin in the absence or presence of the tested compound in a buffer solution containing (in mM): 20 HEPES/NaOH (pH 7.3), 118 NaCl, 4.8 KCl, 2.5 $CaCl_2$, 1.2 $MgSO_4$ and 0.1% BSA. Nonspecific binding was determined in the presence of 5 µM α-bungarotoxin. Following incubation, the samples are filtered rapidly under vacuum through glass fiber filters (GF/B, Packard) presoaked with 0.3% PEI and rinsed several times with an ice-cold buffer containing 50 mM Tris-HCl, 500 mM NaCl and 0.1% BSA using a 96-sample cell harvester (Unifilter, Packard). The filters were dried then counted for radioactivity in a scintillation counter (Topcount, Packard) using a scintillation cocktail (Microscint 0, Packard). The results are expressed as a percent inhibition of the control radioligand specific binding. The standard reference compound is α-bungarotoxin, which is tested in each experiment at several concentrations to obtain a competition curve from which its IC_{50} is calculated.[282]

Preparation of oocytes and RNA injections.

Electrophysiology experiments were performed in the laboratory of Dr. Carlos A. Villalba-Galea (University of the Pacific, Stockton, California, USA). *Xenopus laevis* oocyte isolation, preparation and injection were performed using methods published from the lab and elsewhere.[283,284] Animal protocols were approved by Institutional Animal Care and Use Committees at University of the Pacific and conform to the requirements in the Guide for the Care and Use of Laboratory Animals from the U.S. National Academy of Sciences. Frogs were purchased from *Xenopus* 1 (Dexter, MI). Oocytes were maintained at 16-17 ºC in an incubation solution of (in mM): 99 NaCl, 1 KCl, 2 $CaCl_2$, 1 $MgCl_2$ or $MgSO_3$, 10

HEPES, 2 pyruvic acid, and 20-50 mg/L of gentamycin. The incubation solution was titrated to pH 7.5 with NaOH. Results from many batches of oocytes were combined.

For expression, plasmids encoding for the α_1, β_1, δ_1, and γ_1 subunits of the embryonic nAChR from rat were prepared in the laboratory from original samples kindly gifted by Dr. Roger Papke. The plasmids were transcribed into cRNA using a SP6 RNA polymerase kit (mMessage mMachine, Ambion). Oocytes were injected with a mix containing 2.5 ng of each *in vitro*-transcribed cRNA. Injected oocytes were kept in incubation solution at 16-17 ^{o}C for 2-4 days before recordings.

Electrophysiology

Ionic currents were recorded using the TEVC technique employing a GeneClamp amplifier (Axon Instruments). For these recordings, the membrane potential was held at -60 mV with constant perfusion by recirculation. Two LEDs with emission centered at 335-340 nm (UV light) and 400-450 nm (blue light) were used to induce photo-isomerization of the compounds. All LED emission spectra had a 20 - 35 nm full width at half maximum per manufacturer specifications. The LEDs were powered using an in house-built circuit controlled by the acquisition system to synchronize LED irradiation with the electrophysiological recordings.

Receptor activation was driven by external application of ACh using a nano-injector (Nanoject II, Drummond Scientific) with a sharpen glass capillary. Briefly, 2.3 to 18.4 nL of 50 μM of ACh were applied on the surface of the oocytes at a rate of 46 nL/s. These "puffs" of ACh were allowed to freely diffuse for 100-1000 ms and subsequently washed out by recording solution recirculation. An in house-made micro-recirculation system was built using a piezoelectric-based peristaltic pump (Bartels Mikrotechnik, Germany). The powering system for the pump was controlled by the acquisition system. The chamber volume was 100-150 μL and the total "dead" volume of the tubing and pump was 100 μL.

For TEVC recordings, oocytes were bathed in a recording solution containing (in mM): 99 NaCl, 1 KCl, 2 $CaCl_2$, 1 $MgCl_2$ or $MgSO_3$, and 10 HEPES titrated to pH 7.4 with NaOH.

Glass sharp electrodes (resistance = 0.2-2.0 MΩ) were filled with a solution containing (in mM) 1000 KCl, 10 HEPES and 10 EGTA, at pH 7.4 (KOH). Voltage control and current acquisition was performed using a USB-6251 multi-function acquisition board (National Instruments) controlled by an in house-made program coded in LabVIEW (National Instruments) (C.A. Villalba-Galea, details available upon request). In addition, the nano-injector delivering the "ACh puffs", the LEDs and the micro-recirculation system were controlled with the multi-function board to synchronize their actions. Current signals were filtered at 100 kHz, oversampled at 1-2 MHz, and stored at 5-25 kHz for offline analysis. Data were analyzed using a custom Java-based software (C.A. Villalba-Galea, details available upon request) and Origin 2018 (OriginLab).

Measurement of cell viability with MTT

Cell viability, virtually the mitochondrial activity of living cells, was measured in Raw 264.7 macrophages by quantitative colorimetric assay with MTT (Sigma Aldrich, Madrid, Spain), based on the ability of viable cells to reduce yellow MTT to blue formazan as was described previously.[262]

Briefly, cells were plated in wells of 96-well plates and incubated for 24 h at 37 °C. The cells were treated with or without the compounds. At the end of the treatment, the medium was removed, and the cells were incubated with 100 µL of MTT (5 mg/mL in phosphate buffered saline; PBS) in a fresh medium for 4 h at 37 °C. After 4 h, formazan crystals, formed by mitochondrial reduction of MTT, were solubilized in DMSO (150 µL per well). After mixing, the absorbance of the cells was measured at 540 nm.

BIBLIOGRAPHY

BIBLIOGRAPHY

(1) Maresova, P.; Mohelská, H.; Dolejs, J.; Kuca, K. Socio-economic aspects of Alzheimer's disease. *Curr. Alzheimer Res.* **2015**, *12*, 903-911.

(2) Holtzman, D. M.; Morris, J. C.; Goate, A. M. Alzheimer's disease: the challenge of the second century. *Sci. Transl. Med.* **2011**, *3*, 77sr71-77sr71.

(3) Hroudová, J.; Singh, N.; Fišar, Z.; Ghosh, K. K. Progress in drug development for Alzheimer's disease: an overview in relation to mitochondrial energy metabolism. *Eur. J. Med. Chem.* **2016**, *121*, 774-784.

(4) Ansari, M. A.; Scheff, S. W. Oxidative stress in the progression of Alzheimer disease in the frontal cortex. *J. Neuropathol. Exp. Neurol.* **2010**, *69*, 155-167.

(5) E Abdel Moneim, A. Oxidant/antioxidant imbalance and the risk of Alzheimer's disease. *Curr. Alzheimer Res.* **2015**, *12*, 335-349.

(6) Fernández-Moriano, C.; González-Burgos, E.; Gómez-Serranillos, M. P. Mitochondria-targeted protective compounds in Parkinson's and Alzheimer's diseases. *Oxid. Med. Cell. Long.* **2015**, *2015*.

(7) Cuadrado, A.; Manda, G.; Hassan, A.; Alcaraz, M. J.; Barbas, C.; Daiber, A.; Ghezzi, P.; León, R.; López, M. G.; Oliva, B. Transcription factor NRF2 as a therapeutic target for chronic diseases: a systems medicine approach. *Pharmacol. Rev.* **2018**, *70*, 348-383.

(8) Kang, M. I.; Kobayashi, A.; Wakabayashi, N.; Kim, S. G.; Yamamoto, M. Scaffolding of Keap1 to the actin cytoskeleton controls the function of Nrf2 as key regulator of cytoprotective phase 2 genes. *Proc. Natl. Acad. Sci. U. S. A.* **2004**, *101*, 2046-2051.

(9) McBean, G. J.; López, M. G.; Wallner, F. K. Redox-based therapeutics in neurodegenerative disease. *Br. J. Pharmacol.* **2017**, *174*, 1750-1770.

(10) Johnson, J. A.; Johnson, D. A.; Kraft, A. D.; Calkins, M. J.; Jakel, R. J.; Vargas, M. R.; Chen, P. C. The Nrf2-ARE pathway: an indicator and modulator of oxidative stress in neurodegeneration. *Ann. N. Y. Acad. Sci.* **2008**, *1147*, 61-69.

(11) Magesh, S.; Chen, Y.; Hu, L. Small molecule modulators of Keap1-Nrf2-ARE pathway as potential preventive and therapeutic agents. *Med. Res. Rev.* **2012**, *32*, 687-726.

(12) Copple, I. M.; Shelton, L. M.; Walsh, J.; Kratschmar, D. V.; Lister, A.; Odermatt, A.; Goldring, C. E.; Dinkova-Kostova, A. T.; Honda, T.; Park, B. K. Chemical tuning enhances both potency toward nrf2 and in vitro therapeutic index of triterpenoids. *Toxicol Sci.* **2014**, *140*, 462-469.

(13) Stangel, M.; Linker, R. A. Dimethyl fumarate (BG-12) for the treatment of multiple sclerosis. *Expert Review of Clinical Pharmacology* **2013**, *6*, 355-362.

(14) Toto, R. D. Bardoxolone—the Phoenix? *J. Am. Soc. Nephrol.* **2018**, *29*, 360-361.

(15) Pallesen, J. S.; Tran, K. T.; Bach, A. Non-covalent Small-Molecule Kelch-like ECH-Associated Protein 1-Nuclear Factor Erythroid 2-Related Factor 2 (Keap1-Nrf2) Inhibitors and Their Potential for Targeting Central Nervous System Diseases. *J. Med. Chem.* **2018**, *61*, 8088-8103.

(16) Richardson, B. G.; Jain, A. D.; Speltz, T. E.; Moore, T. W. Non-electrophilic modulators of the canonical Keap1/Nrf2 pathway. *Bioorg. Med. Chem. Lett.* **2015**, *25*, 2261-2268.

(17) Zhuang, C.; Narayanapillai, S.; Zhang, W.; Sham, Y. Y.; Xing, C. Rapid Identification of Keap1–Nrf2 Small-Molecule Inhibitors through Structure-Based Virtual Screening and Hit-Based Substructure Search. *J. Med. Chem.* **2014**, *57*, 1121-1126.

(18) Abed, D. A.; Goldstein, M.; Albanyan, H.; Jin, H.; Hu, L. Discovery of direct inhibitors of Keap1–Nrf2 protein–protein interaction as potential therapeutic and preventive agents. *Acta Pharm. Sin. B* **2015**, *5*, 285-299.

(19) Richardson, B. G.; Jain, A. D.; Potteti, H. R.; Lazzara, P. R.; David, B. P.; Tamatam, C. R.; Choma, E.; Skowron, K.; Dye, K.; Siddiqui, Z. Replacement of a Naphthalene Scaffold in Kelch-like ECH-Associated Protein 1 (KEAP1)/Nuclear factor (erythroid-derived 2)-like 2 (NRF2) Inhibitors. *J. Med. Chem.* **2018**, *61*, 8029-8047.

(20) Zhao, F.; Wu, T.; Lau, A.; Jiang, T.; Huang, Z.; Wang, X. J.; Chen, W.; Wong, P. K.; Zhang, D. D. Nrf2 promotes neuronal cell differentiation. *Free Radic. Biol. Med.* **2009**, *47*, 867-879.

(21) Karkkainen, V.; Pomeshchik, Y.; Savchenko, E.; Dhungana, H.; Kurronen, A.; Lehtonen, S.; Naumenko, N.; Tavi, P.; Levonen, A. L.; Yamamoto, M.; Malm, T.; Magga, J.; Kanninen, K. M.; Koistinaho, J. Nrf2 regulates neurogenesis and protects neural progenitor cells against Abeta toxicity. *Stem Cells* **2014**, *32*, 1904-1916.

(22) Sun, H.; Zhu, J.; Lin, H.; Gu, K.; Feng, F. Recent progress in the development of small molecule Nrf2 modulators: a patent review (2012-2016). *Expert Opin. Ther. Pat.* **2017**, *27*, 763-785.

(23) Kerr, F.; Sofola-Adesakin, O.; Ivanov, D. K.; Gatliff, J.; Gomez Perez-Nievas, B.; Bertrand, H. C.; Martinez, P.; Callard, R.; Snoeren, I.; Cocheme, H. M.; Adcott, J.; Khericha, M.; Castillo-Quan, J. I.; Wells, G.; Noble, W.; Thornton, J.; Partridge, L. Direct Keap1-Nrf2 disruption as a potential therapeutic target for Alzheimer's disease. *PLoS Genet.* **2017**, *13*, e1006593.

(24) Vianello, R.; Repič, M.; Mavri, J. How are Biogenic Amines Metabolized by Monoamine Oxidases? *Eur. J. Org. Chem.* **2012**, *2012*, 7057-7065.

(25) Gaweska, H.; Fitzpatrick, P. F. Structures and mechanism of the monoamine oxidase family. *Biomol. concepts* **2011**, *2*, 365-377.

(26) Binda, C.; Li, M.; Hubálek, F.; Restelli, N.; Edmondson, D. E.; Mattevi, A. Insights into the mode of inhibition of human mitochondrial monoamine oxidase B from high-resolution crystal structures. *Proc. Natl. Acad. Sci.* **2003**, *100*, 9750-9755.

(27) Youdim, M. B.; Edmondson, D.; Tipton, K. F. The therapeutic potential of monoamine oxidase inhibitors. *Nat. Rev. Neurosci.* **2006**, *7*, 295-309.

(28) Edmondson, D. E.; Bhattacharyya, A. K.; Walker, M. C. Spectral and kinetic studies of imine product formation in the oxidation of p-(N, N-dimethylamino) benzylamine analogs by monoamine oxidase B. *Biochemistry* **1993**, *32*, 5196-5202.

(29) Schedin-Weiss, S.; Inoue, M.; Hromadkova, L.; Teranishi, Y.; Yamamoto, N. G.; Wiehager, B.; Bogdanovic, N.; Winblad, B.; Sandebring-Matton, A.; Frykman, S. Monoamine oxidase B is elevated in Alzheimer disease neurons, is associated with γ-secretase and regulates neuronal amyloid β-peptide levels. *Alzheimer's Res. Ther.* **2017**, *9*, 57.

(30) Tripathi, A. C.; Upadhyay, S.; Paliwal, S.; Saraf, S. K. Privileged scaffolds as MAO inhibitors: Retrospect and prospects. *Eur. J. Med. Chem.* **2018**, *145*, 445-497.

(31) Ramsay, R.; Tipton, K. Assessment of enzyme inhibition: a review with examples from the development of monoamine oxidase and cholinesterase inhibitory drugs. *Molecules* **2017**, *22*, 1192.

(32) Dubocovich, M. L.; Delagrange, P.; Krause, D. N.; Sugden, D.; Cardinali, D. P.; Olcese, J. International Union of Basic and Clinical Pharmacology. LXXV. Nomenclature, classification, and pharmacology of G protein-coupled melatonin receptors. *Pharmacol. Rev.* **2010**, pr. 110.002832.

(33) Vu, T. K.; Patil, S. P.; Park, Y. J.; Thao, D. T. Synthesis and In Vitro Cytotoxic Activity Evaluation of Novel Mannich Bases and Modified AZT Derivatives Possessing Mannich Base Moieties via Click Chemistry. *Lett. Drug Des. Discov.* **2013**, *10*, 585-593.

(34) Jiaranaikulwanitch, J.; Govitrapong, P.; Fokin, V. V.; Vajragupta, O. From BACE1 inhibitor to multifunctionality of tryptoline and tryptamine triazole derivatives for Alzheimer's disease. *Molecules* **2012**, *17*, 8312-8333.

(35) Nosjean, O.; Ferro, M.; Cogé, F.; Beauverger, P.; Henlin, J.-M.; Lefoulon, F.; Fauchère, J.-L.; Delagrange, P.; Canet, E.; Boutin, J. A. Identification of the Melatonin-binding SiteMT 3 as the Quinone Reductase 2. *J. Biol. Chem.* **2000**, *275*, 31311-31317.

(36) Nosjean, O.; Nicolas, J.-P.; Klupsch, F.; Delagrange, P.; Canet, E.; Boutin, J. A. Comparative pharmacological studies of melatonin receptors: mt1, mt2 and mt3/qr2. tissue distribution of mt3/qr2 1. *Biochem. Pharmacol.* **2001**, *61*, 1369-1379.

(37) Dubocovich, M. L. Melatonin receptors: are there multiple subtypes? *Trends Pharmacol. Sci.* **1995**, *16*, 50-56.

(38) Jockers, R.; Delagrange, P.; Dubocovich, M. L.; Markus, R. P.; Renault, N.; Tosini, G.; Cecon, E.; Zlotos, D. P. Update on melatonin receptors: IUPHAR Review 20. *Br. J. Pharmacol.* **2016**, *173*, 2702-2725.

(39) Zlotos, D. P.; Jockers, R.; Cecon, E.; Rivara, S.; Witt-Enderby, P. A. MT1 and MT2 melatonin receptors: ligands, models, oligomers, and therapeutic potential. *J. Med. Chem.* **2013**, *57*, 3161-3185.

(40) De Bodinat, C.; Guardiola-Lemaitre, B.; Mocaër, E.; Renard, P.; Muñoz, C.; Millan, M. J. Agomelatine, the first melatonergic antidepressant: discovery, characterization and development. *Nat. Rev. Drug Discov.* **2010**, *9*, 628.

(41) Kato, K.; Hirai, K.; Nishiyama, K.; Uchikawa, O.; Fukatsu, K.; Ohkawa, S.; Kawamata, Y.; Hinuma, S.; Miyamoto, M. Neurochemical properties of ramelteon (TAK-375), a selective MT1/MT2 receptor agonist. *Neuropharmacology* **2005**, *48*, 301-310.

(42) Lavedan, C.; Forsberg, M.; Gentile, A. J. Tasimelteon: a selective and unique receptor binding profile. *Neuropharmacology* **2015**, *91*, 142-147.

(43) Liu, J.; Clough, S. J.; Hutchinson, A. J.; Adamah-Biassi, E. B.; Popovska-Gorevski, M.; Dubocovich, M. L. MT1 and MT2 melatonin receptors: a therapeutic perspective. *Annu. Rev. Pharmacol. Toxicol.* **2016**, *56*, 361-383.

(44) Fu, Y.; Buryanovskyy, L.; Zhang, Z. Quinone reductase 2 is a catechol quinone reductase. *J. Biol. Chem.* **2008**, *283*, 23829-23835.

(45) Cassagnes, L.-E.; Perio, P.; Ferry, G.; Moulharat, N.; Antoine, M.; Gayon, R.; Boutin, J. A.; Nepveu, F.; Reybier, K. In cellulo monitoring of quinone reductase activity and reactive oxygen species production during the redox cycling of 1, 2 and 1, 4 quinones. *Free Radic. Biol. Med.* **2015**, *89*, 126-134.

(46) Hashimoto, T.; Nakai, M. Increased hippocampal quinone reductase 2 in Alzheimer's disease. *Neurosci. Lett.* **2011**, *502*, 10-12.

(47) Cassagnes, L.-E.; Chhour, M.; Pério, P.; Sudor, J.; Gayon, R.; Ferry, G.; Boutin, J. A.; Nepveu, F.; Reybier, K. Oxidative stress and neurodegeneration: The possible contribution of quinone reductase 2. *Free Radic. Biol. Med.* **2018**, *120*, 56-61.

(48) Boutin, J. A. Quinone reductase 2 as a promising target of melatonin therapeutic actions. *Expert Opin. Ther. Targets* **2016**, *20*, 303-317.

(49) Heneka, M. T.; Carson, M. J.; El Khoury, J.; Landreth, G. E.; Brosseron, F.; Feinstein, D. L.; Jacobs, A. H.; Wyss-Coray, T.; Vitorica, J.; Ransohoff, R. M. Neuroinflammation in Alzheimer's disease. *Lancet Neurol.* **2015**, *14*, 388-405.

(50) Fan, Z.; Brooks, D. J.; Okello, A.; Edison, P. An early and late peak in microglial activation in Alzheimer's disease trajectory. *Brain* **2017**, *140*, 792-803.

(51) Rådmark, O.; Werz, O.; Steinhilber, D.; Samuelsson, B. 5-Lipoxygenase: regulation of expression and enzyme activity. *Trends Biochem. Sci.* **2007**, *32*, 332-341.

(52) Manev, H.; Uz, T.; Sugaya, K.; Qu, T. Putative role of neuronal 5-lipoxygenase in an aging brain. *FASEB J.* **2000**, *14*, 1464-1469.

(53) Ikonomovic, M. D.; Abrahamson, E. E.; Uz, T.; Manev, H.; DeKosky, S. T. Increased 5-lipoxygenase immunoreactivity in the hippocampus of patients with Alzheimer's disease. *J. Histochem. Cytochem.* **2008**, *56*, 1065-1073.

(54) Panigrahi, S.; Li, D.-D.; Surai, S.; Ghosh, A.; Hong, H. 5-lipoxygenase: Emerging Therapeutic Targets in Central Nervous System Disorders. *Int. J. Adv. Res. Biol. Sci* **2018**, *5*, 20-29.

(55) Giannopoulos, P. F.; Joshi, Y. B.; Praticò, D. Novel lipid signaling pathways in Alzheimer's disease pathogenesis. *Biochem. Pharmacol.* **2014**, *88*, 560-564.

(56) Firuzi, O.; Zhuo, J.; Chinnici, C. M.; Wisniewski, T.; Praticò, D. 5-Lipoxygenase gene disruption reduces amyloid-β pathology in a mouse model of Alzheimer's disease. *FASEB J.* **2008**, *22*, 1169-1178.

(57) Chu, J.; Giannopoulos, P. F.; Ceballos-Diaz, C.; Golde, T. E.; Praticò, D. 5-Lipoxygenase gene transfer worsens memory, amyloid, and tau brain pathologies in a mouse model of alzheimer disease. *Ann. Neurol.* **2012**, *72*, 442-454.

(58) Chu, J.; Li, J.-G.; Pratico, D. Zileuton improves memory deficits, amyloid and tau pathology in a mouse model of Alzheimer's disease with plaques and tangles. *PLoS One* **2013**, *8*, e70991.

(59) Chu, J.; Praticò, D. The 5-Lipoxygenase as modulator of Alzheimer's γ-secretase and therapeutic target. *Brain Res. Bull.* **2016**, *126*, 207-212.

(60) Altman, J. Are new neurons formed in the brains of adult mammals? *Science* **1962**, *135*, 1127-1128.

(61) Decimo, I.; Bifari, F.; Krampera, M.; Fumagalli, G. Neural stem cell niches in health and diseases. *Curr. Pharm. Des.* **2012**, *18*, 1755-1783.

(62) Urbán, N.; Guillemot, F. Neurogenesis in the embryonic and adult brain: same regulators, different roles. *Front. Cell. Neurosci.* **2014**, *8*, 396.

(63) Kempermann, G.; Gage, F. H.; Aigner, L.; Song, H.; Curtis, M. A.; Thuret, S.; Kuhn, H. G.; Jessberger, S.; Frankland, P. W.; Cameron, H. A.; Gould, E.; Hen, R.; Abrous, D. N.; Toni, N.; Schinder, A. F.; Zhao, X.; Lucassen, P. J.; Frisen, J. Human adult neurogenesis: Evidence and remaining questions. *Cell Stem Cell* **2018**, *23*, 25-30.

(64) Boldrini, M.; Fulmore, C. A.; Tartt, A. N.; Simeon, L. R.; Pavlova, I.; Poposka, V.; Rosoklija, G. B.; Stankov, A.; Arango, V.; Dwork, A. J.; Hen, R.; Mann, J. J. Human hippocampal neurogenesis persists throughout aging. *Cell Stem Cell* **2018**, *22*, 589-599 e585.

(65) Wang, J. M.; Singh, C.; Liu, L.; Irwin, R. W.; Chen, S.; Chung, E. J.; Thompson, R. F.; Brinton, R. D. Allopregnanolone reverses neurogenic and cognitive deficits in mouse model of Alzheimer's disease. *Proc. Natl. Acad. Sci. USA* **2010**, *107*, 6498-6503.

(66) Hernandez, G. D.; Brinton, R. D., Allopregnanolone as a Therapeutic to Regenerate the Degenerated Brain. In *Sex Steroids' Effects on Brain, Heart and Vessels*, Springer: 2019; pp 111-123.

(67) Bolijn, S.; Lucassen, P. J. How the Body Talks to the Brain; Peripheral Mediators of Physical Activity-Induced Proliferation in the Adult Hippocampus. *Brain Plast.* **2015**, *1*, 5-27.

(68) Herrera-Arozamena, C.; Martí-Marí, O.; Estrada, M.; de la Fuente Revenga, M.; Rodríguez-Franco, M. I. Recent advances in neurogenic small molecules as innovative treatments for neurodegenerative diseases. *Molecules* **2016**, *21*, 1165-1185.

(69) Ramírez-Rodríguez, G.; Vega-Rivera, N. M.; Benítez-King, G.; Castro-García, M.; Ortiz-López, L. Melatonin supplementation delays the decline of adult hippocampal neurogenesis during normal aging of mice. *Neurosci. Lett.* **2012**, *530*, 53-58.

(70) López-Iglesias, B.; Pérez, C.; Morales-García, J. A.; Alonso-Gil, S.; Pérez-Castillo, A.; Romero, A.; López, M. G.; Villarroya, M.; Conde, S.; Rodríguez-Franco, M. I. New melatonin-*N*,*N*-dibenzyl(*N*-methyl)amine hybrids: potent neurogenic agents with antioxidant, cholinergic, and neuroprotective properties as innovative drugs for Alzheimer's disease. *J. Med. Chem.* **2014**, *57*, 3773-3785.

(71) de la Fuente Revenga, M.; Pérez, C.; Morales-García, J. A.; Alonso-Gil, S.; Pérez-Castillo, A.; Caignard, D. H.; Yáñez, M.; Gamo, A. M.; Rodríguez-Franco, M. I. Neurogenic potential assessment and pharmacological characterization of 6-methoxy-1,2,3,4-tetrahydro-beta-carboline (pinoline) and melatonin-pinoline hybrids. *ACS Chem. Neurosci.* **2015**, *6*, 800-810.

(72) de la Fuente Revenga, M.; Fernández-Sáez, N.; Herrera-Arozamena, C.; Morales-García, J. A.; Alonso-Gil, S.; Pérez-Castillo, A.; Caignard, D.-H.; Rivara, S.; Rodríguez-Franco, M. I. Novel *N*-acetyl bioisosteres of melatonin: melatonergic receptor pharmacology, physicochemical studies, and phenotypic assessment of their neurogenic potential. *J. Med. Chem.* **2015**, *58*, 4998-5014.

(73) Morales-García, J. A.; de la Fuente Revenga, M.; Alonso-Gil, S.; Rodríguez-Franco, M. I.; Feilding, A.; Perez-Castillo, A.; Riba, J. The alkaloids of *Banisteriopsis caapi*, the plant source of the Amazonian hallucinogen Ayahuasca, stimulate adult neurogenesis *in vitro*. *Sci. Rep.* **2017**, *7*, 5309.

(74) Rodríguez-Franco, M. I.; de la Fuente Revenga, M.; Pérez, C.; Pérez-Castillo, A.; Morales-García, J. A.; Alonso-Gil, S.; Figueiró, J.; Carro, E. Neurogenic compounds comprising melatonin and the efficacy thereof in in vivo experiments for use in the treatment of diseases of the nervous system. WO2014154925A1 (Oct 2, **2014**).

(75) Figueiró-Silva, J.; Antequera, D.; Pascual, C.; de la Fuente Revenga, M.; Volt, H.; Acuña-Castroviejo, D.; Rodríguez-Franco, M. I.; Carro, E. The Melatonin Analog IQM316 May Induce Adult Hippocampal Neurogenesis and Preserve Recognition Memories in Mice. *Cell Transplant.* **2018**, *27*, 423-437.

(76) Liu, L.; Zhang, Q.; Cai, Y.; Sun, D.; He, X.; Wang, L.; Yu, D.; Li, X.; Xiong, X.; Xu, H.; Yang, Q.; Fan, X. Resveratrol counteracts lipopolysaccharide-induced depressive-like behaviors via enhanced hippocampal neurogenesis. *Oncotarget* **2016**, *7*, 56045-56059.

(77) Thiel, G.; Rossler, O. G. Resveratrol regulates gene transcription via activation of stimulus-responsive transcription factors. *Pharmacol. Res.* **2017**, *117*, 166-176.

(78) Truong, V. L.; Jun, M.; Jeong, W. S. Role of resveratrol in regulation of cellular defense systems against oxidative stress. *Biofactors* **2018**, *44*, 36-49.

(79) Tan, C.-C.; Yu, J.-T.; Wang, H.-F.; Tan, M.-S.; Meng, X.-F.; Wang, C.; Jiang, T.; Zhu, X.-C.; Tan, L. Efficacy and safety of donepezil, galantamine, rivastigmine, and memantine for the treatment of Alzheimer's disease: a systematic review and meta-analysis. *J. Alzheimer's Dis.* **2014**, *41*, 615-631.

(80) Morphy, R.; Rankovic, Z. Designed multiple ligands. An emerging drug discovery paradigm. *J. Med. Chem.* **2005**, *48*, 6523-6543.

(81) Cavalli, A.; Bolognesi, M. L.; Minarini, A.; Rosini, M.; Tumiatti, V.; Recanatini, M.; Melchiorre, C. Multi-target-directed ligands to combat neurodegenerative diseases. *J. Med. Chem.* **2008**, *51*, 347-372.

(82) Bansal, Y.; Silakari, O. Multifunctional compounds: smart molecules for multifactorial diseases. *Eur. J. Med. Chem.* **2014**, *76*, 31-42.

(83) Swerdlow, R. H. Alzheimer's disease pathologic cascades: who comes first, what drives what. *Neurotox. Res.* **2012**, *22*, 182-194.

(84) Hroudova, J.; Singh, N.; Fisar, Z.; Ghosh, K. K. Progress in drug development for Alzheimer's disease: an overview in relation to mitochondrial energy metabolism. *Eur. J. Med. Chem.* **2016**, *121*, 774-784.

(85) Ortiz, C. J. C.; de Freitas Silva, M.; Gontijo, V. S.; Viegas, F. P. D.; Dias, K. S. T.; Viegas, C. Design of Multi-target Directed Ligands as a Modern Approach for the Development of Innovative Drug Candidates for Alzheimer's Disease. *Multi-Target Drug Design Using Chem-Bioinformatic Approaches* **2019**, 255-351.

(86) Ramsay, R. R.; Popovic-Nikolic, M. R.; Nikolic, K.; Uliassi, E.; Bolognesi, M. L. A perspective on multi-target drug discovery and design for complex diseases. *Clin. Transl. Med.* **2018**, *7*, 3.

(87) Majidinia, M.; Reiter, R. J.; Shakouri, S. K.; Yousefi, B. The role of melatonin, a multitasking molecule, in retarding the processes of ageing. *Ageing Res. Rev.* **2018**, *47*, 198-213.

(88) Yang, J. H.; Kondratyuk, T. P.; Jermihov, K. C.; Marler, L. E.; Qiu, X.; Choi, Y.; Cao, H.; Yu, R.; Sturdy, M.; Huang, R.; Liu, Y.; Wang, L. Q.; Mesecar, A. D.; van Breemen, R. B.; Pezzuto, J. M.; Fong, H. H.; Chen, Y. G.; Zhang, H. J. Bioactive compounds from the fern Lepisorus contortus. *J. Nat. Prod.* **2011**, *74*, 129-136.

(89) Peperidou, A.; Pontiki, E.; Hadjipavlou-Litina, D.; Voulgari, E.; Avgoustakis, K. Multifunctional Cinnamic Acid Derivatives. *Molecules* **2017**, *22*, E1247.

(90) Cai, H.; Huang, X.; Xu, S.; Shen, H.; Zhang, P.; Huang, Y.; Jiang, J.; Sun, Y.; Jiang, B.; Wu, X.; Yao, H.; Xu, J. Discovery of novel hybrids of diaryl-1,2,4-triazoles and caffeic acid as dual inhibitors of cyclooxygenase-2 and 5-lipoxygenase for cancer therapy. *Eur. J. Med. Chem.* **2016**, *108*, 89-103.

(91) Bar-Am, O.; Amit, T.; Weinreb, O.; Youdim, M. B.; Mandel, S. Propargylamine containing Compounds as modulators of proteolytic cleavage of amyloid protein precursor: involvement of MAPK and PKC activation. *J. Alzheimers Dis.* **2010**, *21*, 361-371.

(92) Kumar, V.; Kaur, S.; Kumar, S. ZrCl4 catalyzed highly selective and efficient Michael addition of heterocyclic enamines with α, β-unsaturated olefins. *Tetrahedron Lett.* **2006**, *47*, 7001-7005.

(93) Zhang, X.; Breslav, M.; Grimm, J.; Guan, K.; Huang, A.; Liu, F.; Maryanoff, C. A.; Palmer, D.; Patel, M.; Qian, Y. A new procedure for preparation of carboxylic acid hydrazides. *J. Org. Chem.* **2002**, *67*, 9471-9474.

(94) Ottoni, O.; Neder, A. d. V.; Dias, A. K.; Cruz, R. P.; Aquino, L. B. Acylation of Indole under Friedel− Crafts Conditions An Improved Method To Obtain 3-Acylindoles Regioselectively. *Org. Lett.* **2001**, *3*, 1005-1007.

(95) Guo, T.; Han, S.-L.; Liu, Y.-C.; Liu, Y.; Liu, H.-M. Convenient synthesis of antiproliferative 2,3-dihydro-2,3′-bisindoles via dimerization of N-*H* indole derivatives. *Tetrahedron Lett.* **2016**, *57*, 1097-1099.

(96) Dupeyre, G.; Lemoine, P.; Ainseba, N.; Michel, S.; Cachet, X. A one-pot synthesis of 7-phenylindolo [3, 2-a] carbazoles from indoles and β-nitrostyrenes, via an unprecedented reaction sequence. *Org. Biomol. Chem.* **2011**, *9*, 7780-7790.

(97) Qu, H.; Qin, W.; Chang, Q.; Hu, Q.; Liu, L. Iron (III) Trichloride-Catalyzed One-Pot Three-Component Coupling of Indoles and Sodium Nitrite: A Convenient Synthesis of 2, 3'-Bi (3H-indol)-3-one oximes. *Curr. Org. Chem.* **2013**, *17*, 756-762.

(98) Noland, W. E.; Brown, C. D.; Zabronsky, A. E.; Tritch, K. J. Synthesis of 2-(9H-carbazol-1-yl) anilines from 2, 3′-biindolyl and ketones. *Tetrahedron* **2018**, *74*, 2391-2404.

(99) Noland, W. E.; Kumar, H. V.; Lu, C.; Brown, C. D.; Wiley-Schaber, E.; Johansson, A.; LaBelle, E. V.; O'Brian, N. C.; Jensen, R. C.; Tritch, K. J. N′-Acylation of (3, 2′)-indole dimers. *Tetrahedron Lett.* **2016**, *57*, 2158-2160.

(100) Bianco, G. G.; Ferraz, H. M.; Costa, A. M.; Costa-Lotufo, L. V.; Pessoa, C.; de Moraes, M. O.; Schrems, M. G.; Pfaltz, A.; Silva Jr, L. F. (+)-and (−)-Mutisianthol: First Total Synthesis, Absolute Configuration, and Antitumor Activity. *J. Org. Chem.* **2009**, *74*, 2561-2566.

(101) Carreno, M. C.; Enriquez, A.; Garcia-Cerrada, S.; Sanz-Cuesta, M. J.; Urbano, A.; Maseras, F.; Nonell-Canals, A. Towards configurationally stable [4]helicenes: enantioselective synthesis of 12-substituted 7,8-dihydro[4]helicene quinones. *Chem. Eur. J.* **2008**, *14*, 603-620.

(102) Ghaffarzadeh, M.; Bolourtchian, M.; Gholamhosseni, M.; Mohsenzadeh, F. Synthesis of arylaldehydes: Br2/DMSO catalytic system for the chemoselective oxidation of methylarenes. *Appl. Catal., A* **2007**, *333*, 131-135.

(103) Surendra, K.; Rajendar, G.; Corey, E. Useful catalytic enantioselective cationic double annulation reactions initiated at an internal π-bond: Method and applications. *J. Am. Chem. Soc.* **2013**, *136*, 642-645.

(104) Magedov, I. V.; Evdokimov, N. M.; Karki, M.; Peretti, A. S.; Lima, D. T.; Frolova, L. V.; Reisenauer, M. R.; Romero, A. E.; Tongwa, P.; Fonari, A. Reengineered epipodophyllotoxin. *Chem. Commun.* **2012**, *48*, 10416-10418.

(105) Cabri, W.; Candiani, I.; Bedeschi, A.; Santi, R. 1, 10-Phenanthroline derivatives: a new ligand class in the Heck reaction. Mechanistic aspects. *J. Org. Chem.* **1993**, *58*, 7421-7426.

(106) Scott, W. J.; Pena, M. R.; Sward, K.; Stoessel, S. J.; Stille, J. Palladium-catalyzed olefination of vinyl triflates. *J. Org. Chem.* **1985**, *50*, 2302-2308.

(107) Arcadi, A.; Cacchi, S.; Fabrizi, G.; Moro, L. Palladium-Catalyzed Cyclocarbonylation of o-Ethynylphenols and Vinyl Triflates To Form 3-Alkylidene-2-coumaranones. *Eur. Jour. Org. Chem.* **1999**, *1999*, 1137-1141.

(108) Stang, P. J.; Treptow, W. Single-step improved synthesis of primary and other vinyl trifluoromethanesulfonates. *Synthesis* **1980**, *1980*, 283-284.

(109) Schoffmann, A.; Wimmer, L.; Goldmann, D.; Khom, S.; Hintersteiner, J.; Baburin, I.; Schwarz, T.; Hintersteininger, M.; Pakfeifer, P.; Oufir, M.; Hamburger, M.; Erker, T.; Ecker, G. F.; Mihovilovic, M. D.; Hering, S. Efficient modulation of gamma-aminobutyric acid type A receptors by piperine derivatives. *J. Med. Chem.* **2014**, *57*, 5602-5619.

(110) McOmie, J.; Watts, M.; West, D. Demethylation of aryl methyl ethers by boron tribromide. *Tetrahedron* **1968**, *24*, 2289-2292.

(111) Fernández-Bachiller, M. I.; Pérez, C.; Monjas, L.; Rademann, J.; Rodríguez-Franco, M. I. New tacrine--4-oxo-4*H*-chromene hybrids as multifunctional agents for the treatment of Alzheimer's disease, with cholinergic, antioxidant, and beta-amyloid-reducing properties. *J. Med. Chem.* **2012**, *55*, 1303-1317.

(112) Ramadas, K.; Srinivasan, N. Iron-ammonium chloride-a convenient and inexpensive reductant. *Synth. Commun.* **1992**, *22*, 3189-3195.

(113) Lappert, M.; Prokai, B. Chloroboration and allied reactions of unsaturated compounds II. Haloboration and phenylboration of acetylenes; and the preparation of some alkynylboranes. *J. Organom. Chem.* **1964**, *1*, 384-400.

(114) Blackborow, J. R. The haloboration of n-hexyne-1. *J. Organom. Chem.* **1977**, *128*, 161-166.

(115) Suzuki, A. New application of organoboron compounds in organic synthesis. *Pure Appl. Chem.* **1986**, *58*, 629-638.

(116) La Regina, G.; Silvestri, R.; Gatti, V.; Lavecchia, A.; Novellino, E.; Befani, O.; Turini, P.; Agostinelli, E. Synthesis, structure–activity relationships and molecular modeling studies of new indole inhibitors of monoamine oxidases A and B. *Bioorg. Med. Chem.* **2008**, *16*, 9729-9740.

(117) Fang, H.-J.; Shou, X.-A.; Liu, Q.; Gan, C.-C.; Duan, H.-Q.; Qin, N. Synthesis and anti-metastatic effects of novel chiral ionone alkaloid derivatives. *Eur. J. Med. Chem.* **2015**, *101*, 245-253.

(118) Marco, J. L. Improved preparation of N-propargyl-2-(5-benzyloxyindolyl) methylamine [a]. *J. Heterocyclic Chem.* **1998**, *35*, 475-476.

(119) Unpublished results.

(120) Witt-Enderby, P. A.; Dubocovich, M. L. Characterization and regulation of the human ML1A melatonin receptor stably expressed in Chinese hamster ovary cells. *Mol. Pharmacol.* **1996**, *50*, 166-174.

(121) Beresford, I. J.; Browning, C.; Starkey, S. J.; Brown, J.; Foord, S. M.; Coughlan, J.; North, P. C.; Dubocovich, M. L.; Hagan, R. M. GR196429: a nonindolic agonist at high-affinity melatonin receptors. *J. Pharmacol. Exp. Ther.* **1998**, *285*, 1239-1245.

(122) Pickering, D. S.; Niles, L. P. Pharmacological characterization of melatonin binding sites in Syrian hamster hypothalamus. *Eur. J. Pharmacol.* **1990**, *175*, 71-77.

(123) Depreux, P.; Lesieur, D.; Mansour, H. A.; Morgan, P.; Howell, H. E.; Renard, P.; Caignard, D.-H.; Pfeiffer, B.; Delagrange, P. Synthesis and structure-activity relationships of novel naphthalenic and bioisosteric related amidic derivatives as melatonin receptor ligands. *J. Med. Chem.* **1994**, *37*, 3231-3239.

(124) Einhorn, L.; Krapfenbauer, K. HTRF: a technology tailored for biomarker determination-novel analytical detection system suitable for detection of specific autoimmune antibodies as biomarkers in nanogram level in different body fluids. *EPMA J.* **2015**, *6*, 23.

(125) Dávalos, A.; Gómez-Cordovés, C.; Bartolomé, B. Extending applicability of the oxygen radical absorbance capacity (ORAC-fluorescein) assay. *J. Agric. Food Chem.* **2004**, *52*, 48-54.

(126) Monjas, L.; Arce, M. P.; León, R.; Egea, J.; Pérez, C.; Villarroya, M.; López, M. G.; Gil, C.; Conde, S.; Rodríguez-Franco, M. I. Enzymatic and solid-phase synthesis of new donepezil-based L- and D-glutamic acid derivatives and their pharmacological evaluation in models related to Alzheimer's disease and cerebral ischemia. *Eur. J. Med. Chem.* **2017**, *130*, 60-72.

(127) Estrada Valencia, M.; Herrera-Arozamena, C.; de Andrés, L.; Pérez, C.; Morales-García, J. A.; Pérez-Castillo, A.; Ramos, E.; Romero, A.; Viña, D.; Yáñez, M.; Laurini, E.; Pricl, S.; Rodríguez-Franco, M. I. Neurogenic and neuroprotective donepezil-flavonoid hybrids with sigma-1 affinity and inhibition of key enzymes in Alzheimer's disease. *Eur. J. Med. Chem.* **2018**, *156*, 534-553.

(128) Estrada-Valencia, M.; Herrera-Arozamena, C.; Pérez, C.; Viña, D.; Morales-García, J. A.; Pérez-Castillo, A.; Ramos, E.; Romero, A.; Laurini, E.; Pricl, S.; Rodríguez-Franco, M. I. New flavonoid – *N*,*N*-dibenzyl(*N*-methyl)amine hybrids: Multi-target-directed agents for Alzheimer´s disease endowed with neurogenic properties. *J. Enzyme Inhib. Med. Chem.* **2019**, *34*, 712-727.

(129) Sofic, E.; Rimpapa, Z.; Kundurovic, Z.; Sapcanin, A.; Tahirovic, I.; Rustembegovic, A.; Cao, G. Antioxidant capacity of the neurohormone melatonin. *J. Neural. Transm. (Vienna)* **2005**, *112*, 349-358.

(130) Matos, M. J.; Rodríguez-Enríquez, F.; Vilar, S.; Santana, L.; Uriarte, E.; Hripcsak, G.; Estrada, M.; Rodríguez-Franco, M. I.; Viña, D. Potent and selective MAO-B inhibitory activity: Amino-versus nitro-3-arylcoumarin derivatives. *Bioorg. Med. Chem. Lett.* **2015**, *25*, 642-648.

(131) Pufahl, R. A.; Kasten, T. P.; Hills, R.; Gierse, J. K.; Reitz, B. A.; Weinberg, R. A.; Masferrer, J. L. Development of a fluorescence-based enzyme assay of human 5-lipoxygenase. *Anal. Biochem.* **2007**, *364*, 204-212.

(132) Wang, X. J.; Hayes, J. D.; Wolf, C. R. Generation of a stable antioxidant response element–driven reporter gene cell line and its use to show redox-dependent activation of Nrf2 by cancer chemotherapeutic agents. *Cancer Res.* **2006**, *66*, 10983-10994.

(133) Gameiro, I.; Michalska, P.; Tenti, G.; Cores, Á.; Buendia, I.; Rojo, A. I.; Georgakopoulos, N. D.; Hernández-Guijo, J. M.; Ramos, M. T.; Wells, G. Discovery of the first dual GSK3β inhibitor/Nrf2 inducer. A new multitarget therapeutic strategy for Alzheimer's disease. *Sci. Rep.* **2017**, *7*, 45701.

(134) Gameiro, I.; Michalska, P.; Tenti, G.; Cores, Á.; Buendia, I.; Rojo, A. I.; Georgakopoulos, N. D.; Hernández-Guijo, J. M.; Ramos, M. T.; Wells, G. Discovery of the first dual GSK3β inhibitor/Nrf2 inducer. A new multitarget therapeutic strategy for Alzheimer's disease. *Sci Rep.* **2017**, *7*, 45701.

(135) Di, L.; Kerns, E. H.; Fan, K.; McConnell, O. J.; Carter, G. T. High throughput artificial membrane permeability assay for blood–brain barrier. *Eur. J. Med. Chem.* **2003**, *38*, 223-232.

(136) Estrada-Valencia, M.; Herrera-Arozamena, C.; Pérez, C.; Viña, D.; Morales-García, J. A.; Pérez-Castillo, A.; Ramos, E.; Romero, A.; Laurini, E.; Pricl, S.; Rodríguez-Franco, M. I. New flavonoid – *N*,*N*-dibenzyl(*N*-methyl)amine hybrids: Multi-target-directed agents for Alzheimer´s disease endowed with neurogenic properties. *J. Enzyme Inhib. Med. Chem.* **2019**, *34*, 712-727.

(137) Estrada, M.; Pérez, C.; Soriano, E.; Laurini, E.; Romano, M.; Pricl, S.; Morales-García, J. A.; Pérez-Castillo, A.; Rodríguez-Franco, M. I. New neurogenic lipoic-based hybrids as innovative Alzheimer's drugs with sigma-1 agonism and beta-secretase inhibition. *Future Med . Chem.* **2016**, *8*, 1191-1207.

(138) Estrada, M.; Herrera-Arozamena, C.; Pérez, C.; Viña, D.; Romero, A.; Morales-García, J. A.; Pérez-Castillo, A.; Rodríguez-Franco, M. I. New cinnamic - *N*-benzylpiperidine and cinnamic - *N*,*N*-dibenzyl(*N*-methyl)amine hybrids as Alzheimer-directed multitarget drugs with antioxidant, cholinergic, neuroprotective and neurogenic properties. *Eur. J. Med. Chem.* **2016**, *121*, 376-386.

(139) López-Iglesias, B.; Pérez, C.; Morales-García, J. A.; Alonso-Gil, S.; Pérez-Castillo, A.; Romero, A.; López, M. G.; Villarroya, M.; Conde, S.; Rodríguez-Franco, M. I. New Melatonin–N,N-Dibenzyl(N-methyl)amine Hybrids: Potent Neurogenic Agents with Antioxidant, Cholinergic, and Neuroprotective Properties as Innovative Drugs for Alzheimer's Disease. *J. Med. Chem.* **2014**, *57*, 3773-3785.

(140) Morales-Garcia, J. A.; Alonso-Gil, S.; Gil, C.; Martinez, A.; Santos, A.; Perez-Castillo, A. Phosphodiesterase 7 inhibition induces dopaminergic neurogenesis in hemiparkinsonian rats. *Stem Cells Transl. Med.* **2015**, *4*, 564-575.

(141) Kempermann, G.; Jessberger, S.; Steiner, B.; Kronenberg, G. Milestones of neuronal development in the adult hippocampus. *Trends Neurosci.* **2004**, *27*, 447-452.

(142) Kamat, P. K.; Rai, S.; Swarnkar, S.; Shukla, R.; Nath, C. Molecular and cellular mechanism of okadaic acid (OKA)-induced neurotoxicity: a novel tool for Alzheimer's disease therapeutic application. *Mol. Neurobiol.* **2014**, *50*, 852-865.

(143) Reiter, R. J.; Mayo, J. C.; Tan, D. X.; Sainz, R. M.; Alatorre-Jimenez, M.; Qin, L. Melatonin as an antioxidant: under promises but over delivers. *J. Pineal Res.* **2016**, *61*, 253-278.

(144) Jin, G.; Lee, S.; Choi, M.; Son, S.; Kim, G. W.; Oh, J. W.; Lee, C.; Lee, K. Chemical genetics-based discovery of indole derivatives as HCV NS5B polymerase inhibitors. *Eur. J. Med. Chem.* **2014**, *75*, 413-425.

(145) Xu, Y.-Y.; Li, S.-N.; Yu, G.-J.; Hu, Q.-H.; Li, H.-Q. Discovery of novel 4-anilinoquinazoline derivatives as potent inhibitors of epidermal growth factor receptor with antitumor activity. *Bioorg. Med. Chem.* **2013**, *21*, 6084-6091.

(146) Carvalho, S. A.; Feitosa, L. O.; Soares, M.; Costa, T. E.; Henriques, M. G.; Salomao, K.; de Castro, S. L.; Kaiser, M.; Brun, R.; Wardell, J. L.; Wardell, S. M.; Trossini, G. H.; Andricopulo, A. D.; da Silva, E. F.; Fraga, C. A. Design and synthesis of new (E)-cinnamic N-acylhydrazones as potent antitrypanosomal agents. *Eur. J. Med. Chem.* **2012**, *54*, 512-521.

(147) Saunthwal, R. K.; Patel, M.; Kumar, S.; Danodia, A. K.; Verma, A. K. Pd(II)-Catalyzed C-H Activation of Styrylindoles: Short, Efficient, and Regioselective Synthesis of Functionalized Carbazoles. *Chem. Eur. J.* **2015**, *21*, 18601-18605.

(148) Farlow, D. S.; Flaugh, M. E.; Horvath, S. D.; Lavagnino, E. R.; Pranc, P. Two efficient syntheses of indole-3-propionic esters and acids. further applications of meldrum's acid. *Org. Prep. Proced. Int.* **1981**, *13*, 39-48.

(149) Liu, Y.; Xu, Y.; Jung, S. H.; Chae, J. A facile and green protocol for nucleophilic substitution reactions of sulfonate esters by recyclable ionic liquids [bmim][X]. *Synlett* **2012**, *23*, 2692-2698.

(150) Su, J.; Qiu, Y.; Ma, K.; Yao, Y.; Wang, Z.; Li, X.; Zhang, D.; Tu, Z.; Jiang, S. Design, synthesis, and biological evaluation of largazole derivatives: alteration of the zinc-binding domain. *Tetrahedron* **2014**, *70*, 7763-7769.

(151) Levins, C. G.; Wan, Z.-K. Efficient phosphonium-mediated synthesis of 2-amino-1, 3, 4-oxadiazoles. *Org. Lett.* **2008**, *10*, 1755-1758.

(152) Barreca, M. L.; Ferro, S.; Rao, A.; De Luca, L.; Zappalà, M.; Monforte, A.-M.; Debyser, Z.; Witvrouw, M.; Chimirri, A. Pharmacophore-based design of HIV-1 integrase strand-transfer inhibitors. *J. Med. Chem.* **2005**, *48*, 7084-7088.

(153) Dhurjati, M. S. K.; Sarma, J. A. R. P.; Desiraju, G. R. Unusual [2 + 2] topochemical cycloadditions of 3-cyano- and 4-cyano-cinnamic acids: temperature dependent solid state photochemical reactions. *J. Chem. Soc., Chem. Commun.* **1991**, 1702-1703.

(154) Wittstruck, T. A.; Trachtenberg, E. N. A nuclear magnetic resonance study of transmission of electronic effects. Ethylbenzenes, dihydrocinnamic acids, and cis-and trans-cinnamic acids. *J. Am. Chem. Soc.* **1967**, *89*, 3803-3809.

(155) Coutrot, P.; Snoussi, M.; Savignac, P. An improvement in the Wittig-Horner synthesis of 2-alkenoic acids. *Synthesis* **1978**, *1978*, 133-134.

(156) Rault, S.; Lancelot, J. C.; Suzanne, P.; Voisin-Chiret, A.-S.; Pecquet, R.; Joseph, J.-C., Guanidine derivatives in cinnamic series. Google Patents: 2014.

(157) Chaaban, I.; El Sayeda, M.; Mahran, M. A.; El Razik, H. A. A.; El Salamouni, N. S.; Wahab, A. E. A. Synthesis and biological evaluation of novel hydroquinone dimethyl ethers as potential anticancer and antimicrobial agents. *Med. Chem. Res.* **2013**, *22*, 3760-3778.

(158) TANAKA, K.; MATSUO, K.; Nakanishi, A.; HATANO, T.; IZEKI, H.; ISHIDA, Y.; MORI, W. Syntheses and anti-inflammatory and analgesic activities of hydroxamic acids and acid hydrazides. *Chem. Pharm. Bull.* **1983**, *31*, 2810-2819.

(159) Katritzky, A. R.; Wang, M.; Zhang, S. One-pot synthesis of cinnamoyl hydrazides. *Arkivoc* **2001**, *9*, 19-23.

(160) Rosen, G. M.; Popp, F. D. 2-Benzyl-1, 3, 4-oxadiazolin-5-one and related compounds. *J. Heterocycl. Chem.* **1971**, *8*, 659-662.

(161) Cohen, A. 94. The synthesis of compounds related to the sterols, bile acids, and oestrus-producing hormones. Part V. The synthesis of conjugated arylhexadienes, and their

behaviour in the Diels-Alder reaction. *J. Chem. Soc.* **1935**, 10.1039/JR9350000429, 429-436.

(162) Langley, W. D.; Adams, R. Condensation of certain nitriles and various poly-hydroxyphenols to form phenolic acids. *J. Am. Chem. Soc.* **1922**, *44*, 2320-2330.

(163) Piccolrovazzi, N.; Pino, P.; Consiglio, G.; Sironi, A.; Moret, M. Electronic effects in homogeneous indenylzirconium Ziegler-Natta catalysts. *Organometallics* **1990**, *9*, 3098-3105.

(164) Yang, Z.; Zhang, Y.; Chen, X.; Li, W.; Li, G.-B.; Wu, Y. Total Synthesis and Evaluation of New B-homo Palmatine and Berberine Derivatives as p300 Histone Acetyltransferase Inhibitors. *Eur. J. Org. Chem.*

(165) Hanif, M.; Khan, I.; Rama, N. H.; Noreen, S.; Choudhary, M. I.; Jones, P. G.; Iqbal, M. Synthesis, crystal structure and β-glucuronidase inhibition activity of some new hydrazinecarboxamides and their 1, 2, 4-triazole derivatives. *Med. Chem. Res.* **2012**, *21*, 3885-3896.

(166) Prata, J. V.; Clemente, D.-T. S.; Prabhakar, S.; Lobo, A. M.; Mourato, I.; Branco, P. S. Intramolecular addition of acyldiazenecarboxylates onto double bonds in the synthesis of heterocycles. *J. Chem. Soc., Perkin Trans. 1* **2002**, 513-528.

(167) Desforges, G.; Bombrun, A.; Quattropani, A. An efficient and expeditious synthesis of di-and trisubstituted amino-phenyl and-benzyl derivatives of tetrazole and [1, 3, 4] oxadiazol-2-one. *J. Comb. Chem.* **2008**, *10*, 671-680.

(168) Wipf, P.; Hopkins, C. R. Efficient Synthesis of 1, 4-Dihydro-2 H-isoquinoline-3, 5, 8-triones via Cyclobutene Ring Expansion. *J. Org. Chem.* **1999**, *64*, 6881-6887.

(169) Di Gioia, M. L.; Leggio, A.; Guarino, I. F.; Leotta, V.; Romio, E.; Liguori, A. A simple synthesis of anilines by LiAlH4/TiCl4 reduction of aromatic nitro compounds. *Tetrahedron Lett.* **2015**, *56*, 5341-5344.

(170) Ou, B.; Hampsch-Woodill, M.; Prior, R. L. Development and Validation of an Improved Oxygen Radical Absorbance Capacity Assay Using Fluorescein as the Fluorescent Probe. *J. Agric. Food Chem.* **2001**, *49*, 4619-4626.

(171) Matos, M. J.; Rodríguez-Enríquez, F.; Borges, F.; Santana, L.; Uriarte, E.; Estrada, M.; Rodríguez-Franco, M. I.; Laguna, R.; Viña, D. 3-Amidocoumarins as Potential

Multifunctional Agents against Neurodegenerative Diseases. *ChemMedChem* **2015**, *10*, 2071-2079.

(172) Pufahl, R. A.; Kasten, T. P.; Hills, R.; Gierse, J. K.; Reitz, B. A.; Weinberg, R. A.; Masferrer, J. L. Development of a fluorescence-based enzyme assay of human 5-lipoxygenase. *Anal. Biochem.* **2007**, *364*, 204-212.

(173) Rodríguez-Franco, M. I.; Fernández-Bachiller, M. I.; Pérez, C.; Hernández-Ledesma, B.; Bartolomé, B. Novel tacrine-melatonin hybrids as dual-acting drugs for Alzheimer disease, with improved acetylcholinesterase inhibitory and antioxidant properties. *J. Med. Chem.* **2006**, *49*, 459-462.

(174) Rodríguez-Franco, M. I.; Fernández-Bachiller, M. I.; Pérez, C.; Hernández-Ledesma, B.; Bartolomé, B. Novel Tacrine−Melatonin Hybrids as Dual-Acting Drugs for Alzheimer Disease, with Improved Acetylcholinesterase Inhibitory and Antioxidant Properties. *J. Med. Chem.* **2006**, *49*, 459-462.

(175) Morales-García, J. A.; Luna-Medina, R.; Alfaro-Cervello, C.; Cortés-Canteli, M.; Santos, A.; García-Verdugo, J. M.; Pérez-Castillo, A. Peroxisome proliferator-activated receptor gamma ligands regulate neural stem cell proliferation and differentiation *in vitro* and *in vivo*. *Glia* **2011**, *59*, 293-307.

(176) Verhulst, C.; Coiffard, C.; Coiffard, L. J.; Rivalland, P.; De Roeck-Holtzhauer, Y. In vitro correlation between two colorimetric assays and the pyruvic acid consumption by fibroblasts cultured to determine the sodium laurylsulfate cytotoxicity. *J. Pharmacol. Toxicol. Methods* **1998**, *39*, 143-146.

(177) Liu, Y.; Nair, M. G. An efficient and economical MTT assay for determining the antioxidant activity of plant natural product extracts and pure compounds. *J. Nat. Prod.* **2010**, *73*, 1193-1195.

(178) Lemoine, D.; Jiang, R.; Taly, A.; Chataigneau, T.; Specht, A.; Grutter, T. Ligand-gated ion channels: new insights into neurological disorders and ligand recognition. *Chem. Rev.* **2012**, *112*, 6285-6318.

(179) Karlin, A. Ion channel structure: emerging structure of the nicotinic acetylcholine receptors. *Nature Reviews Neuroscience* **2002**, *3*, 102.

(180) Dani, J. A., Neuronal nicotinic acetylcholine receptor structure and function and response to nicotine. In *Int. Rev. Neurobiol.*, Elsevier: 2015; Vol. 124, pp 3-19.

(181) Shimohama, S.; Kawamata, J., Roles of Nicotinic Acetylcholine Receptors in the Pathology and Treatment of Alzheimer's and Parkinson's Diseases. In *Nicotinic Acetylcholine Receptor Signaling in Neuroprotection*, Springer: 2018; pp 137-158.

(182) Kalamida, D.; Poulas, K.; Avramopoulou, V.; Fostieri, E.; Lagoumintzis, G.; Lazaridis, K.; Sideri, A.; Zouridakis, M.; Tzartos, S. J. Muscle and neuronal nicotinic acetylcholine receptors. Structure, function and pathogenicity. *FEBS J.* **2007**, *274*, 3799-3845.

(183) Unwin, N. Nicotinic acetylcholine receptor and the structural basis of neuromuscular transmission: insights from Torpedo postsynaptic membranes. *Q. Rev. Biophys.* **2013**, *46*, 283-322.

(184) Karlin, A.; Holtzman, E.; Yodh, N.; Lobel, P.; Wall, J.; Hainfeld, J. The arrangement of the subunits of the acetylcholine receptor of Torpedo californica. *J. Biol. Chem.* **1983**, *258*, 6678-6681.

(185) Mishina, M.; Takai, T.; Imoto, K.; Noda, M.; Takahashi, T.; Numa, S.; Methfessel, C.; Sakmann, B. Molecular distinction between fetal and adult forms of muscle acetylcholine receptor. *Nature* **1986**, *321*, 406.

(186) Witzemann, V.; Barg, B.; Nishikawa, Y.; Sakmann, B.; Numa, S. Differential regulation of muscle acetylcholine receptor γ-and ϵ-subunit mRNAs. *FEBS letters* **1987**, *223*, 104-112.

(187) Nayak, T. K.; Bruhova, I.; Chakraborty, S.; Gupta, S.; Zheng, W.; Auerbach, A. Functional differences between neurotransmitter binding sites of muscle acetylcholine receptors. *Proc. Natl. Acad. Sci. USA* **2014**, *111*, 17660-17665.

(188) Zhong, W.; Gallivan, J. P.; Zhang, Y.; Li, L.; Lester, H. A.; Dougherty, D. A. From ab initio quantum mechanics to molecular neurobiology: a cation–π binding site in the nicotinic receptor. *Proc. Natl. Acad. Sci. USA* **1998**, *95*, 12088-12093.

(189) Schmitt, J. D.; Sharples, C. G.; Caldwell, W. Molecular recognition in nicotinic acetylcholine receptors: The importance of π− cation interactions. *J. Med. Chem.* **1999**, *42*, 3066-3074.

(190) Dougherty, D. A. Cation-π interactions in chemistry and biology: a new view of benzene, Phe, Tyr, and Trp. *Science* **1996**, *271*, 163-168.

(191) Fagerlund, M.; Eriksson, L. Current concepts in neuromuscular transmission. *Br. J. Anaesth.* **2009**, *103*, 108-114.

(192) Farooq, K.; Hunter, J. M. Neuromuscular blocking agents and reversal agents. *Anaesth. Intensive Care Med.* **2017**, *18*, 279-284.

(193) Bowman, W. Neuromuscular block. *Br. J. Pharmacol.* **2006**, *147*.

(194) Miyazaki, Y.; Sunaga, H.; Hobo, S.; Miyano, K.; Uezono, S. Pancuronium enhances isoflurane anesthesia in rats via inhibition of cerebral nicotinic acetylcholine receptors. *J. Anesth.* **2016**, *30*, 671-676.

(195) Hunter, J. M. Reversal of residual neuromuscular block: complications associated with perioperative management of muscle relaxation. *Br. J. Anaesth.* **2017**, *119*, i53-i62.

(196) Hartley, G. The cis-form of azobenzene. *Nature* **1937**, *140*, 281.

(197) García-Amorós, J.; Velasco, D. Recent advances towards azobenzene-based light-driven real-time information-transmitting materials. *Beilstein J. Org. Chem.* **2012**, *8*, 1003.

(198) Zollinger, H., Color Chemistry, Syntheses, Properties, and Applications of Organic Dyes and Pigments, VCHA, Verlag Helvetica Chimica Acta AG, Zürich und. Wiley-VCH GmbH & Co. KGaA, Weinheim: 1987; p 85.

(199) Athey, R. D. Free radical initiator basics. *Eur. Coat. J.* **1998**, 146-149.

(200) Baroncini, M.; Ragazzon, G.; Silvi, S.; Venturi, M.; Credi, A. The eternal youth of azobenzene: new photoactive molecular and supramolecular devices. *Pure Appl. Chem.* **2015**, *87*, 537-545.

(201) Li, Z.; Yuan, X.; Feng, Y.; Chen, Y.; Zhao, Y.; Wang, H.; Xu, Q.; Wang, J. A reversible conductivity modulation of azobenzene-based ionic liquids in aqueous solutions by UV/Vis light. *Phys. Chem. Chem. Phys.* **2018**.

(202) Velema, W. A.; Szymanski, W.; Feringa, B. L. Photopharmacology: beyond proof of principle. *J. Am. Chem. Soc.* **2014**, *136*, 2178-2191.

(203) Lerch, M. M.; Hansen, M. J.; van Dam, G. M.; Szymanski, W.; Feringa, B. L. Emerging targets in Photopharmacology. *Angew. Chem. Int. Ed. Engl.* **2016**, *55*, 10978-10999.

(204) Hull, K.; Morstein, J.; Trauner, D. In vivo photopharmacology. *Chem. Rev.* **2018**, *118*, 10710-10747.

(205) Harvey, A. J.; Abell, A. D. α-Ketoester-based photobiological switches: synthesis, peptide chain extension and assay against α-chymotrypsin. *Bioorg. Med. Chem. Lett.* **2001**, *11*, 2441-2444.

(206) Banghart, M. R.; Volgraf, M.; Trauner, D. Engineering light-gated ion channels. *Biochemistry* **2006**, *45*, 15129-15141.

(207) Banghart, M.; Borges, K.; Isacoff, E.; Trauner, D.; Kramer, R. H. Light-activated ion channels for remote control of neuronal firing. *Nat. Neurosci.* **2004**, *7*, 1381.

(208) Bregestovski, P.; Maleeva, G.; Gorostiza, P. Light-induced regulation of ligand-gated channel activity. *Br. J. Pharmacol.* **2017**.

(209) Pittolo, S.; Gómez-Santacana, X.; Eckelt, K.; Rovira, X.; Dalton, J.; Goudet, C.; Pin, J.-P.; Llobet, A.; Giraldo, J.; Llebaria, A. An allosteric modulator to control endogenous G protein-coupled receptors with light. *Nat. Chem. Biol.* **2014**, *10*, 813.

(210) Tochitsky, I.; Kienzler, M. A.; Isacoff, E.; Kramer, R. H. Restoring vision to the blind with chemical photoswitches. *Chem. Rev.* **2018**, *118*, 10748-10773.

(211) Laprell, L.; Tochitsky, I.; Kaur, K.; Manookin, M. B.; Stein, M.; Barber, D. M.; Schon, C.; Michalakis, S.; Biel, M.; Kramer, R. H.; Sumser, M. P.; Trauner, D.; Van Gelder, R. N. Photopharmacological control of bipolar cells restores visual function in blind mice. *J. Clin. Invest.* **2017**, *127*, 2598-2611.

(212) Deal, W. J.; Erlanger, B. F.; Nachmansohn, D. Photoregulation of biological activity by photochromic reagents, III. Photoregulation of bioelectricity by acetylcholine receptor inhibitors. *Proc. Natl. Acad. Sci. USA* **1969**, *64*, 1230-1234.

(213) Bieth, J.; Wassermann, N.; Vratsanos, S. M.; Erlanger, B. F. Photoregulation of biological activity by photochromic reagents, IV. A model for diurnal variation of enzymic activity. *Proc. Natl. Acad. Sci. USA* **1970**, *66*, 850-854.

(214) Damijonaitis, A.; Broichhagen, J.; Urushima, T.; Hüll, K.; Nagpal, J.; Laprell, L.; Schönberger, M.; Woodmansee, D. H.; Rafiq, A.; Sumser, M. P. AzoCholine enables optical control of alpha 7 nicotinic acetylcholine receptors in neural networks. *ACS Chem. Neurosci.* **2015**, *6*, 701-707.

(215) Tochitsky, I.; Banghart, M. R.; Mourot, A.; Yao, J. Z.; Gaub, B.; Kramer, R. H.; Trauner, D. Optochemical control of genetically engineered neuronal nicotinic acetylcholine receptors. *Nat. Chem.* **2012**, *4*, 105-111.

(216) Damijonaitis, A.; Barber, D. M.; Trauner, D., The photopharmacology of nicotinic acetylcholine receptors. Neurotransmitter: 2016.

(217) Bregestovski, P.; Iljin, V.; Jurchenko, O. P.; Veprintsev, B.; Vulfius, C. A. Acetylcholine receptor conformational transition on excitation masks disulphide bonds against reduction. *Nature* **1977**, *270*, 71.

(218) Bartels, E.; Wassermann, N. H.; Erlanger, B. F. Photochromic activators of the acetylcholine receptor. *Proc. Natl. Acad. Sci. USA* **1971**, *68*, 1820-1823.

(219) Nerbonne, J. M.; Sheridan, R. E.; Chabala, L.; Lester, H. A. cis-3, 3'-Bis-[alpha-(trimethylammonium) methyl] azobenzene (cis-Bis-Q). Purification and properties at acetylcholine receptors of Electrophorus electroplaques. *Mol. Pharmacol.* **1983**, *23*, 344-349.

(220) Lester, H. A.; CHANG, H. W. Response of acetylcholine receptors to rapid photochemically produced increases in agonist concentration. *Nature* **1977**, *266*, 373.

(221) Lester, H. A.; Krouse, M. E.; Nass, M. M.; Wassermann, N. H.; Erlanger, B. F. A covalently bound photoisomerizable agonist. Comparison with reversibly bound agonists at Electrophorus electroplaques. *J. Gen. Physiol.* **1980**, *75*, 207.

(222) Gurney, A. M.; Lester, H. A. Light-flash physiology with synthetic photosensitive compounds. *Physiol. Rev* **1987**, *67*, 583-617.

(223) Chabala, L.; Gurney, A. M.; Lester, H. A. Dose-response of acetylcholine receptor channels opened by a flash-activated agonist in voltage-clamped rat myoballs. *J. Physiol.* **1986**, *371*, 407-433.

(224) Wassermann, N.; Bartels, E.; Erlanger, B. Conformational properties of the acetylcholine receptor as revealed by studies with constrained depolarizing ligands. *Proc. Natl. Acad. Sci. USA* **1979**, *76*, 256-259.

(225) Krouse, M. E.; Lester, H. A.; Wassermann, N. H.; Erlanger, B. F. Rates and equilibria for a photoisomerizable antagonist at the acetylcholine receptor of Electrophorus electroplaques. *J. Gen. Physiol.* **1985**, *86*, 235-256.

(226) Merino, E. Synthesis of azobenzenes: the coloured pieces of molecular materials. *Chem. Soc. Rev.* **2011**, *40*, 3835-3853.

(227) Hamon, F.; Djedaini-Pilard, F.; Barbot, F.; Len, C. Azobenzenes—synthesis and carbohydrate applications. *Tetrahedron* **2009**, *65*, 10105-10123.

(228) Harvey, J. H.; Butler, B. K.; Trauner, D. Functionalized azobenzenes through cross-coupling with organotrifluoroborates. *Tetrahedron Lett.* **2007**, *48*, 1661-1664.

(229) Haghbeen, K.; Tan, E. W. Facile synthesis of catechol azo dyes. *J. Org. Chem.* **1998**, *63*, 4503-4505.

(230) Murtaza, S.; Ashraf, J. Synthesis, Antioxidant and Antimicrobial Activity of 4-Aminophenol and 2-Aminobenzoic Acid Based Novel Azo Compounds. *Asian J. Chem.* **2015**, *27*, 3551.

(231) Pizzolatti, M. G.; Yunes, R. A. Azoxybenzene formation from nitrosobenzene and phenylhydroxylamine. A unified view of the catalysis and mechanisms of the reactions. *J. Chem. Soc., Perkin Trans. 2* **1990**, 759-764.

(232) Nanjundaswamy, H.; Pasha, M. Facile, Product-Selective Reduction of Azoxyarenes into Azoarenes or Hydrazoarenes by Aluminium/Hydrazine Hydrate. *Synth. commun.* **2005**, *35*, 2163-2168.

(233) Greene, F. D.; Gilbert, K. E. Cyclic azo dioxides. Preparation, properties, and consideration of azo dioxide-nitrosoalkane equilibriums. *J. Org. Chem.* **1975**, *40*, 1409-1415.

(234) Taylor, E. C.; Tseng, C. P.; Rampal, J. B. Conversion of a primary amino group into a nitroso group. Synthesis of nitroso-substituted heterocycles. *J. Org. Chem.* **1982**, *47*, 552-555.

(235) Gowenlock, B. G.; Richter-Addo, G. B. Preparations of C-nitroso compounds. *Chem. Rev.* **2004**, *104*, 3315-3340.

(236) Zhu, Z.; Espenson, J. H. Kinetics and mechanism of oxidation of anilines by hydrogen peroxide as catalyzed by methylrhenium trioxide. *J. Org. Chem.* **1995**, *60*, 1326-1332.

(237) Priewisch, B.; Rück-Braun, K. Efficient preparation of nitrosoarenes for the synthesis of azobenzenes. *J. Org. Chem.* **2005**, *70*, 2350-2352.

(238) Yu, B.-C.; Shirai, Y.; Tour, J. M. Syntheses of new functionalized azobenzenes for potential molecular electronic devices. *Tetrahedron* **2006**, *62*, 10303-10310.

(239) Huskić, I.; Halasz, I.; Friščić, T.; Vančik, H. Mechanosynthesis of nitrosobenzenes: a proof-of-principle study in combining solvent-free synthesis with solvent-free separations. *Green Chem.* **2012**, *14*, 1597-1600.

(240) Wawzonek, S.; McIntyre, T. Electrolytic preparation of azobenzenes. *J. Electrochem. Soc.* **1972**, *119*, 1350-1350.

(241) Heravi, M. M.; Ajami, D.; Ghassemzadeh, M. Wet alumina Supported Chromium (VI) oxide: A Mild, Efficient and Inexpensive reagent for Oxidative Deprotection of Trimethylsilyl and Tetrahydropyranyl Ethers in Solventless System. *Synth. Commun.* **1999**, *29*, 781-784.

(242) Zhang, C.; Jiao, N. Copper-Catalyzed Aerobic Oxidative Dehydrogenative Coupling of Anilines Leading to Aromatic Azo Compounds using Dioxygen as an Oxidant. *Angew. Chem.* **2010**, *122*, 6310-6313.

(243) Thorwirth, R.; Bernhardt, F.; Stolle, A.; Ondruschka, B.; Asghari, J. Switchable selectivity during oxidation of anilines in a ball mill. *Chem. Eur. J.* **2010**, *16*, 13236-13242.

(244) Hutchins, R. O.; Lamson, D. W.; Rua, L.; Milewski, C.; Maryanoff, B. Reduction of aromatic nitro compounds with sodium borohydride in dimethyl sulfoxide or sulfolane. Synthesis of azo or azoxy derivatives. *J. Org.Chem.* **1971**, *36*, 803-806.

(245) Nystrom, R. F.; Brown, W. G. Reduction of Organic Compounds by Lithium Aluminum Hydride. III. Halides, Quinones, Miscellaneous Nitrogen Compounds1. *J. Am. Chem. Soc.* **1948**, *70*, 3738-3740.

(246) Gund, S. H.; Shelkar, R. S.; Nagarkar, J. M. An efficient catalyst-free and chemoselective synthesis of azobenzenes from nitrobenzenes. *RSC Advances* **2014**, *4*, 42947-42951.

(247) Wang, Q.; Yi, L.; Liu, L.; Zhou, C.; Xi, Z. A thermostable azo-linker for reversible photoregulation of DNA replication. *Tetrahedron Lett.* **2008**, *49*, 5087-5089.

(248) Wang, J.; Hu, L.; Cao, X.; Lu, J.; Li, X.; Gu, H. Catalysis by Pd nanoclusters generated in situ of high-efficiency synthesis of aromatic azo compounds from nitroaromatics under H 2 atmosphere. *RSC Advances* **2013**, *3*, 4899-4902.

(249) Stappert, K.; Muthmann, J.; Spielberg, E. T.; Mudring, A.-V. Azobenzene-based organic salts with ionic liquid and liquid crystalline properties. *Cryst. Growth Des.* **2015**, *15*, 4701-4712.

(250) Tian, X.; Zhang, C.; Xu, Q.; Li, Z.; Shao, X. Azobenzene-benzoylphenylureas as photoswitchable chitin synthesis inhibitors. *Org. Biomol. Chem.* **2017**, *15*, 3320-3323.

(251) Bard, B.; Martel, S.; Carrupt, P.-A. High throughput UV method for the estimation of thermodynamic solubility and the determination of the solubility in biorelevant media. *Eur. J. Pharm. Sc.* **2008**, *33*, 230-240.

(252) Avdeef, A.; Comer, J. E. A.; Thomson, S. J. pH-Metric log P. 3. Glass electrode calibration in methanol-water, applied to pKa determination of water-insoluble substances. *Anal. Chem.* **1993**, *65*, 42-49.

(253) Griffiths, J. II. Photochemistry of azobenzene and its derivatives. *Chem. Soc. Rev.* **1972**, *1*, 481-493.

(254) Birnbaum, P.; Linford, J.; Style, D. The absorption spectra of azobenzene and some derivatives. *Transactions of the Faraday Society* **1953**, *49*, 735-744.

(255) Fischer, E.; Frankel, M.; Wolovsky, R. Wavelength dependence of photoisomerization equilibria in azocompounds. *J. Chem. Phys.* **1955**, *23*, 1367-1367.

(256) Moniruzzaman, M.; Talbot, J.; Sabey, C.; Fernando, G. The use of 1H NMR and UV–vis measurements for quantitative determination of trans/cis isomerization of a photo-responsive monomer and its copolymer. *J. Appl. Polym. Sci.* **2006**, *100*, 1103-1112.

(257) Wazzan, N. Cis-trans isomerisation of azobenzenes studied by NMR spectroscopy with in situ laser irradiation and DFT calculations. *PhD Thesis* **2009**.

(258) Tait, K. M.; Parkinson, J. A.; Bates, S. P.; Ebenezer, W. J.; Jones, A. C. The novel use of NMR spectroscopy with in situ laser irradiation to study azo photoisomerisation. *J. Photochem. Photobiol. A: Chem.* **2003**, *154*, 179-188.

(259) Tait, K. M.; Parkinson, J. A.; Jones, A. C.; Ebenezer, W. J.; Bates, S. P. Comparison of experimental and calculated 1H NMR chemical shifts of geometric photoisomers of azo dyes. *Chem. Phys. Lett.* **2003**, *374*, 372-380.

(260) Lever, L. S.; Bradley, M. S.; Johnson Jr, C. S. Comparison of pulsed field gradient NMR and holographic relaxation spectroscopy in the study of diffusion of photochromic molecules. *J. Magn. Reson.* **1986**, *68*, 335-344.

(261) Purohit, P.; Bruhova, I.; Gupta, S.; Auerbach, A. Catch-and-hold activation of muscle acetylcholine receptors having transmitter binding site mutations. *Biophys. J.* **2014**, *107*, 88-99.

(262) Denizot, F.; Lang, R. Rapid colorimetric assay for cell growth and survival: modifications to the tetrazolium dye procedure giving improved sensitivity and reliability. *J. Immunol. Methods* **1986**, *89*, 271-277.

(263) Denizot, F.; Lang, R. Rapid colorimetric assay for cell growth and survival. Modifications to the tetrazolium dye procedure giving improved sensitivity and reliability. *J. Immunol. Methods* **1986**, *89*, 271-277.

(264) Zuo, S.-J.; Zhang, S.; Mao, S.; Xie, X.-X.; Xiao, X.; Xin, M.-H.; Xuan, W.; He, Y.-Y.; Cao, Y.-X.; Zhang, S.-Q. Combination of 4-anilinoquinazoline, arylurea and tertiary amine moiety to discover novel anticancer agents. *Bioorg. Med. Chem.* **2016**, *24*, 179-190.

(265) Russell, G. A.; Wang, K. Electron transfer processes. 53. Homolytic alkylation of enamines by electrophilic radicals. *J. Org. Chem.* **1991**, *56*, 3475-3479.

(266) Rice, K. D.; Anand, N. K.; Arcalas, A.; Blazey, C. M.; Bussenius, J.; Chan, W. K. V.; Du, H.; Epshteyn, S.; Ibrahim, M. A.; Kearney, P., Pyrimidinones as Casein Kinase II (CK2) modulators. WO 2004046107: 2012.

(267) Molander, G. A.; Sandrock, D. L. Aminomethylations via cross-coupling of potassium organotrifluoroborates with aryl bromides. *Org. Lett.* **2007**, *9*, 1597-1600.

(268) Tsou, H.-R.; Ayral-Kaloustian, S.; Birnberg, G. H.; Floyd, M. B.; Kaplan, J.; Kutterer, K. M.; Liu, X.; Nilakantan, R.; Otteng, M. A.; Tang, Z., Substituted isoquinoline-1, 3 (2H, 4H)-diones, 1-thioxo, 1, 4-dihydro-2H-isoquinoline-3-ones and 1, 4-dihyro-3 (2H)-isoquinolones and methods of use thereof. Google Patents: 2010.

(269) Goss, F. R.; Ingold, C. K.; Wilson, I. S. CCCXXIV.—The nature of the alternating effect in carbon chains. Part VIII. The nitration of some benzylamine derivatives with special reference to the respective rôles of the ions, salts, and bases. *J. Chem. Soc.* **1926**, *129*, 2440-2462.

(270) Ibrahim, E.-S.; Montgomerie, A. M.; Sneddon, A. H.; Proctor, G. R.; Green, B. Synthesis of indolo [3, 2-c] quinolines and indolo [3, 2-d] benzazepines and their interaction with DNA. *Eur. J. Med. Chem.* **1988**, *23*, 183-188.

(271) Hanada, S.; Tsutsumi, E.; Motoyama, Y.; Nagashima, H. Practical Access to Amines by Platinum-Catalyzed Reduction of Carboxamides with Hydrosilanes: Synergy of Dual Si− H Groups Leads to High Efficiency and Selectivity. *J. Am. Chem. Soc.* **2009**, *131*, 15032-15040.

(272) Shiraishi, M.; Aramaki, Y.; Seto, M.; Imoto, H.; Nishikawa, Y.; Kanzaki, N.; Okamoto, M.; Sawada, H.; Nishimura, O.; Baba, M. Discovery of novel, potent, and selective small-molecule CCR5 antagonists as anti-HIV-1 agents: synthesis and biological evaluation of anilide derivatives with a quaternary ammonium moiety. *J. Med. Chem.* **2000**, *43*, 2049-2063.

(273) Roth, G. J.; Heckel, A.; Colbatzky, F.; Handschuh, S.; Kley, J. r.; Lehmann-Lintz, T.; Lotz, R.; Tontsch-Grunt, U.; Walter, R.; Hilberg, F. Design, synthesis, and evaluation of indolinones as triple angiokinase inhibitors and the discovery of a highly specific 6-methoxycarbonyl-substituted indolinone (BIBF 1120). *J. Med. Chem.* **2009**, *52*, 4466-4480.

(274) Zhang, L.; Xia, J.; Li, Q.; Li, X.; Wang, S. Fast Synthesis of Hydrazine and Azo Derivatives by Oxidation of Rare-Earth-Metal− Nitrogen Bonds. *Organometallics* **2011**, *30*, 375-378.

(275) Gingras, B. A.; Waters, W. A. Properties and reactions of free alkyl radicals in solution. Part VII. Reactions with quinone imides, nitric oxide, and nitroso-compounds. *J. Chem. Soc.* **1954**, 1920-1924.

(276) Wassermann, N.; Erlanger, B. Agents related to a potent activator of the acetylcholine receptor of Electrophorus electricus. *Chem.-Biol. Interact.* **1981**, *36*, 251-258.

(277) Bard, B.; Martel, S.; Carrupt, P.-A. High throughput UV method for the estimation of thermodynamic solubility and the determination of the solubility in biorelevant media. *Eur. J. Pharm. Sci.* **2008**, *33*, 230-240.

(278) Tan, H.; Semin, D.; Wacker, M.; Cheetham, J. An automated screening assay for determination of aqueous equilibrium solubility enabling SPR study during drug lead optimization. *J. Lab. Autom.* **2005**, *10*, 364-373.

(279) Caine, B. A.; Dardonville, C.; Popelier, P. L. Prediction of Aqueous p K a Values for Guanidine-Containing Compounds Using Ab Initio Gas-Phase Equilibrium Bond Lengths. *ACS Omega* **2018**, *3*, 3835-3850.

(280) Lukas, R. J. Characterization of curaremimetic neurotoxin binding sites on membrane fractions derived from the human medulloblastoma clonal line, TE671. *J. Neurochem.* **1986**, *46*, 1936-1941.

(281) Sharples, C. G.; Kaiser, S.; Soliakov, L.; Marks, M. J.; Collins, A. C.; Washburn, M.; Wright, E.; Spencer, J. A.; Gallagher, T.; Whiteaker, P. UB-165: a novel nicotinic

agonist with subtype selectivity implicates the α4β2* subtype in the modulation of dopamine release from rat striatal synaptosomes. *J. Neurosci.* **2000**, *20*, 2783-2791.

(282) Gopalakrishnan, M.; Monteggia, L. M.; Anderson, D. J.; Molinari, E. J.; Piattoni-Kaplan, M.; Donnelly-Roberts, D.; Arneric, S. P.; Sullivan, J. P. Stable expression, pharmacologic properties and regulation of the human neuronal nicotinic acetylcholine alpha 4 beta 2 receptor. *J. Pharmacol. Exp. Ther.* **1996**, *276*, 289-297.

(283) Corbin-Leftwich, A.; Mossadeq, S. M.; Ha, J.; Ruchala, I.; Le, A. H.; Villalba-Galea, C. A. Retigabine holds KV7 channels open and stabilizes the resting potential. *J. Gen. Physiol.* **2016**, *147*, 229-241.

(284) Boland, L. M.; Drzewiecki, M. M.; Timoney, G.; Casey, E. Inhibitory effects of polyunsaturated fatty acids on Kv4/KChIP potassium channels. *Am. J. Physiol. Cell Physiol.* **2009**, *296*, C1003-1014.